THESIS AND ABSTRACT

Autophagy is Indispensable for Normal Maturation and Function of Macrophages and Neutrophils

Amanda Jane Stranks

University College, Oxford
Nuffield Department of Clinical Medicine
MRC Human Immunology Unit, Weatherall Institute of Molecular Medicine

Thesis submitted in fulfilment of the requirements for the degree of Doctor of Philosophy,

University of Oxford

Trinity Term 2013

Contents

Abstract

Autophagy is Indispensable for Normal Maturation and Function of Macrophages and Neutrophils

Amanda Jane Stranks, University College, Oxford

Thesis submitted in fulfilment of the requirements for the degree Doctor of Philosophy, University of Oxford, Trinity Term, 2013

Macrophages and neutrophils are vital cells of the immune system, performing crucial innate functions and bridging innate and adaptive immunity. However, inappropriate activation or poor resolution of responses results in chronic inflammatory and autoimmune conditions due to accumulation of myeloid cells and uncontrolled cytokine production, as is commonly seen in the aging immune system. It is not clear what is required to maintain healthy myeloid cells throughout life or what links inflammation and myeloid dysfunction during the aging process.

We have shown that autophagy, a vital intracellular degradation mechanism, is required for normal macrophage innate and adaptive immune functions such as phagocytosis and antigen presentation, as well as being an important regulator of the inflammatory response. Loss of autophagy also results in reduced surface antigen expression and increased glycolysis. We found that autophagy-deficient macrophages have a similar phenotype to aged macrophages. Furthermore, aged macrophages exhibit reduced autophagy compared with young macrophages, suggesting a link between reduced autophagy and acquisition of the aging macrophage phenotype. Finally, we show that autophagy plays a vital role in normal neutrophil differentiation, with autophagy-deficient neutrophils exhibiting altered nuclear morphology and aberrant granule formation.

These data show that autophagy plays a critical role in the maintenance of essential macrophage homeostasis and functions by regulating inflammation and metabolism, thereby preventing immunosenescence. We postulate that autophagy modulation in macrophages and neutrophils may be used to prevent excess inflammation, such as in inflammatory and autoimmune diseases. Moreover, inflammation due to aging may potentially be delayed by induction or preservation of autophagy, which could improve immune responses and reduce the morbidity and mortality associated with “inflamm-aging”.

Acknowledgements

Completing a DPhil and writing a thesis is a huge undertaking, and cannot be done without the help and invaluable support of many people. I would like to thank the following people and organisations, without which this work would not have been possible.
Firstly, I would like to thank the Nuffield Department of Medicine for awarding me the Studentship that provided my funding throughout the four years of my DPhil. Without the faith of the selection board, I would not have had the chance to complete my DPhil at Oxford and, for such an opportunity, I am truly grateful.

Secondly, I would like to thank my fellow lab members and the wider WIMM community of researchers. Thanks to Monika Mortensen, for your help and advice when I first arrived in the lab, and helping me get set up. Thanks also to my lab mates, Dan and Alec, for your scientific input and ideas, help with weaning enormous mice and for sharing a general whinge about the various difficulties faced by autophagy researchers and DPhil students in general! Your support was invaluable and made it much easier to get through difficult days in the lab. Sharon, Anne and Kanchan, a special thanks to you also, for many hours spent on the ImageStream on my behalf, or helping me plan or analyse experiments. Several vital pieces of data came out of our experiments, without which this thesis would not have had the outcomes it did. Your time and expertise was much appreciated. Thanks also to the members of Jackson lab (and not just for answering the phone!), and other members of the WIMM who provided company or advice, or took the time to help me learn the techniques I needed. Thanks also to Matt and Keith for autoclaving countless forceps and mortar and pestles and returning them to me. Thanks to Alastair and Becky for keeping everything in such good running order, and to Kevin and Craig for the time spent solving my FACS dilemmas and sorting my samples.

Thirdly, to my friends and family members, scientifically inclined and otherwise, for your patience and support throughout my DPhil. Four years is a long time to be so far away from family, and I have appreciated your understanding and encouragement, not just in giving your blessing to travel around the world, but for remembering to let me know that you miss me! Thanks for being willing to ask about (and try to understand) my project, and for being understanding when I didn't keep in touch as much as I should or come home as often as you'd like. To my Oxford friends, thanks so much for your friendship during our time in Oxford. The people we have met and the friendships we have formed have really made our time here, and I would never remember Oxford half as fondly were it not for all the memories formed through countless college dinners, BOPs, balls, and particularly the many nights when you let me cook for you and we sat late into the night just chatting with a glass of wine (and the odd game of cards).

Fourthly, to my wonderful, wonderful husband Sam. Hard to believe that this time almost 5 years ago we were arguing about me applying for my scholarship while on our

honeymoon! Thanks for winning that argument, and making me apply – your dreams for me were bigger than I'd had even for myself and they've opened doors I'd never even have thought to look behind. Thanks for listening, for providing a source of encouragement and strength, and for taking my side when problems struck! You have been amazing during these past months, taking on the running of this house to allow me to write full time, while also taking the time to proof-read the entire manuscript and generally listening to me complain about how hard it was to write. I can't even begin to put into words the many ways in which this thesis would not have happened without you. I can't wait to see where our next steps, post-Oxford and post-DPhil, lie.

Finally, to my supervisor Katja, a very big and grateful thank you. Thanks for your patience and encouragement to keep me going throughout this DPhil, even when your words were not what I wanted to hear! It may not have always seemed like it, but I really valued and appreciated your effort and ability to keep me motivated. Thank you for your many (many!) ideas and for always being able to come up with something when things seemed to be going wrong (which was a lot of the time). Thanks for providing so many opportunities to present our research and for allowing me to teach on the methods and techniques course, which I enjoyed so much. I also appreciated our conversations on science as a career, women in science and the pros and cons of being a scientist – they have provided much food for thought as to what my next steps post-DPhil will be. I'm looking forward to writing those papers, and seeing what direction research in the Katja Simon lab will take next.

Abbreviations

2DG	2-Deoxyglucose
3MA	3-Methyladenine
AAM	Alternately activated macrophages
ADP	Adenosine diphosphate
AGE	Advanced glycosylation end-product
AKT	AKT8 virus oncogene cellular homolog
AML	Acute myeloid leukaemia
AMPK	AMP-activated protein kinase
APC	Antigen presenting cell
APL	Acute promyelocytic leukaemia
Arf	ADP-ribosylation factor 6
Arp 2/3	Actin-related protein 2/3
Atg	Autophagy related gene
ATP	Adenosine triphosphate
BCA	Bicinchoninic acid
BDS	Bright detail similarity (a measure of colocalisation)
BMMϕ	Bone marrow derived macrophages
BSA	Bovine serum albumin
C/EBPε	CCAAT enhancer binding protein epsilon
cAMP	Cyclic adenosine monophosphate
CCL3	Chemokine C-C motif ligand 3
CD	Clusters of differentiation
CD62L	L-selectin
CFSE	Carboxyfluorescein diacetate succinimidyl ester
CIITA	Class II transactivator
CMA	Chaperone mediated autophagy
CO_2	Carbon dioxide
CR	Caloric restriction
CXCR4	C-X-C Chemokine receptor 4
DAMP	Damage/danger associated molecular pattern
DAPI	4',6-Diamidino-2-Phenylindole, Dihydrochloride
DAPK	Death-associated protein kinase

DC	Dendritic cell
DC-SIGN	Dendritic Cell-Specific Intercellular adhesion molecule-3-Grabbing Non-integrin
DEPC	Diethylpyrocarbonate
DHAP	Dihydroxyacetone phosphate
DHEA	Dehydroepiandrosterone
DMEM	Dulbecco's Modified Eagle's medium
DNA	Deoxyribonucleic acid
DPI	Diphenylene iodonium
ECAR	Extracellular acidification rate
EDTA	Ethylenediaminetetraacetic acid
ELISA	Enzyme-linked immunosorbent assay
EM	Electron microscopy
ENMA	Endosome mediated autophagy
ER	Endoplasmic reticulum
ERK	Extra-cellular signal related kinase
FACS	Fluoresence activated cell sorting
FAD	Flavin adenine dinucleotide
$FADH_2$	Flavin Adenine Dinucleotide, Reduced
FCCP	Trifluorocarbonylcyanide Phenylhydrazone
FCS	Foetal calf serum
FIH	Factor inhibiting HIF-1
FITC	Fluorescein isothiocyanate
FS	Forward scatter
Fwd	Forward
G6DP	Glucose-6-phosphate dehydrogenase
GAPDH	Glyceraldehyde-3 phosphate dehydrogenase
GDP	Guanosine diphosphate
Glrx	Glutaredoxin
Glut	Glucose transporter
GM-CSF	Granulocyte-macrophage colony stimulating factor
GMP	Granulocyte macrophage progenitor
GTP	Guanosine triphosphate
HIF	Hypoxia inducible factor
HKLM	Heat killed *Listeria Monocytogenes*

HMGB1	High-mobility group protein B1
HRE	Hypoxia response elements
HRP	Horseraddish peroxidase
Hrs	Hours
HSC	Hematopoietic stem cell
Hsc70	Heat shock cognate protein of 70 kDa
HSP	Heat shock protein
HSV1	Herpes simplex virus 1
IC	Intracellular
IFN	Interferon
IKK	IκB kinase
IL	Interleukin
iNOS	Inducible nitric oxide synthase
IR	Insulin receptor
JNK	c-Jun amino-terminal kinase
Keap-1	Kelch-like ECH-associated protein 1
KO	Knock out ($Atg7^{-/-}$ cells)
LAMP	Lysosome-associated membrane protein
LC3	Microtubule-associated protein 1A/1B-light chain 3
LDH	Lactate dehydrogenase
LPS	Lipopolysaccharide
Ltf	Lactoferrin
M	Molar
M1	Classically activated macrophages
M2	Alternately activated macrophages
MACS	Magnetic-activated cell sorting
MAPK	Mitogen-activated protein kinase
M-CSF	Macrophage colony stimulating factor
MDS	Myelodysplastic syndrome
MFI	Mean fluorescence intensity
MG	Methylglyoxal
MHC	Major Histocompatibility Complex
MIIC	MHC II loading compartments
Min	Minutes
MIP	Macrophage inflammatory protein

MMP	Matrix metalloproteinase
MPO	Myeloperoxidase
MR	Mannose receptor
MRC	Maximum respiratory capacity
mROS	Mitochondrial reactive oxygen species
mtDNA	Mitochondrial DNA
mTOR	Mammalian target of rapamycin
MVB	Multi vesicular body
MyD88	Myeloid differentiation primary response gene (88)
N	Normality (a measure of acid concentration)
NAC	N-acetylcysteine
NAD	Nicotinamide adenine dinucleotide
NADH	Nicotinamide adenine dinucleotide (reduced)
NADPH	Nicotinamide adenine dinucleotide phosphate
NED	N-1-napthylethylenediamine dihydrochloride
NET	Neutrophil extracellular trap
NF-κB	Nuclear factor kappa-light-chain-enhancer of activated B cells
NGAL	Neutrophil gelatinase
NK	Natural killer (cell)
NLR	NOD-like receptor
NLRP3	NACHT, LRR and PYD domains-containing protein 3
NO	Nitric oxide
NOD	Nucleotide-binding and oligomerization domain
Nrf2	Nuclear factor erythroid 2-related factor 2
OCR	Oxygen consumption rate
OLA-1	Obg-like ATPase 1
OxPhos	Oxidative Phosphorylation (mitochondrial respiration)
PAMP	Pathogen associated molecular pattern
PAS	Pre-autophagosomal structure
PBMC	Peripheral blood mononuclear cells
PBS	Phosphate buffered saline
PCR	Polymerase chain reaction
PE	Phosphatidylethanolamine
PFK2	Phosphofructokinase
Pi	Phosphate

PI3K	Phosphoinositide 3-kinase
PMA	Phorbol myristate acetate
Poly I:C	Polyinosinic-polycytidylic acid
PPP	Pentose Phosphate Pathway
PRR	Pattern recognition receptor
Prxn	Peroxiredoxin
PtdIns	Phosphatidylinositol
PTEN	Phosphatase and tensin homolog
qPCR	Quantitative polymerase chain reaction
R10	RPMI 1640 + 10% FCS + glutamine and PenStrep (media)
RANTES	Regulated on activation, normal T-cell expressed and secreted (chemokine)
RAR	Retinoic acid receptor
RBC	Red blood cell
Ref	Reference
Rev	Reverse
RIPA	Radioimmunoprecipitation assay buffer
RLR	Rig-like receptor
RNA	Ribonucleic acid
ROS	Reactive oxygen species
RPMI	Roswell Park Memorial Institute medium
RT	Reverse transcription/room temperature
RUBICON	RUN domain and cysteine-rich domain containing, Beclin 1-interacting protein
SDS	Sodium dodecyl sulfate
Sec	Seconds
SEM	Standard error of the mean
siRNA	Small interfering RNA
SIRT1	Mammalian silent information regulator 2 homolog
SOCS	Suppressor of cytokine signalling
SPF	Specific pathogen free
SQSTM1	Sequestosome-1 (also known as p62)
SRC	Spare respiratory capacity
SS	Side scatter
STING	Stimulator of interferon genes
TAP	Transporter for antigen processing

TBE	Tris/Borate/EDTA (buffer)
TCA	Citric acid cycle
TCR	T-cell receptor
TGN	Trans-Golgi network
T_H1	T helper type 1 cell
T_H2	T helper type 2 cell
TIGAR	TP53-inducible glycolysis and apoptosis regulator
TLR	Toll-like receptor
TMRM	Tetramethylrhodamine, methyl ester
TNF	Tumour necrosis factor
tPMET	trans-plasma membrane electron transport
TRAF6	TNF receptor-associated factor 6
TRAPS	TNF receptor associated syndrome
TSC	Tuberous sclerosis protein
V	Volts
VAMP	Vesicle associated membrane protein
VASP	Vasodilator-stimulated phosphoprotein
WST-1	Water soluble tetrazolium salts
WT	Wildtype

Chapter 1: General Introduction

The autophagy pathway and its regulation

1.1 Autophagy

The word 'autophagy' comes from the Greek *auto* (self) and *phagy* (to eat), and describes a catabolic intracellular pathway for the degradation of bulk protein aggregates and organelles. The pathway is an evolutionarily-conserved process ubiquitous to all eukaryotic cells(1) and is controlled by the *autophagy-related genes* (Atg). Autophagy has two central physiological roles; degradation of damaged organelles, and recycling cytoplasmic elements to recover amino acids to maintain homeostasis during periods of starvation. Autophagy plays a critical role during cellular development and differentiation(2), cell death(3) and has been linked to cancer(4) and aging(5). It also plays diverse roles in innate and adaptive immunity, including immunity to intracellular pathogens(6), regulation of the inflammatory response(7), and antigen presentation(8, 9), and is important in several diseases, including Crohn's disease(10), diabetes(11), Alzheimer's(12) and Huntington's disease(13).

1.2 Autophagy pathways

Autophagy can describe one of several pathways that facilitate digestion of cytoplasmic contents in lysosomes - including macroautophagy, microautophagy and chaperone-mediated autophagy. Classical macroautophagy, hereafter denoted autophagy, describes the sequestration of cytoplasmic contents by a double-membraned vesicle termed the autophagosome, which fuses with a lysosome for degradation of the internal contents. The degraded cargo is then recycled into the cytoplasm and the energy, nucleotides and other building blocks reused in times of cellular stress or starvation(14). Classical autophagy is the main focus of this thesis.

Microautophagy differs from classical autophagy in that cytosolic contents are degraded by direct invagination of the lysosome, rather than first being sequestered by the

autophagosome(15). Microautophagy allows maintenance of organelle size, membrane homeostasis, and cell survival during episodes of starvation, and uses similar molecular machinery to classical autophagy.

Chaperone-mediated autophagy (CMA) refers to a selective form of autophagy that modulates the degradation of specific soluble proteins(16). Proteins degraded by CMA contain a motif in their amino acid sequence required for targeting to lysosomes(17). The motif is recognised by the chaperone heat shock cognate protein of 70 kDa (Hsc70), which directs the protein to the lysosome, where the protein-chaperone complex docks at the lysosome-associated membrane protein type 2A (LAMP-2a), which acts as a receptor for CMA. The protein then unfolds and is translocated across the lysosomal membrane for degradation(15).

1.3 Autophagy signalling

Autophagy is tightly regulated, both during development(18) and by extracellular stimuli such as growth factors(19), cytokines(20) and pathogen components such as LPS(21). The Atg genes were identified during genetic screens of yeast mutants(22) and, to date, 36 autophagy-related genes have been described(23). Mammalian orthologs have been identified for many of the genes, and their functions identified within the autophagy pathway.

The two key molecules in autophagy regulation are serine/threonine kinase mammalian Target of Rapamycin (mTOR) and the class I and class III phosphoinositide 3-kinases (PI3Ks), whose actions on downstream molecules inhibit or initiate autophagy respectively. During optimal growth factor signalling, mTOR is activated by class I PI3K action upon phosphatidylinositol-3,4,5-triphosphate (PtdIns(3,4,5)P_3), and autophagy is inhibited(24), as illustrated in figure 1. Thus, inhibitors of mTOR or class I PI3K, such as

rapamycin and PTEN, respectively, induce autophagy. Under starvation conditions, however, class III PI3K positively regulates autophagy by producing phosphatidylinositol-3-phosphate (PtdIns3P), an essential molecule for the complex required for autophagy induction(25). Thus, PI3K inhibitors such as 3-methyladenine (3MA) and wortmannin are inhibitors of autophagy(26).

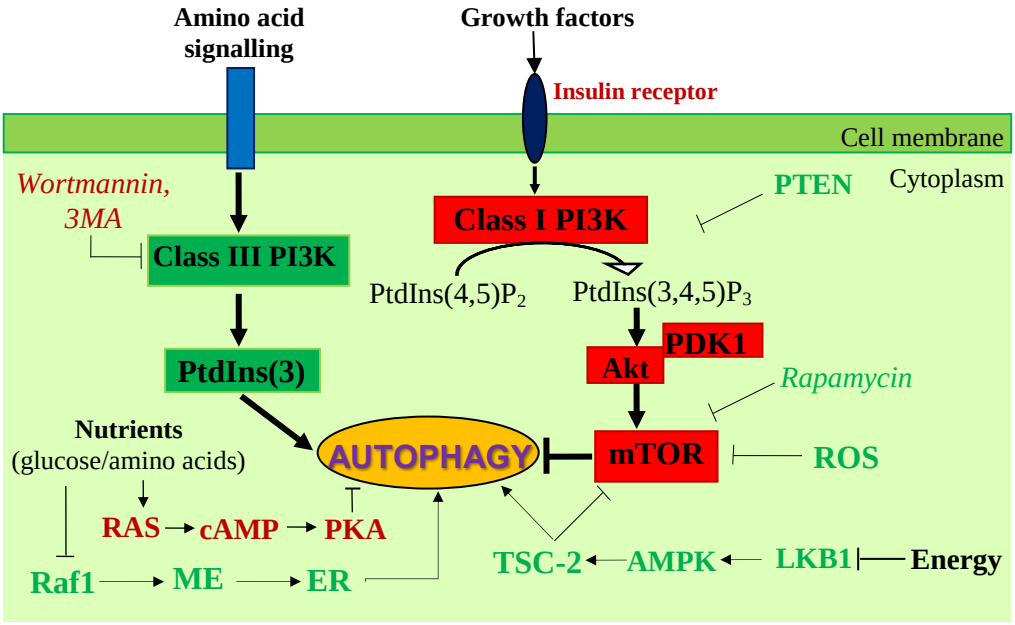

Figure 1 *– Autophagy is closely regulated by a variety of signalling pathways, responding to extra- and intra-cellular signalling. Red boxes highlight the inhibitory type I PI3K pathway, which consists of PtdIns(4,5)P_2 and PtdIns(3,4,5)P_3, phosphoinositide-dependent kinase (PDK1) and Akt (also known as protein kinase B), which phosphorylate a GTPase-activating protein for the protein Rheb (not shown), whose GTP form activates mTOR, resulting in the inhibition of autophagy. Other inhibiting pathways (in red) include nutrient signalling through the Ras/Protein kinase A (PKA) pathway and inhibitors of PI3K such as Wortmannin and 3MA. Green boxes highlight the major inducing pathway, via the type III PI3K, which produces PtdIns(3)P, an essential component of autophagosome formation. Other inducing pathways (in green) include nutrient-derived inhibition of ERK 1/2, ROS, Rapamycin, and decreases in cellular ATP which inhibit mTOR via the action of AMP-activated protein kinase (AMPK). Phosphatase and tensin homolog (PTEN) hydrolyses PtdIns(3,4,5)P_3 to PtdIns(4,5)P_2, counteracting the action of the type 1 PI3K pathway and inducing autophagy.*

In addition to class I and III PI3K activity, mTORC1 can be regulated by cellular energy changes through the AMPK/TSC pathway, and thereby control autophagy initiation(27). AMPK is a sensor of the AMP/ATP ratio within the cell and, during conditions of low

energy or metabolic stress, phosphorylates Tuberous sclerosis protein 2 **(**TSC-2), inhibiting mTOR or directly activating autophagy by phosphorylation of ULK1 (mammalian Atg1) and Beclin 1(mammalian Atg6)(27). Autophagy can also be regulated via the cAMP pathway, where elevation of intracellular cAMP levels is an inhibitor of autophagy through PKA activity(28).

1.4 The Mammalian Autophagy pathway

Initiation of autophagy requires stepwise recruitment of autophagy proteins into multi-protein kinase complexes. Cellular starvation induces phosphorylation of ULK1(29) and Atg13, allowing the formation of the ULK1-Atg13-FIP200 complex (FIP200 is mammalian Atg17(30)), which is essential for autophagosome development(31). Concomitantly, Beclin-1 associates with Atg14 and activated-type III PI3K (also called Vps34) to form a second essential kinase complex(32, 33). The membrane components required for autophagosome formation are recruited under the control of Atg9(34) to the pre-autophagosomal structure (PAS), where the isolation membrane is formed. Autophagic membranes are thought to originate from various sources, including mitochondria, Golgi, the plasma membrane and the endoplasmic reticulum (ER)(23, 35, 36). Elongation of the isolation membrane is mediated by two ubiquitin-like conjugation systems (Figure 1.2), through which Atg 12 is conjugated to Atg5(37), and LC3 (mammalian Atg8) is modified via a lipidation reaction with phosphatidylethanolamine (PE)(38). The C-terminal glycine residue (G_{140}) of Atg12 is coupled to a lysine residue of Atg5 by the action of the E1- and E2- like enzymes Atg7 and Atg10. This complex binds Atg16 and attaches to the exterior of the isolation membrane. In the second system, LC3 (Atg8) is cleaved of five C-terminal amino acids by Atg4, exposing a glycine residue (G_{120}) that is then transferred to PE,

catalysed by the E1- and E2- like enzymes, Atg7 and Atg3. The lipidation of LC3 causes a conformational change necessary for membrane formation(39).

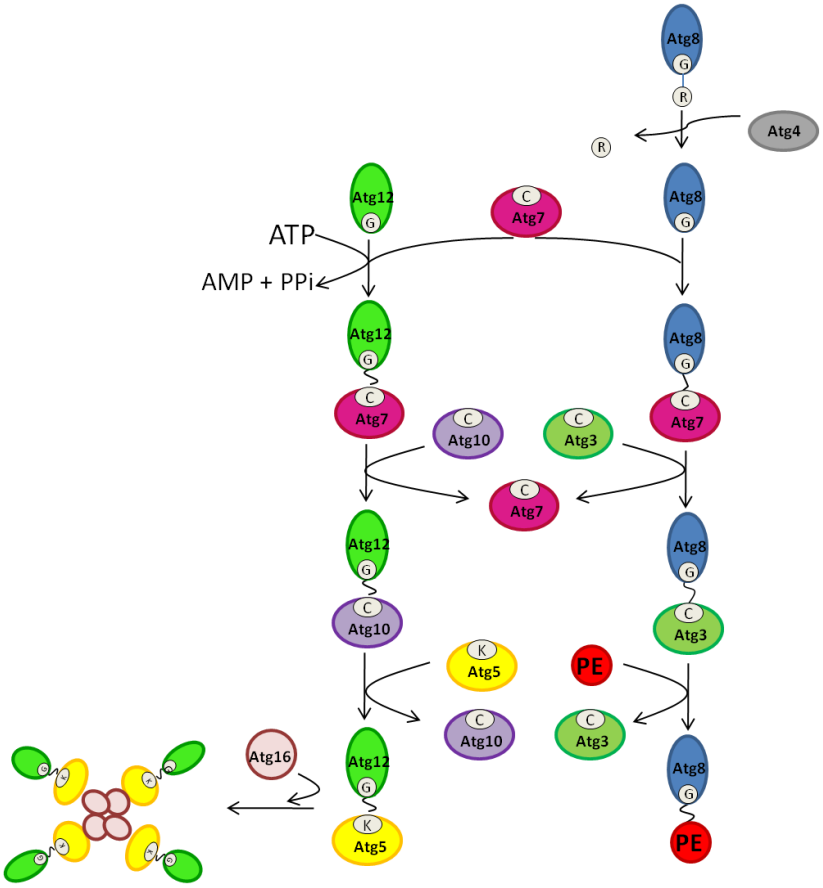

Figure 1.2 *– Two ubiquitin-like conjugation systems are essential for the formation of the autophagic membrane. Atg7, homologous to the E1 ubiquitin-activating enzyme, hydrolyses ATP to activate Atg12 through the formation of a thioester bond between the C-terminal glycine of Atg12 and the activated cysteine on Atg7. Activated Atg12 is then transferred to the active site of Atg10, an E2-like enzyme, which allows Atg5 to be conjugated to Atg12 by the formation of an isopeptide bond. Atg12-Atg5 is then complexed to Atg16, which then forms a tetramer to facilitate the construction of the multimeric complex. The Atg8-PE complex begins with the cleavage of the C-terminal arginine of Atg8 by Atg4, a protease. The resultant exposed glycine is bound to the active cysteine site of Atg7, and the activated Atg8 transferred to another E2-like enzyme, Atg3. Finally, Atg3 catalyses the conjugation of Atg8 to Atg8-PE. Both complexes facilitate vesicle formation at the pre-autophagosomal structure. Adapted from Ref. (40).*

Following autophagosome completion (figure 1.3), the Atg5-Atg12-Atg16 complex dissociates away and the LC3-PE complex is de-conjugated by Atg4. Atg8 remains bound to the internal membrane of the autophagosome where it is degraded. The exact function

of either complex is unknown, although it is postulated that the Atg5-Atg12-Atg16 complex may play a role in determining the curvature of the developing phagosome(41), whereas LC3 (Atg8) may form a membrane anchor for autophagy substrates(42).

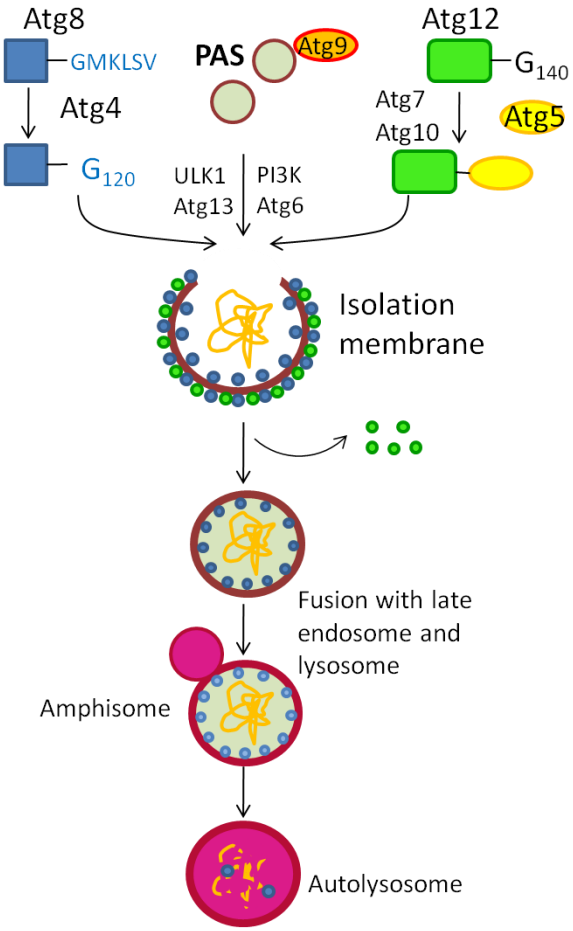

Figure 1.3 *– Schematic overview of autophagy. The Atg6-PI3K and Atg1 kinase complexes together initiate autophagosome formation in response to mTOR signalling. Two ubiquitin-like pathways give rise to the Atg8/LC3-PE and Atg5-Atg12-Atg16 complexes, which are integral in formation of the isolation membrane. Once the autophagosome is complete, the Atg5-Atg12-Atg16 complex recycles into the cytoplasm, whereas Atg8 remains associated with the internal membrane of the phagosome. The pathway is completed when the autophagosome fuses with late endosomes and lysosomes, and the internalised cargo is degraded.*

Once substrates have been fully packaged, the autophagosome undergoes a series of maturation steps, which may include fusion with endosomes to form the amphisome(43), and finally fuses with a lysosome to form the autolysosome, a process that involves

Rab7(44, 45). Once fusion is complete, the contents of the autolysosome are degraded and released into the cytoplasm for recycling.

1.5 Degradation substrates

In addition to its role in survival during starvation periods, autophagy functions to remove misfolded proteins or protein aggregates, and damaged organelles from the cytoplasm. Accumulation of abnormal proteins and organelles is a common feature in cells in which autophagy has been ablated or reduced(46, 47). Specific organelle degradation has also been observed, giving rise to the terms mitophagy (degradation of mitochondria), pexophagy (peroxisomes), ribophagy (ribosomes), ER-phagy (ER) and nucleophagy (nuclei)(48-52). Accumulation of damaged organelles or protein aggregates can cause serious cellular damage and contribute to the development of degenerative diseases such as Alzheimer's(12) and promote tumorigenesis(53). Accumulation of damaged mitochondria is also highly detrimental to cells, and can inhibit maturation and survival of red blood cells (RBCs) and T lymphocytes(54, 55).

1.6 Use of degradation products

One of the primary objectives of autophagy is to recycle amino acids from intracellular constituents during times of starvation. The recycled amino acids are then thought to be used in three ways. Firstly, during extended periods of starvation when carbohydrate stores have been consumed, gluconeogenesis occurs in the liver to generate further glucose, a process which requires amino acids(56). Secondly, amino acids are processed through the tricarboxylic acid (TCA) cycle into energy. Finally, amino acids generated through autophagy can be used for protein synthesis, which is vital for cellular adaption during starvation periods(56).

1.7 Thesis Summary: The role of autophagy in macrophage and neutrophil development and function

The aim of the research presented in this thesis was to investigate the role(s) of autophagy in the development and function of macrophages and neutrophils using a mouse model in which the essential autophagy gene, Atg7, was selectively deleted in the hematopoietic system. Loss of Atg7 in the hematopoietic system, among other symptoms, gives rise to a significant myeloproliferation characterised by increased numbers of macrophages and neutrophils in hematopoietic and non-hematopoietic tissues, many of which show signs of immaturity. Previous work in our lab had shown that this myeloproliferation was not leukemic in nature(57), and thus this work explores alternate hypotheses for increased immature myeloid burden in the tissues. The main focus of this work, however, was investigating the links between autophagy and normal macrophage and neutrophil function. This thesis presents novel roles for autophagy in normal macrophage biology and function, and uncovers a requirement for autophagy in normal neutrophil development. Furthermore, links between defective or reduced autophagy and altered immune function in aging are investigated, due to the known connections between autophagy and aging. The data described herein suggest that interventions involving modulation of autophagy in the immune system may be beneficial to prevent or improve altered innate immune function with aging, and suggest areas for future research into maintenance of autophagy levels during aging in the hope of retaining improved immune function in later life.

Chapter 2: Materials and Methods

2.1 Mice

All mice were bred and housed in the animal facilities at Biomedical Services Oxford. Mice were maintained in filter top cages under SPF conditions and fed *ad libitum*. $Atg7^{flox/flox}$ mice were obtained from M. Komatsu and vav-iCre mice were kindly gifted by D. Kioussis, London. Wildtype controls for each experiment were taken from $Atg7^{flox/flox}$; Cre^{-} , $Atg7^{flox/wt}$; Cre^{-} or $Atg7^{flox/wt}$; Cre^{+} littermate controls of the experimental $Atg7^{flox/flox}$; Cre^{+} mice, and were used interchangeably, as no phenotype was observed in the heterozygous mice. All mice were bred on a C57BL/6 background and all procedures were carried out in accordance with the Home Office Animals (Scientific Procedures) Act 1986 and as allowed under personal and project licences (PIL: 30/8801; PPL:30/2809). Experimental mice were used at 7 – 8 weeks of age unless otherwise specified.

2.2 Genotyping

DNA extraction and PCR

Mice were identified and genotyped by ear tissue samples. Small tissue sections were digested for 2 hrs at 55° C in lysis buffer (5mM EDTA, 0.1 M Tris-HCl, 0.2% SDS, 0.2 M NaCl and 7.8 mg/ml proteinase K [Sigma]) and solids pelleted by centrifugation (16000 × g, 10 min). Supernatant was transferred to a clean Eppendorf tube and DNA precipitated using an equal volume of isopropanol and gentle mixing by inversion. The resultant precipitate was pelleted (16000 x g, 10 min) and washed in 70% ethanol. Following air drying, the DNA was dissolved in 50µL MilliQ water and incubated at 65° C for 30 min to aid suspension. DNA samples were stored at -20° C.

All PCR reactions were carried out in a total volume of 20 µL, using MyTaq™ Red Mix combined PCR mix (Applied Biosystems, USA). Primers for the Cre and Atg7 flox transgenes were as follows:

iCre PCR

iCre-Fwd: 5'-AGATGCCAGGACATCAGGAACCTG-3'
iCre-Rev: 5'-ATCAGCCACACCAGACACAGAGATC-3'

Atg7 flox PCR

(WT fwd Primer) 752: 5'-CCATGCTGATGGCTAATGTCTC-3'
(Flox fwd Primer) 753: 5'-CTGCAGGAATTCGATATCATAACTTCG-3'
(Reverse Primer) Atg7-14R: 5'-GTCCAGAGTCCGGTCTCTGGTTG-3'

DNA was amplified under the following conditions:

1. 95° C, 1 min
2. 95° C, 15 sec
3. 55° C, 15 sec
4. 72° C, 10 sec
5. 30× cycles from step 2
6. Hold at 4° C

Amplified DNA was analysed on a 2% agarose gel (Invitrogen), prepared in 50 ml 1× TBE buffer (45 mM Tris-Borate, 1mM EDTA, stained with 5 µL SYBR® Safe DNA Gel Stain [Invitrogen, Life Technologies]). Gels were run at 70 V for ~35 min until the bands were sufficiently separated.

2.3 Preparation of Primary Cells

Bone Marrow-Derived Macrophages

Bone marrow-derived macrophages (BMMϕ) were obtained by crushing hind limb bones from 6 – 9 week old mice in PBS/5% FCS. The bone marrow suspension was filtered through 70 µm cell strainers (BD Falcon) and counted by Trypan Blue (Sigma) exclusion.

Macrophages were cultured in RPMI 1640 (Invitrogen) supplemented with FCS (10%), glutamine, penicillin, streptomycin and 20 ng/ml recombinant murine M-CSF (Peprotech). Cultures were maintained at 37° C/5% CO_2 and fed 50% of the initial volume of media on the third day after plating. Macrophages were stimulated on day 7 as described in the relevant figure legends. Macrophages were identified in all flow cytometry experiments as $F4/80^{+}CD11b^{+}$ double positive cells. An example of the gating strategy for identifying macrophages is shown below (figure 1):

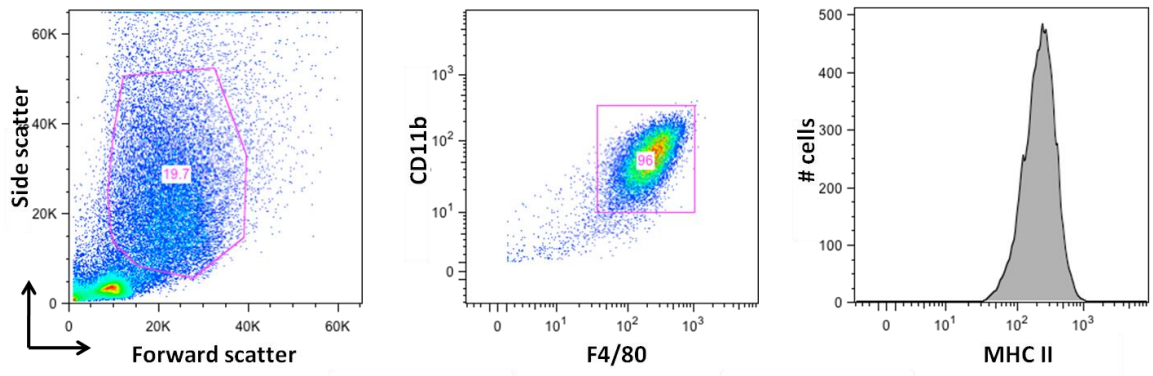

Peritoneal Macrophages

Unstimulated macrophages were harvested by injection of 5 ml of PBS/5% FCS into the peritoneal cavity using a 19 gauge needle, gentle massage to dislodge cells and recovery of 4 ml of injected solution. Recovered cells were placed on ice, washed with 5 ml PBS/5% FCS and either used immediately or cultured at 37° C overnight in R10, supplemented with 20 ng/ml M-CSF.

Splenic Macrophages

Spleens were harvested in PBS/5% FCS and maintained on ice until use. A single cell suspension was created by gentle disruption through a 70 μM filter using the blunt end of a syringe, with frequent rinses of PBS/5% FCS (approximately 10 ml). Cells were washed in 10 ml PBS and centrifuged at 1000× g to pellet for 5 min. The supernatant was

removed and replaced with 1 ml 1× RBC Lysis buffer (eBioscience), and incubated at room temperature for 5 min. The lysed cells were washed in a further 10 ml of PBS/5% FCS, re-suspended in R10 supplemented with 10 ng/ml M-CSF and macrophages were allowed to adhere to the culture dish overnight at 37° C. The following day, non-adherent cells were rinsed away with ice cold PBS, and the splenic macrophages harvested with ice-cold PBS/FCS/0.1M EDTA.

Neutrophils

Neutrophils were harvested from the peritoneal cavity in the same manner as described above for macrophages. Neutrophils were isolated *ex vivo* from bone marrow by producing a single cell suspension in the same manner described above for BMMϕ, and used immediately for flow cytometry, or stimulated overnight as described in relevant figure legends. Blood neutrophils were also used in several experiments. Blood was collected in heparinized tubes from heart puncture following euthanasia, and centrifuged at 1000× g to pellet the cells. RBCs were lysed with 1 ml of 1× RBC Lysis buffer (eBioscience) at room temperature for 5 min and washed in a further 10 ml of PBS/5% FCS prior to being stained for analysis.

MACS enrichment

Magnetic cell labelling was used to positively enrich peritoneal exudates or bone marrow suspensions for macrophages or neutrophils. Macrophages were collected as described above, pelleted by centrifugation (300 × g, 10 min), and the supernatant discarded. The cell pellet was re-suspended in 90 µL of MACS buffer (PBS pH 7.2, 0.5% BSA and 2 mM EDTA) to which 10 µL of anti-F4/80 PE (eBioscience) antibody was added, and incubated for 15 min at 4° C. This was followed by 20 µL anti-PE MicroBeads (Miltenyi Biotech), and further 10 min incubation. The cells were then washed in 2 ml of buffer, the

supernatant was removed and discarded, and the cell pellet was suspended in 500 µL of buffer. An MS separation column (Miltenyi Biotech) was placed in the separation magnet and rinsed with 500 µL of MACS buffer prior to the addition of the cell suspension to the column. After the cells had passed through the column, the column was rinsed 3× with 500 µL MACS buffer and the unlabelled cell fraction collected and kept on ice. Labelled macrophages were then collected by removing the column from the magnet and flushing with 1ml of buffer and depressing the syringe firmly. Bone marrow neutrophils were enriched in a similar manner using anti-Ly6g MicroBeads (Miltenyi Biotech).

2.4 qPCR

RNA extraction

Cells were pelleted (16000×g, 15 min) and supernatant discarded before re-suspension in 1ml Trizol reagent (Invitrogen) per 3×10^6 cells. Cells were allowed to lyse for 2 hrs or overnight. 200 µL of chloroform/isomyl (49:1) (Fluka) was added to each tube and mixed by inversion. Phases were separated by centrifugation (16000 × g, 15 min, 4° C) and the aqueous phase transferred to a fresh Eppendorf tube before precipitation with 500 µL of isopropanol. Following 15 min of incubation at room temperature, RNA was pelleted (16000 × g, 15 min, 4° C) and washed in 200 µL ice cold 70% ethanol. The pellet was allowed to air dry, prior to re-suspension in 10 – 20 µL DEPC-H_2O (Invitrogen). RNA concentration and quality was determined using a NanoDrop spectrophotometer (Thermo Scientific USA). Samples were stored at -80° C.

Reverse Transcription

RNA was reverse transcribed to cDNA using a High Capacity RNA to cDNA kit (Applied Biosystems). All reactions were completed in 20 µL (9 µL RNA, 1 µL RT Enzyme Mix

[20×] and 10 µL RT Buffer Mix [2×]) per tube. Reactions were incubated at 37° C for 1 hr, followed by 5 min at 95° C, and finished with 10 min at 4° C. Transcribed cDNA was stored at -20° C until analysis by qPCR.

Real-time qPCR

The comparative Ct ($\Delta\Delta C_T$) method was used to evaluate relative gene expression in wildtype and $Atg7^{-/-}$ macrophages and neutrophils under different conditions. Validated TaqMan primer probes (Applied Biosystems) were used for all reactions (Table 1). Quantitative PCR reactions were carried out in a total of 20 µL (9 µL reverse transcribed RNA, 10 µL TaqMan® Gene Expression Mix [Applied Biosystems] and 1 µL of the relevant 20× TaqMan probe) in 96 well MicroAmp® reaction plates (Applied Biosystems) sealed with MicroAmp Optical Adhesive Film (Applied Biosystems). Reactions were completed in standard mode of a 7500 Fast Real-time PCR system (Applied Biosystems). Cycling conditions were as follows:

1. 50° C, 2 min
2. 95° C, 10 min
3. 95°, 15 sec
4. 60° C, 1 min
5. 40× cycles from step 3.

***Table 1**: List of TaqMan probes used in qPCR experiments:*

Gene	TaqMan Gene Expression Assay ID	RefSeq
Atg7	Mm00512209_m1	NM_028835.3
Gapdh	Mm99999915_g1	NM_008084.2
Atg6	Mm01265461_m1	NM_019584.3
Atg5	Mm01187300_m1	NM_053069.5
TLR4	Mm00445273_m1	NM_021297.2
M-CSFR	Mm01266652_m1	NM_001037859.2
HIF-1α	Mm00468869_m1	NM_010431.2

Nrf2	Mm00477784_m1	NM_010902.3
SOCS3	Mm00545913_s1	NM_007707.3
Cepbε	Mm02030363_s1	NM_207131.1
H2-Ab1 (MHC II)	Mm00439216_m1	NM_207105.2
MMP9	Mm00442991_m1	NM_013599.2
Lactoferrin	Mm00434787_m1	NM_008522.3
MPO	Mm01298424_m1	NM_010824.2

2.5 Flow Cytometry and Image Stream Analysis

Surface markers

Macrophages were harvested by removing the incubation media, replacing with cold FACS buffer (PBS, 5% FCS and 0.2% azide) and gently pipetting up and down to dislodge the cells. Cells were then transferred to the appropriate wells of a round-bottomed 96 well plate for staining and analysis, and centrifuged (1500 × g, 5 min) to form pellets. The supernatant was discarded. Pellets were re-suspended in 50 µL of the relevant antibody mix and the plate was covered in foil before incubation for 20 min at 4° C on a shaker. Following incubation, each pellet was washed with 250 µL of FACS buffer and centrifuged at 1500 × g for 5 min. Cells that were to be analysed immediately were re-suspended in FACS buffer and transferred to FACS tubes or small Eppendorf tubes as appropriate. Cells to be analysed at a later date were re-suspended in 300 µL of FACS fixation solution (PBS, 2% paraformaldehyde and 1% FCS) and kept at 4° C, protected from light with foil. Table 2 lists the antibodies and other reagents used for experiments.

***Table 2** – Reagents used for flow cytometry analysis*

Antibody	Flurochrome Or Ex/Em	Supplier	Experimental Dilution
Annexin V	PE	BD Biosciences	1:1000
Annexin V binding buffer	N/A	BD Biosciences	1×
Anti-caspase 3	FITC	BD Biosciences	1:20
Anti-goat IgG	Alexa fluor 488	Invitrogen	1:500
Anti-mouse CD11b	eFluor450	eBioscience	1:400
Anti-mouse CD11b	FITC	eBioscience	1:200
Anti-mouse CD13	FITC	AbD Serotec	1:50
Anti-mouse CD14	APC	eBioscience	1:400
Anti-mouse CD47	FITC	eBioscience	1:100
Anti-mouse CD48	PE	eBioscience	1:200
Anti-mouse CD62L	PE-Cy7	eBioscience	1:400
Anti-mouse CD86	PE	eBioscience	1:200
Anti-mouse CXCR4	PE	eBioscience	1:300
Anti-mouse F4/80	APC	eBioscience	1:400
Anti-mouse F4/80	PE-Cy7	eBioscience	1:400
Anti-mouse Fc Receptor II/III (CD16/32)	PE	eBioscience	1:200
Anti-mouse G-CSF	APC	eBioscience	0.75 µL/well
Anti-mouse GM-CSF	FITC	eBioscience	1 µL/well
Anti-mouse Gr1	PE-Cy7	eBioscience	1:400
Anti-mouse IL-10	PE	eBioscience	1 µL/well
Anti-mouse IL-12	eFluor450	eBioscience	1 µL/ well
Anti-mouse IL-6	FITC	eBioscience	1 µL/ well
Anti-mouse iNOS	PE	eBioscience	1:200
Anti-mouse Lactoferrin	Unlabelled	Santa Cruz biotech	1:500
Anti-mouse Ly6g	PE-Cy7	Biolegend	1:400
Anti-mouse Ly6g	FITC	Biolegend	1:200
Anti-mouse Ly6g	Pacific blue	Biolegend	1:100
Anti-mouse M-CSFR	PE	eBioscience	1:200
Anti-mouse MHC I	FITC	eBioscience	1:100

Anti-mouse MHC II	PE	eBioscience	1:200
Anti-mouse MHC II	APC	eBioscience	1:400
Anti-mouse MIP1α	PE	eBioscience	0.75 µL/well
Anti-mouse MR	Alexafluor 647	Biolegend	1:400
Anti-mouse NGAL	Unlabelled	Santa Cruz biotech	1:500
Anti-mouse TLR 4	PE	eBioscience	1:200
Anti-Mouse TNFα	PE-Cy7	eBioscience	0.75 µL/well
Draq5	652/675 nm	Cell Signaling Technology	1:1000
Fixable live/dead stain	Violet 1	Invitrogen	1:1000
Fixation and permeabilisation kit	N/A	eBioscience	
Latex beads	FITC	Invitrogen	1 µg/ml
Nile Red	552/636 nm	Invitrogen	1 µM
Streptavidin	PE-Cy7	eBioscience	1:200

Intracellular Staining

After staining cell surface molecules as above, cells were fixed with 100 µL Fixation buffer (eBioscience) and incubated in the dark for 20 min at room temperature. Cells were permeabilised with 100 µL of 1× Permeabilisation buffer (eBioscience) diluted in distilled water and pelleted by centrifugation at 1500 × g for 5 min. The cells were re-suspended in the intracellular antibody mix diluted in permeabilisation buffer and incubated for >60 minutes in the dark at room temperature. Cells were washed twice with 100 µL of permeabilisation buffer prior to re-suspension in 300 µL of FACS buffer for analysis. Unstained cells and cells, beads or a mixture of cells and beads stained with a single colour were used to set up the flow cytometer (Dako Cyan) in each experiment. Data were analysed using FlowJo 9.0 and Graphpad Prism software.

ImageStream

Cells for analysis by ImageStream (Amnis Corporation, Seattle) were stained for surface and intracellular markers as described in the protocols above. Unstained cells and cells, beads or a mixture of cells and beads stained with a single colour were used to set up the ImageStream prior to each experiment. Samples were run with the aid of Kanchan Phadwal, Sharon Sanderson and Anne Hansen.

Phagocytosis Assay

Bone marrow or peritoneal macrophages were prepared as described above and maintained at 37° C/5% CO_2. Green fluorescent latex beads (Invitrogen) were added to macrophages at a concentration of (1 μg/ml), approximately 1μL/well in a 12 well plate, with or without LPS (1 μg/ml) and the macrophages incubated overnight. The following day, macrophages were harvested as described above, and any beads present on the surface of the macrophages quenched with 2.5 μL of 0.4% Trypan Blue (Invitrogen) diluted in PBS. Macrophage surface markers were stained as described above and latex bead uptake was measured by flow cytometry.

2.6 ELISA

eBioscience ELISA Ready-SET-Go!® kits were used to detect IL-1β, TNF-α, IL-10, 1L-12 and IL-6 in the supernatant of macrophage cultures. Briefly, 50 μL capture antibody was incubated overnight at 4° C in Corning Costar 9018 ELISA plates. Wells were aspirated and washed 5× with 300 μL/well of wash buffer (PBS, 0.05% Tween-20) with 1 minute of soaking between washes, blocked with 1× assay diluent (eBioscience) for 1 hr at room temperature, followed by a further 5 washes. Standards were diluted according to the relevant certificate of analysis and added in duplicates of 2-fold serial dilutions

(50 µL/well) to produce a standard curve. Supernatant was added to remaining wells in duplicate at 50 µL/well and the plate incubated at 4° C overnight. The following day, wells were aspirated and the plate washed 5× with wash buffer and blotted on paper towel. The detection antibody was diluted in 1× assay buffer and 50 µL added to each well, followed by 1 hr of incubation at room temperature. After a further 5 washes, 50 µL of Avidin-HRP was added to each well and the plate incubated at room temperature for 30 min. Prior to development, the plate was washed a total of 7× in wash buffer, with 2 min of soaking between each wash. Finally, 50 µL of substrate was incubated in each well for 15 min and the colourimetric reaction stopped with 50 µL of stop solution (H_2SO_4). The plate was read at 450 nm (Bio-Rad microplate reader, model 690), with wavelength 595 nm subtracted and the results analysed using Excel.

2.7 Griess Assay

Nitrite concentration in the medium was analysed as an indicator of NO production, using the Griess reaction. Sample supernatant (25 µL) was added to Sulfanilamide Solution (50 µL) in appropriate wells of a 96 well plate and incubated for 10 min at room temperature, as per kit instructions (Promega). 50 µL of NED solution was added to each well, and incubated a further 10 min in the dark before reading at 550 nm on a plate reader. Nitrite concentration was then determined based on a standard curve.

2.8 Glucose Assay

Glucose uptake was measured using a serum glucose kit based on glucose oxidase (Sigma). Supernatant samples from macrophage cultures were harvested following overnight LPS stimulation and stored at -20° C prior to analysis. Samples were diluted 1:25 to bring their estimated glucose concentration to within the optimal testing range of

20 – 80 µg/mL (R10 has a starting glucose concentration of 2 mg/ml), and added to appropriate wells of a 96 well plate in triplicate. D-glucose standards were prepared at a range of 0 – 150 mg/ml in deionized water and added to the plate in triplicate. o-Dianisidine reagent was added to the glucose oxidase/peroxidase reagent as described in the protocol to give the working reagent, and also added to each of the standards and samples at 100 µL/well, followed by incubation at 37° C for 30 min. 100 µL of 12 N sulphuric acid solution was added to each well to stop the colour change reaction, and the absorbance at 540 nm recorded using a plate reader. Sample glucose concentrations were calculated using a standard curve and used to determine the proportion of glucose taken up by the macrophage cultures. Values were normalized to cell number by analysis of protein content of the cells in each culture sample well.

2.9 Myeloperoxidase Assay

Neutrophils were harvested as described above and adjusted to a concentration of 2.5×10^7/ml. Myeloperoxidase release was assessed by addition of 25 µL of cell suspension to appropriate wells of a 96 well plate in triplicate in 75 µL R10 ± LPS (1 µg/ml), and incubation at 37° C/5% CO_2 for 30 min. 50 µL of TMB (eBioscience) and 50 µL H_2O_2 (5 mM) were added to each well and the colour change reaction allowed to proceed for 5 min at RT prior to addition of 50 µL sulphuric acid (2 M). Total myeloperoxidase content was assessed in the same manner, with the addition of 25 µL of 0.5% Triton-X 100 (Sigma) following incubation. The plate was read at 405 nm, and relative MPO concentration assessed by comparison of average absorbencies.

2.10 Electron Microscopy

Bone marrow-derived macrophages were harvested and washed with PBS as described above prior to being stained with F4/80 PE (eBioscience) and labelled with anti-PE magnetic beads (Miltenyi). Labelled macrophages were then isolated using a MACS column (Miltenyi) as described above, and fixed for electron microscopy. Bone marrow neutrophils were harvested as described above, and stained for the neutrophil markers Gr1 and CD11b for sorting by flow cytometry. Sorted $Gr1^{+}CD11b^{+}$ cells were then fixed and analysed by electron microscopy. Image collection was kindly carried out by Professor David Fergusson.

2.11 Light Microscopy

Macrophages or neutrophils were harvested and cultured as described above. For some experiments, macrophages and neutrophils were allowed to adhere to Poly-L-lysine (Invitrogen) coated slides by pipetting 100 µL of cells directly onto slides and incubating at 37° C for 2 hrs or until sufficiently adhered. In other experiments, myeloid cells were adhered to slides by cytospinning. Cells were prepared as required, harvested and diluted to a concentration of 1×10^{6} cells/ml in PBS/5% FCS. 100 µL of the required cells were added to a cytospin chamber, and the cells adhered to the slides for 3 min at 900 rpm. Slides were allowed to dry, then stained with Differential Quik Stain (Modified Giemsa, Polysciences, USA), mounted in DPX (Sigma Aldrich) and analysed by light microscopy (Zeiss Axiovert S100 inverted microscope or Zeiss Axioskop Upright with Q imaging camera). Some macrophage cultures were also analysed direct in their culture dishes with no slide preparation.

2.12 Confocal Microscopy

Macrophages were grown on coverslips, rinsed 3× with PBS and fixed with 500 µL IC Fixation Buffer (eBioscience) for 30 minutes in the dark at RT. Wells were washed twice with 300 µL 1× Permeabilisation Buffer (perm buffer) (eBioscience) and all liquid removed by careful pipetting. Primary antibodies were diluted in 300 µL/well 1× perm buffer, and incubated with the cells for 1 hr at RT, no shaking. Wells were rinsed twice with perm buffer prior to incubation with secondary antibodies. Secondaries were diluted in 500 µL 1× perm buffer, and incubated on the cells for 30 – 60 min in the dark. Stained coverslips were then washed and mounted as above. Slides were viewed on a Zeiss 510 Inverted Confocal Microscope, and images produced using Fiji software. Stained slides were stored at 4° C for short periods, or -70° C for long term storage. Antibodies used for confocal are listed in table 3.

***Table 3**: Antibodies used in confocal experiments*

Antibody	Supplier	Dilution
Rabbit α-LC3	Kind gift from Christian Munz	1:500
Phalloidin Alexa Fluor 488	Invitrogen Life Technologies	1:500
Rabbit α-Prxn1	Sigma	1:500
Anti-Rabbit IgG 488	Invitrogen Life Technologies	1:500
Anti-Rabbit 568	Invitrogen Life Technologies	1:500

2.13 Protein Extraction

Macrophages or neutrophils were stimulated as required and harvested or cultured as described above. Cells were washed twice in ice cold PBS to remove any residual culture medium, harvested in ice cold PBS into Eppendorf tubes and centrifuged at 1000 × g to pellet the cells. The supernatant was removed and cells suspended in 500 µL RIPA buffer

(Sigma Aldrich) per 5×10^6 cells, supplemented with 1 cOmplete Protease Inhibitor Cocktail Tablet (Roche) per 10 ml RIPA buffer. Cell membrane rupture was aided by vigorous pipetting, and tubes incubated on ice for 5 – 10 min. Protein samples were centrifuged at 16000 × g for 15 minutes to remove debris, and the resultant supernatant transferred to a clean tube. Where required, protein samples were concentrated using Microcon® Centrifugal Filters Spin Columns (Millipore). Up to 500 µL protein was added to the filter, placed in the collection tube and centrifuged at 10000 × g for 10 min. The filtrate was discarded, and the concentrated protein collected by inverting the filter into a clean tube and centrifuging for 5 min at 1000 × g. Protein samples were stored at -70° C.

2.14 Protein Quantification

Protein extracts were quantified using the BCA assay. Standards were prepared by appropriate dilution of a 2 µg/ml BSA aliquot (Thermo Scientific), and added in triplicate to a 96 well plate. Protein samples were diluted as required and 25 µL of each sample added to the plate in triplicate. An appropriate volume of working solution was prepared by mixing sufficient volumes of reagent A and reagent B (Thermo Scientific BCA Protein Assay Kit) in a ratio of 50:1 to allow 200 µL of working solution per sample and standard. 200 µL of working solution was added to each well of the plate by multichannel pipette, and the plate was incubated at 37° C for 30 min before reading absorbance at 562 nm. Protein concentration in samples was determined using a standard curve.

2.15 Proteomics

BMMϕ were cultured as described above and washed twice in PBS to remove any media. Cytoplasmic extracts were obtained by addition of 1 ml M-PER® Mammalian Protein Extraction Reagent (Thermo Scientific) to each sample and vigorously pipetting to disrupt

cell membranes. Protein concentration determined by BSA Assay as described above, and samples adjusted to the same concentration with further M-PER. Sample analysis by tandem mass spectrometry and assessment of the relative quantitation of identified proteins were performed as described previously(58). Mass Spectrometry and sample analysis was done in collaboration with Dr Benedikt Kessler.

2.16 Seahorse Analysis of Peritoneal Macrophages

Murine peritoneal macrophages were harvested as described above, washed in PBS/5% FCS and live cells enumerated by Trypan Blue exclusion. Following counting, cell concentration was adjusted to 1×10^6 cells/ml in R10 to allow plating of 2×10^5 cells/well of a XF24 Cell Culture Microplate (Seahorse Bioscience), the required volume to allow a close monolayer of macrophages to form. Macrophages were plated (10 replicates each of wildtype and $Atg7^{-/-}$ macrophages) in 300 μL/well R10 medium supplemented with 10 ng/ml M-CSF and incubated for 48 hr at 37° C/5% CO_2 to allow macrophage adherence and apoptosis of any contaminating neutrophils. Immediately prior to the experiment, 200 μL of media were removed from each well and gently replaced by 900 μL of un-buffered DMEM. A further 2 exchanges of 900 μL/well un-buffered DMEM (supplemented with Glutamax 200 mM (Gibco) and Sodium Pyruvate 100 mM [Sigma]) were very gently undertaken to completely remove any traces of previous media, followed by a final addition of 575 μL DMEM to give a total volume of 675 μL in each well. The plate was allowed to equilibrate for 30 min at 37° C in the absence of CO_2 and then loaded onto a XF24 XF Seahorse analyser (Seahorse Bioscience, Billerica, MA, USA). Rates of glycolysis and oxidative phosphorylation were determined by measuring lactic acid release (extracellular acidification rate, ECAR) and oxygen consumption rate (OCR) following sequential addition of Oligomycin (400 nM), FCCP (400 nM) and Rotenone (1 μM).

Seahorse experiments were carried out with the assistance of Professors Marion MacFarlane and Kelvin Cain, Leicester University.

2.17 Antigen Presentation Experiment

BMMϕ were generated from male mice, as described above. Male DCs were used as a positive control and were derived using GM-CSF and IL-4 (both at 20 ng/ml), in the same manner as the macrophages. Wildtype male macrophages, DCs and $Atg7^{-/-}$ macrophages (1×10^6 cells per mouse) were harvested on day 7, washed in PBS and injected into female recipients via the tail vein. The response was then boosted via vaccinia-UTY injection 7 days later, and antigen response analysed via tetramer specific anti-UTY CD8+ T-cells. Blood (50 μL) was harvested from each vaccinated mouse and RBCs lysed with RBC lysis buffer (eBioscience). Cells were stained with anti-mouse CD19, anti-mouse CD8 and UTY-tetramer (kind gift from Mariolina Salio), followed by streptavidin PE-Cy7. $CD19^{neg}CD8^{+}$ UTY-tetramer positive cells were identified by flow cytometry(59).

2.18 Statistics

Statistics were calculated using GraphPad Prism software. The specific statistical test applied to each experiment and the values for significance are given in the figure legends.

Chapter 3: Introduction

Autophagy influences innate macrophage functions

3.1 Autophagy in the immune system

Autophagy was originally thought to be solely a degradation mechanism for internal proteins and organelles. However, the discovery that autophagy can engulf and degrade intracellular bacteria opened a new avenue of investigation for autophagy as an active participant of the immune system. Autophagy has since been shown to participate in many aspects of both innate and adaptive immunity, including pathogen resistance, lymphocyte development and tolerance, regulation of inflammation, and antigen presentation (figure 3.1).

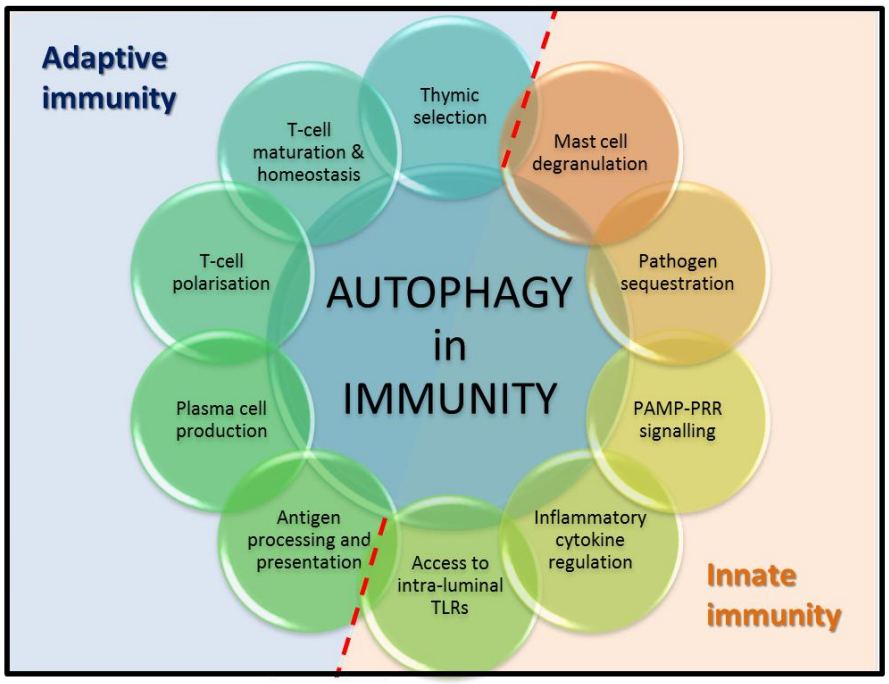

Figure 3.1 *– The roles of autophagy in the innate and adaptive immune systems. Autophagy can sequester and destroy intracellular bacteria, influence the inflammatory response and aid in the activation of the adaptive immune response by signalling through Toll-Like Receptors (TLRs) and other Pattern Recognition Receptors (PRRs) in response to Pathogen Associated Molecular Patterns (PAMPs). Autophagy also influences the function of some immune cells, such as mast cell degranulation. In the adaptive immune system, autophagy is vital to the development, selection and homeostasis of lymphocytes, and in the processing and presentation of peptide antigens in antigen-presenting cells (APCs).*

3.2 Immune signalling regulates autophagy

Signalling via bacterial or viral products and immune cell-derived cytokines can regulate autophagy, either activating or dampening the autophagic response depending on the requirements of the immune response or the invading pathogen. Activation of PRRs through signalling via PAMPs or DAMPs has been shown to activate autophagy, possibly as a mechanism of pathogen clearance from the cytoplasm and initiation of peptide production for antigen presentation. TLR4 signalling induces ubiquitylation of Beclin 1 through TNF receptor-associated factor 6 (TRAF6)(60), activating ULK1 and thus autophagy. Induction of autophagy by TLR9 following stimulation with CpG-rich DNA has also been reported(61).

NOD-like receptors (NLRs) also participate in autophagy signalling, recruiting Atg16-like 1 (Atg16L-1) to the site of bacterial entry, in reaction to signalling via NOD1 and 2(62). In contrast to TLRs and NLRs, signalling through Rig-Like Receptors (RLR) appears to negatively regulate autophagy(63). However, molecules downstream of RLRs potentially have an RLR-independent function in autophagy induction. Sensing of nucleic acid downstream of RLRs causes STimulator of IFN Genes (STING)-mediated activation of type I IFN production, but can also induce autophagy. Indeed, infection with double-stranded DNA viruses, such as herpes simplex virus 1 (HSV1), induces autophagy in a STING-dependent manner(64).

Reactive oxygen species (ROS) are important effectors and signalling molecules of the immune system, which can also regulate autophagy(65). NADPH oxidase, a ROS generator, interacts with the autophagy regulatory protein RUBICON (run domain Beclin 1-interacting and cysteine-rich-containing protein), thereby activating two antibacterial mechanisms (autophagy and ROS production)(66). Conversely, nitric oxide (NO), another

ROS, acts as an autophagy inhibitor by inactivating Jun N-terminal kinase 1 (JNK1) and IKKβ, and inhibiting AMPK-dependent autophagy initiation(67).

Inflammatory cytokines, such as IL-1β, can also induce autophagy. IL-1β signals through the IL-1 receptor, resulting in the recruitment of TRAF6, activation of beclin-1 and, thereby, autophagy(60). T-helper cell type 1 (T_H1) cytokines such as IFNγ also induce autophagy, potentially also through phosphorylation of Beclin-1(68). Similarly, TNF-α can stimulate autophagy as a protective mechanism against intracellular bacterial infection(69). In contrast to T_H1 cytokines, T_H2 cytokines are suppressors of autophagy. During periods of starvation, IL-4, IL-13 and IL-10 can all stimulate AKT signalling(70, 71), which suppresses autophagy.

3.3 Autophagy and adaptive immunity

Autophagy plays a significant role in the adaptive immune system, affecting the development and maintenance of lymphocytes and the processing and presentation of peptide antigens (discussed in more detail in 3.5). T-cells undergo low levels of constitutive autophagy, but upregulate it strongly following TCR interaction or infection with certain viruses(72, 73). Autophagy is required for the survival of activated lymphocytes, as Atg5 or Atg7-deficient T-cells cannot proliferate or effectively remove mitochondria on exit from the thymus(55). Autophagy also regulates T-cell metabolism, with inhibition of autophagy blocking the expected increase in ATP production following TCR stimulation(74), and influences T-cell selection in the thymus. Thymic epithelial cells from $Atg5^{-/-}$ thymi gave rise to an altered selection of MHC II-restricted T-cell specificities, which in turn resulted in colitis and general inflammation(75, 76).

Whereas T-cells develop normally in the absence of autophagy, B-cells require autophagy to progress past the pro-B stage(77). Mice with a haematopoietic-specific deletion of Atg7

have significantly reduced numbers of peripheral B-cells(54), while mice that lack Atg5 specifically in the B-lineage showed a particular requirement for autophagy in B-1a B-cell homeostasis, and in normal plasma cell function(78). Autophagy levels also differ according to T-cell polarisation, with Th2 cells found to be more resistant to autophagic cell death(79). Autophagy is induced in B-cells upon ligation of the B-cell receptor but inhibited upon co-receptor stimulation, preventing apoptosis of the B-cell whilst maintaining tolerance(80). Autophagy is fundamental to the survival, function and proliferation of lymphocytes, albeit with slightly different roles in each subset.

3.4 Autophagy in innate immunity

Autophagy plays a major role in the induction and regulation of the innate immune system, and has specialised roles within various innate cells, including macrophages. As discussed above, autophagy is connected to TLR-mediated macrophage activation, with LPS signalling via TLR4 known to induce autophagy(21, 81), as does signalling through other TLRs(82). Furthermore, autophagy aids recognition of viruses by facilitating delivery of viral peptides to intra-luminal TLRs, where they are able to induce type-1 interferon-based responses(83).

Autophagy is also vital in the defence against intracellular bacteria. Uptake of cytosolic bacteria during autophagy is facilitated by a central adaptor protein called p62 (also SQSTM1), which recognises bacteria and links them to LC3-positive phagophores(84). Autophagy mediates clearance of intracellular pathogens, such as *Listeria monocytogenes*(85), extracellular bacteria in the host cytoplasm, such as Group A *Streptococcus*(86), and bacteria that disrupt phagosome maturation, such as *Mycobacterium tuberculosis*(87). However, some bacteria have evolved to avoid clearance

by autophagy or to use it to their replicative advantage, such as *Brucella abortus*(88), *Chlamydia trachomatis*(89) and *Legionella pneumophila*(90).

The phagocytic pathway has also been linked to the autophagic pathway, though the exact manner in which autophagy and phagocytosis are linked is controversial. Autophagy during macrophage development has been shown to be required for acquisition of phagocytic functions(91), and autophagy machinery is linked to phagocytosis through its connection to TLR signalling(92). However, other researchers have provided evidence that autophagy negatively regulates phagocytosis, as autophagy induction inhibits phagocytic capacity(93). Furthermore, macrophages lacking Atg7 accumulated greater numbers of *M. tuberculosis*, due to increased expression of scavenger receptors(94). It has been proposed that autophagy may regulate levels of phagocytosis via participation in a negative feedback loop, such that accumulation of intracellular bacteria sends signals to halt further internalisation of bacteria(95).

In neutrophils, autophagy is important in the formation of neutrophil extra-cellular traps (NETs). NETs are made up of extracellular chromatin released by neutrophils during a specialised type of cell death called NETosis, and act by trapping and facilitating destruction of bacteria(96). PMA-induced NETosis is severely inhibited when autophagy is blocked using the autophagy inhibitor Wortmannin(97).

Mast cell degranulation, a cause of anaphylaxis, also requires autophagy(98). Autophagy has been shown to be constitutively induced in mast cells even under full nutrient conditions, with LC3 localising to secretory vesicles(99). However, mast cell development was not adversely affected in the absence of autophagy. Autophagy has no known specialised roles in basophils and eosinophils. A summary of known roles of autophagy in myeloid cells can be seen in figure 3.2.

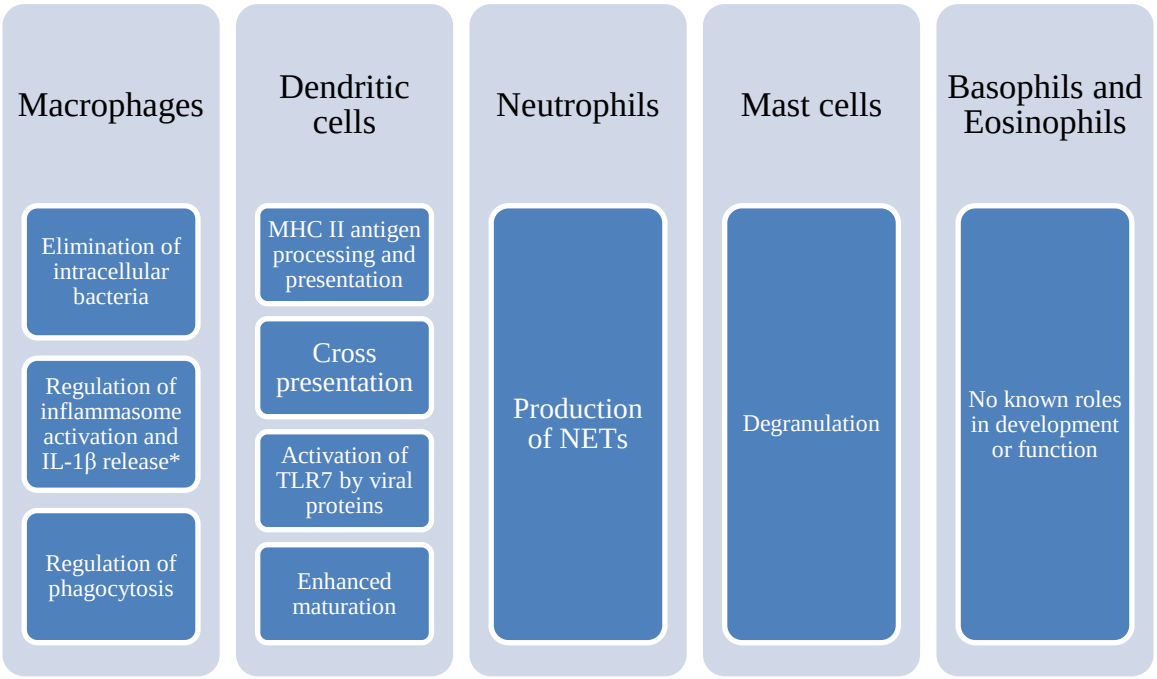

Figure 3.2 *– Currently known functions of autophagy within myeloid cells (exclusive of stimuli/effects that induce/inhibit autophagy within myeloid cells). Aside from the well-studied roles of autophagy in the elimination of intracellular pathogens and antigen presentation, little is known about the functions of autophagy in the development and function of myeloid cells. Autophagic regulation of inflammasome activation and control of inflammation will be discussed in detail in chapter 4.*

3.5 Autophagy and antigen presentation

During infections, T-cells recognise antigenic epitopes presented on Major Histocompatibility Complex (MHC) I and II. Antigenic peptides are generated from pathogenic fragments and self-proteins via several pathways where peptides are processed, delivered to MHC molecules and finally presented on the surface of the APC. $CD8^+$ T-cells recognise peptide presented in the context of MHC I molecules, expressed on the surface of all nucleated cells. MHC I molecules present antigen from various intracellular sources, including viral proteins, tumour antigens and cytoplasmic and nuclear self-antigens. Evidence regarding the role of autophagy in classical MHC I presentation is conflicting, with several studies showing no change in MHC I expression to $CD8^+$ T-cells following ablation of autophagy(9, 100, 101). However, inhibition of autophagy decreases

MHC I surface expression on B16 murine melanoma cells and reduces the subsequent T-cell response, suggesting that autophagy may influence this pathway under some conditions(102). Furthermore, autophagy enhances presentation of endogenous viral antigens via MHC I during HSV-1 infection(103), and induction of autophagy in *M. tuberculosis*-infected DCs prior to use as a vaccine results in increased proliferation of $CD8^+$ T-cells in mice(104).

MHC II molecules are constitutively expressed on the surface of specialised APCs such as dendritic cells (DCs), B-cells, macrophages and, under some circumstances, neutrophils(105). Antigen presented on MHC II molecules is recognised by $CD4^+$ T-cells. In contrast to MHC I presentation, the role of autophagy in the presentation of endogenous and exogenous antigens via MHC II is less equivocal. Autophagosomes produce a variety of peptide antigens and autophagosome fusion with MHC II loading compartments has been demonstrated experimentally(100), with 50% of MHC II compartments (MIICs) co-localising with autophagosomes. Investigation of the influence of autophagy on the MHC-II ligandome indicated that peptide presentation is improved by induction of autophagy, significantly increasing presentation of intracellular and lysosomal source proteins rather than peptides from membrane and secreted proteins. Furthermore, autophagy influenced the MHC-II antigen-processing machinery(8). Autophagy also augments MHC II processing and presentation of phagocytosed extracellular particulate antigens. NOD2-mediated autophagy has been shown to be vital for generation of MHC II antigen-specific $CD4^+$ T-cell responses in DCs(106), and Atg5 was found to be required for processing and presentation of extracellular antigen on MHC II by DCs(9). The roles of autophagy in antigen presentation are summarised in figure 3.3 below.

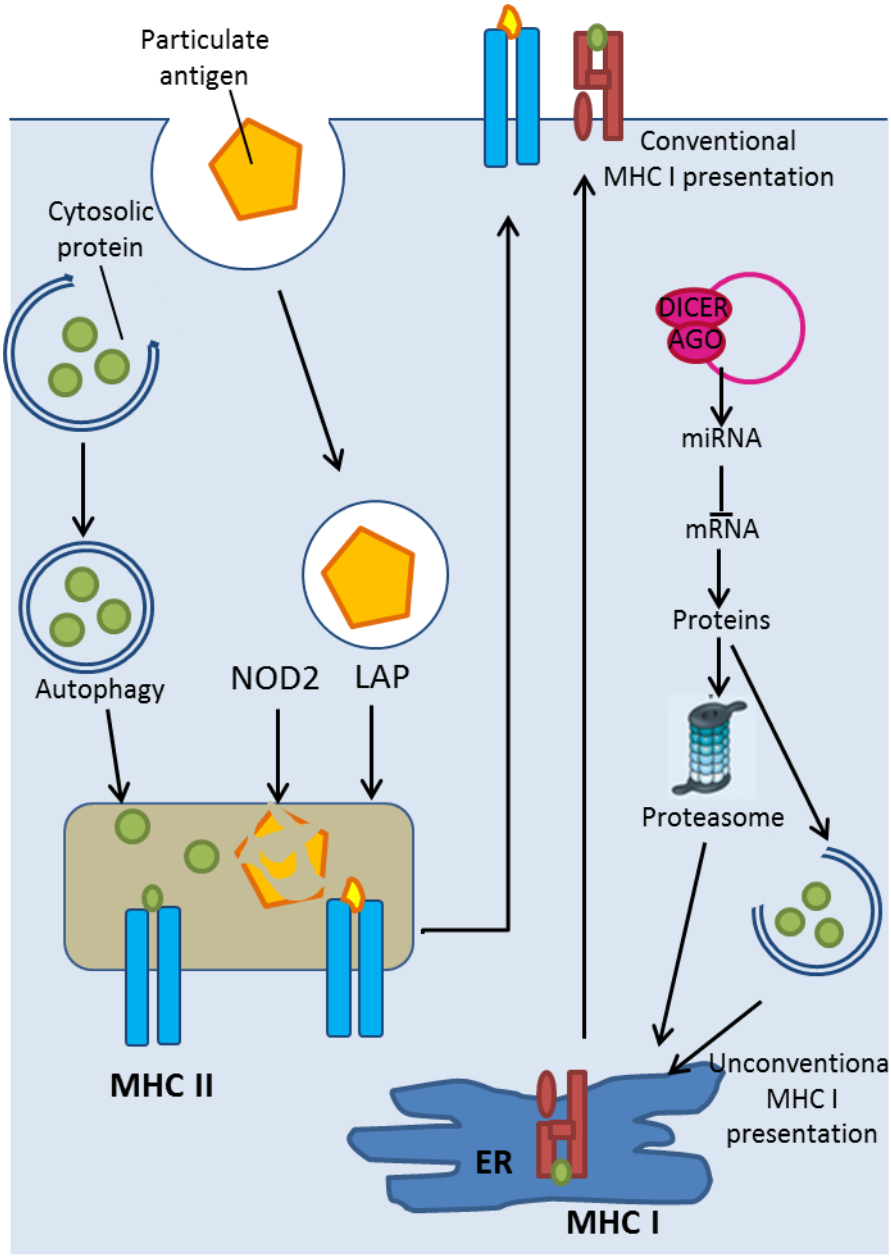

***Figure 3.3**: The role of autophagy in antigen presentation. Autophagy can increase the MHC class II presentation of cytoplasmic antigens, including self or viral antigens. LAP can also facilitate particulate antigen processing for MHC class II presentation. NOD2 enhances autophagic antigen presentation. Furthermore autophagy may support unconventional MHC class I presentation by providing degraded antigens from the autolysosome to the ER. Adapted from Ref. (107).*

3.6 Autophagy in cell death and survival

It is generally accepted that one of the main roles of autophagy is to promote cellular survival during periods of stress by providing important nutrients and by maintaining

cellular quality control of organelles and accumulated proteins. However, autophagy also interacts with cell death pathways on several levels. The three main pathways of cell death are apoptosis, necrosis and autophagic cell death. Apoptosis is characterised by caspase activation, chromatin condensation and nuclear fragmentation, cell shrinkage and the formation of apoptotic bodies(108). Apoptosis is a vital component of many processes including cellular turnover, development and regulation of the immune system. By contrast, necrosis is characterised by cellular swelling and membrane rupture and was initially considered to be un-programmed. More recently, however, evidence of programmed necrosis has appeared(109), with finely regulated signal transduction pathways and machinery(110). Autophagic cell death is morphologically defined as cell death occurring in the absence of chromatin condensation and accompanied by massive accumulation of autophagic vacuoles in the cytoplasm(111).

Autophagy and apoptosis overlap in several ways, both in function, activation of pathways and machinery. Atg5 and Bcl-2 proteins have been shown to be active in both autophagy and apoptotic pathways(112). Atg5 is cleaved following death stimuli, and the resulting cleavage product appears to promote apoptosis via the mitochondrial pathway. Bcl-2 acts during autophagy by binding and inhibiting Beclin 1-mediated autophagy and autophagic cell death(112).

Autophagy can promote cell survival and prevent the activation of apoptosis, a process exploited by some tumours to enable survival under stress(113). In addition to its general role in promotion of cellular survival, autophagy facilitates survival during the neonatal starvation period soon after birth(46, 114). Furthermore, autophagy is activated to promote survival in response to chemotherapeutic treatment(4) and following apoptotic cytochrome-c release in the absence of caspase activation(115). Conversely, inhibition of autophagy can result in apoptosis in a variety of situations(3).

Whether autophagy is protective or detrimental to cellular survival has also been linked to the level of autophagy taking place. In a cell undergoing starvation or cellular stress, autophagy initially acts as a survival mechanism by degrading surplus organelles and cytoplasmic contents. However, this cannot continue indefinitely as organelles and autophagic substrates eventually become limiting, at which point continued autophagy results in cell death. In a *C. elegans* model system, physiological levels of autophagy were found to promote survival. However, both insufficient and excessive levels of autophagy resulted in hypersensitivity to starvation(116).

The relationship between autophagy and other death pathways is highly complex and overlapping. Nevertheless, it is clear that autophagy functions in both cell death and survival under different conditions.

3.7 The influence of autophagy on macrophage function

In this chapter we show that autophagy plays an important role in many aspects of macrophage function. Loss of Atg7 in macrophages results in a significant abrogation of basal and induced autophagy. Loss of autophagy appears to influence macrophage morphology both in *ex vivo* macrophages and bone marrow-derived macrophages. Furthermore, it reduces several processes vital for macrophage defence against pathogens, such as phagocytosis, NO burst and antigen presentation.

Chapter 3: Results

Autophagy influences innate macrophage functions

3.8 Atg7 is efficiently excised from BMMϕ

To show that Atg7 is efficiently excised from macrophages from Vav-Atg7$^{-/-}$ mice, Atg7 gene expression was analysed by qPCR. Macrophages were cultured for 7 days from wildtype and Atg7$^{-/-}$ bone marrow and total RNA extracted and reverse transcribed for Atg7 gene expression analysis by qPCR. Relative gene expression was studied using the comparative Ct method ($\Delta\Delta C_T$), in which the Ct value of Atg7$^{-/-}$ macrophages was compared with control RNA from wildtype macrophages. The Ct values of both the control and the sample of interest were normalized to the endogenous housekeeping gene, GAPDH. Macrophages derived from Atg7$^{-/-}$ mice express significantly lower amounts of Atg7 mRNA than wildtype macrophages, with Atg7 expression only around 7% of wildtype mRNA abundance (figure 3.4). This indicates that Atg7 is successfully and efficiently excised from Atg7$^{-/-}$ BMMϕ.

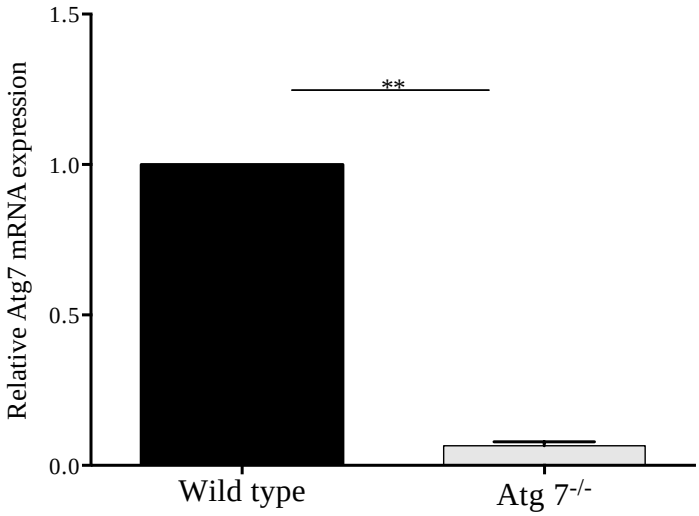

Figure 3.4: *Relative Atg7 gene expression in macrophages cultured from Vav-Atg7$^{-/-}$ bone marrow. Values determined using the $\Delta\Delta C_T$ method, normalised to GAPDH and compared to wildtype macrophages cultured under the same conditions. Error bars represent standard deviation of 3 experiments, **p<0.01.*

3.9 Atg7$^{-/-}$ mice have higher numbers of macrophages in the spleen, peritoneal cavity and blood

Macrophages represent one of the most flexible cells of the immune system, with essential roles in both the innate and adaptive arms of immune responses. They are incredibly plastic cells and specialised subsets appear in many of the main tissues and organs in the body, from where they influence the initiation and conclusion of immune responses, development, homeostasis and tissue repair. Autophagy has been implicated in several important macrophage functions, such as clearance of intracellular pathogens(87, 89) and access to intra-luminal TLRs(83). However, there is little research investigating the role of autophagy in macrophage development and maturation, and how this affects their function. In order to investigate the role of autophagy in macrophage development, macrophage numbers were first assessed in Vav-Atg7$^{-/-}$ mice to ascertain if they have normal macrophage populations in the peritoneal cavity, spleen and blood. F4/80^{+} CD11b^{+} double positive cells were assessed by flow cytometric analysis of non-elicited peritoneal wash and lysed spleen and blood samples from 8 week old mice. Macrophages were present in each of the investigated samples, making up a higher than expected proportion of total cell number from each sample. All three macrophage populations were significantly increased in Atg7$^{-/-}$ mice (Figure 3.5), in contrast to lymphocytes, which are significantly decreased in this model. The presence of macrophages in this model demonstrates that autophagy is not required for macrophage differentiation or survival *in vivo*. Not only are they present, but significantly increased in number, suggesting that autophagy has a role in macrophage proliferation or survival or in the prevention of inflammation leading to increased proliferation and macrophage migration to tissues.

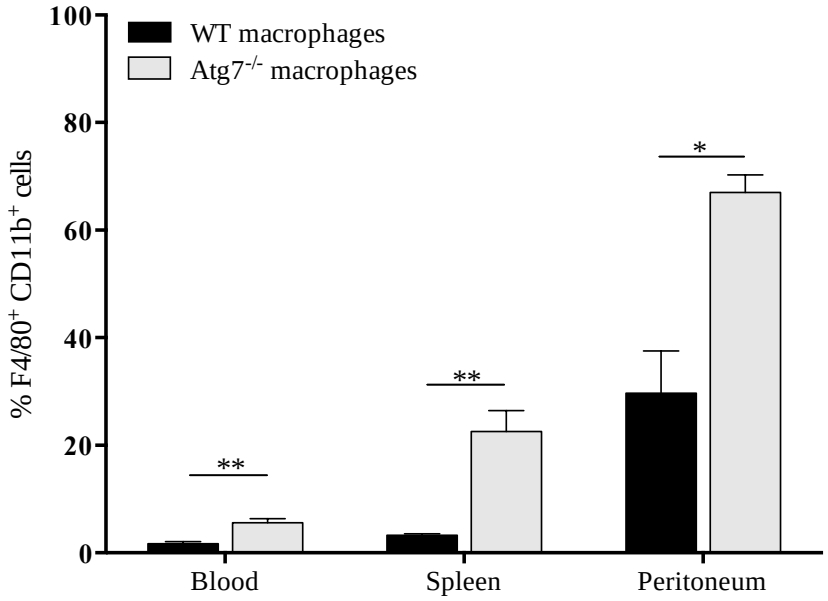

Figure 3.5: *Vav-Atg7$^{-/-}$ mice have increased proportions of macrophages in major organs. Numbers of F4/80^{+}/CD11b^{+} cells in the blood, spleen and peritoneal cavity of 8 week old mice are increased as detected by flow cytometry. Data are representative of three independent experiments. Error bars represent SEM, n = 4. *p<0.05 and **p<0.01, unpaired t-test.*

3.10 *Ex vivo* Atg7$^{-/-}$ macrophages are identifiable as macrophages, but show some alterations in morphology

Macrophages from wildtype and Atg7$^{-/-}$ mice were analysed *ex vivo* by light and confocal microscopy in order to determine whether loss of Atg7$^{-/-}$ caused any morphological changes. Cultures were viewed directly by light microscopy or stained with FITC-labelled Phalloidin and DAPI to visualise F-actin and nuclei respectively. Splenic macrophages were harvested from 8 week old mice and allowed to adhere to glass coverslips for 3 days in R10 culture medium supplemented with 10 ng/ml M-CSF, followed by overnight stimulation with LPS. Macrophages were visible in each culture as strongly adherent, dark stellate cells (figure 3.6), and the morphology of the adherent cells did not change following LPS stimulation, though increased numbers of cells were adherent in LPS stimulated cultures. However, Atg7$^{-/-}$ splenic macrophages showed slightly altered morphology, with shorter processes and a more rounded appearance than wildtype

macrophages. Additionally, Atg7$^{-/-}$ macrophages appeared less flat and firmly adhered to the culture plate than wildtype macrophages.

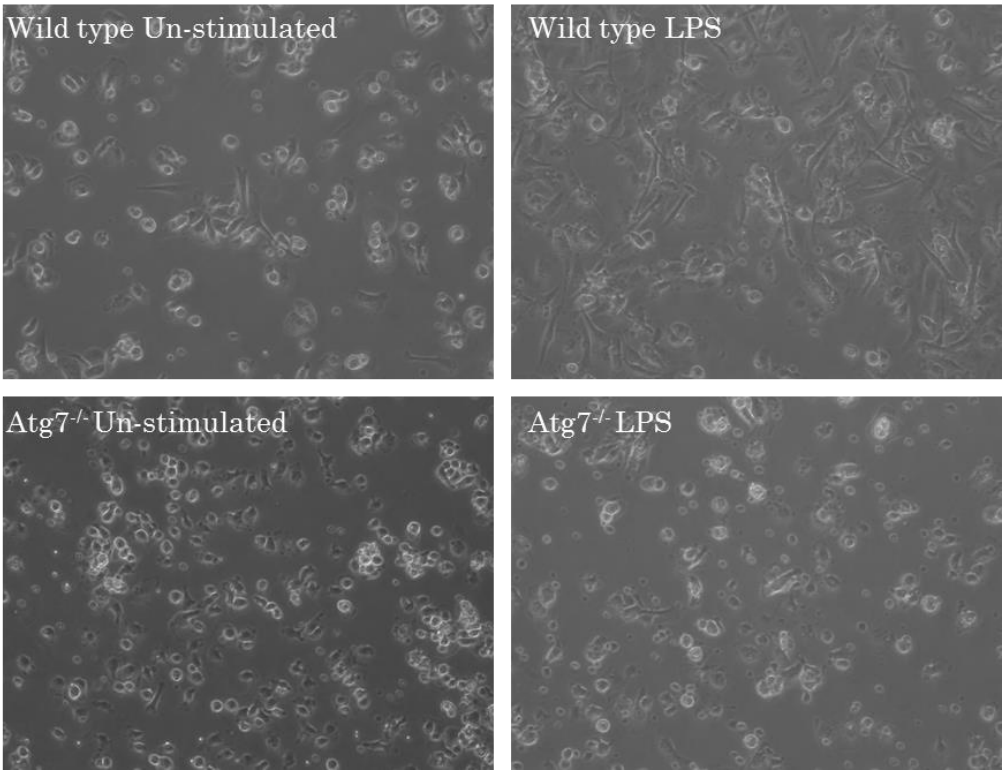

Figure 3.6: *Atg7$^{-/-}$ ex vivo splenic macrophage cultures show altered morphology by light microscopy. A single cell suspension was produced from the spleens of 8 week old mice and allowed to adhere to tissue culture plates following RBC lysis. Macrophages were cultured in R10 media supplemented with 10 ng/ml M-CSF and non-adherent cells removed after 3 days, followed by overnight stimulation with LPS (1µg/ml). Representative images from 3 cultures, 100x magnification.*

Adherent Atg7$^{-/-}$ peritoneal exudates are also clearly identifiable as macrophages (figure 3.7), with a relatively large cell size, stellate appearance and presence of visible cytoplasmic vesicles. Staining with trypan blue indicated similar numbers of live cells in both cultures (not shown). However, Atg7$^{-/-}$ macrophages also display some qualitative differences in appearance, being larger, more rounded and appearing less flat than their wildtype counterparts. Although Atg7$^{-/-}$ macrophages have the expected stellate morphology, they also appear to have shorter, fatter extensions than their wildtype

counterparts, possibly representing an impaired or altered macrophage development or activation state.

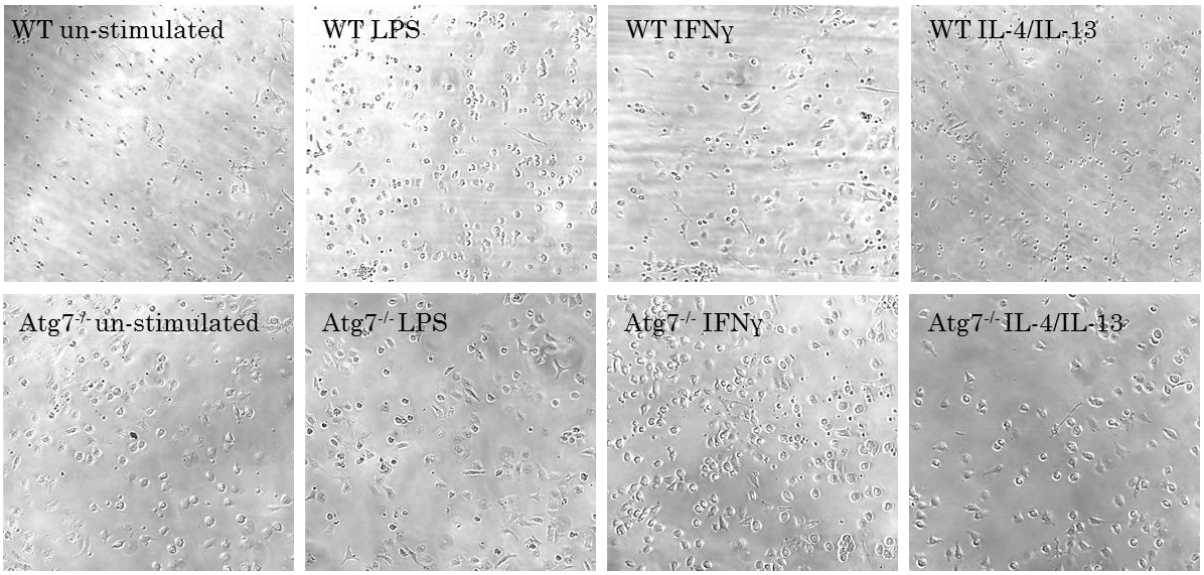

Figure 3.7: *Atg7$^{-/-}$ ex vivo peritoneal macrophage cultures from 8 week old mice show altered morphology by light microscopy. Non-elicited peritoneal macrophages were harvested and allowed to adhere to tissue culture plates. Macrophages were cultured in R10 media supplemented with 10 ng/ml M-CSF and non-adherent cells removed after 3 days, followed by overnight stimulation with LPS (1µg/ml), IFN γ (10 ng/ml) or IL-4/IL-13 (1 µg/ml). Representative images from 3 cultures, taken using 20x lens, Phase 1.*

Peritoneal macrophages were also stained using Phalloidin, a phallotoxin that binds F-actin(117), enabling visualisation of cellular morphology by fluorescence microscopy. Atg7$^{-/-}$ macrophages appear similar to wildtype macrophages, and show a similar degree of filopodial projection (figure 3.8). However, as in phase microscopy, Atg7$^{-/-}$ macrophages appear to show fewer long protrusions, and are rounder in general than wildtype macrophages. Nevertheless, the lack of these projections does not seem to adversely affect their migration ability, as significant myeloid (and macrophage) infiltration of multiple tissues is a feature of this mouse model(57).

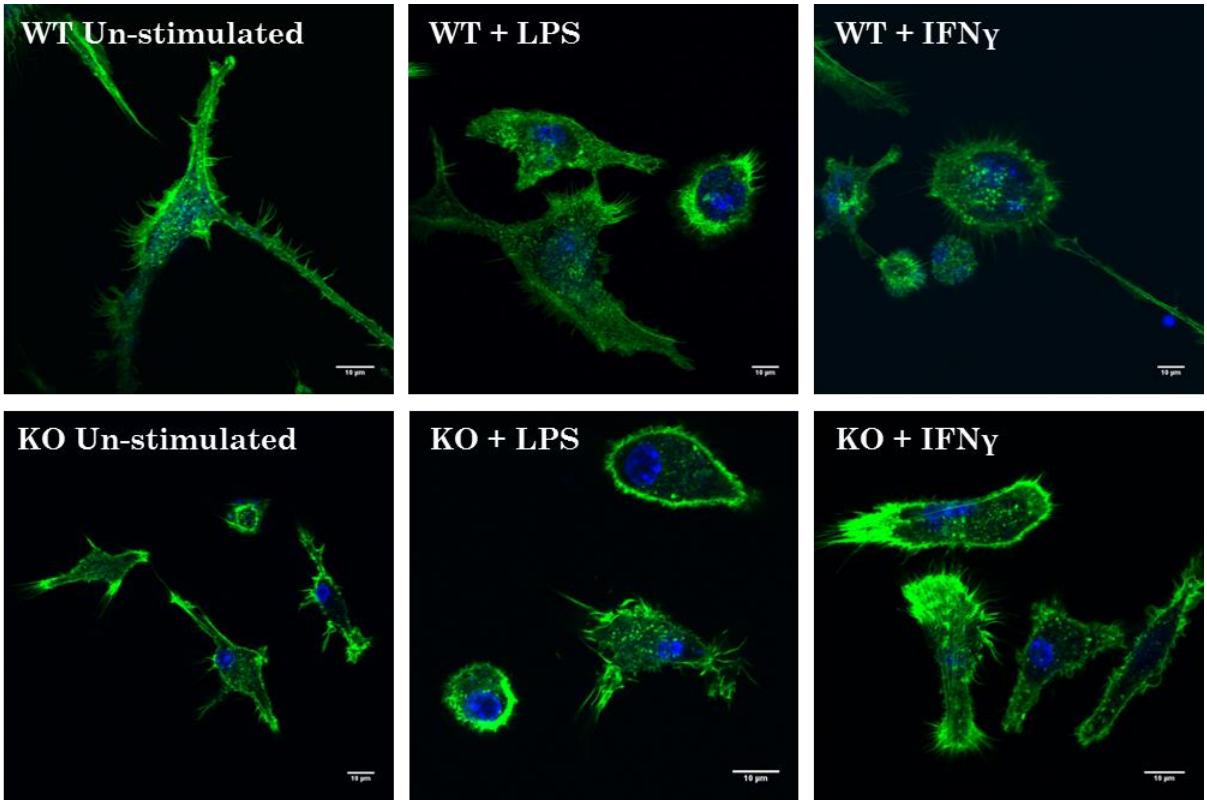

Figure 3.8: *Atg7$^{-/-}$ ex vivo peritoneal macrophage cultures from 8 week old mice show fewer long, actin rich projections by confocal microscopy. Macrophages were cultured on glass coverslips in complete R10 medium and stimulated for 3 hours with LPS (1µg/ml) or IFNγ (10 ng/ml). Coverslips were stained with FITC labelled Phalloidin and DAPI and viewed by confocal microscopy, 60x lens. Representative images from three separate cultures.*

3.11 Atg7$^{-/-}$ bone marrow derived macrophages express F4/80 and CD11b and show increased granularity

Macrophages can be derived in large numbers from bone marrow precursors using CSF-1 (Macrophage Colony Stimulating Factor, M-CSF), enabling experiments that require high cell numbers to be more easily performed. Bone marrow-derived macrophages (BMMϕ) can be used for a variety of functional assays and are regarded as a model for the role of resident macrophages in the innate immune system(118). BMMϕ can be identified by the surface antigens F4/80(119) and macrophage-1 antigen (CD11b)(120) using flow cytometry. In order to demonstrate that cultured BMMϕ expressed the expected

macrophage surface markers, BMMϕ were cultured for 7 days in the presence of M-CSF and then stained for FACS analysis with F4/80 and CD11b. Unstimulated Atg7$^{-/-}$ macrophages express similar levels of both macrophage antigens (Figure 3.9), and similar proportions of double positive cells are present in both cultures, indicating that in the absence of autophagy, macrophages are still able to be derived successfully from bone marrow.

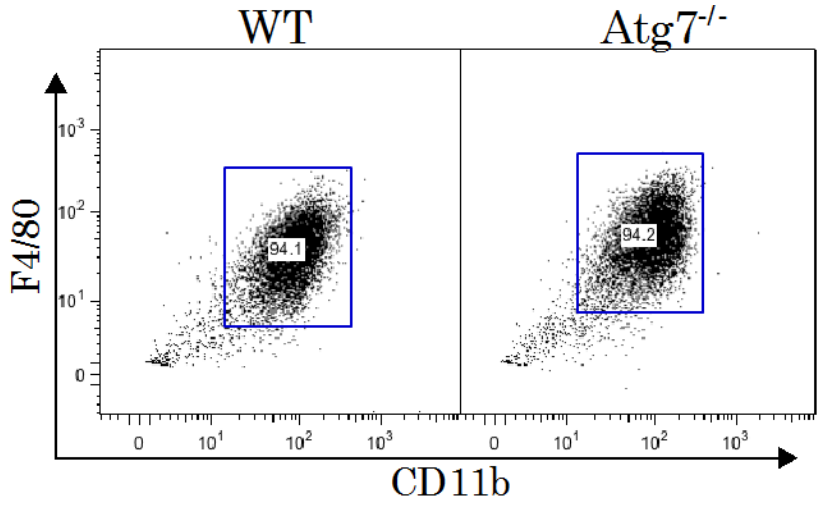

Figure 3.9*: Flow cytometric analysis of BMMϕ cultures using the macrophage surface antigens F4/80 and CD11b. BMMϕ were cultured for 7 days in the presence of M-CSF (20 ng/ml) and stained for flow cytometry. Gated on F4/80$^+$ CD11b$^+$ cells. FACS plots representative of >50 experiments.*

In addition to investigating the expression of macrophage specific surface markers, the macrophages were further analysed by comparing their forward scatter (FS) and side scatter (SS) profiles. FS and SS are generated by the light beam passing directly through the cell or being scattered off to the side, respectively. FS provides information about the relative size of the cells, whereas SS gives an indication of cellular density and complexity/granularity, allowing identification of various immune subsets based on their unique FS vs. SS profile. High SS can be an indicator of macrophage differentiation, due to increased numbers of membrane bound organelles, such as lysosomes and mitochondria(121), following stimulation. Analysis of overlaid side scatter histograms

showed that Atg7$^{-/-}$ BMMϕ display significantly increased granularity (figure 3.10, top image). Granularity increased in both cultures following LPS stimulation (figure 3.10, bottom image), however the increase in Atg7$^{-/-}$ macrophages was smaller than in wildtype macrophages. This could indicate that Atg7$^{-/-}$ macrophages are more activated than wildtype macrophages, even prior to external stimulation, or it could be the result of increased organelles and protein aggregates present in the cytoplasm, due to lack of autophagy.

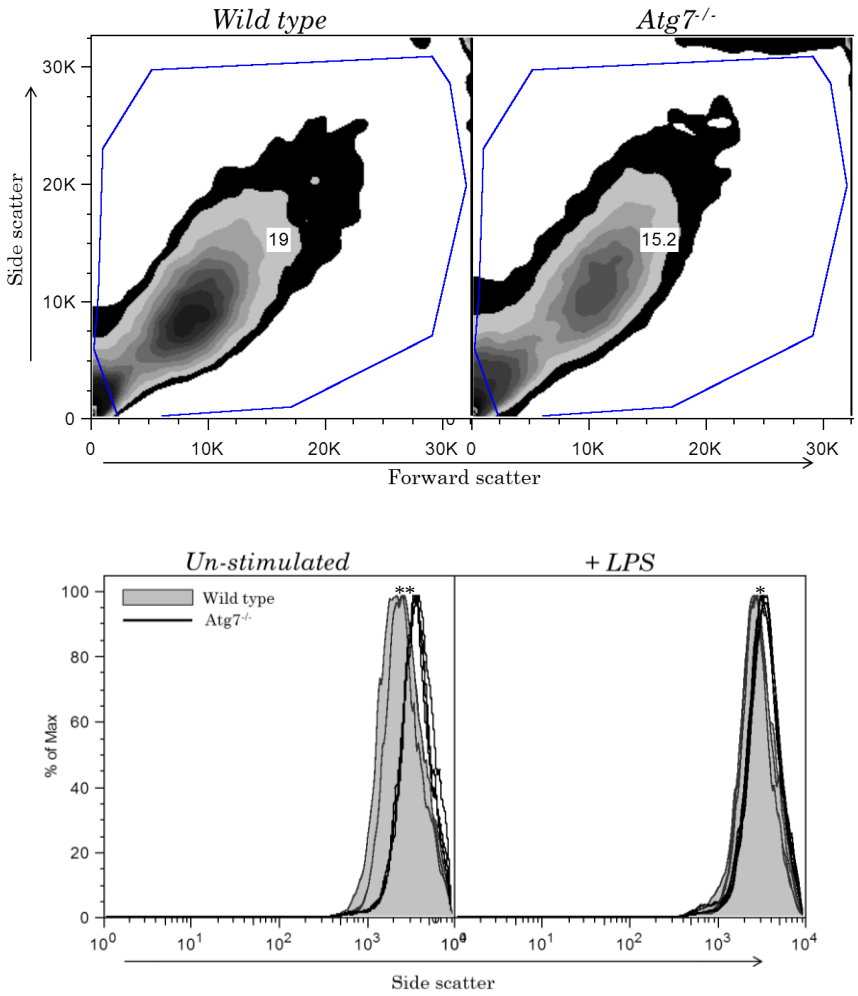

Figure 3.10: *Flow cytometric analysis of BMMϕ cultures based on their FS vs. SS profile. BMMϕ were cultured for 7 days in the presence of M-CSF (20 ng/ml) and stained for flow cytometry. Top: FS vs. SS plots for unstimulated wildtype and Atg7$^{-/-}$ macrophage cultures. All cells shown. Bottom: Overlaid histograms of macrophages side scatter (log). Gated on F4/80^{+} CD11b^{+} cells. FACS plots in both images representative of >50 experiments. *p<0.05, **p<0.01, calculated on mean MFI of SS Log, un-paired t-test.*

3.12 Atg7$^{-/-}$ BMMϕ exhibit defective autophagy

In order to demonstrate that loss of Atg7 expression in macrophages results in an autophagy defect, BMMϕ were stimulated with either LPS or IFNγ, both of which are strong inducers of autophagy in macrophages(21, 87). BMMϕ were cultured in R10 medium on glass coverslips, stimulated with LPS or IFNγ for 3 hours and then stained with anti-LC3 antibody and DAPI to show the presence of autophagosomes and nuclei, respectively. Wildtype macrophages contained a small number of autophagosomes, even in complete media and without stimulation (figure 3.11). Following overnight stimulation, the proportion of cells showing autophagosomes was close to 70% for LPS stimulated macrophages and 93% following stimulation with IFNγ (figure 3.12). Unstimulated Atg7$^{-/-}$ macrophages showed significantly fewer autophagosomes, with less than 20% showing visible autophagosomes. LPS produced a small but significant increase in autophagosomes, but significantly fewer than wild type LPS stimulated macrophages. IFNγ treatment caused no increase in autophagosomes in Atg7$^{-/-}$ macrophages. These data indicate that both basal and induced levels of autophagy are significantly lower in Atg7$^{-/-}$ macrophages, though some induction of autophagosome formation appears possible using LPS. It is possible that these puncta do not represent completed autophagosomes, but rather isolation membranes that have not fully formed, although this would not explain the lack of similar induction in IFNγ stimulated Atg7$^{-/-}$ macrophages.

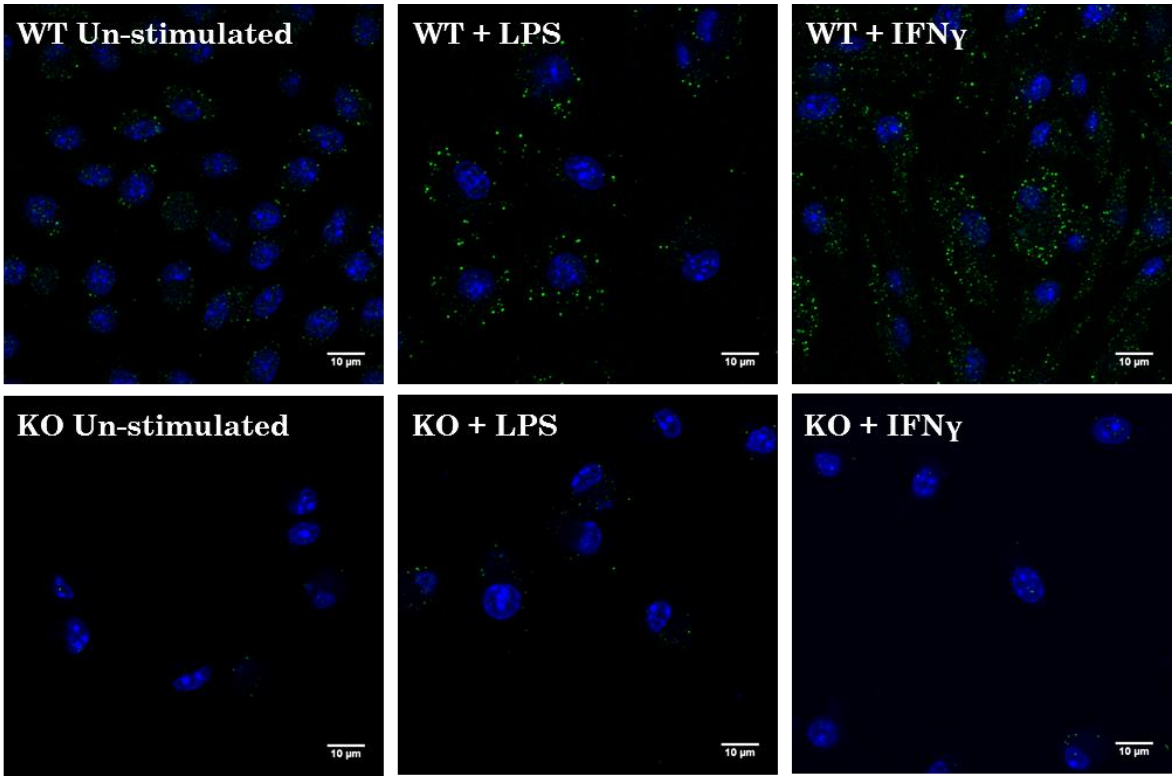

Figure 3.11*: Atg7$^{-/-}$ macrophages have significantly fewer LC3^{+} autophagosomes following autophagic stimuli, indicating defective autophagy. Macrophages were cultured on glass coverslips in complete R10 medium and stimulated for 3 hours with LPS (1µg/ml) or IFNγ (10 ng/ml) to induce autophagy. Coverslips were stained with anti-mouse LC3 and DAPI and viewed by confocal microscopy.4 images taken per slide, n = 4 mice/group. Images representative of 2 separate experiments.*

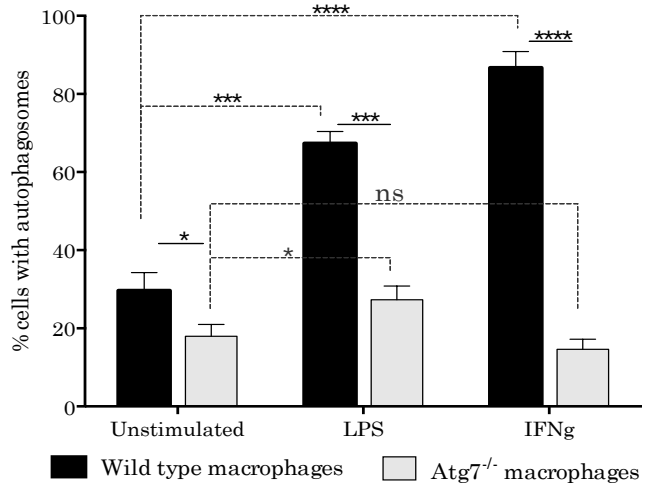

Figure 3.12: *Proportions of BMMϕ undergoing autophagy following stimulation with LPS or IFNγ. Macrophages were cultured on glass coverslips in complete R10 medium and stimulated for 3 hours with LPS (1µg/ml) or IFNγ (10 ng/ml) to induce autophagy. Coverslips were stained with anti-mouse LC3 and DAPI and viewed by confocal microscopy. 40 cells for each sample were counted and the percentage of cells positive for autophagosomes calculated. Error bars represent SEM, n = 3. *p<0.05, ***p<0.001 and ****p<0.0001, un-paired t-test.*

3.13 Atg7$^{-/-}$ bone marrow derived macrophages have increased vacuolisation of the cytoplasm

Analysis by flow cytometry confirmed that the BMMϕ expressed macrophage specific surface antigens, indicating that macrophages can be successfully derived from Atg7$^{-/-}$ bone marrow. However, in order to assess whether the cells identified showed differences in organelle appearance or membranous structures, cultures were investigated by electron microscopy. BMMϕ from 8 week old mice were cultured for 7 days in the presence of M-CSF and their morphology investigated by electron microscopy. Naive macrophages showed no gross morphological abnormalities when compared with wildtype macrophages (figure 3.13). Incomplete autophagosomes could also be clearly seen (inset) in the Atg7$^{-/-}$ macrophages. A substantial vacuolisation (black arrows, figure 3.13 d) was found in LPS stimulated, Atg7$^{-/-}$ macrophages, possibly due to unfinished autophagosomes failing to fuse with lysosomes or increased numbers of lipid droplets(122). Very few similar vacuoles were visible in wildtype macrophages; however, there were several unstimulated Atg7$^{-/-}$ macrophages that also contained the vacuolisation. These vacuoles may contribute to the increased SS visible in the Atg7$^{-/-}$ macrophages by flow cytometry. Atg7$^{-/-}$ macrophages also show a reduction in the length of membrane protrusions, as had been seen by light and confocal microscopy.

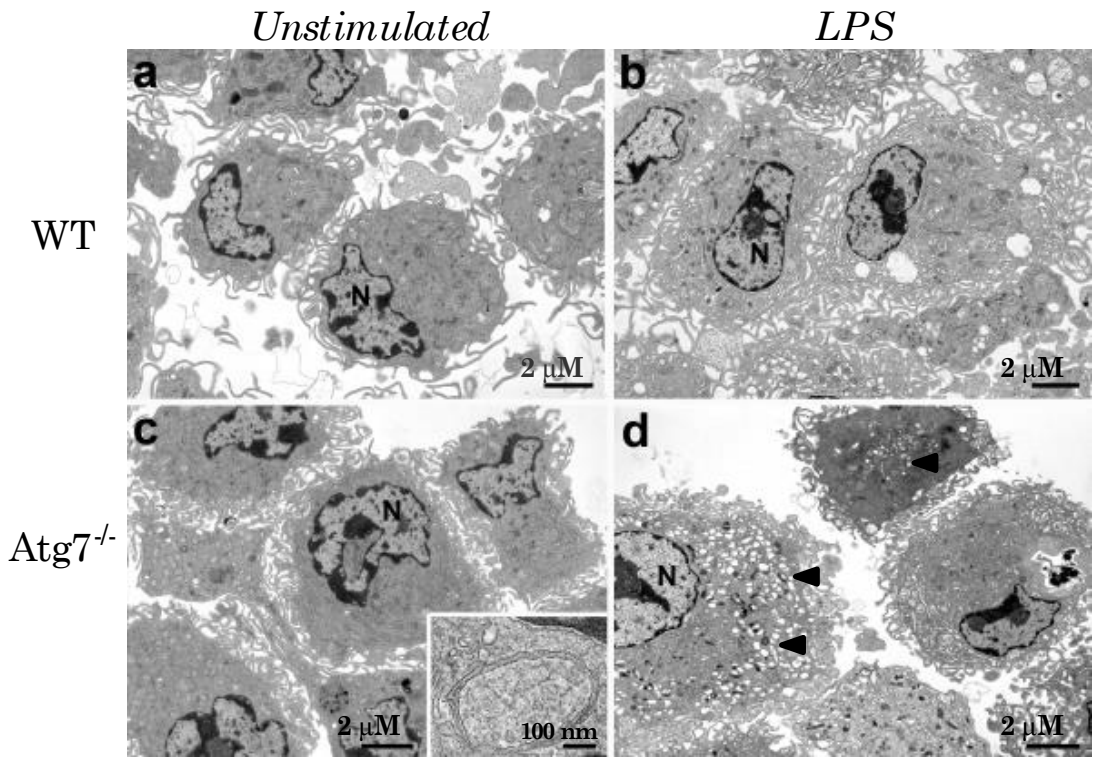

***Figure 3.13**: Bone marrow derived Atg7$^{-/-}$ macrophages have slightly altered morphology and increased vacuolisation. F4/80^{+} macrophages were enriched by MACS and fixed for electron microscopy analysis. Cells from 4 Atg7$^{-/-}$ bone marrow derived macrophage cultures were pooled for analysis. Images shown are representative of two independent experiments. Scale bar in images a – d is 2μM, inset in c is 100 nm. N – Nucleus. Black arrow head: Increased vacuoles in LPS stimulated Atg7$^{-/-}$ macrophages. Inset shows an incomplete autophagosome in an Atg7$^{-/-}$ macrophage. Grateful acknowledgements to Professor David Fergusson for acquiring these images and helping with their analysis.*

3.14 Atg7$^{-/-}$ macrophages have increased numbers of lipid droplets in the cytoplasm

As electron microscopy and flow cytometry suggested the presence of cytoplasmic vacuoles that could represent increased numbers of lipid droplets, other lysosomal organelles, and as autophagy is known to play a role in the degradation of cholesterol droplets(122), we assessed the lipid content of Atg7$^{-/-}$ macrophages. Nile red is a lipophilic stain that fluoresces intensely red-gold in lipid rich environments, with very little fluorescence in other polar solvents. Autophagy-deficient macrophages showed higher Nile red staining than wildtype macrophages for all stimuli (figure 3.14). However, Atg7$^{-/-}$

macrophages showed no increase in staining following LPS stimulation, whereas wildtype macrophages showed a significant increase. This is in contrast to the vacuolisation visible by electron microscopy, which was much more visible in Atg7$^{-/-}$ macrophages following LPS stimulation. As such, though lipid droplets may contribute to the increased granularity and vacuolisation present in Atg7$^{-/-}$ macrophages, they are not the main cause.

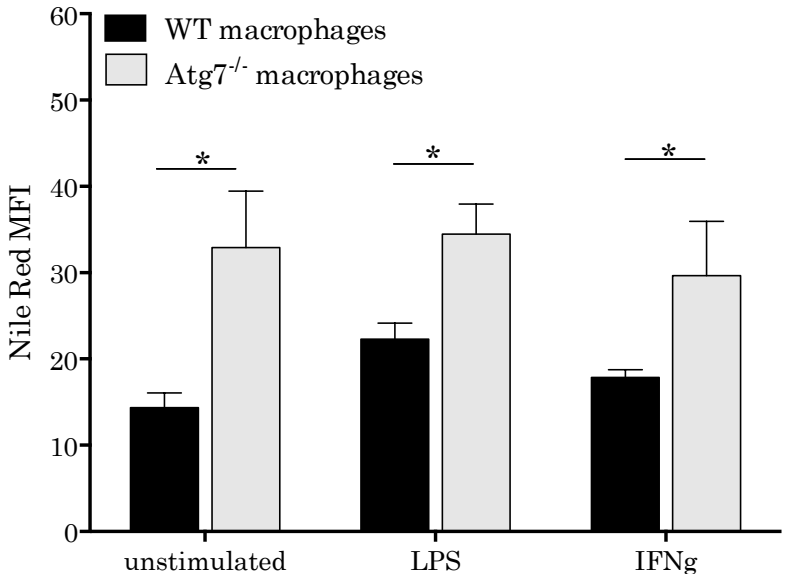

***Figure 3.14**: Nile Red Lipid droplet staining in bone marrow derived macrophages. BMMϕ were cultured and stimulated overnight with LPS or IFNγ, followed by staining with Nile red (1 μM) for analysis by flow cytometry. Average MFI of Nile red fluorescence for F4/80$^+$ CD11b$^+$ macrophages shown. Error bars represent SEM, n = 3. *p<0.05, un-paired t-test.*

3.15 Loss of autophagy causes higher levels of cell death in macrophages

The presence of increased numbers of macrophages in Vav-Atg7 mice suggested that they could have a proliferative or survival advantage over other cells of the hematopoietic system. Furthermore, autophagy is known to be a survival mechanism in some cells(123, 124), and therefore levels of apoptosis were investigated in wildtype and Atg7$^{-/-}$ BMMϕ. Early cell death can be detected using Annexin V to detect cells that have expressed phosphatidylserine, a phospholipid component usually on the cytosolic side of the

membrane, on their cell surface. Annexin V positive cells are thus in the early stages of apoptosis. In unstimulated Atg7$^{-/-}$ macrophage cultures, 20% of cells were Annexin V^{+}, a small but significant increase on the 15% of cells Annexin V^{+} in wildtype cultures (Figure 3.15). Following stimulation with LPS or IFNγ, there was a decrease in the proportion of Annexin V^{+} wildtype macrophages. However, no such decrease in Annexin V^{+} cells was observed following stimulation in Atg7$^{-/-}$ cells. In some cultures IFNγ stimulation appeared to slightly decrease numbers of positive cells, but this was variable between cultures, and was not statistically significant.

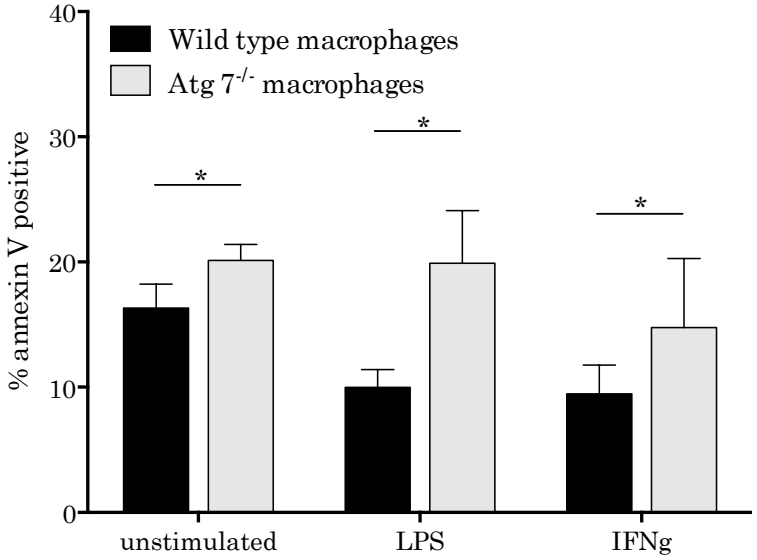

Figure 3.15*: Increased numbers of Annexin V^{+} cells in Atg7$^{-/-}$ macrophage cultures. BMMϕ were stained with F4/80, CD11b and Annexin V and analysed by flow cytometry. The graph shows proportions of Annexin V^{+} cells in BMMϕ cultures following overnight stimulation with LPS or IFNγ. Error bars represent SEM, n = 4. *p<0.05, un-paired t-test.*

Caspase-3 is an executioner caspase activated in both the extrinsic (death ligand) and intrinsic (mitochondrial) apoptosis pathways, and thus activated caspase 3 makes a useful target for assessing later apoptotic events in cells. A significantly higher proportion of Atg7$^{-/-}$ macrophages were found to be positive for activated caspase 3 (figure 3.16), with even higher numbers found following LPS stimulation. LPS stimulation also increased the proportion of wildtype caspase 3^{+} cells from around 2.5% to 7.5%. Stimulation with IFNγ

produced no increase in caspase 3^+ cells in wildtype or $Atg7^{-/-}$ macrophages. These data indicate that loss of autophagy in macrophages increases their susceptibility to cell death, and suggests that increased macrophage numbers in Vav-Atg7 mice is not due to increased macrophage survival, but rather increased proliferation or production of macrophage precursors from the bone marrow.

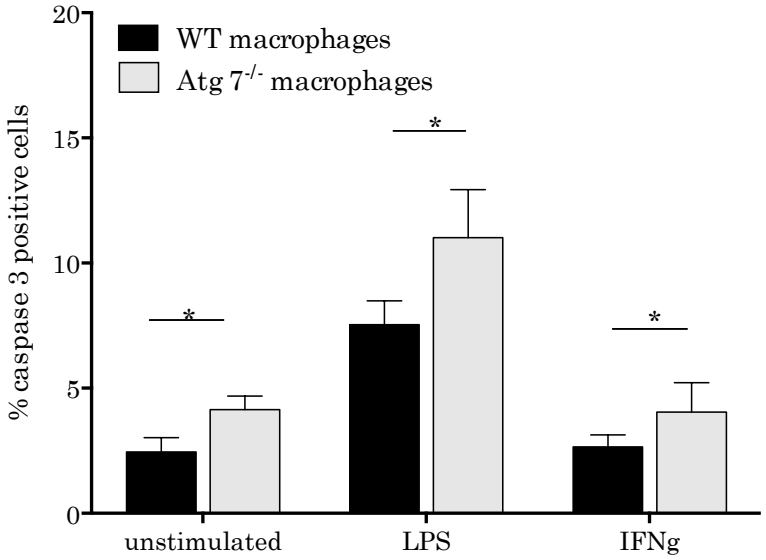

***Figure 3.16**: Higher proportions of activated-caspase 3 positive cells in $Atg7^{-/-}$ BMMϕ cultures following overnight stimulation with LPS or IFNγ. BMMϕ were stained with F4/80, CD11b and Annexin V and analysed by flow cytometry. The graph shows proportions of macrophages staining positive for activated caspase-3 following overnight stimulation with LPS or IFNγ. Error bars represent SEM, n = 4. *p<0.05, un-paired t-test.*

3.16 $Atg7^{-/-}$ BMMϕ show decreased phagocytic capacity and nitrite burst following stimulation

Macrophages play a vital role in the innate immune response by phagocytosing invading pathogens and releasing reactive nitrogen and oxygen species. In order to analyse the functional capacity of $Atg7^{-/-}$ macrophages, the ability of macrophages to phagocytose FITC labelled latex beads was analysed by flow cytometry. Both $Atg7^{-/-}$ and wildtype macrophages were capable of latex bead uptake (figure 3.17). However, unstimulated $Atg7^{-/-}$ macrophages exhibited a small, but significant, reduction in phagocytosis compared

with their wildtype counterparts, with 50% of autophagy-deficient macrophages positive for beads, compared with 60% of wildtypes. Furthermore, whereas phagocytic capacity significantly increased in wildtype macrophages following stimulation with LPS, a much smaller increase was observed for Atg7$^{-/-}$ macrophages. Stimulation with LPS increased phagocytic capacity in Atg7$^{-/-}$ macrophages similar to that of unstimulated wildtype macrophages, but this was still significantly lower than the 80% bead-positive wildtype macrophages following LPS stimulation. Although autophagy is evidently dispensable for phagocytosis in macrophages, its loss results in a reduction in phagocytic capacity, which could result in reduced pathogen clearance.

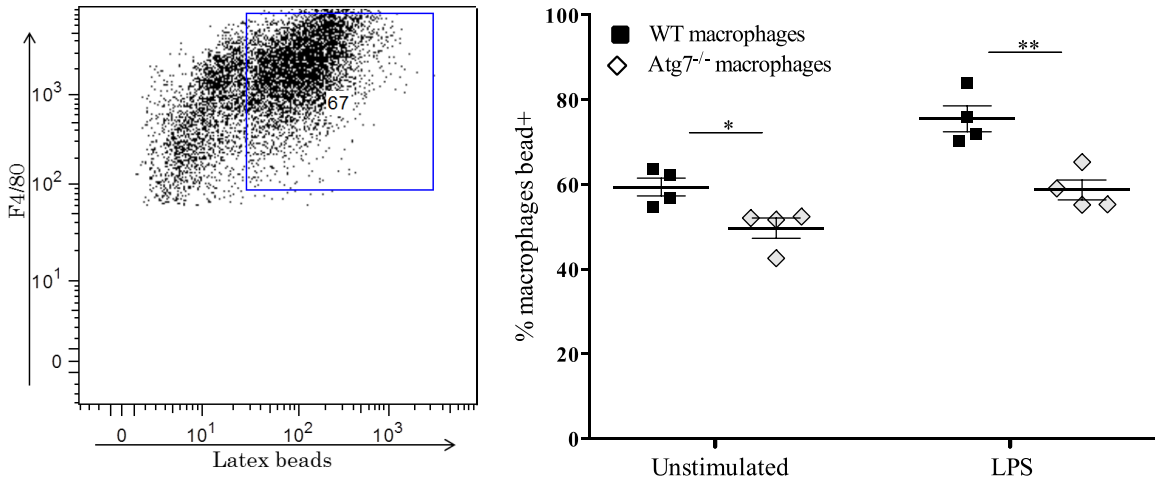

Figure 3.17: *Decreased phagocytic capacity of Atg7$^{-/-}$ BMMϕ before and after LPS stimulation. FITC labelled latex beads were cultured for 3 hours with BMMϕ in the presence or absence of LPS (1 µg/ml) and analysed by flow cytometry. Surface associated bead fluorescence was quenched with trypan blue. Left: An example of bead^{+} macrophages (gated). Right: Graph of average bead^{+} macrophages. Error bars represent SEM (n = 4), *p<0.05, **p<0.01, unpaired t-test.*

NO is a short lived free radical that is produced by a variety of immune and non-immune cells. NO is vital for the cytotoxic and microbicidal activity of macrophages and plays an important role in the respiratory burst, thus protecting the host from bacterial infection. NO is detected as nitrite (NO_2^-) in the supernatant by formation of a pink colour upon treatment with the Griess reagent, with maximum absorption at 550 nm. BMMϕ were

stimulated overnight with LPS or IFNγ and supernatants harvested and analysed for the presence of NO using the Griess reagent to identify secreted nitrite. Atg7$^{-/-}$ and wildtype macrophages produced similar basal levels of NO (figure 3.18). However, following overnight stimulation with LPS, wildtype macrophages showed a significant increase in nitrite expression to produce a supernatant nitrite concentration of 2 μM, four times the basal level. Similarly, stimulation of wildtype macrophages with IFNγ resulted in a supernatant nitrite concentration of 1.6 μM. In contrast, stimulation of Atg7$^{-/-}$ macrophages with LPS resulted in no increased production of nitrite above basal levels, and stimulation with IFNγ resulted in a small, but significant increase of production. Overall, Atg7$^{-/-}$ macrophages show a reduced nitrate burst following stimulation, compared with wildtype macrophages. A reduced NO burst following pathogenic stimuli, coupled with decreased phagocytic capacity could significantly reduce the ability of autophagy-deficient macrophages to respond to and eliminate invading pathogens, thereby severely impeding the immune response to infection.

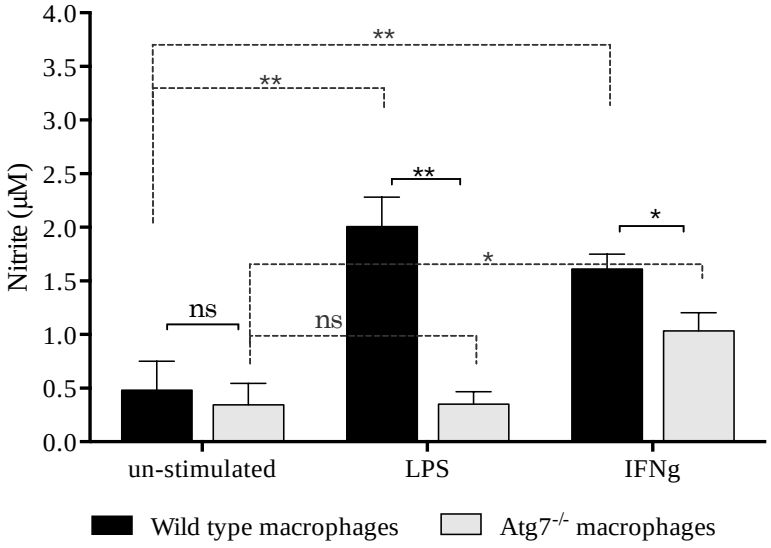

Figure 3.18: *Loss of autophagy results in a reduced nitrite burst in stimulated macrophages. BMMϕ were stimulated overnight with LPS (1 μg/ml) or IFNγ (10 ng/ml) and supernatant samples taken the following day for nitrite analysis using the Griess reagent. Samples were analysed in triplicate and absorbance was measured at 550 nm. Nitrite concentration was determined using a standard curve. Error bars represent SD, n = 4. *p<0.05, **p<0.01, un-paired t-test.*

3.17 Lack of Atg7 reduces antigen presentation capacity in macrophages

In addition to a major role in the orchestration of the early innate response to pathogenic infection, macrophages are professional APCs, and as such play an important role in the initiation of the adaptive immune response(125). Autophagy is known to play a role in antigen presentation by other APCs(8, 9), and as such we investigated the ability of the $Atg7^{-/-}$ macrophages to present antigen in a male-antigen-into-female experiment, using male-antigen (UTY)-specific CD8 T-cell responses as a readout for a specific immune response(126). Male APCs (macrophages or dendritic cells) were injected into female recipients and the resultant CD8 response assessed using a male-antigen specific tetramer, following a boosting injection with cross-linked vaccinia-UTY. Ten days after boosting, wildtype male DCs raised a robust anti-male $CD8^{+}$ response in female recipients. Female recipients of male wildtype macrophages registered double the number of UTY-specific $CD8^{+}$ T-cells compared to animals that received male $Atg7^{-/-}$ macrophages, indicating that Atg7 deficient macrophages had a significantly lower antigen presentation capacity (figure 3.19). These data demonstrate reduced *in vivo* antigen presentation capacity by autophagy-deficient macrophages to T-cells, and confirm previous data from other groups showing a role for autophagy in antigen presentation. Together with the impaired innate immune responses in $Atg7^{-/-}$ macrophages, the reduced antigen presentation capacity would substantially blunt their capacity to initiate and direct an appropriate immune response to invading pathogens. This demonstrates that autophagy plays a vital role in macrophage ability to produce correct responses following immune stimuli.

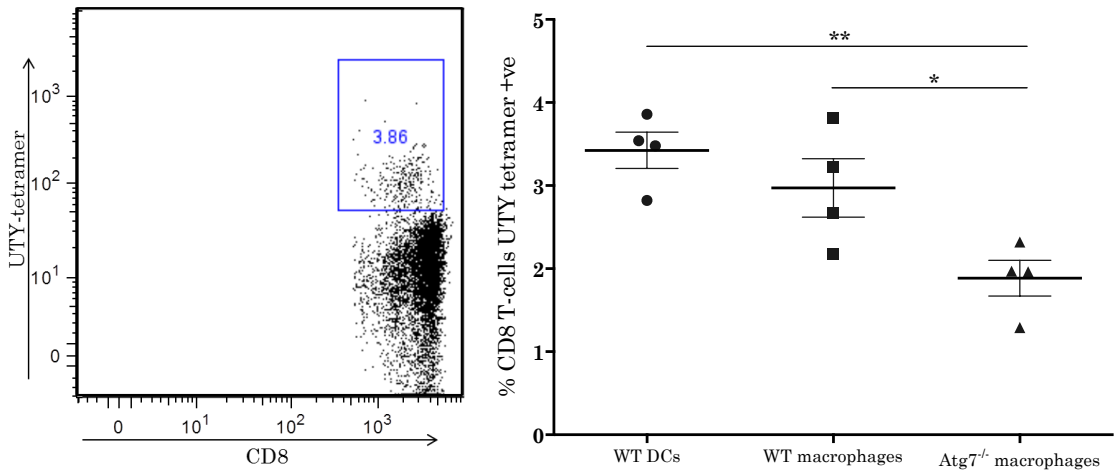

Figure 3.19: *Atg7$^{-/-}$ BMMϕ have impaired antigen presentation in vivo. Wildtype and Atg7$^{-/-}$ macrophages and wildtype DCs were derived from male donors and injected into female recipients via the tail vein. Immune response was analysed by detection of male-antigen specific (UTY^{+}) CD8^{+} T-cells in the blood 2 weeks post injection. Gating strategy for tetramer staining (left): UTY-tetramer positive cells shown are CD19^{neg}CD8^{+} cells from lysed blood samples. Graph shows average tetramer positive CD8 T-cells. Data representative of two independent experiments, n=4 mice. Error bars represent SEM, *p<0.05, **p<0.01, un-paired t-test.*

3.18 Atg7$^{-/-}$ macrophages have altered expression of proteins associated with cell structure and function

Proteomic analysis provides a useful overview of all proteins present in a cell at a particular point in time. Protein extracts were taken from wildtype and Atg7$^{-/-}$ macrophages and investigated by tandem mass spectrometry, in order to gain a better understanding of how loss of autophagy affects cellular biology and function in macrophages (Figure 3.20). Important structural proteins such as vimentin, desmin and moesin and assembly molecules such as cofilin were found to be significantly upregulated in Atg7$^{-/-}$ macrophages. Proteins such as latrophilin, which modulates cellular adhesion and Ena/VASP like proteins, which regulate the actin cytoskeleton, were also significantly upregulated in Atg7$^{-/-}$ macrophages. Alterations in expression of such proteins may be partly responsible for the altered morphology of Atg7$^{-/-}$ macrophages visible by

microscopy. In addition to these structurally related proteins, the autophagy substrate p62 was expressed at higher levels in $Atg7^{-/-}$ macrophages, reflecting its accumulation in the absence of autophagy.

Protein ID	Protein Name	Score	WT:KO ratio	p value
	Structural Proteins			
P20152	Vimentin	1755	0.47	0
P26041	Moesin	974	0.76	0
P18760	Cofilin	812	0.68	0
Q80TS3	Latrophilin	779	KO only	KO only
P24452	Macrophage capping protein	697	0.73	0
P70429	Ena/VASP like protein	333	KO only	KO only
P63028	Translationally-controlled tumour protein	261	WT only	WT only
Q7TPR4	F-actin cross linking protein	769	1.99	1
Q9JM76	Actin-related protein 2/3 complex subunit 3	182	1.48	0.98
P13001	Desmin	464	KO only	KO only
	Autophagy			
Q64337	Sequestrome 1 (p62)	429	KO only	KO only

***Figure 3.20**: $Atg7^{-/-}$ macrophages show altered expression of many structural proteins. Bone marrow derived macrophages were cultured for 7 days and stimulated overnight with LPS (1 µg/ml). Protein extracts were produced from pooled wildtype and $Atg7^{-/-}$ macrophages, adjusted to the same protein concentration and analysed by tandem mass spectrometry. Protein score is a measure of protein abundance. Significance is denoted as $p<0.05$ for proteins with increased expression in $Atg7^{-/-}$ macrophages, and $p>0.95$ for proteins with increased expression in wildtype macrophages. Grateful acknowledgements to Dr Benedikt Kessler for performing the proteomic experiments and assisting with their analysis.*

Chapter 3: Discussion

Autophagy influences innate macrophage functions

3.19 Increased macrophages in Vav-Atg7 mice

Study of the role of autophagy in the immune system, and more specifically in macrophages, has been greatly facilitated by the use of a mouse model in which the essential autophagy gene, Atg7, has been deleted in hematopoietic cells. These mice, known as Vav-Atg7 mice, have a particularly strong phenotype, characterised by severe and progressive anaemia and lymphopenia resulting from a stem cell defect, and eventually culminating in death at a median age of 12 weeks(54). In spite of the stem cell defect, and in contrast to the lymphocytes and erythrocytes, however, cells of the myeloid system appear relatively unaffected. The presence of mature macrophages (based on their high expression of F4/80 and CD11b) suggests that autophagy is not essential for macrophage survival and development in the same manner as it is for lymphocytes and erythrocytes. In addition to significantly increased numbers of myeloid cells, including macrophages, detected in the blood, spleen and peritoneal cavity, infiltration of non-hematopoietic tissues, such as the heart, liver and pancreas, was also clear in tissue sections taken from the mice(57). The infiltrates stained positive for CD68, CD11b and myeloperoxidase, and included a high number of immature and maturing macrophages, described as reminiscent of MDS or AML. Although resident macrophages appear in most major tissues, such high numbers are not normally found in healthy individuals. The increased numbers of macrophages may be as a result of a proliferative advantage, reduced cell death, response to pathogenic infection, aseptic inflammation or as a result of a proliferative, dysplastic or malignant syndrome. No proliferative advantage was observed in macrophages cultured from bone marrow, however, with similar numbers of $F4/80^{+}$ $CD11b^{+}$ cells derived from the same number of bone marrow cells. Where there was a discrepancy between final macrophage numbers, $Atg7^{-/-}$ macrophages were invariably lower, as a result of increased cell death in the absence of autophagy. Thus macrophage

accumulation in tissues is also unlikely to be as a result of a survival advantage conferred by loss of autophagy, as more cell death rather than less cell death was detected. However, macrophages were only enumerated on the final day of culture, so an early (but limited) proliferative burst cannot be discounted. Macrophage proliferation in culture could be assessed by labelling bone marrow with a cell proliferation dye, such as CFSE, and analysing numbers and proliferation of $F4/80^{+}$ $CD11b^{+}$ cells at different time points during culture.

High levels of myeloid infiltration are also found in MDS, myeloproliferative disorders and myeloid leukaemias. However, when bone marrow from $Atg7^{-/-}$ mice was used to reconstitute irradiated mice, little reconstitution was observed and tissue infiltrates in the recipients were rarely, if ever, seen(57), suggesting that the macrophage and myeloid infiltration is not leukemic in origin. The presence of blasts and anaemia could also suggest myelodysplastic syndrome. However, the anaemia is attributable to a cell specific loss of autophagy, as a RBC specific deletion of Atg7 also gives rise to anaemia in mice, though not as severe as in the Vav-Atg7 model(2) and increased blasts can also be attributed to acute infection or inflammation. Single cell colony formation assays performed in our lab have shown that both $Atg7^{-/-}$ HSCs and the myeloid granulocyte-macrophage progenitor (GMP) give rise to fewer and smaller colonies than their wildtype counterparts, shedding doubt on the proliferative capacity of myeloid precursors, at least *ex vivo* (*Alec Watson, unpublished observations*). Furthermore, karyotype analysis of infiltrates showed no evidence of translocations or major deletions, though there were some minor deletions (unpublished data from our lab). This does not rule out MDS as the cause of increased macrophage (and neutrophil, as will be discussed in future chapters) numbers but, given the lack of genetic alterations and proliferative capacity of myeloid precursors, other non-proliferative explanations are also possible. Increased numbers of

macrophages also migrate to and proliferate at the site of infection, however infection is unlikely to be the cause of the increased macrophage numbers in this case as the animals are kept under SPF conditions and no signs of infection have ever been observed by the researcher or the animal house staff, or present in histological sections, macrophage cultures or by microscopy. Localised acute infection would increase macrophage numbers at the site of infection and potentially increase monocytes in the blood, but would be unlikely to cause increased macrophages in non-hematopoietic tissues away from the site of infection. Chronic infection could possibly give rise to a more general infiltration; however, with such severely reduced lymphocytes any infection would quickly overwhelm Vav-Atg7 mice.

Systemic inflammation and chronic inflammatory signalling could also result in increased numbers of macrophages in various tissues. With high levels of cell death amongst RBCs, lymphocytes and other autophagy-deficient cells and reduced phagocytic capacity, macrophages could be activated to release inflammatory cytokines and chemokines by ingestion of necrotic cells or DAMPs released by the dying cells(127), thereby attracting neutrophils into tissues as well. As will be discussed in chapters 4 and 5, autophagy-deficient macrophages do indeed secrete high amounts of inflammatory cytokines and chemokines even in the absence of externally applied stimuli, potentially resulting in a feedback loop of inflammation and contributing to the eventual stem cell failure. Levels of cytokines and other immune products could be assessed in the tissues by ELISA or multiplex to assess levels of systemic inflammation. Infant mice could also be treated with anti-inflammatory or cytokine blocking substances to see if this could prevent or reduce the myeloproliferation and potentially the bone marrow failure.

3.20 Altered macrophage morphology in the absence of Atg7 and accumulation of cytoplasmic vacuoles

Ex vivo and bone marrow-derived Atg7$^{-/-}$ macrophages were found to have altered membrane morphology on microscopic analysis, with reduced numbers and length of characteristic macrophage projections clearly visible by light, confocal and, particularly, electron microscopy. Membrane ruffling and pseudopodia/filopodia formation are vital to macrophage function, playing important roles in macrophage polarisation(128), adhesion, migration(129) and phagocytosis(130). Pseudopodia are composed of microtubule and filamentous structures and polymerised actin. A lamellipodium (small protrusion) extends from the plasma membrane, supported by filaments that assemble at the leading edge. Cytoplasm fills the growing lamellipodium, forming pseudopodia(131). Proteomic analysis found altered expression of several actin and microfilament related proteins, which may influence membrane ability to form into pseudopodia or lamellipodia. Desmin, a type III intermediate filament that was found at increased levels in Atg7$^{-/-}$ mice, helps give cells structure. Accumulation of desmin aggregates in muscle cells results in cardiomyopathy, a process which is usually controlled by autophagy(132). Such aggregations in macrophages may play a role in blocking pseudopodia formation. Vimentin is another intermediate-type filament, overexpression of which is important in macrophage differentiation(133). Vimentin is also known to inhibit autophagy by binding with beclin-1 and 14-3-3, thereby contributing to tumorigenesis(134). Macrophage capping protein is a member of the actin-binding protein family, which is crucial for the organisation of the actin cytoskeleton, and is thought to play a role in migration and metastasis(135). Overexpression, such as seen in Atg7$^{-/-}$ macrophages, increases motility, and may partly explain how macrophages are able to so easily infiltrate tissues in Vav-Atg7 mice. These proteins may be autophagic substrates under normal cellular conditions,

and therefore accumulate in the absence of autophagy, potentially interfering with cell shape and motility. Unlike the previously mentioned proteins, which had increased expression in $Atg7^{-/-}$ macrophages by proteomic analysis, F-actin cross linking protein (Alpha actinin-1) has reduced expression. Alpha actinin is a major component of lamellipodia(136), and a reduction in expression could well result in decreased membrane processes. The actin related protein 2/3 (Arp2/3) complex also had lower expression in $Atg7^{-/-}$ macrophages. Arp2/3 builds lamellipodial networks by initiating actin filament branching, and plays a major role in lamellipodia extension(137), but is dispensable for migration and chemotaxis(138). It is not clear how loss of autophagy, which is primarily a protein degradation mechanism, would result in decreased protein expression. However, proteins from the Arp complex are known to interact with autophagic machinery(139), potentially generating signals required for Arp2/3 initiation or up-regulation of expression(140). Autophagy has also been shown to modulate cell shape and spreading in macrophages through the action of Rho GTPase pathways(141).

In addition to altered morphology, a significant vacuolisation of the cytoplasm was seen in LPS stimulated $Atg7^{-/-}$ macrophage electron micrographs. Staining with Nile Red revealed increased lipid droplets, which contain cholesterol and are known to be degraded through the action of autophagy(122), thereby contributing to the pathogenesis of atherosclerosis(142). However, the degree of staining cannot fully explain the vacuolisation visible by EM. The vacuoles are light in colour and appear to contain little or no cytoplasm. They are bounded by a single membrane, and are therefore not composed of incomplete autophagosomes. Their relatively close position to the cell membrane suggests they could be pinosomes, which at 50 – 250 nm in size fit the dimensions of the observed vacuoles. Pinosomes can be autophagic substrates(143), and loss of autophagy is not known to negatively influence pinocytosis. Thus the vacuolisation

may be less visible in the LPS-stimulated wildtype macrophages due to degradation of the pinosomes via autophagy. A pinocytosis inhibitor such as amiloride(144) could be used to block pinocytosis in macrophages and assess whether the vesicles are not present following treatment. However, amiloride can also affect actin, which may cause other morphological problems(145). Similarly, the vacuoles could represent small endosomes formed under the same conditions, which could be assessed by staining for endosomal markers such as LAMP, VAMP and Arf6, or by use of endocytosis inhibitors, such as Chlorpromazine or Filipin(144).

The presence of cytoplasmic vacuoles may also contribute to the increased granularity observed by flow cytometry in Atg7$^{-/-}$ macrophages, as could the lipid droplets. Although SS was higher in both unstimulated and LPS stimulated-Atg7$^{-/-}$ macrophages, the increase following stimulation was not as great as that observed in wildtype macrophages. Granularity is often taken as a measure of differentiation or activation due to the increased lysosomes and other organelles, including mitochondria, in activated macrophages(121). This suggests that unstimulated Atg7$^{-/-}$ macrophages may have a higher activation state than unstimulated wildtype macrophages, possibly from endogenous production of cytokines or sensitivity to serum present in the media. It is also possible that accumulation of protein aggregates and organelles in the absence of autophagy creates more light scattering in the cytoplasm, thereby contributing to higher SS by flow cytometry.

3.21 Defective autophagy in Atg7$^{-/-}$ macrophages

Deletion of the essential autophagy gene Atg7 in hematopoietic cells leads to defective autophagy in macrophages. Very few autophagosomes were present in unstimulated or IFNγ stimulated Atg7$^{-/-}$ macrophages, though a small but significant increase in autophagosomes was visible in LPS stimulated macrophages by fluorescence microscopy.

Atg7 is essential for canonical autophagy(46), however an Atg7/Atg5 independent, non-canonical pathway has since been described(146), which does not require Atg7 or Atg5 and does not result in lipidation of LC3. Non-canonical autophagy was detected in several embryonic tissues and appeared to have a role in clearance of mitochondria during erythrocyte maturation under the conditions tested. Although lipidation of LC3 is not involved in the non-canonical pathway, double-membraned autophagosomes are still formed, which may be what is seen in LPS-stimulated $Atg7^{-/-}$ macrophages. However, the alternative pathway is clearly not able to completely substitute for canonical autophagy in these macrophages, or in Vav-Atg7 mice in general, as the phenotype of the mice is still severe. Non-canonical autophagy also appears to have different inducing stimuli than classical autophagy, being stimulated by etoposide but not rapamycin, though both pathways can be stimulated by starvation. This differential signalling requirement may also explain why autophagosomes were only visible in LPS, but not IFNγ-stimulated $Atg7^{-/-}$ macrophages. Additionally, punctate LC3 has been observed previously in macrophages transfected with LC3-GFP, even in the absence of autophagic stimulation(92), in $Atg7^{-/-}$ hepatocytes(46), and in primary $Atg7^{-/-}$ macrophages in our laboratory, using Imagestream analysis or particular antibodies. The origin of these puncta is possibly non-lipidated LC3, or incomplete autophagosomes, such as those that are visible by electron microscopy, and therefore likely not representative of true classical autophagosomes. Further assessment of the origin of LC3 puncta in autophagy-deficient cells may need to be done via very high resolution confocal microscopy in order to confidently assert that the occasionally higher LC3 staining observed in $Atg7^{-/-}$ cells is not due to autophagy.

Some autophagosomes were also present in unstimulated wildtype macrophages that had been incubated in complete medium. These could represent basal autophagy due to

normal cellular function, or as a result of declining nutrient content in the media after 7 days of culture.

3.22 Higher cell death in Atg7$^{-/-}$ macrophages

Autophagy is known to be involved in cellular survival in both tumours(4) and primary cells(77, 124). As such it is not surprising to find higher cell death in Atg7$^{-/-}$ macrophages than in wildtype macrophages. However, unlike in T-cells and B-cells, which are severely reduced(72, 77) as a result of loss of autophagy, numbers of macrophages in the tissues, blood and peritoneal cavity of Vav-Atg7 mice are increased, not decreased, in spite of their increased susceptibility to cell death. This suggests that autophagy is not as important as a survival factor in macrophages as in lymphocytes. Indeed, while Atg7$^{-/-}$ CD4 and CD8 T-cells had 2 and 2.4 times, respectively, the proportion of caspase-3^{+} cells(147), the proportion of Atg7$^{-/-}$ bone marrow-derived macrophages was only 20% higher than in wildtype unstimulated macrophages, increasing to 30% higher following LPS stimulation. A similar pattern was observed in Annexin V staining, though cell death did increase by a larger amount following LPS stimulation. Reduced survival in lymphocytes in the absence of autophagy is likely due to the accumulation of damaged mitochondria, as autophagy plays an essential role in mitochondrial control in peripheral T lymphocytes(148). Macrophages (and neutrophils) have comparatively fewer mitochondria(149) and, as such, mitophagy is likely less important to macrophages. Macrophages do, however, produce large amounts of ROS(150), which are vital for macrophage killing mechanisms(151) as well as playing a major signalling role(152). As such, macrophages have specially adapted antioxidant and ROS scavenging responses that help to control ROS levels within the cell, and prevent damage, such as the Nrf2 pathway, which results in upregulation of antioxidant molecules(153). However, ROS also stimulate autophagy(154), and autophagy

plays a role in protection against ROS by removing damaged mitochondria(155). This suggests that although macrophages have developed antioxidant mechanisms to help them prevent oxidative stress, the loss of one such pathway, autophagy, renders them more sensitive to cell death, particularly following stimulation. This hypothesis could be tested by culturing macrophages in the presence of antioxidants such as N-acetyl-Cysteine (NAC) or the mitochondrial ROS-specific antioxidant diphenylene iodonium (DPI)(156), and assessing whether their addition reduced cell death levels in $Atg7^{-/-}$ macrophages.

2.23 Loss of autophagy results in reduced phagocytosis and nitric oxide burst in macrophages

Phagocytosis is one of the fundamental anti-pathogenic defences in the macrophage arsenal. In $Atg7^{-/-}$ macrophages, phagocytosis of latex beads was found to be significantly reduced, but not abolished, with 50% of macrophages bead positive in $Atg7^{-/-}$ cultures compared with 60% in wildtype, and little increase observed in $Atg7^{-/-}$ macrophage phagocytosis following LPS stimulation. The residual phagocytosis suggests that autophagy is not directly required for phagocytosis of beads, but rather that its role is indirect. Other forms of phagocytosis (e.g. bacteria or opsonised RBC) were not assessed, and may require autophagy to a greater or lesser extent, though similar machinery is required for most phagocytic substrates. Investigation of downstream events of phagocytosis would be an interesting follow up to this experiment, to determine whether loss of autophagy also inhibited intracellular killing, as in the case of *Mycobacterium Tuberculosis,* or degradation of phagosomes contents.

As discussed earlier, lamellipodia formation appears to be affected by the loss of autophagy. Reorganisation of actin filaments at the surface is required for particle engulfment(130), and changes in expression of this type of protein were observed in

$Atg7^{-/-}$ macrophages, potentially reducing the phagocytic response. Alterations in membrane dynamics may also affect the expression of phagocytic receptors, such as CD11b and Fc Receptor. Likewise, the increased levels of cell death observed in macrophages could also reduce their phagocytic potential. Autophagy and Atg7 have also been shown to have other links with phagocytosis. For example, Atg7, but not autophagy, was found to be important for the recruitment of LC3 to phagosomes (not autophagosomes) following TLR mediated phagocytosis(92). Autophagy has also been shown by some groups to be required for acquisition of phagocytic functions by macrophages, using macrophages derived from $Atg7^{-/-}$ bone marrow(91). By contrast, it has also been shown that initiation of autophagy inhibits phagocytosis(93), though this may be temporally dependent, with phagocytic particles potentially initiating autophagy to prevent the further uptake of particles and allow degradation of phagosomes already present. Recently, loss of autophagy has been shown to enhance, not decrease, phagocytic uptake of *M. Tuberculosis*, a phenomenon that was traced to increased scavenger receptor expression(94). These data all indicate a close relationship between phagocytic and autophagic pathways, which is not surprising due to their close evolutionary relationship(157), under varying circumstances of stimulation and phagocytic target (bacteria vs. beads, in the presence or absence of stimulation). However, phagocytosis is clearly not dependent on functioning autophagy or Atg7 in some circumstances, suggesting phagocytic pathways that are completely independent from autophagy.

The release of NO following stimulation was also affected by lack of Atg7 in macrophages, with very little NO detected in $Atg7^{-/-}$ macrophage supernatants even following stimulation with LPS, a known NO stimulant in macrophages(158). NO is generated from L-arginine by three different NO synthases, two of which are inducible and the third which is upregulated by transactivation of the appropriate gene(159) during

inflammation. The role played by NO during inflammation is controversial, with conflicting inflammatory and anti-inflammatory roles reported(160). Reduced expression of iNOS and inhibition of autophagy have been induced by the same agents, suggesting an interconnection of pathways may exist(161). Furthermore, NO exhibits potent inhibitory effects on autophagy by reduction of Bcl-2 phosphorylation, which strengthens the Bcl-2-Beclin 1 interaction and thus disrupts hVps34/Beclin 1 complex formation and initiation of autophagy(67). This illustrates a differential role for different species of ROS (of which NO is one), with superoxide signalling inducing autophagy(162), whereas NO inhibits autophagy(163). Together they could create a signalling feedback loop, whereby increased ROS signals to induce autophagy but cannot, and therefore activation of iNOS is inhibited, reducing NO production as seen in $Atg7^{-/-}$ macrophages. This could be partly investigated through the use of ROS scavengers to block ROS signalling to determine whether this could restore normal NO production.

3.24 Reduced antigen presentation in capacity in $Atg7^{-/-}$ macrophages

Antigen presentation by professional APCs such as macrophages connects the innate immune system to the adaptive response. Antigen presentation requires antigen uptake, either by phagocytosis or by infection of the antigen presenting cell, with antigens from different sources being processed in different ways. Autophagy has been demonstrated to play a role in many aspects of antigen presentation, both *in vitro* and *in vivo*, by providing an intersection of exogenous or cytosolic antigen, via autophagosomes, with antigen processing machinery. However, no research to date has specifically looked at the role of autophagy in macrophage antigen presentation. We used a male-antigen into female model to investigate whether loss of autophagy in macrophages influences MHC I

restricted antigen presentation to CD8 T-cells, which is known to rely on CD4 help(164). Female recipients of male wildtype macrophages registered double the number of UTY-specific $CD8^+$ T-cells compared to animals that received male $Atg7^{-/-}$ macrophages, indicating that Atg7 deficient macrophages did not efficiently present UTY-antigen. This could be as a result of impaired antigen processing, which has been shown to involve autophagy(165-167), or as a result of reduced surface expression of MHC molecules(168), as will be discussed in the following chapter. Furthermore, it is possible that the alterations in innate functions caused by loss of autophagy, such as reduced phagocytosis and increased cell death, could also indirectly reduce antigen presentation. In order to fully understand the role of autophagy in macrophage antigen processing, a more comprehensive series of experiments would need to be done to investigate each pathway in more detail. Vav-Atg7 mice would not be an ideal model for this, due to lack of lymphocytes, but a macrophage specific $Atg7^{-/-}$ model, using Cre under the control of the LysM promoter, could be useful for this investigation(169).

3.25 Conclusions

These data reveal that although autophagy is dispensable for macrophage differentiation, it nevertheless plays an important role in macrophage innate functions, both directly and indirectly, and that, in the absence of autophagy, many innate functions are significantly reduced. Deletion of Atg7 results in a significant blunting of autophagic potential, with little evidence of autophagosome formation in unstimulated or IFNγ-stimulated macrophages. However, it is possible that low levels of non-canonical autophagy are taking place in response to LPS stimulation, though if true it is insufficient to rescue the altered innate functions of macrophages. Loss of autophagy results in alterations in macrophage shape and production of lamellipodia, which may then have knock-on effects

in the reduction of phagocytosis, adhesion and migration, all of which are vital to macrophage function. Phagocytosis was not fully abolished in the absence of autophagy, suggesting an indirect role for autophagy or Atg7 in this instance. However, it is also possible that even this level of reduction in phagocytic capacity could severely hamper immune responses. In addition, the NO burst from stimulated and unstimulated macrophages was severely blunted in the absence of autophagy, possibly as a result of increased ROS supressing NO production. Finally, presentation of the male-antigen UTY was also significantly reduced in the absence of autophagy, indicating that autophagy in macrophages influences the initiation of adaptive responses as well as influencing vital innate functions. Together, this shows that autophagy has a vital role in the capacity of macrophages to generate appropriate innate responses to challenge, and to initiate adaptive immune responses by antigen presentation to T-cells.

Chapter 4: Introduction

Loss of autophagy influences surface receptor recycling and regulation of inflammation in macrophages

4.1 Surface receptor trafficking

All immune cells rely on the surface expression of specific receptors for activation, signalling and vital effector functions. Most surface markers are synthesised and trafficked to the cell surface via the ER-Golgi standard secretion system. However, some receptors, such as MHC I and MHC II, have specialised pathways for transport to the cell surface, to allow for processing and binding of antigenic peptides in the correct manner or for other modification vital to receptor function.

Surface, and other, proteins are synthesised in the ER, which is responsible for the folding, quality control and glycosylation of much of the cellular proteome. Following synthesis, most proteins are transported to the Golgi, which provides a membrane scaffold for binding of various vital signalling and sorting proteins that are essential for further transport(170). The Golgi are stacked in a highly ordered morphology, with the outer cisternae facing the trans-Golgi network (TGN), which is a tubular vesicular cluster required for execution of final sorting steps to post-Golgi destinations such as the endocytic pathway. From the TGN, proteins can either traffic directly to the plasma membrane, or be sorted into early or recycling endosomes(171).

MHC I transport to the plasma membrane occurs through a slightly different mechanism. MHC I molecules are generated in the ER, from where they receive their antigenic peptide sequences via the transporter for antigen processing (TAP), which translocates peptides into the lumen of the ER from the cytosol or nucleus in an ATP-dependent manner. Successful peptide binding allows the release of MHC I molecule from the MHC class-I-loading complex for delivery to the cell surface via the Golgi as part of the standard secretory pathway(172).

MHC II molecules are composed of α- and β-chains that are assembled in the ER, together with a chaperone protein called the invariant chain (Ii) that serves to stabilize the αβ

heterodimer and prevent inappropriate binding of antigen to the peptide-binding groove(173). Once formed, the αβ-Ii complex leaves the ER, traffics through the Golgi and trans-Golgi TGN, and is delivered to endocytic multivesicular bodies (MVBs) and lysosomes, which are collectively called MHC II compartments (MIICs). MIICs are proteolytically active compartments where proteins are processed into peptides. However, there is debate about whether MHC II complexes traffic via endocytic compartments at all, with some research arguing that they are able to travel directly from the TGN to the plasma membrane, and from there enter early recycling endosomes or the endocytic pathway(174). It is possible that neither pathway is mutually exclusive, with some complexes trafficking directly to the cell surface, and others travelling via MVBs and MIICs. The use of multiple pathways may ensure that newly-synthesized MHC II molecules have maximum access to potential foreign antigens present in many different intracellular compartments(175). Antigens can bind MHC II following degradation of the Ii(176). Trafficking of MHC II-peptide complexes from the MVBs to the membrane is much less understood. Some experiments using time-lapse fluorescence microscopy have shown direct fusion of MIICs with the plasma membrane, however this is not thought to be the major pathway used(177). Other studies have shown that MHC II traffics from within MVBs to the plasma membrane via the formation of long tubular organelles that extended into the cellular periphery. Vesicles form from the tips of the tubules and non-selectively incorporate MHC II, from where they are thought to travel to the plasma membrane(178).

4.2 Autophagy and regulation of inflammation

The autophagy pathway and associated proteins also play a role in regulation of the inflammatory response, through control of inflammatory transcriptional responses and

induction of the inflammasome. Genetic disruption of autophagy is associated with several inflammatory diseases, including Crohn's disease(179-181), systemic lupus erythematosus(182), asthma(183) and rheumatoid arthritis(184). The inflammasome is a multi-protein complex induced by pathogens or other stressors to release pro-inflammatory cytokines(185). Endotoxin-stimulated autophagy-deficient macrophages release increased levels of the inflammatory cytokines IL-1β and IL-18 due to increased activation of caspase 1(186) or mitochondrial DNA (mtDNA) release and elevated reactive oxygen species present in the cytoplasm(7). Autophagy normally acts to remove damaged mitochondria from the cytoplasm, thereby reducing mtDNA release and regulating the inflammatory response. Conversely, activation of autophagy by inflammatory signalling serves to dampen the immune response and inflammatory cytokine production by targeting ubiquitinated inflammasomes for destruction(187).

Inflammasome-independent regulation of the inflammatory response has also been reported. Inhibition of autophagy in PBMCs resulted in significantly increased IL-1β production following stimulation with TLR2 or TLR4 ligands, while simultaneously reducing TNFα expression, whereas induction of autophagy by starvation resulted in decreased IL-1β production. Inflammasome activation was not observed, but rather changes in cytokine production occurred on a transcriptional level, possibly involving inhibition of p38 MAPK phosphorylation(188). Furthermore, accumulation of p62 in autophagy-deficient cells results in activation of the pro-inflammatory transcription factor NF-κB(189) and enhanced activity of the stress-induced transcription factor Nrf2(190), which can also result in increased inflammatory cytokine expression.

Control of inflammation by autophagy illustrates its diverse role in the immune system, whereby it not only ensures the initiation of the correct immune response, but also prevents excessive inflammatory signalling at the conclusion of infection.

4.3 Autophagy in the regulation of surface antigen presentation and the inflammatory response

This chapter explores a novel role for autophagy in surface expression of important macrophage surface markers such as MHC II and CD86. Loss of autophagy results in reduced surface expression of such important receptors and a diminished upregulation following stimulation. However, similar levels of protein are produced, but trapped inside the cell, suggesting that autophagy or autophagy machinery contributes to the surface marker expression pathways. Furthermore, autophagy-deficient macrophages are shown to be highly inflammatory, producing higher levels not only of inflammasome-associated cytokines, but other inflammatory cytokines, chemokines and growth factors. Together, these may contribute to the increased numbers of myeloid cells present in Vav-Atg7 mice.

Chapter 4: Results

Loss of autophagy influences surface receptor recycling and regulation of inflammation in macrophages

4.4 Atg7$^{-/-}$ macrophages inefficiently up-regulate MHC II and other surface molecules following stimulation with LPS or IFNγ

To effectively respond to immune stimuli and generate appropriate responses, macrophages need to be able to up-regulate surface antigens associated with immunity, such as the antigen presentation molecule MHC II. MHC II levels were assessed by flow cytometry after overnight stimulation with LPS or IFNγ. Expression of MHC II was

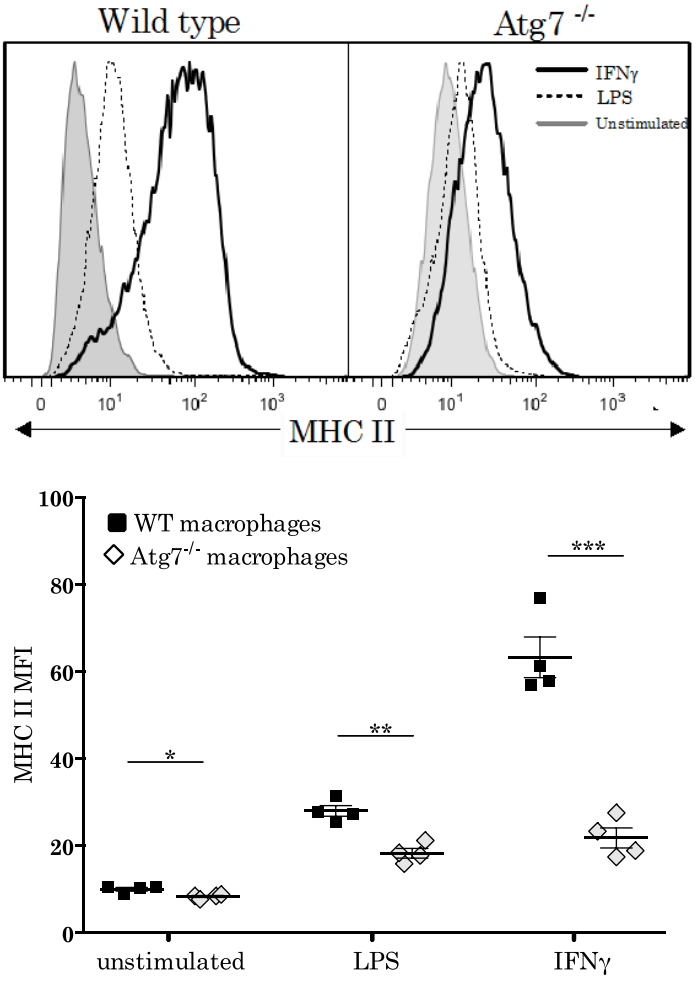

Figure 4.1: *Expression of the antigen presentation molecule MHC II on BMMϕ. BMMϕ were stimulated overnight with LPS (1µg/ml) or IFNγ (10 ng/ml) and analysed by flow cytometry. Top: Representative histograms of MHC II on wildtype and Atg7$^{-/-}$ macrophages following stimulation. Bottom: MHC II expression on wildtype and Atg7$^{-/-}$ macrophages as represented by MFI. Results are representative of six independent experiments, n = 4. Error bars represent SD. *p<0.05, **p<0.01.*

detectable on Atg7$^{-/-}$ macrophages and generally increased following stimulation (figure 4.1). In the majority of experiments, expression was significantly lower on Atg7$^{-/-}$ macrophages.

However, there were instances where MHC II expression was similar or slightly increased on unstimulated Atg7$^{-/-}$ macrophages (not shown). Expression following LPS or IFNγ stimulation was always lower on Atg7$^{-/-}$ macrophages, nevertheless. Decreased MHC II expression following stimulation could indicate that Atg7$^{-/-}$ macrophages cannot fully

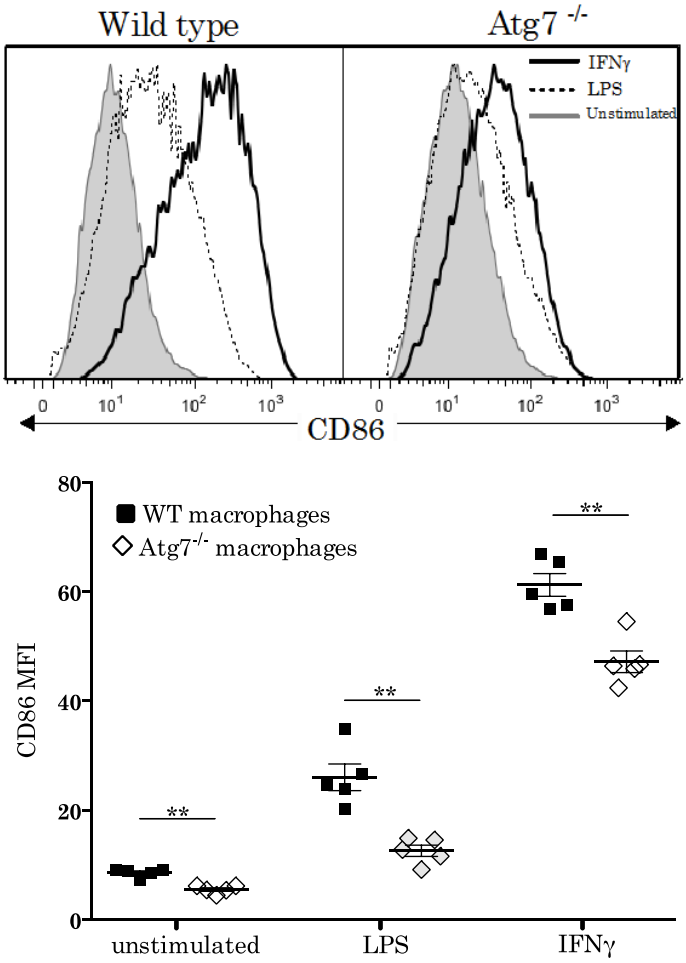

Figure 4.2: *Expression of the co-stimulatory molecule CD86 on BMMϕ. Macrophages were cultured as described in figure 1.8.1 and analysed by flow cytometry. Top: Representative histograms of CD86 on wildtype and Atg7$^{-/-}$ macrophages. Bottom: CD86 expression on wildtype and Atg7$^{-/-}$ macrophages as represented by MFI. Results are representative of six independent experiments. Error bars represent SD, n = 5. **p<0.01.*

mature in response to immune stimuli, which could reduce their functional capacity in response to pathogens. CD86 is expressed on APCs such as macrophages, and provides co-stimulatory signals that are required for T-cell activation concomitantly with TCR/MHC interactions. Both wildtype and Atg7$^{-/-}$ macrophages express CD86 in the resting state (figure 4.2), and CD86 expression increased on both following stimulation with LPS or IFNγ. However, Atg7$^{-/-}$ macrophages expressed a significantly lower level of CD86 than wildtype macrophages, and similarly to MHC II, had a significantly smaller up-regulation following stimulation.

TLR4 is a PRR that is highly expressed on macrophages and recognises the bacterial endotoxin LPS. Signal transduction through TLR4 and its co-receptor CD14 creates a cascade of signalling events that result in differential expression of surface molecules and expression of cytokines amongst other things(191). As reduced TLR4 expression could result in reduced downstream signalling, and therefore potentially altered expression of many other surface antigens, TLR4 and CD14 expression were investigated on Atg7$^{-/-}$ macrophages.

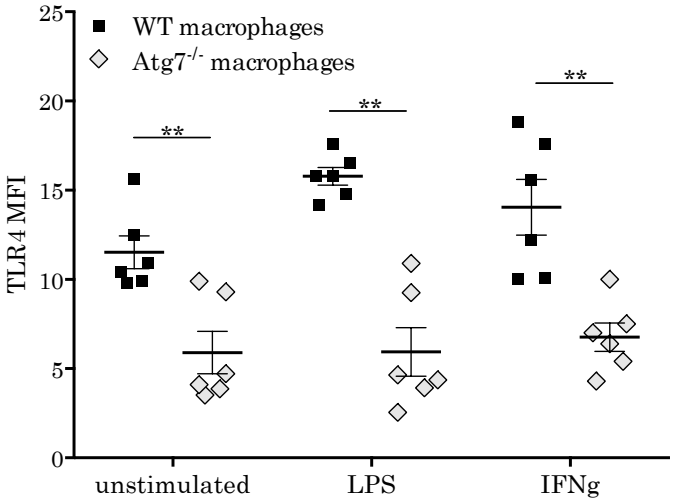

Figure 4.3: *TLR4 expression on BMMϕ. Macrophages were cultured as described in figure 1.8.1 and analysed by flow cytometry. TLR4 expression on wildtype and Atg7$^{-/-}$ macrophages was assessed by plotting MFI of TLR4 fluorescence for each sample. Results are representative of six independent experiments. Error bars represent SD, n = 6. **p<0.01.*

TLR4 and CD14 expression was significantly reduced on autophagy-deficient macrophages, both before and after stimulation. TLR4 was variable on both wildtype and Atg7$^{-/-}$ mice (figure 4.3), but was lower on average on Atg7$^{-/-}$ macrophages for all stimuli. Furthermore, TLR4 was not significantly up-regulated on autophagy-deficient macrophages following LPS stimulation, unlike in wildtype macrophages, where expression increased by almost 50%. IFNγ stimulus also caused a small increase in TLR4 expression on wildtype macrophages that was not seen Atg7$^{-/-}$ macrophages. Expression of the co-receptor CD14 was much more consistent between mice from both experimental groups (Figure 4.4). Atg7$^{-/-}$ macrophage CD14 levels were significantly lower for all stimuli. However, the magnitude of expression increase following LPS stimulation was similar in both groups.

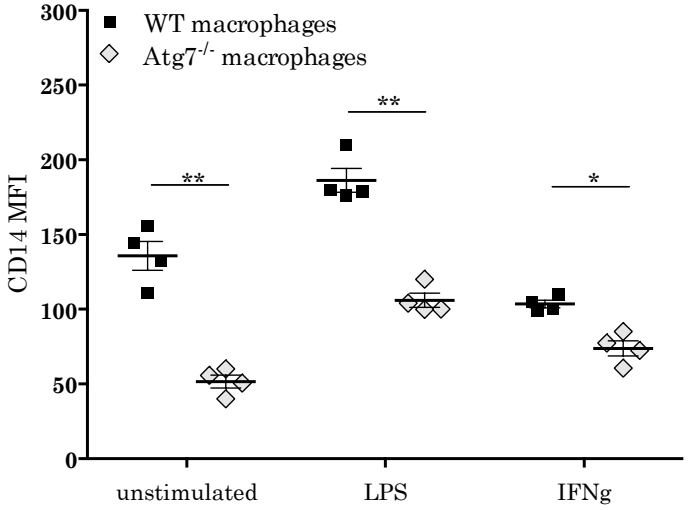

Figure 4.4: *Decreased CD14 expression on Atg7$^{-/-}$ BMMϕ. Macrophages were cultured as described in figure 4.1 and surface marker expression analysed by flow cytometry. CD14 expression on wildtype and Atg7$^{-/-}$ macrophages was assessed by plotting the MFI of CD14 fluorescence for each sample. Result shown is representative of six independent experiments. Error bars represent SD, n = 6. *p<0.05, **p<0.01, un-paired t-test.*

Other macrophage specific (e.g. M-CSFR) and non-specific (e.g. CD48) surface markers were also analysed by flow cytometry in order to determine whether all surface markers were similarly affected by loss of autophagy (figure 4.5). The majority of surface markers investigated show reduced expression on Atg7$^{-/-}$ macrophages.

Marker	**Atg7$^{-/-}$**
F4/80	±/●
CD11b	●
MHC I	↓
MHC II	↓
CD47	↓
CD48	↓
TLR4	↓
CD86	↓
Mannose receptor	↓
CD13	±
CD14	↓
M-CSFR	↓

Figure 4.5 *– Surface marker expression on autophagy-deficient macrophages relative to wildtype. BMMϕ were stimulated overnight as previously indicated, prior to staining for analysis by flow cytometry. Expression of each marker is determined by average geometric mean of fluorescence (MFI) relative to wildtype macrophages. Only significant results are shown. ↓ Decreased expression in Atg7$^{-/-}$ macrophages, ● similar expression in Atg7$^{-/-}$ macrophages, ± variable expression on Atg7$^{-/-}$ macrophages.*

4.5 Disruption of surface antigen expression is not Atg7 specific

Our animal model has a hematopoietic system-specific deletion of Atg7 in order to inhibit the autophagy pathway. However, several Atg genes have separate roles outside the autophagy pathway(192), and it is likewise possible that the defect in surface antigen

expression is due to an autophagy-independent role for Atg7. As such, chemical inhibitors of autophagy were applied to wildtype macrophages to determine whether altered expression of surface antigens is Atg7 specific or due to lack of autophagy. BMMϕ were cultured from wildtype mice in media supplemented with wortmannin and stimulated overnight before analysis of certain antigens by flow cytometry. Similar to $Atg7^{-/-}$ macrophages, wildtype macrophages cultured in the presence of the autophagy inhibitor wortmannin expressed less MHC II than untreated macrophages (figure 4.6). Furthermore, LPS stimulation of wortmannin treated macrophages decreased mean MHC II fluorescence, unlike untreated macrophages where MHC II expression increased with stimulation. IFNγ induced a small increase in MHC II expression in treated macrophages, but expression remained significantly lower than in untreated macrophages. CD86 and TLR4 expression were also analysed on wortmannin treated macrophages (not shown) and found to be significantly lower, in a similar manner to $Atg7^{-/-}$ macrophages.

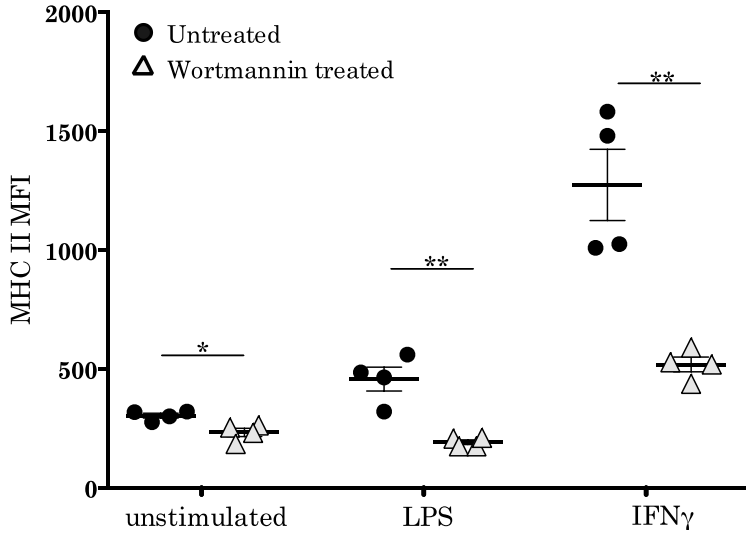

Figure 4.6: *Chemical inhibition of autophagy using wortmannin also causes a reduction in MHC II expression. Wildtype macrophages were cultured in the presence of the autophagy inhibitor, wortmannin (100nM) for 7 days, stimulated overnight with LPS or IFNγ as previously described and stained for flow cytometry. MHC II expression on wildtype and $Atg7^{-/-}$ macrophages was assessed by plotting MFI of MHC II fluorescence for each sample. Results are representative of 2 independent experiments. Error bars represent SEM, n = 4. *p<0.05, **p<0.01, students t-test.*

To determine whether induction of autophagy could positively modulate surface antigen expression, wildtype macrophages were cultured in the presence of the autophagy inducer, rapamycin. Induction of autophagy resulted in increased MHC II expression following stimulation with LPS or IFNγ, though there was some variation in expression following IFNγ stimulus (figure 4.7). Rapamycin treatment of unstimulated macrophages, however, resulted in similar expression to untreated macrophages. Expression of CD86, TLR4 and MHC I were also analysed after treatment with rapamycin, and were found to be increased in a similar manner to MHC II (not shown).

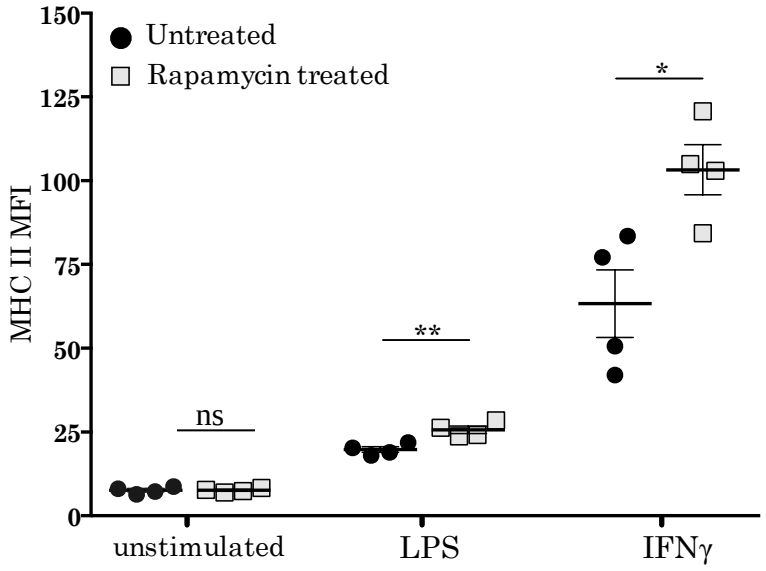

Figure 4.7: *Chemical induction of autophagy using rapamycin causes increased MHC II expression following stimulation. Wildtype macrophages were cultured in the presence of the autophagy inducer, rapamycin (1 μM) for 7 days, stimulated overnight with LPS or IFNγ as previously described. MHC II expression on wildtype and Atg7$^{-/-}$ macrophages was assessed by plotting MFI of MHC II fluorescence for each sample. Results are representative of 2 independent experiments. Error bars represent SEM, n = 4. *p<0.05, **p<0.01, ns = not significant, students t-test.*

Finally, expression levels of important surface markers such as MHC II were analysed on macrophages derived from the bone marrow of mice in which the essential autophagy gene Atg5(114) had been deleted using the same vav-iCre system used to delete Atg7 in our model. BMMϕ were cultured and stimulated in the same manner as for Atg7$^{-/-}$

macrophages. Atg5$^{-/-}$ macrophages showed a similar reduction in MHC II expression as seen for Atg7 deficient macrophages (figure 4.8), both prior to stimulation and after stimulation with LPS or IFNγ.

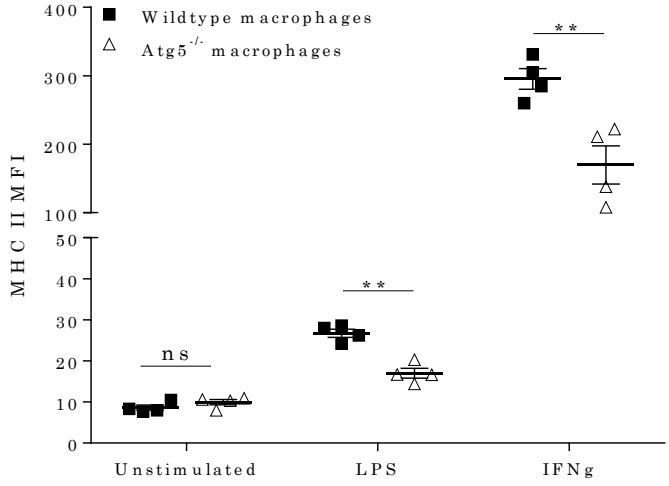

***Figure 4.8**: Reduced expression of MHC II on macrophages deficient in the essential autophagy gene Atg5. Macrophages were cultured from Atg5$^{-/-}$ bone marrow for 7 days in the presence of M-CSF (20 ng/ml), stimulated overnight as previously described. MHC II expression on wildtype and Atg5$^{-/-}$ macrophages as represented by MFI. Results are representative of 2 independent experiments, n=4. Error bars represent SEM. *p<0.05, **p<0.01.*

Previous data from our laboratory has also shown reduced MHC II surface marker expression on Atg7$^{-/-}$ dendritic cells upon LPS stimulation and reduced TCR expression on Atg7$^{-/-}$ T-cells(147), suggesting that this effect is not restricted to the macrophage lineage.

4.6 Altered expression of surface antigens is not limited to stimulation via TLR4

Macrophages are able to recognize a variety of PAMPs via different TLRs in addition to TLR4. Given the relationship between TLRs and autophagy, we investigated whether the effect is extended to signalling in response to other TLR ligands. Atg7$^{-/-}$ macrophages were stimulated overnight with heat killed *Listeria Monocytogenes* (HKLM), a TLR2 ligand, or

polyinosinic-polycytidylic acid (Poly I:C), a synthetic double stranded RNA and TLR3 ligand. Stimulation via alternate TLR pathways did not overcome the surface expression defect, with levels of MHC II on Poly I:C or HKLM stimulated macrophages significantly lower than on wildtype macrophages (figure 4.9). Indeed, Poly I:C stimulation resulted in no significant up-regulation of expression in Atg7$^{-/-}$ macrophages at all, whereas HKLM produced a small increase in expression. The surface markers CD86, MHC I, CD47 and CD48 were also investigated following Poly I:C and HKLM stimulation, and were also found to be significantly lower in Atg7$^{-/-}$ macrophages (data not shown), suggesting that this defect is not specific to signalling via a specific receptor.

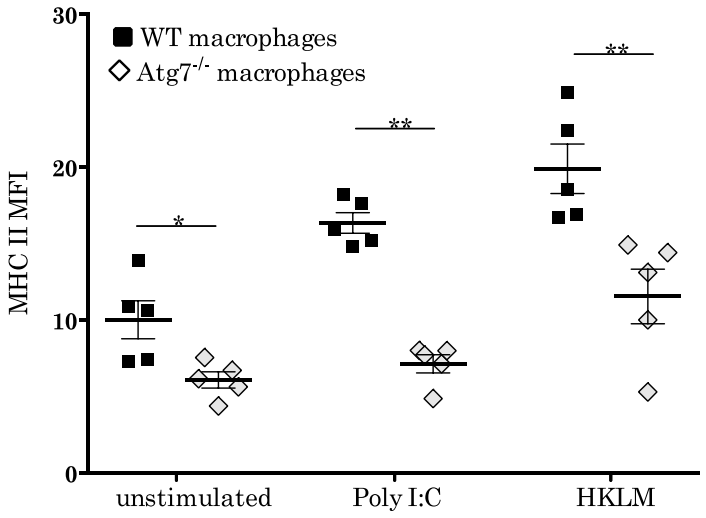

Figure 4.9 *– MHC II up-regulation is significantly impaired following Poly I:C and HKLM stimulation in Atg7$^{-/-}$ macrophages. BMMϕ were cultured for 7 days, stimulated overnight with HKLM (10^8 particles/well) or Poly I:C (1µg/ml) and stained for flow cytometry. Expression levels compared using geometric means of fluorescence of BMMϕ. n = 5, two independent experiments. *p<0.05, **P<0.01, un-paired t-test.*

Pathogen or immune signalling through TLRs drives macrophages toward an inflammatory phenotype, characterised by up-regulation of certain surface markers as described above, the production of various cytokines and increased antigen presentation(193). However, macrophages can also be stimulated by Th2 type cytokines (e.g. IL-4, IL-10 and IL-13) or tumour products to become alternately activated

macrophages (AAM)(194), producing polyamines and proline which induce cellular proliferation and collagen production(59). AAM are characterised by increased expression of the mannose receptor (MR), a C-type lectin carbohydrate-binding protein that is involved in pathogen recognition. In order to determine whether the surface marker expression and up-regulation defect was limited to type 1, inflammatory macrophages, BMMϕ were cultured as before and stimulated with IL-4 and IL-13 to become AAM. MR expression was significantly lower on Atg7$^{-/-}$ macrophages following stimulation with LPS or IL-4/IL-13 (figure 4.10). However, in contrast to other surface markers, expression on unstimulated Atg7$^{-/-}$ macrophages was not significantly different than wildtype macrophages.

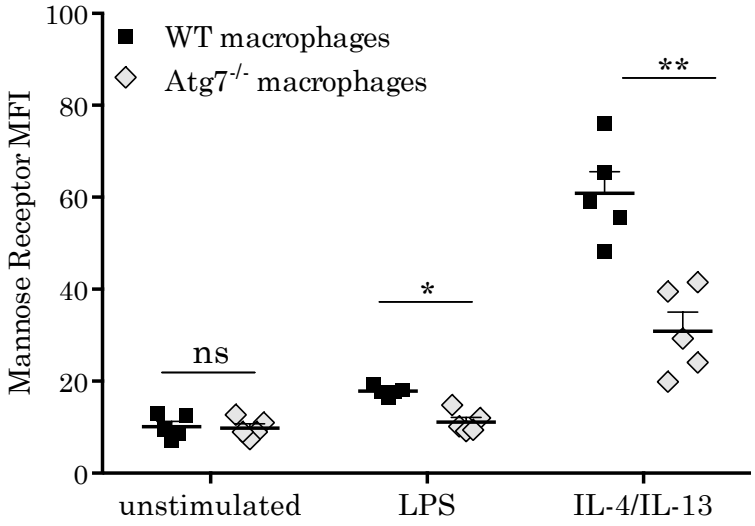

Figure 4.10: *Mannose receptor expression on BMMϕ. Macrophages were cultured as described previously, stimulated overnight with IL-4 and IL-13 (each 1 μg/ml) and surface marker expression analysed by flow cytometry. Results are representative of two independent experiments, n = 4. Error bars represent SD, n = 5.*p<0.05, **p<0.01, un-paired t-test.*

Finally, different concentrations of LPS were used to stimulate the macrophages to determine whether increasing the signal was sufficient to fully mature the macrophages. The highest expression of MHC II was found occurring the at second lowest concentration of LPS, and no tested LPS concentration was sufficient to bring Atg7$^{-/-}$ MHC II expression

levels in line with their wildtype counterparts (figure 4.11). These data suggest that the maturational defect is not limited to specific stimulation pathways and cannot be overcome by saturating amounts of stimulation.

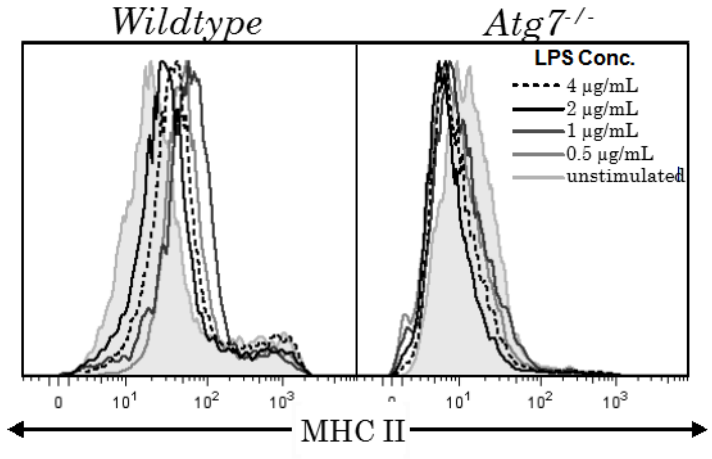

Figure 4.11*: Increasing concentration of stimuli cannot overcome the up-regulation defect. BMMϕ were cultured as previously described and stimulated overnight using increasing concentrations of LPS as shown. Overlaid histograms of MFI of MHC II fluorescence from wildtype and Atg7$^{-/-}$ macrophages shown. Representative histograms of three independent experiments, n = 4.*

4.7 Loss of Atg7 results in increased cell size in macrophages

As reduced cell size may also appear as reduced apparent surface expression, we compared wildtype and Atg7$^{-/-}$ cell size using an imaging flow cytometer. Surface area of F4/80^{+} CD11b^{+} cells was compared using a cell size Wizard in the ImageStream IDEAS software. Atg7$^{-/-}$ macrophages were found to have a larger average surface area than wildtype macrophages (figure 4.12), ruling out the possibility that reduced surface expression is due to smaller cell size.

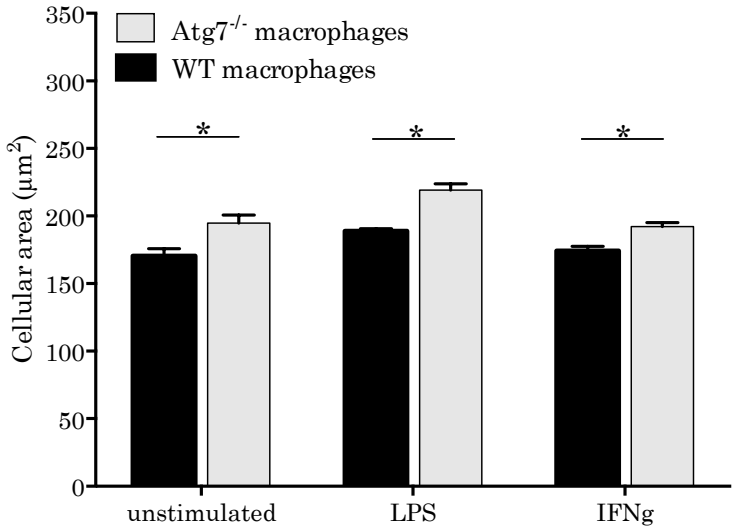

***Figure 4.12**: Atg7$^{-/-}$ macrophages have a larger surface area than wildtype macrophages. BMMϕ were cultured, stimulated and stained for surface markers as previously described. Cell size was assessed on F4/80^{+} CD11b^{+} cells using an image flow cytometer to evaluate surface area. Graph shows average cell size, error bars represent SEM, n = 4. Data representative from two separate experiments, *p<0.05 un-paired t-test.*

4.8 Autophagy influences expression of some genes for cell surface proteins

Lower surface marker expression could be due to reduced or altered gene transcription, and thus levels of MHC II, TLR4 and M-CSFR gene expression were investigated. Gene expression was investigated by qPCR analysis of macrophage mRNA using specific primers and normalising expression to GAPDH expression within the cells. Naive Atg7$^{-/-}$ macrophages were found to produce 77% of wildtype MHC II mRNA, but similar levels were observed following stimulation with LPS (figure 4.13).

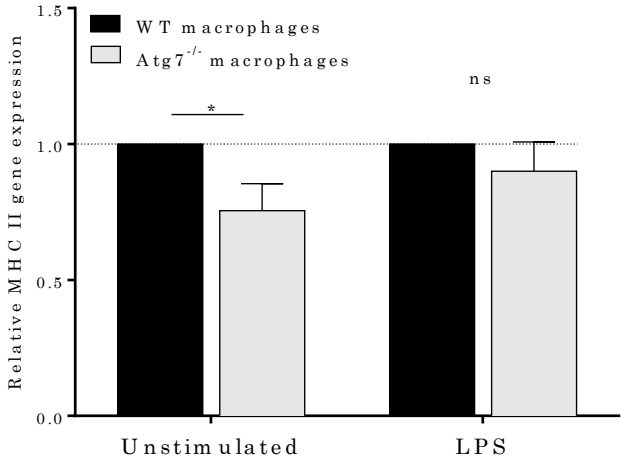

Figure 4.13: *Relative MHC II mRNA expression in Atg7$^{-/-}$ macrophages. BMMϕ were cultured and stimulated overnight with LPS as previously described. Total RNA was extracted using Trizol reagent and reverse transcribed to cDNA. Values determined using the ΔΔCT method, normalised to GAPDH and compared to wildtype macrophages cultured under the same conditions. Dotted line represents wildtype expression levels. Error bars represent standard deviation of 3 experiments, *p<0.05, un-paired t-test.*

Analysis of TLR4 gene expression, however, revealed a significant reduction in expression in Atg7$^{-/-}$ macrophages, of less than 50% of wildtype in unstimulated macrophages, and increasing to 61% following stimulation with LPS (figure 4.14).

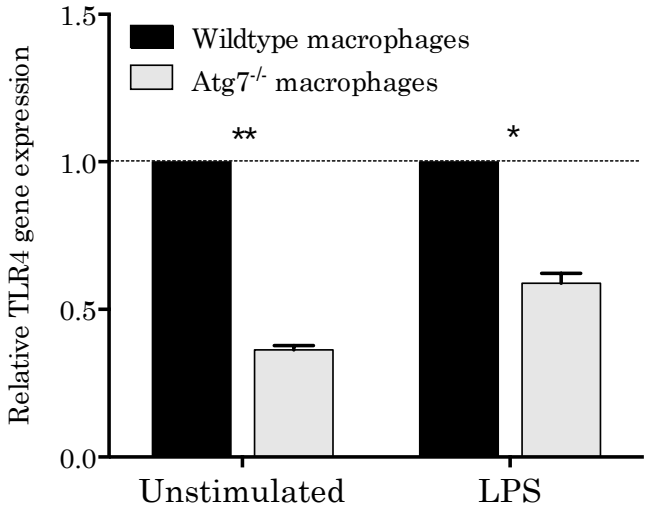

Figure 4.14*: Relative TLR4 mRNA expression in Atg7$^{-/-}$ macrophages. BMMϕ were cultured and stimulated overnight with LPS as previously described. Total RNA was extracted using Trizol reagent and reverse transcribed to cDNA. Values determined using the ΔΔCT method, normalised to GAPDH and compared to wildtype macrophages cultured under the same conditions. Dotted line represents wildtype expression levels. Error bars represent standard deviation of 3 experiments, *p<0.05, un-paired t-test.*

Finally, levels of another macrophage specific gene, the M-CSF receptor, were analysed. In contrast to TLR4 gene expression, levels of M-CSFR transcripts were found to be similar in Atg7$^{-/-}$ and wildtype macrophages (figure 4.15). Unlike MHC II and TLR4 gene expression, there was even a small increase above wildtype levels following LPS stimulation, though this was not found to be statistically significant. Together, these data suggest that autophagy may influence expression of surface marker genes, though its influence varies for each gene and may only be indirect.

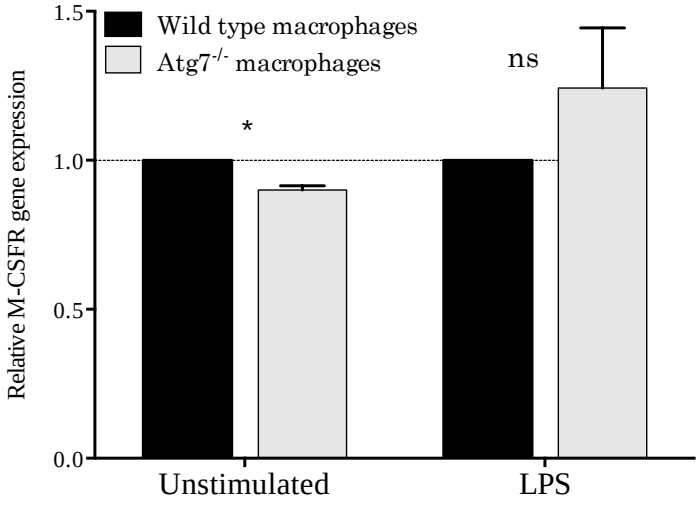

Figure 4.15: *Relative M-CSFR mRNA expression in Atg7$^{-/-}$ macrophages. BMMϕ were cultured and stimulated overnight with LPS as previously described. Total RNA was extracted using Trizol reagent and reverse transcribed to cDNA. Values determined using the ΔΔCT method, normalised to GAPDH and compared to wildtype macrophages cultured under the same conditions. Dotted line represents wildtype expression levels. Error bars represent standard deviation of 3 experiments, *p<0.05, un-paired t-test.*

4.9 Total MHC II expression is similar in Atg7$^{-/-}$ macrophages

As analysis of gene expression had revealed some differences between surface marker mRNA levels in Atg7$^{-/-}$ macrophages, it was important to ascertain whether total protein levels were altered in a similar fashion. As such, we investigated whether similar amounts of MHC II protein were being produced and thereby eliminate the possibility of a protein

synthesis defect or low protein production due to reduced gene expression. To determine whether wildtype and Atg7$^{-/-}$ macrophages synthesise similar amounts of MHC II protein, surface and intracellular staining of MHC II was combined to assess total MHC II intensity using an imaging flow cytometer. Despite minor changes in mRNA expression, Atg7$^{-/-}$ macrophages unexpectedly showed comparable total levels of MHC II to wildtype macrophages (figure 4.16). Total MHC II fluorescence increased by equivalent amounts following stimulation with either LPS or IFNγ, indicating that similar amounts of MHC II were being produced in both unstimulated macrophages and following activating stimuli.

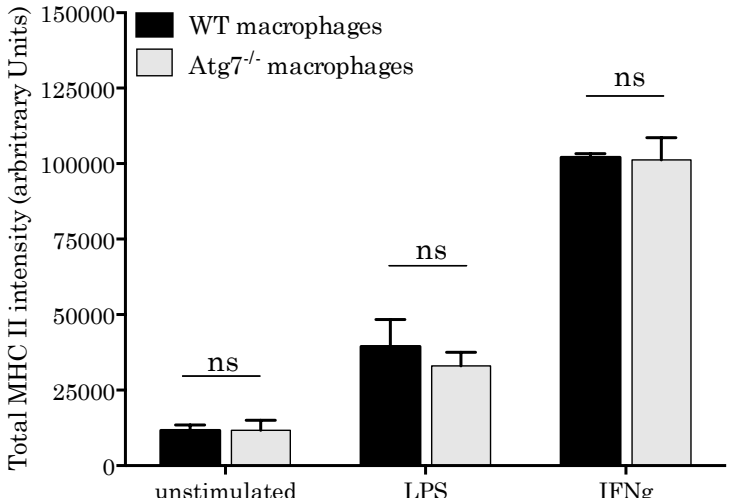

***Figure 4.16**: Total MHC II expression in macrophages as assessed by ImageStream. BMMϕ were cultured and stimulated overnight with LPS as previously described. Harvested macrophages were stained for surface markers, and fixed and permeabilised for intracellular MHC II staining. Total MHC II was analysed by ImageStream analysis of internal and external MHC II fluorescence intensity of CD11b^{+}F4/80^{+} macrophages. Data representative of 2 independent experiments. Error bars represent SEM, n = 4, ns = not significant, un-paired t-test.*

4.10 Atg7$^{-/-}$ macrophages have higher intracellular levels of MHC II

Reduced MHC II surface expression coupled with similar total expression suggested that MHC II may be trapped intracellularly in Atg7$^{-/-}$ macrophages. Intracellular MHC II content was investigated by permeabilising fixed BMMϕ to allow internal MHC II

staining in addition to surface MHC II. The internal MHC II load was assessed by applying a surface mask, using CD11b staining, to the macrophages using ImageStream IDEAS software. Intracellular levels of MHC II in Atg7$^{-/-}$ macrophages were significantly higher than those of wildtype macrophages (figure 4.17), with the highest internal MHC II load occurring in unstimulated macrophages. Stimulation with either LPS or IFNγ resulted in a decrease in internal staining in wildtype and Atg7$^{-/-}$ macrophages, suggesting that in Atg7$^{-/-}$ macrophages, intracellular MHC II is still trafficked to the surface following stimulation, but not to the same extent as in wildtype macrophages.

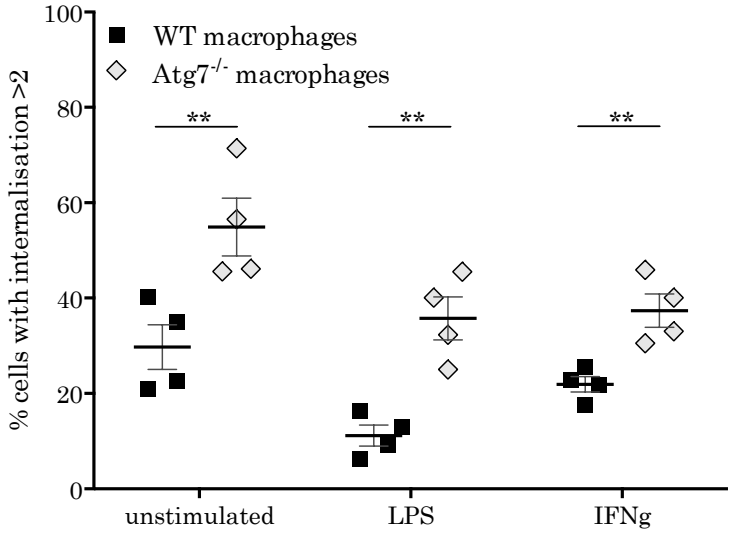

Figure 4.17: *Intracellular MHC II staining in BMMϕ as assessed by ImageStream analysis. Macrophages were cultured, stimulated overnight and stained for the macrophage surface markers, F4/80 and CD11b. Cells were then fixed and permeabilised to allow surface and internal MHC II staining. Internal MHC II was evaluated using a mask to exclude surface staining and using the internalisation wizard available from Amnis. The lower threshold for internal fluorescence was set at 2 arbitrary units. Data representative of two independent experiments. Error bars represent SEM, n = 4. **p<0.01, un-paired t-test.*

The micrograph images showed brighter, more punctate internal staining in Atg7$^{-/-}$ macrophages, relative to the bright surface but diffuse internal staining shown by the wildtype macrophages (figure 4.18). There was also significantly less surface MHC II visible on the Atg7$^{-/-}$ macrophages, in agreement with the flow cytometry data. These

results suggest that MHC II is produced at normal levels in autophagy-deficient macrophages, but that it is trapped intracellularly and not presented efficiently on the surface of the macrophages during development or maturation.

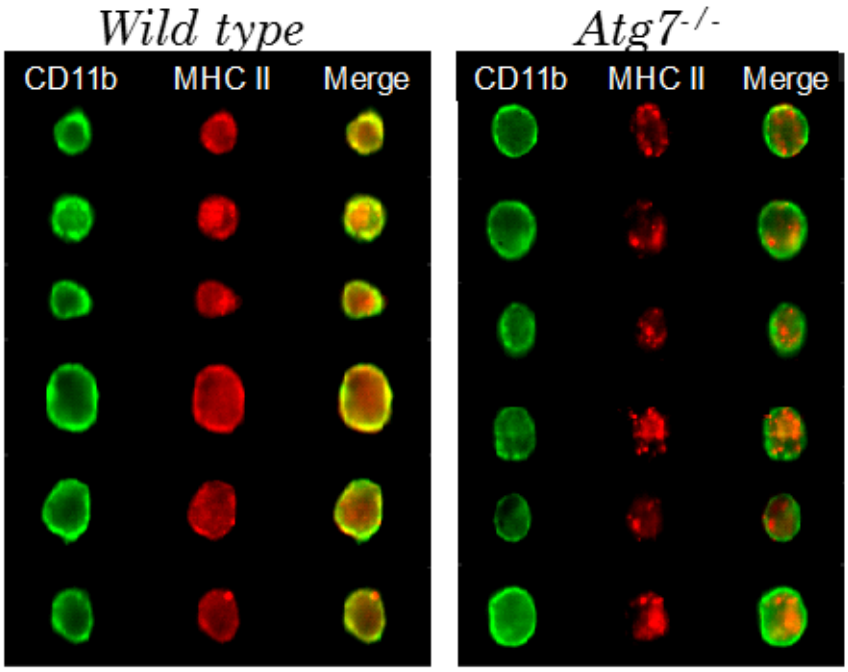

Figure 4.18: *Surface and internal MHC II staining in BMMϕ. Macrophages were cultured, stimulated and stained as described above. Representative micrographs of F4/80$^+$ CD11b$^+$ cells from wildtype and Atg7$^{-/-}$ macrophages, selection of six random images for each genotype.*

4.11 Atg7$^{-/-}$ macrophages show different expression of many proteins involved with protein and lysosomal trafficking

Proteomic analysis of protein extracts taken from Atg7$^{-/-}$ and wildtype macrophages revealed differential expression of a variety of proteins involved in trafficking, which may be responsible for the reduced surface marker expression capacity of Atg7$^{-/-}$ macrophages (figure 4.19). Transport proteins that had increased expression in Atg7$^{-/-}$ macrophages include vimentin, an intermediate filament protein that has a role in integrin recycling(195), and ezrin, a peripheral membrane protein that facilitates interactions between the cytoskeleton and the plasma membrane and has a direct role in the trafficking

of some receptors(196). Tumour protein D52 is also known to have a major role in lysosomal trafficking to the plasma membrane, with overexpression leading to an accumulation of the lysosomal marker LAMP1 on the plasma membrane(196). Cytohesin-associated scaffolding protein (CASP), is important for the recruitment and assembly of protein complexes that are associated with intracellular trafficking and signalling(197), and is particularly expressed during times of cellular stress to improve intracellular signalling and trafficking. Strikingly, there are also a major group of transport proteins that show reduced expression in $Atg7^{-/-}$ macrophages – the Rab proteins, part of the Ras superfamily of small GTPases proteins, which have central roles in many aspects of cellular trafficking(198). Through their actions, Rabs regulate membrane fusion and vesicle movement and formation, and reductions in their expression have been linked to reduced surface expression of various receptors(199-201). Higher levels of cytosolic MHC II were also observed by proteomic analysis, providing supporting evidence to the data suggesting normal production of MHC II, with reduced trafficking to the cell surface.

Protein ID		**Protein Name**	**Score**	**WT:KO ratio**
Transport Related Proteins				
P20152	Vimentin	1755.1	0.5	0
Q62393	Tumour protein D52	235.5	0.6	0.01
P70403	Protein CASP	659.7	KO only	KO only
P26040	Ezrin	744.1	KO only	KO only
P61027	Rab 10	231	1.77	1
P35283	Rab 13	195	WT only	WT only
Q91V41	Rab14	339	1.79	0.96
Q8K386	Rab 15	140	2.44	0.98
P62821	Rab 1A	270	1.63	1
Q9D1G1	Rab 1B	249	1.88	1
Q504M8	Rab 26	231	1.72	0.98
Q921E2	Rab 31	406	WT only	WT only

P63011	Rab 3A	200	WT only	WT only
Q9CZT8	Rab 3B	214	WT only	WT only
P62823	Rab 3C	170	WT only	WT only
P35276	Rab 3D	195	WT only	WT only
Q91ZR1	Rab 4B	234	WT only	WT only
P51150	Rab 7a	332	WT only	WT only
P55258	Rab 8A	213	2.1	1
P61028	Rab 8B	233	2	1
Surface markers				
P01904	H-2 class II histocompatibility antigen, E-D alpha chain	229	KO only	KO only
P04224	H-2 class II histocompatibility antigen, E-K alpha chain	228	KO only	KO only

***Figure 4.19**: Atg7$^{-/-}$ macrophages show altered expression of many proteins associated with intracellular trafficking. Bone marrow derived macrophages were cultured for 7 days and stimulated overnight with LPS (1 µg/ml). Protein extracts were produced from pooled wildtype and Atg7$^{-/-}$ macrophages, adjusted to the same protein concentration and analysed by tandem mass spectrometry. Protein score is a measure of protein abundance. Significance is denoted as p<0.05 for proteins with increased expression in Atg7$^{-/-}$ macrophages, and p>0.95 for proteins with increased expression in wildtype macrophages. Grateful acknowledgements to Dr Benedikt Kessler for performing the proteomic experiments and assisting with their analysis.*

4.12 Autophagy-deficient macrophages are highly inflammatory

As TLR4 expression was shown to be reduced, it was important to determine whether signalling was impaired downstream of TLRs. Downstream signalling was assessed by investigating the expression of several cytokines following LPS stimulation using ELISA analysis of supernatants and intracellular flow cytometry. In agreement with others(7, 186), we find increased IL-1β in the supernatant (figure 4.20) following overnight stimulation with LPS. However, we also find significantly increased IL-1β secretion in

unstimulated macrophages, suggesting an increased inflammatory phenotype in autophagy-deficient macrophages even in the resting state.

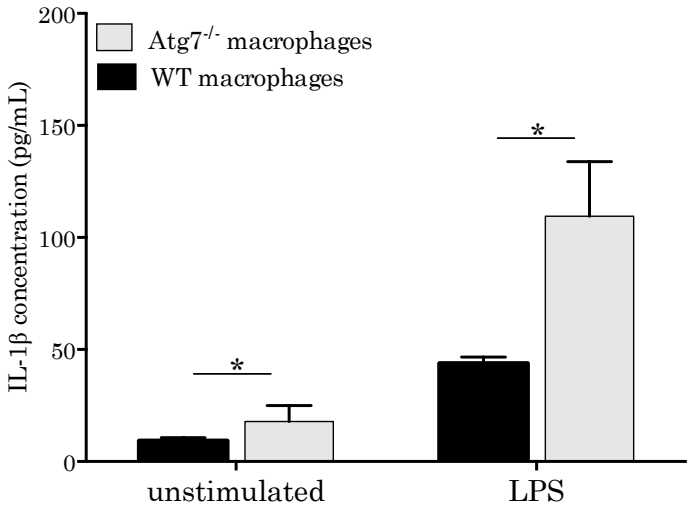

Figure 4.20: *Increased IL-1β secretion by Atg7$^{-/-}$ BMMϕ. Cytokine production was assessed by ELISA of macrophage supernatants following overnight stimulation with LPS (1 µg/ml). Error bars represent SEM, graph representative of four separate experiments, n=3. *p<0.05, un-paired t-test.*

However, in contrast to work by other groups(188), we also find significantly increased expression of other inflammatory cytokines, namely TNF-α and IL-6. As for IL-1β, production of TNF-α was also increased in unstimulated macrophages, with almost 50% of Atg7$^{-/-}$ macrophages producing TNF-α in the absence of any external stimulus (figure 4.21). Furthermore, even when the macrophages were alternately activated using IL-4 and IL-13 to produce an anti-inflammatory phenotype, TNF-α production only declined slightly on unstimulated macrophages, and still remained significantly above alternately activated wildtype macrophages. TNF-α levels present in macrophage supernatants were also analysed, and found to be significantly increased from both LPS and unstimulated macrophages (not shown).

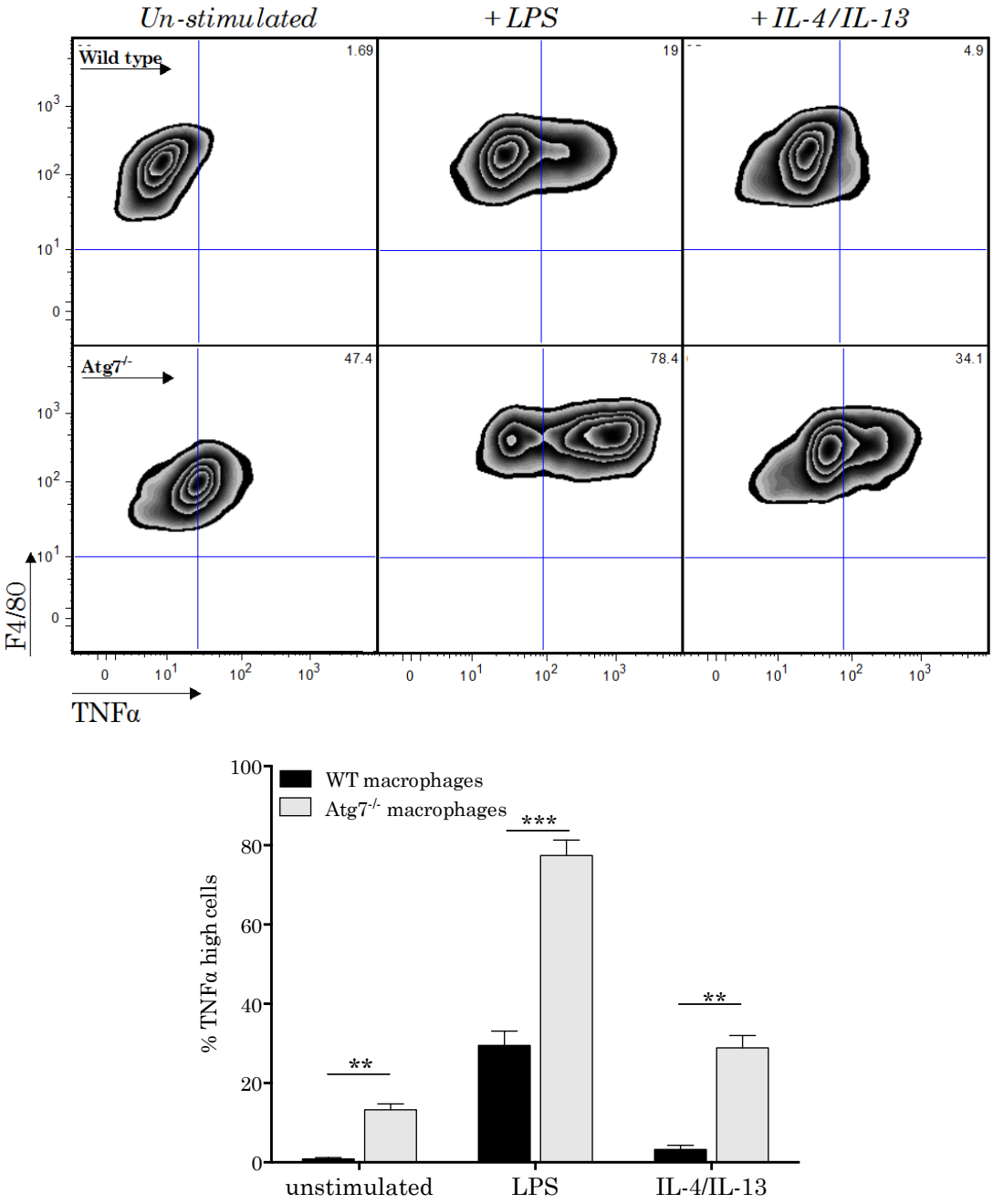

Figure 4.21: *Increased production of TNF-α in Atg7$^{-/-}$ macrophages. BMMϕ were cultured as previously described and stimulated overnight with LPS (1 µg/ml) or IL-4 and IL-13 (1 µg/ml) in the presence of 1x Brefeldin A. Gates for positive cytokine secretion placed according to isotype control staining, plots above show only F4/80^{+} CD11b^{+} cells. Top: Representative plots showing TNF-α^{+} macrophages. Bottom: Mean TNF-α expressing macrophages per culture. Error bars represent SEM, n=4. **p<0.01 and ***p<0.001, unpaired t-test.*

IL-6 production showed a slightly different expression pattern to TNF-α, with very little increase in expression in Atg7$^{-/-}$ macrophages following stimulation in many cultures (figure 4.22).

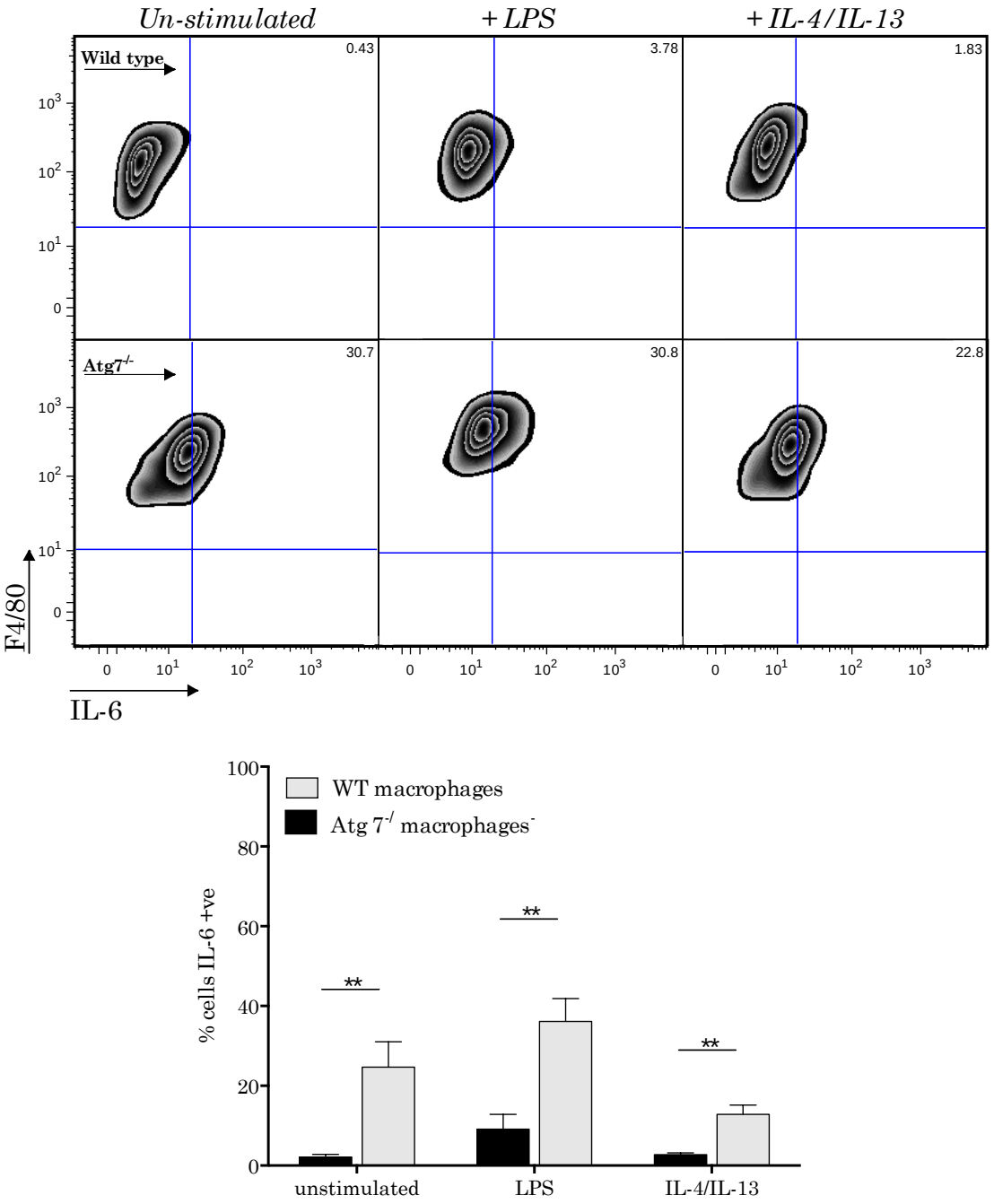

***Figure 4.22**: Increased production of IL-6 in Atg7$^{-/-}$ macrophages. BMMϕ were cultured as previously described and stimulated overnight with LPS (1 µg/ml) or IL-4 and IL-13 (1 µg/ml) in the presence of 1x Brefeldin A. Gates for positive cytokine secretion placed according to isotype control staining, plots above show only F4/80^{+} CD11b^{+} cells. Top: Representative plots showing IL-6^{+} macrophages. Bottom: Mean IL-6 expressing macrophages per culture. Error bars represent SEM, n=4. **p<0.01, un-paired t-test.*

This may be because the autophagy-deficient macrophages are already chronically stimulated, as IL-6 expression was already very high in unstimulated macrophages. Alternate activation decreased expression slightly in Atg7$^{-/-}$ macrophages, but as with TNF-α, expression remained significantly higher than in wildtype macrophages.

In order to assess what effect loss of autophagy has on production of anti-inflammatory cytokines, we next analysed production of IL-10. In direct contrast to other groups(202), we find IL-10 is also significantly increased in Atg7$^{-/-}$ macrophages, particularly following LPS stimulation (figure 4.23). Stimulation using IL-4 and IL-13 also resulted in increased IL-10 production in wildtype and Atg7$^{-/-}$ macrophages, though not as strongly as LPS stimulation. Although TLR4 and other signalling receptor expression is reduced in Atg7$^{-/-}$ macrophages, signalling downstream of TLRs is intact and even amplified, as demonstrated by cytokine expression. These data suggest that reduced receptor expression and up-regulation in the absence of autophagy is not due to decreased signalling via TLR4 or other signalling receptors.

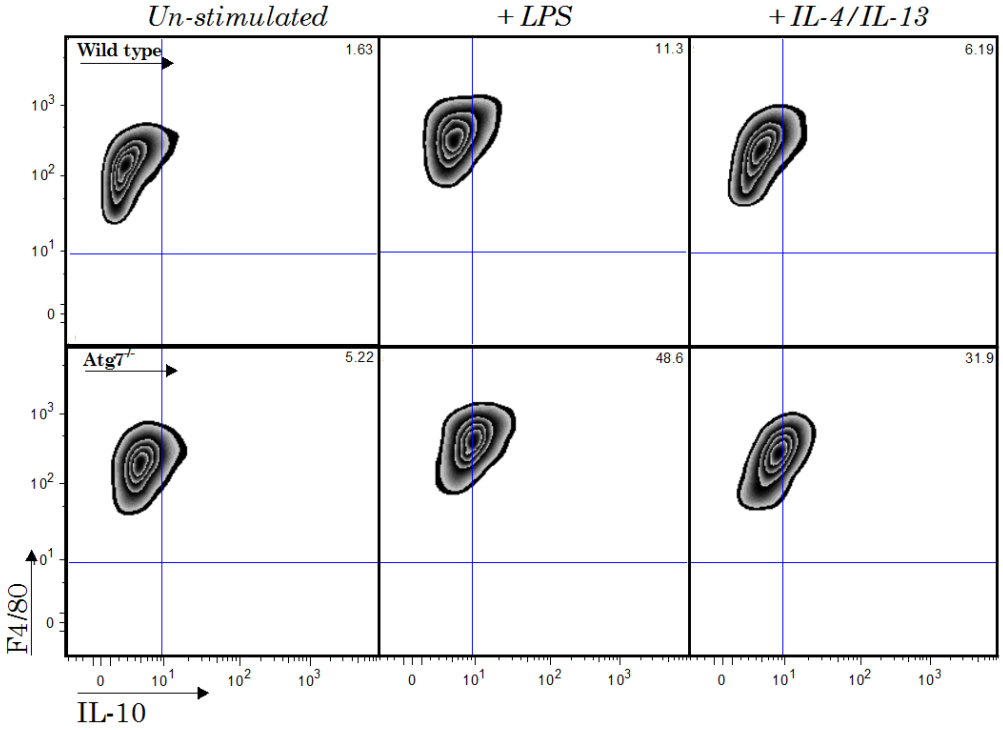

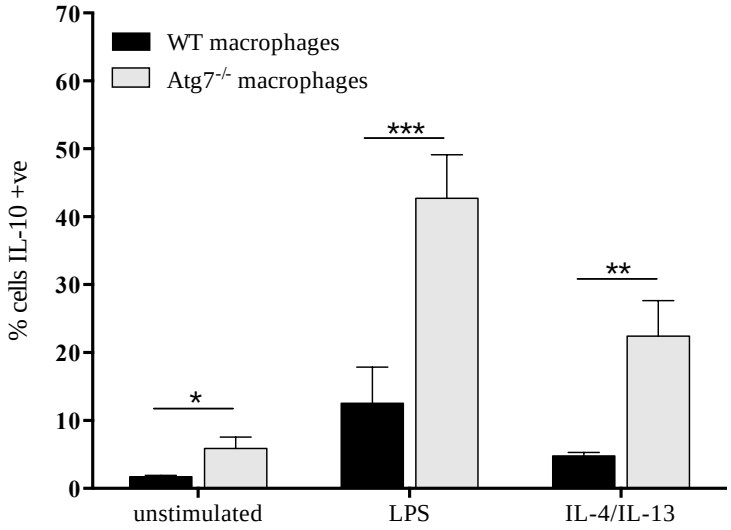

Figure 4.23*: Increased production of IL-10 in Atg7$^{-/-}$ macrophages. BMMϕ were cultured as previously described and stimulated overnight with LPS (1 µg/ml) or IL-4 and IL-13 (1 µg each/ml) in the presence of 1x Brefeldin A. Gates for positive cytokine secretion placed according to isotype control staining, showing F4/80^{+} CD11b^{+} cells. Top: Representative plots showing IL-10^{+} macrophages. Bottom: Mean IL-10 expressing macrophages per culture. Error bars represent SEM, n=4. *p<0.05, **p<0.01 and ***p<0.001, un-paired t-test.*

In addition to cytokines, macrophages produce a plethora of growth factors and chemokines which modulate growth and proliferation of other immune cells and attract immune effectors to the site of inflammation. The high levels of inflammatory cells in the tissues of Vav-Atg7 mice suggest the presence of increased inflammatory signalling, including signalling to the bone marrow to up-regulation production of further myeloid cells. As such, macrophage production of the growth factors Granulocyte Colony Stimulating Factor (G-CSF) and Granulocyte-Monocyte Colony Stimulating Factor (GM-CSF) were assessed by intracellular flow cytometry. Close to 100% of macrophages in either culture secreted some level of growth factor, based on isotype controls (figure 4.24), and as such expression was compared by average MFI. Similar to the cytokines, Atg7$^{-/-}$ macrophages secreted significantly higher levels of growth factors than wildtype cells. Stimulation with LPS appears to result in increased growth factor production, but this was not statistically significant.

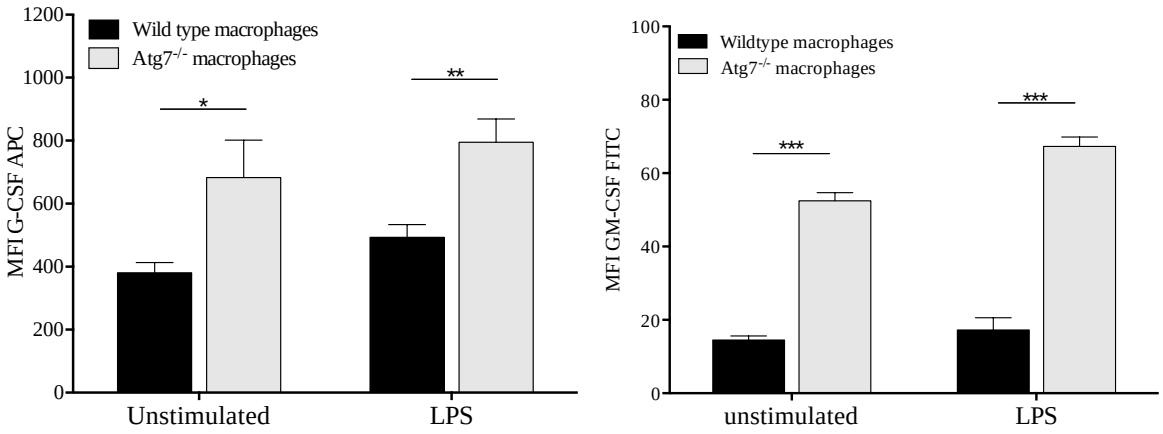

Figure 4.24: *Increased production of growth factors G-CSF and GM-CSF in Atg7$^{-/-}$ macrophages. BMMϕ were stimulated overnight with LPS (1 µg/ml) in the presence of 1× Brefeldin A to block protein secretion. Macrophages were stained for surface markers F4/80 and CD11b, then fixed and permeabilised for growth factor staining. Left: Increased G-CSF expression in Atg7$^{-/-}$ macrophages. MFI of isotype control was 265. Right: Increased GM-CSF expression in Atg7$^{-/-}$ macrophages. MFI of isotype control was 11. Graphs show average MFI, error bars represent SEM, n = 5. *p<0.05, **p<0.01, ***p<0.001, un-paired t-test.*

Macrophages also secrete a number of chemokines to attract other immune cells to the sites of infection or inflammation, thereby initiating and directing the immune response. One such chemokine is the Macrophage Inflammatory Protein (MIP-1α), also known as CCL3, which regulates trans-endothelial migration of lymphocytes, DCs and neutrophils(203). As with the growth factors and cytokines, expression of MIP-1α was significantly elevated in LPS stimulated Atg7$^{-/-}$ macrophages (figure 4.25). In unstimulated macrophages, there was variable expression in Atg7$^{-/-}$ macrophages, meaning expression was not significantly different. However, there does seem to be a trend of increased expression.

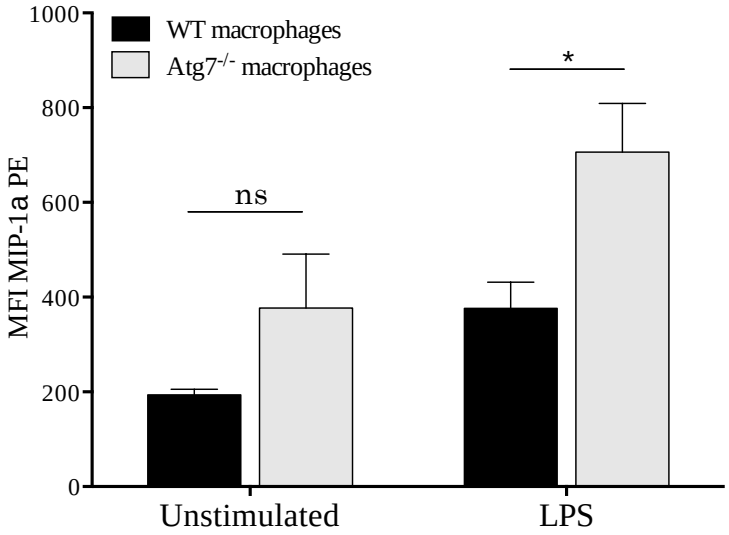

Figure 4.25: *Increased production of the chemokine MIP-1α (CCL3) in Atg7$^{-/-}$ macrophages. BMMϕ were stimulated overnight with LPS (1 µg/ml) in the presence of 1× Brefeldin A to block protein secretion. Macrophages were stained for surface markers F4/80 and CD11b, then fixed and permeabilised for intracellular staining. MFI of isotype control was 95. Graph shows average MFI, error bars represent SEM, n = 4. *p<0.05, un-paired t-test.*

Chapter 4: Discussion

Loss of autophagy influences surface receptor recycling and regulation of inflammation in macrophages

4.13 Impaired upregulation of MHC II and other signalling molecules

Analysis of Atg7$^{-/-}$ BMMϕ by flow cytometry revealed a significant defect in their ability to express vital surface markers such as MHC II and CD86 and to upregulate expression following activating stimuli such as LPS or IFNγ, suggesting a novel role for autophagy in surface marker trafficking and expression.

Upregulation of MHC I and II and co-receptors is an essential pre-requisite for efficient antigen presentation, as low expression of either can severely limit their ability to stimulate a T-cell response(168, 204, 205). Although autophagy has been shown to play an important role in antigen processing(8, 9, 206), a reduction in MHC II and co-stimulatory molecule expression also very likely plays a significant role in reduced antigen-specific responses, providing a second route whereby autophagy influences antigen-related immune responses. The comparable contribution of reduced surface marker expression to impaired antigen processing is difficult to assign from our experiments alone. As mentioned above, reduced surface expression with normal autophagy appears sufficient to reduce antigen presentation, though autophagy levels were not specifically analysed in those experiments. In their DC-specific Atg5 deletion to assess antigen presentation, Lee *et al* suggested that MHC II and CD86 expression were 'comparable' – although their provided expression histograms suggest a slight reduction in both following viral stimulation, and no statistical analysis of expression is provided to enable a true evaluation of expression(9). Nevertheless, the results do suggest that in the presence of comparable MHC II/CD86 expression, antigen presentation is impaired following abrogation of autophagy. However, research investigating NOD-2 triggering of autophagy in DCs showed a reduction in MHC II expression following siRNA knockdown of Atg5, 7 or 16L(106).These models highlight contrasting phenotypes of various myeloid autophagy

knockouts, as no alterations in phagocytosis or cytokine production were observed by Lee *et al*(9), whereas other research has shown changes in both(92, 94, 186). This may represent cell-intrinsic differences, with differing requirements for autophagy in macrophages and DC, or potentially differing roles for Atg5 and Atg7.

Appropriate expression of other macrophage surface markers is also imperative for their function, particularly expression of activation receptors such as TLR4 and CD14. Low expression of TLR4 correlates with reduced responsiveness to LPS(207) and reduced MHC II upregulation(208). Many important macrophage processes require engagement of cell surface receptors, and as such appropriate expression is intrinsic to optimal macrophage function. Expression of M-CSFR was also significantly decreased in $Atg7^{-/-}$ macrophages, but this does not appear to have affected macrophage development significantly, as similar numbers of macrophages were derived from the same number of bone marrow precursor cells.

Not all surface markers are equally affected by lack of Atg7, suggesting that autophagic regulation of surface markers is limited to particular activation or trafficking pathways. The macrophage specific marker, F4/80, and the adhesion molecule, CD11b, were expressed at normal levels on $Atg7^{-/-}$ macrophages in the majority of experiments. Where there were changes in expression, expression was as likely to be higher as lower, and was often variable between samples of both wildtype and $Atg7^{-/-}$ cultures. However, reduced expression of F4/80 and CD11b during development of macrophages derived from Vav-$Atg7^{-/-}$ bone marrow at day 4 has been observed, which was attributed to a requirement for autophagy in M-CSF dependent macrophage development(91). Although we see no significant reduction in expression of either CD11b or F4/80 on day 7 using our differentiation protocol, it is possible that development is delayed in $Atg7^{-/-}$ macrophages or that the differentiation protocol they used resulted in higher cell death and reduced the

numbers of F4/80^{high}CD11b^{high} macrophages. This could be confirmed by analysing F4/80 expression over each day of the 7 day culture period and comparing the rate of upregulation over the time course.

4.14 Disruption of surface antigen expression is not Atg7 specific

Chemical inhibition of autophagy using Wortmannin produced a similar reduction in MHC II expression to Atg7 deletion, as did deletion of another essential autophagy gene, Atg5. These data suggest that the reduction in surface marker expression is not specific to Atg7, but requires either complete autophagy flux or multiple components of the autophagy machinery. Wortmannin has previously been shown to disrupt antigen presentation by blocking the assembly of MHC II:peptide complexes, though the link to autophagy was not made in the paper(209). Induction of autophagy using rapamycin increased LPS and IFNγ stimulated MHC II and CD86 expression in wildtype macrophages. However, rapamycin treatment had little effect on MHC II expression in unstimulated macrophages, suggesting that simultaneous induction of autophagy with stimulation is required for enhanced effect. As many immune stimuli induce autophagy, this may be an adaptive mechanism to boost antigen presentation capacity and facilitate the optimal stimulation of immune responses by adequate MHC II and co-stimulation receptor expression. mTOR inhibition has been shown to hyper-induce CD86 expression(210) and starvation has been linked to enhanced IFNγ-stimulated MHC II expression(211) in other cell types. These data further support a role for autophagy in surface antigen upregulation. The role of rapamycin in surface antigen presentation is controversial, however, with some groups reporting a significant decrease in MHC II and CD86 expression on DCs cultured in rapamycin(212), as part of its role in immunosuppression. These effects may not be

directly linked to autophagy, but rather other regulated pathways downstream of mTOR. The apparent contradiction between autophagy as an immune enhancer and mTOR inhibition as an immunosuppressant may have an explanation along those lines, as may the concentration, duration and co-stimulation protocols used when assessing immune responses.

4.15 Altered expression of surface antigens is not limited to stimulation via TLR4

The defect in surface marker expression could not be overcome via macrophage stimulation through other TLRs, nor by alternate activation using IL-4 and IL-3. Expression of MHC II, and other investigated surface markers, remained lower after stimulation with the TLR2 agonist, HKLM, and the TLR3 agonist Poly I:C, with neither stimuli able to replicate wildtype expression levels of MHC II. Levels of the mannose receptor appeared unaffected by lack of autophagy on unstimulated macrophages, but stimulation with LPS resulted in no increase in expression, and IL-4 and IL-13 stimulation again failed to replicate MR expression levels seen in wildtype macrophages. Stimulation, at the same concentration and duration, by IFNγ, TLR2, 3 or 4 stimulation or alternate activation, are not sufficient to improve surface marker expression to that seen at wildtype levels, suggesting that the defect is not linked to a particular stimulatory pathway, nor specifically to M1 activated macrophages. Stimulation with increasing concentrations of LPS was also attempted, but did not rescue the presentation defect. Indeed, the highest MHC II expression even in wildtype macrophages did not occur at the highest LPS concentration, but at 1 μg/ml, the concentration used in the majority of experiments described herein. This is possibly a negative feedback mechanism to prevent macrophages against hyper-immune responses. Although saturating amounts of a single stimulus were

not sufficient to improve expression on $Atg7^{-/-}$ macrophages, it is possible that dual or sequential stimulation, for example priming with LPS and stimulating with IFNγ or concurrent stimulation with different TLR agonists, may improve expression if there is a relationship between the stimulation route and reduced expression. Classical macrophage activation was initially thought to require sequential stimulation with LPS followed by exogenous addition of IFNγ(213), however this is now thought to be unnecessary. Nevertheless, use of both stimuli may provide a stronger activation signal and improve surface marker expression. If, however, the defect is more related to the reduced autophagy, then further stimulation is unlikely to improve expression. It is also possible that duration of stimulation has an effect on the expression outcome. All experiments described herein used overnight with LPS stimulation, but further durations of stimulation could be investigated to determine whether increased length of duration eventually results in similar expression. Surface expression is not completely abolished in the absence of autophagy, suggesting that its influence on surface expression is likely contributory and potentially partially redundant. As such, increased periods of stimulation may allow other pathways of surface expression to compensate for the loss of autophagy. Similarly, investigation following shorter durations of stimulation may reveal larger differences in expression, with wildtype cells exploiting all available routes to the surface, and autophagy-deficient cells relying merely on residual expression pathways. Upregulation could potentially be followed in real time by fluorescence microscopy, using cells or cell lines transiently or stably expressing fluorescent surface molecules together with LC3.

4.16 Atg7$^{-/-}$ macrophages have higher intracellular levels of MHC II

Assessment of internal MHC II using an Imagestream flow cytometer showed significantly higher internal MHC II expression in Atg7$^{-/-}$ macrophages. Intracellular MHC II dropped following LPS and IFNγ stimulation, corresponding with increased surface expression. This suggests that autophagy plays a role in the trafficking of MHC II, and possibly other surface receptors to the cell surface. The punctate nature of the staining visible in the micrographs suggests that MHC II may be trapped in vesicles awaiting autophagy-related transport to the cell surface. There are a number of points in the autophagy pathway that interconnect with elements of intracellular transport and endocytic pathways. For example, Vps34, a class III PI3K required in the early stages of autophagy, also plays a vital role in some aspects of vesicular trafficking(214), and recent work implicates Atg6 in a number of membrane trafficking events(215).

Multivesicular bodies (MVB) are another candidate for autophagy-regulated surface antigen presentation. Newly formed MHC II molecules are targeted to endocytic compartments, known as MIIC, where they are loaded with peptide antigen(216). Autophagosomes have been shown to co-localise with MIICs(76), which are a form of MVB, and play a central role in the trafficking of MHC II molecules. Although the exact mechanism by which MVBs transport MHC II to the plasma membrane is not fully elucidated, it is thought that MVBs are reshaped into long tubules, from which vesicles pinch off and carry MHC II to the cell surface(176). The pinching off from the main body of the MVBs is a process that has been shown to be PI3K dependent, and able to be inhibited by Wortmannin(217). In addition to MHC II, the mannose receptor is also surface sorted via MVBs(218), suggesting that multiple surface markers may access the surface in this manner. The autophagy pathway shares molecular machinery with MVB,

and induction of autophagy has been shown to promote fusion of autophagosomes with MVB(219, 220), thus providing a link with which autophagy, or autophagy machinery, could connect with MHC II, mannose receptor and potentially other surface marker traffic to the surface. This could be investigated by concurrent staining of MVBs, MIICs and autophagic markers, ideally in real time, to observe whether this process was active in wildtype macrophages but absent in $Atg7^{-/-}$ macrophages. Imagestream analysis could also be used on fixed cells to assess the level of colocalisation between each marker, and whether it was reduced in the absence of autophagy.

More recently, a novel form of APC specific autophagy has been described, termed ENdosome-Mediated Autophagy (ENMA)(221). In this specialised form of autophagy, LPS stimulation causes autophagosomes to bud from MIICs, containing both the molecular machinery required for antigen processing and the autophagy proteins LC3 and Atg16L. The MIIC-associated autophagosomes were induced by starvation and LPS, and increased by treatment with autophagic flux inhibitors. However, ENMA autophagosomes have some differences compared with classical autophagosomes, particularly an electron-dense lumen, possibly due to a reduction in lipid content and increased proteins, including MHC II. A similar autophagosomal lumen has been observed in NOD2-stimulated human DCs, suggesting that this form of autophagosome is DC or APC specific(106). Macrophages were not studied during the research, and thus investigations would need to be done to determine whether ENMA-like autophagosomes could be found in macrophages as well as DCs. Whether other surface markers could find a route to the surface using a similar mechanism is unclear, and autophagosomal contents would need to be analysed to determine whether other membrane receptors were present. Potentially autophagosomes may form directly from endosomes in a similar manner to MIICs using

autophagic machinery, thereby connecting this route to the general surface expression pathways.

Finally, the role of the Rab GTPase family may be important in autophagy mediated surface antigen presentation. Rab GTPases localise to specific intracellular membranes, functioning as vital regulators of distinct steps in membrane traffic pathways. They recruit specific sets of effector proteins onto membranes, regulating vesicle formation, vesicle movement(198), and membrane fusion, all of which are important steps in surface antigen expression. Rab GTPases also play a role in the regulation of autophagy(222), regulating interactions between autophagosomes, endosomes and lysosomes and facilitating membrane recruitment for autophagosome formation(223). Rab1 plays a role in ER to Golgi transport and has been shown to participate in the early stages of autophagy(224), whereas Rab5 is involved in the inhibition of mTOR at the initiation of autophagy and Rab11 regulates the fusion of MVB with autophagosomes(219). Loss of Rab11 results in the prevention of the required tubulation of recycling endosomes by inhibiting autophagosome formation(225), thereby inhibiting autophagy. Autophagy-based unconventional protein secretion of IL-1β, IL-18 and Acb-1 is also dependent on Rab8(226-228). Finally, Rab7 is a major regulator of autophagosome to lysosome fusion(229), an important part of autophagosome maturation(230). Rab proteins are also necessary during MHC II presentation, including the maturation of early (Rab4, Rab5)(231, 232) and late endosomes (Rab7)(233), and have been implicated in trafficking of CD86(234) and MR(224), demonstrating their role in general surface marker trafficking pathways. Proteomic analysis of protein extracts from $Atg7^{-/-}$ macrophages revealed a distinct down-regulation of Rab proteins in autophagy-deficient cells, which could ultimately contribute to reduced expression of surface markers. Though several Rabs could not be detected in $Atg7^{-/-}$ macrophages at all (Rab3, Rab4, Rab7, Rab13 and Rab31),

many others were reduced by around half, which could account for the residual expression of surface markers on Atg7$^{-/-}$ macrophages. The proteomic analysis of Rab proteins remains to be validated in order to confirm which Rab proteins are altered in the absence of autophagy. Although there are multiple reports of Rab proteins regulating autophagy, no reports of autophagic regulation of Rab protein expression were found. However, expression of Rabs is known to be responsive to endosomal and lysosomal content in maturing DCs(235), and is upregulated on LPS stimulation. Thus, it is possible that in the absence of autophagy, lack of mature autophagosomes may result in downregulation (or a failure to up-regulate) of Rab proteins. It would be interesting to follow the regulation of Rab expression in wildtype and Atg7$^{-/-}$ macrophages in the naïve state, after activation and the resolution of activation by either gene expression analysis or western blotting at different time points. Double knockouts of autophagy genes and specific Rabs could also be a useful tool to investigate the role of individual Rabs in autophagy-associated surface marker expression.

4.17 Autophagy-deficient macrophages are highly inflammatory

Cytokine production was initially assessed as a downstream readout of TLR4 stimulation as an indirect means of determining whether sufficient signal was getting through despite reduced TLR4 surface expression, since reduced TLR4 expression has previously been linked to reduced production of inflammatory cytokines(236). However, rather than reduced expression of pro-inflammatory cytokines, we saw elevated production of IL-1β, TNF-α, IL-6, IL-12, and increased production of the anti-inflammatory cytokine IL-10. Additionally, production of the growth factors GM-CSF and G-CSF and the inflammatory chemokine MIP-1α, were also significantly elevated, suggesting a general inflammatory

phenotype in the absence of autophagy in macrophages, despite reduced surface marker expression.

The first report of autophagy-mediated regulation of cytokine production demonstrated a link between Atg16L and endotoxin-induced inflammasome activation in mice(186). Atg16L deficient macrophages secrete significantly greater levels of IL-1β and IL-18 than wildtype macrophages, due to increased activation of caspase-1 and activation of the inflammasome. The researchers demonstrated a similar increase in production of IL-1β in Atg7-deficient macrophages, but found levels of secreted IL-6 to be similar. Further interaction between autophagy and inflammasome activation was demonstrated by Nakahira *et al*, who showed that autophagy was important for prevention of mitochondrial DNA release and subsequent activation of the inflammasome(7). Deletion of LC3 and Beclin-1 resulted in enhanced activation of caspase-1 and consequent secretion of IL-1β and IL-18, in addition to an accumulation of damaged mitochondria. LPS stimulation resulted in increased levels of cytoplasmic mitochondrial DNA, which increased production of IL-1β/IL-18 by initiating greater activation of caspase-1, in an NALP3 dependent manner. However, inflammasome-independent autophagic modulation of inflammatory cytokine production has also been reported(188). Inhibition of autophagy in human PBMCs resulted in increased production of IL-1β, with a concomitant decrease in TNF-α production. Conversely, activation of autophagy via starvation reduced IL-1β production. However, no activation of the inflammasome was observed, rather the researchers found transcriptional regulation of cytokine production by autophagy, possibly involving inhibition of p38 MAPK phosphorylation(188). These three reports uncover apparently different levels of modulation of cytokine production by autophagy, with differing outcomes in terms of the cytokines influenced. We also find increased secretion of IL-1β from $Atg7^{-/-}$ macrophages, which is likely due to increased caspase-1 mediated

cleavage of pro-IL-1β. However, in contrast to the above reports, we also find significantly increased levels of TNF-α, IL-6, IL-12 and IL-10, suggesting further modulation of inflammatory cytokine production by autophagy under our experimental conditions. We also find significantly higher levels of cytokines, including IL-1β, in the absence of any exogenous stimuli, suggesting an endogenous stimulant or stimulants may be causing increased inflammatory cytokine production, which is then further enhanced by LPS stimulation.

One such candidate is overproduction of mitochondrial ROS (mROS), which has been shown to increase pro-inflammatory cytokine production(237). mROS, driven by mitochondrial respiration, are responsible for normal LPS-stimulated inflammatory cytokine production, and for enhanced production of inflammatory cytokines in conditions associated with elevated mROS, such as TNF-Receptor-Associated Periodic Syndrome (TRAPS)(156) in which increased levels of IL-1β, TNF, and IL-6 are common. TNFR1 mutant cells, like Atg7$^{-/-}$ macrophages (shown in chapter 5), exhibit increased mROS generation due to damaged mitochondria. Blockade of mROS efficiently reduced inflammatory cytokine production following LPS stimulation(156). Increased mROS are present even in unstimulated Atg7$^{-/-}$ macrophages, suggesting that they are a viable candidate for the increased cytokine production. This could be investigated by incubation of Atg7$^{-/-}$ macrophages with general or mitochondrial-specific ROS inhibitors, such as N-acetylcysteine (NAC) or diphenylene iodonium (DPI), respectively, and assessing basal and LPS-stimulated cytokine production. The suggested mechanism for ROS-mediated inflammatory cytokine signalling is via increased MAPK signalling(156), and thus levels of MAPK, JNK, p38, and ERK phosphorylation could also be investigated in Atg7$^{-/-}$ macrophages, in the presence and absence of mROS inhibitors, to assess the relative role of these pathways in excessive cytokine production.

Another endogenously-produced inflammatory candidate is binding of the antioxidant protein, Peroxiredoxin-1 (Prxn1), to TLR4(238). Prxn1 is expressed by macrophages under conditions of oxidative stress(239), such as those present in Atg7$^{-/-}$ macrophages due to build-up of damaged mitochondria and mROS. Incubation of Prxn1 with macrophages or immature DCs resulted in TLR4-dependent secretion of TNF-α and IL-6 in an MyD88 dependent manner(238). Elevated Prxn1 was identified in Atg7$^{-/-}$ protein extracts by proteomics and fluorescence microscopy (chapter 5), likely as an adaptive response to increased mROS, making Prxn1 an attractive candidate for increased cytokine production in Atg7$^{-/-}$ macrophages. However, although increased intracellular stores of Prxn1 were confirmed in Atg7$^{-/-}$ macrophages, increased secretion was not verified. Prxn1 lacks a signal peptide for the ER/Golgi-dependent secretory pathway, suggesting that its secretion from cells may be mediated through a non-classical secretory pathway as per proteins such as IL-1β, which is known to involve autophagy(226). Supernatant levels of Prxn1 could be confirmed by ELISA or western blot, and would demonstrate any secretory problems associated with loss of autophagy. It appears contradictory that an antioxidant should cause increased levels of pro-inflammatory cytokine production, however due to its common secretion by tumours(240) and at times of cellular stress(241), it hypothesised that Prxn1 acts as a 'danger signal'(242) – a so-called 'DAMP'(243), which are released by cells dying by non-programmed methods of cell death, and by immune cells. DAMPs activate immune cells via the same receptors as PAMPs – TLRs and NOD-like receptors, thus resulting in activation of TLR4 and other receptors and inducing the inflammatory response. Common DAMPs include Heat Shock Proteins (HSPs), hyaluronan, high-mobility group box 1 (HMGB1), β-defensins and extracellular ATP(244). Oxidative stress increases release of DAMPs, suggesting that Atg7$^{-/-}$ macrophages and other immune cells from the Vav-Atg7 model are expressing increased levels of DAMPs into their local

environment and initiating an inflammatory response. This could be investigated by looking for evidence of DAMP release in Vav-Atg7 mice and Atg7$^{-/-}$ macrophage supernatants by immunohistochemistry or fluorescence microscopy of stained sections and ELISA of supernatants.

These two possibilities, in addition to activation of the inflammasome, are not mutually exclusive and together could conceivably result in abnormal production of inflammatory cytokines and MIP-1α, which are also stimulated by similar stimuli(245, 246). Likewise, macrophage expression of G-CSF and GM-CSF can be mediated via TLR4 and DAMP signalling(247-249), suggesting similar pathways may also be activating their expression. Chronic inflammatory and growth factor signalling in Vav-Atg7 macrophages could cause recruitment of myeloid cells into tissues, and increase hematopoietic cell egress from the bone marrow, thereby increasing its rate of exhaustion.

4.18 Autophagy influences expression of some surface marker genes but not MHC II protein expression

Surface marker expression can be controlled at the gene expression level, and thus reduced expression could be influenced by decreased gene transcription. Expression of M-CSFR, which regulates macrophage differentiation in response to M-CSF, was found to be normal in Atg7$^{-/-}$ macrophages, suggesting that low surface expression of this receptor was not related to reduced gene transcription. Levels of MHC II mRNA were found to be significantly reduced in unstimulated Atg7$^{-/-}$ macrophages, but levels recovered to similar to wildtype following stimulation with LPS. Gene expression of TLR4, however, was significantly reduced in both unstimulated and LPS stimulated macrophages to around half of that of wildtype. This suggests a differential response to loss of autophagy between genes, but also shows that surface marker expression is still reduced even in the presence

of normal mRNA expression. It also implies that autophagy is not directly regulating surface marker gene expression, or at least that any transcriptional regulation by autophagy is limited to particular surface receptors or receptor families. Regulation of gene expression by autophagy has not been previously reported, but it is possible that downregulation of TLR4 and MHC II mRNA is a secondary effect to loss of autophagy or due to the inflammatory phenotype observed in $Atg7^{-/-}$ macrophages, in an effort to dampen further inflammation. In order to determine whether reduced TLR4 mRNA was influencing TLR4 protein production, and thereby reducing downstream TLR4 signalling, total levels of TLR4 could be assessed by western blot or intracellular staining combined with surface staining. Furthermore, despite the reduction in MHC II mRNA expression in unstimulated $Atg7^{-/-}$ macrophages, total MHC II protein expression was comparable between wildtype and $Atg7^{-/-}$ macrophages, both prior to and following stimulation. This suggests that translation and expression of MHC II protein are unaltered in the absence of autophagy, and shows that the reduction in surface expression is not due to an overall decrease in MHC II within the cell.

4.19 Conclusions

Loss of autophagy in macrophages results in decreased expression of important surface receptors such MHC as I and II, and the co-stimulatory molecule CD86, hampering their ability to mature appropriately in response to stimulation and unveiling a novel role for autophagy in surface receptor trafficking. Although there were some minor variations in surface marker mRNA expression, equivalent amounts of total MHC II protein were present within macrophages, which suggested a defect in trafficking of MHC II and other surface markers, to the cell surface. Both MVB and Rab proteins are known to be involved in autophagy and surface marker recycling, making them ideal candidates for

facilitating autophagy-mediated surface marker expression. However, in spite of reduced maturation based on surface marker expression, $Atg7^{-/-}$ macrophages were found to be highly inflammatory, producing increased levels of cytokines, MIP-1α and the growth factors G-CSF and GM-CSF. In addition to the established role for autophagy in the activation of the inflammasome, we hypothesise that stimulation through mROS and endogenous danger signals results in further excessive inflammatory cytokine and growth factor production. Increased expression of inflammatory cytokines and growth factors by macrophages in the tissues and organs of Vav-Atg7 mice may then result in the recruitment and stimulation of further myeloid cells, and their mobilisation from the bone marrow, thereby contributing to the myeloid infiltration of the tissues and bone marrow exhaustion seen in this model.

Chapter 5: Introduction

Loss of autophagy skews macrophage metabolism to glycolysis

5.1 Energy metabolism

Metabolism of energy sources is a key component of immune cell function beyond energy generation for cellular reactions and repair. Ability to alter metabolic state is essential for many immune cells, which can encounter quickly changing energy requirements and a variety of tissue environments, some of which are low in oxygen. Although there are many metabolic pathways that allow for the use of a variety of substrates as energy sources, this introduction focuses on metabolism of the major energy source in most cells, glucose. Glucose can be metabolised in two ways: In the presence of oxygen, glucose can be metabolised through the Citric Acid Cycle (TCA) and oxidative phosphorylation (OxPhos). In addition to OxPhos, cells can metabolise energy through glycolysis, which can occur independently of oxygen levels.

5.2 Glycolysis

Glycolysis occurs within the cytoplasm, generating two molecules of ATP and two of lactate via a series of metabolic reactions in which one molecule of glucose is catabolized to two molecules of pyruvate with a net gain of two ATP. In the absence of oxygen, NAD^+ is regenerated from NADH by reduction of pyruvate to produce lactic acid, catalysed by lactate dehydrogenase (LDH). The following equation shows the overall glycolytic reaction:

$$\textbf{Glucose + 2 NAD}^+ \textbf{ + 2 ADP + 2P}_\textbf{i} \textbf{ → 2 pyruvate + 2 NADH + 2 H}^+ \textbf{ + 2 ATP + 2 H}_2\textbf{O →}$$

$$\textbf{2 lactate + 2 NAD}^+$$

During the initial phase, two molecules of ATP fuel conversion of glucose to fructose-1,6-bisphosphate by sequential reactions that are catalysed by hexokinase, phosphoglucose isomerase, and phosphofructokinase. During the second phase, fructose-1,6-bisphosphate is further converted stepwise into pyruvate, catalysed by glyceraldehyde-3-phosphate

dehydrogenase, phosphoglycerate kinase, phosphoglycerate mutase, enolase and pyruvate kinase, producing four molecules of ATP and two molecules of NADH and consuming two ADP and two NAD^+. NAD^+ can then be regenerated via reduction of pyruvate to lactate by LDH(250), which is vital for continued glycolysis, as NAD^+ is an important cofactor in the conversion of glyceraldehyde-3-phosphate to 1,3-bisphosphoglycerate. The complete set of ten glycolytic reactions can be seen in the flow chart below (figure 5.1). While most somatic cells primarily use OxPhos, there are a number of cells that preferentially utilise glycolysis even during normoxia, such as macrophages and neutrophils(251). Increased glycolytic flux requires upregulation of key glycolytic enzymes, and shifts from constitutive enzymes to activated enzymes(252). In the case of immune effector cells such as macrophages, elevated glycolysis allows rapid activation of microbicidal activity and phagocytosis(253), and survival amidst the hypoxic conditions frequently encountered at sites of inflammation. Macrophage polarisation also influences their metabolic state, with the longer acting M2 and wound healing macrophages favouring OxPhos to provide the sustained energy required for tissue modelling and repair(254). This illustrates the flexibility of many cells to alter their metabolism to suit their energy and biosynthetic requirements, and according to oxygen availability.

Tumours are also well known for up-regulating glycolysis, known as the Warburg effect(255). This is partly to provide the energy to sustain rapid proliferation, but ATP generated by glycolysis makes up a relatively small proportion of total ATP production(256), suggesting that tumours use glycolysis for reasons other than rapid ATP production. In many tumours, mitochondria are intact and functional. However, in addition to generation of ATP, glycolysis is valuable for production of glycolytic intermediates, from which essential cellular building blocks such as nucleotides and amino acids can be derived(257).

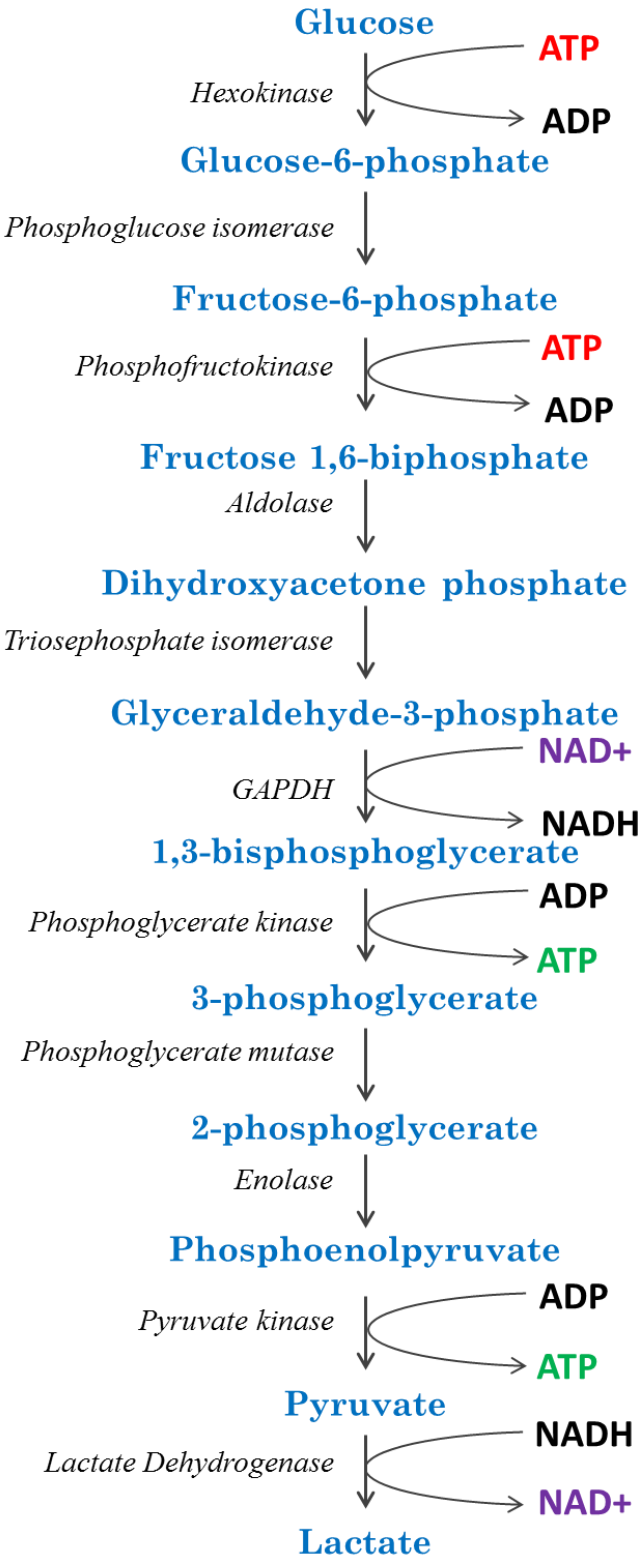

***Figure 5.1**: The ten reactions of glycolysis. Glucose is sequentially catabolised by specific enzymes into pyruvate and then into lactate, yielding 2 ATP molecules. NAD^+ is replaced by reaction of pyruvate with Lactate dehydrogenase to produce lactate. Adapted from ref (250).*

Thus glycolysis acts as more than a mere energy generation mechanism in many cells. Glycolysis is regulated on several levels: glucose availability, rate limiting glycolytic enzymes and oxygen availability. Hypoxia-inducible factor (HIF) is a central transcriptional regulator of cell metabolism and adaptation to cellular stress during hypoxia(258). During hypoxia, HIF-1α accumulates and translocates to the nucleus, where it binds HIF-1β. The HIF complex then binds to core nucleotide sequences called hypoxic response elements (HREs) on target genes, which include many glycolytic enzymes and glucose transporters that control glucose uptake. Activation of these genes decreases mitochondrial oxygen consumption and shifts metabolism to glycolysis. Their actions also balance the low pH caused by increased lactic acid, optimising cell energetics and homeostasis in oxygen poor environments(259). HIF-1α can also be stabilised during normoxia in some conditions, allowing so-called aerobic glycolysis. In macrophages and some cancers, HIF-1α activation during normal oxygen levels is enabled by suppression of Factor Inhibiting HIF-1 (FIH-1) by membrane type-1 matrix metalloproteinase, a membrane protease that regulates various cellular functions(260, 261).

5.3 Oxidative phosphorylation

Under normal oxygen conditions in cells that utilise OxPhos, pyruvate generated through glycolysis is further oxidised to generate more ATP. Pyruvate passes into the mitochondria, where it is converted to Acetyl-CoA. Acetyl CoA then enters the TCA, where the eight-step citric acid cycle generates three NADH molecules and two other carrier molecules: $FADH_2$ and GTP (figure 5.2).

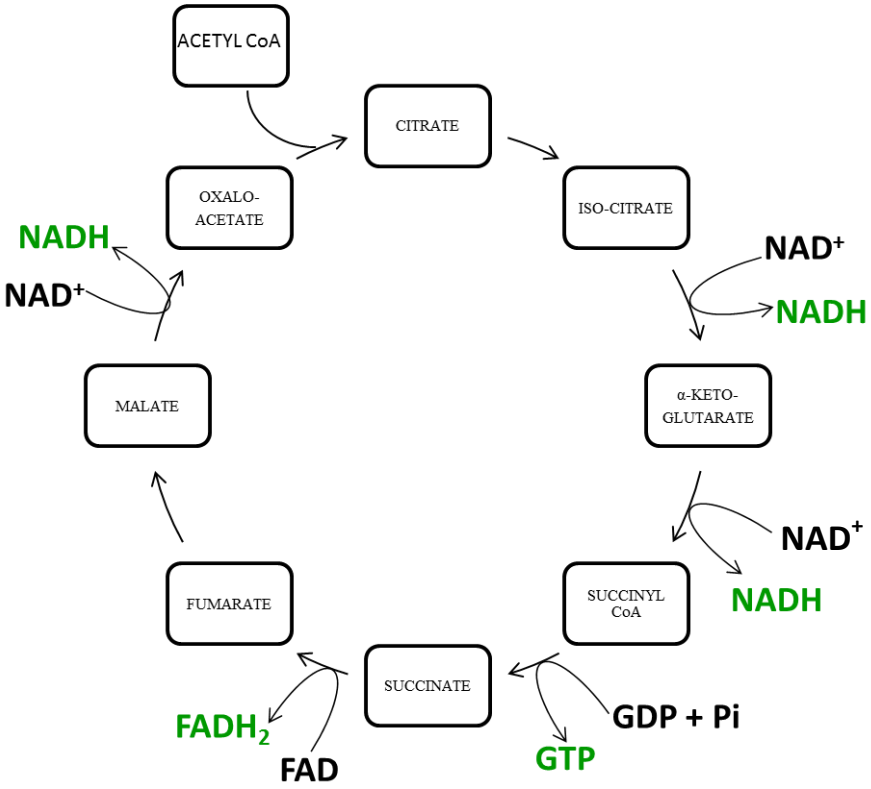

***Figure 5.2**: Generation of NADH, $FADH_2$ and GTP from Acetyl CoA in the citric acid cycle. NADH generated is shuttled to complex I and is converted to NAD^+, driving oxidative phosphorylation. Adapted from ref (262).*

In the third stage, electrons from $FADH_2$ and NADH are transferred to the electron transport chain for oxidative phosphorylation, thereby generating 3 ATP molecules for each electron that enters OxPhos. The electron transport chain is made up of 4 multi-subunit complexes (I, III, IV & V) embedded in the inner mitochondrial membrane. The electrons from NADH and $FADH_2$ power the pumping of protons across the matrix to the inter-membrane space, creating a potential difference that can be used for synthesis of ATP in the last step of oxidative phosphorylation(262).

OxPhos not only produces the vast majority of cellular energy in most cells, but is also involved in oxygen radical production and apoptosis. OxPhos is controlled by three main mechanisms. Firstly, by availability of the ATP substrates, ADP and phosphate, increasing when ATP use re-generates ADP and phosphate. Secondly, allosteric control of OxPhos,

which is mediated by small molecules that bind to enzymes involved, changing their kinetic properties, and finally cellular signalling, for example through the insulin receptor(263). Through these means, cells can up- or downregulate ATP production as cellular circumstances dictate.

5.4 Loss of autophagy skews macrophage metabolism to glycolysis

This chapter demonstrates a novel role for autophagy in the regulation of glycolytic capacity and oxygen consumption in macrophages. Macrophages isolated from Vav-Atg7 mice exhibit significantly increased glucose uptake and levels of glycolysis, suggesting that glycolysis can be used to generate the energy and metabolic intermediates that are lacking due to lost autophagy, as well as potentially allowing the macrophages to maintain mitochondrial potential and thereby avoid premature apoptosis. Despite increased glycolysis, which does not require oxygen consumption, $Atg7^{-/-}$ macrophages exhibit significantly increased rates of oxygen consumption. The origin and implications of this paradox are considered in the context of macrophage survival and ability to transition between metabolic states.

Chapter 5: Results

Loss of autophagy skews macrophage metabolism to glycolysis

5.5 Increased acidification of Atg7$^{-/-}$ macrophage culture medium

During the 7 day macrophage cultures, Atg7$^{-/-}$ macrophages were observed to acidify their culture media much faster than wildtype macrophages, particularly in the first 3 days of culture, resulting in a colour change from red (fresh R10 medium) to light orange or yellow by day 3 (or day 7, following media top up) of culture (figure 5.3). Acidification causes a colour change in the phenol red indicator present in RPMI, due to products from cellular metabolism decreasing media pH.

***Figure 5.3**: Atg7$^{-/-}$ macrophages cause yellowing of the culture medium. Macrophages were cultured from bone marrow in the presence of M-CSF (20 ng/ml) for 7 days at 37° C, 5% CO_2. Images taken from 2 separate experiments, on culture day 3 (left) and 7 (right), WT = wildtype, KO = Atg7$^{-/-}$ macrophages.*

The colour change was assessed quantitatively by analysing the absorbance at 450 nm of a small sample of medium from each culture on days 3 and 7, and after overnight stimulation with LPS and comparing it to fresh R10 culture medium. All samples showed increased absorbance on days 3 and 7, and after LPS stimulation, relative to fresh R10 medium (figure 5.4, dotted black line). However, media samples from Atg7$^{-/-}$ macrophage cultures had significantly higher absorbance than those from wildtype samples at both time points, and following LPS stimulation. These data show that Atg7$^{-/-}$ macrophages acidify their media at a faster rate than wildtype macrophages.

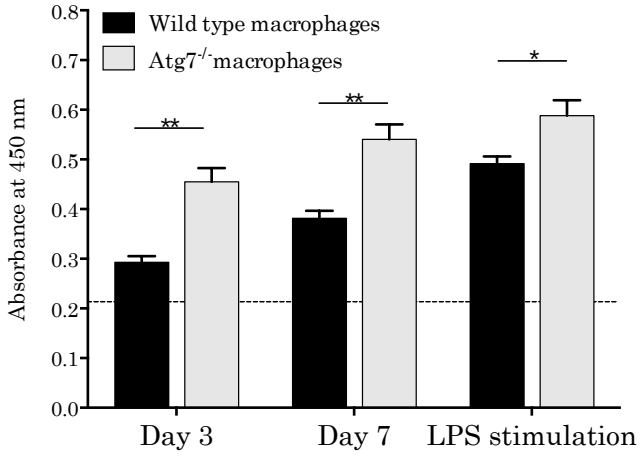

Figure 5.4: *Culture medium from Atg7$^{-/-}$ macrophage cultures shows higher absorbance at 450 nm. Bone marrow macrophages were stimulated overnight with LPS (1µg/ml). 25 µL samples of media were taken from each well on day 3, 7 and following LPS stimulation and absorbance at 450 nm was compared with absorbance from fresh R10 medium (dotted black line). Graph shows mean absorbance, error bars represent SEM, n = 4. *p<0.05. **p<0.01, un-paired t-test.*

5.6 Atg7$^{-/-}$ macrophages rapidly utilise glucose

Glucose is the primary metabolic substrate in macrophages(264), and therefore changes in glucose uptake can indicate alterations in the metabolic rate and/or pathway. Glucose uptake by macrophages was assessed by assaying the concentration of glucose remaining in the medium following the culture period, and comparing this with the glucose concentration in fresh medium. Fresh R10 (made from RPMI 1640) contains 2000 µg/L of glucose. Glucose was analysed by enzymatic conversion to gluconic acid and hydrogen peroxide, and reaction with o-dianisidine in the presence of peroxidase to produce a change in absorbance at 540 nm. Remaining glucose concentration in media from unstimulated Atg7$^{-/-}$ macrophages was significantly lower than in media from wildtype cultures (figure 5.5). A further significant decrease was observed in both cultures following LPS stimulation, with the largest decrease again in Atg7$^{-/-}$ culture medium. Autophagy-deficient macrophages utilise more glucose than wildtype macrophages over

the same culture period, particularly following LPS stimulation, suggesting that loss of Atg7 influences macrophage energy production.

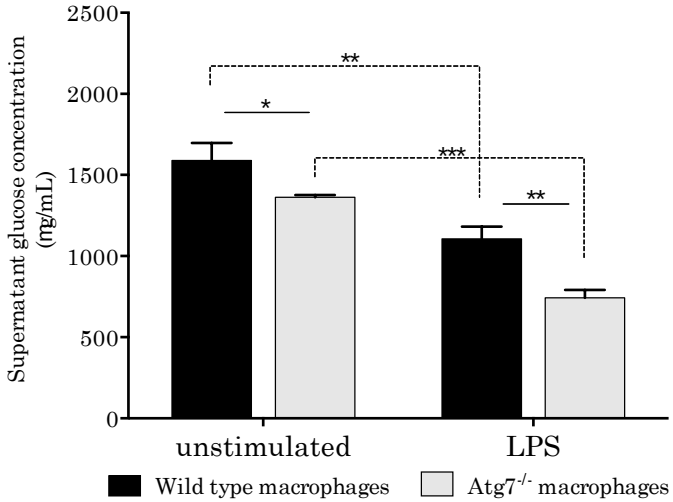

Figure 5.5: *Increased glucose uptake by Atg7$^{-/-}$ macrophages during culture and following LPS stimulation. Macrophages were cultured from bone marrow and stimulated overnight with LPS (1 µg/ml), and media samples taken from stimulated and unstimulated cultures. Samples were diluted 1/25 to bring them into the sensitivity range of the testing kit. Concentration was determined using a standard curve. Graph shows average glucose concentration remaining in media following culture, error bars represent SEM, n = 4. *p<0.05, **p<0.01, ***p<0.001, un-paired t-test.*

Glucose is transported across the macrophage plasma membrane by the glucose transporter 1 (Glut-1)(265). Increased expression of Glut-1 and other glucose transporters is required for increased glucose uptake and metabolism(264), and as such, Glut-1 expression on macrophages was assessed using flow cytometry. Wildtype and Atg7$^{-/-}$ macrophages both showed high levels of Glut-1 expression, reflecting the high energetic demands of macrophages(266) (figure 5.6). However, Atg7$^{-/-}$ macrophages showed significantly higher expression of Glut-1 compared with wildtype macrophages, thereby enabling their enhanced glucose uptake in culture.

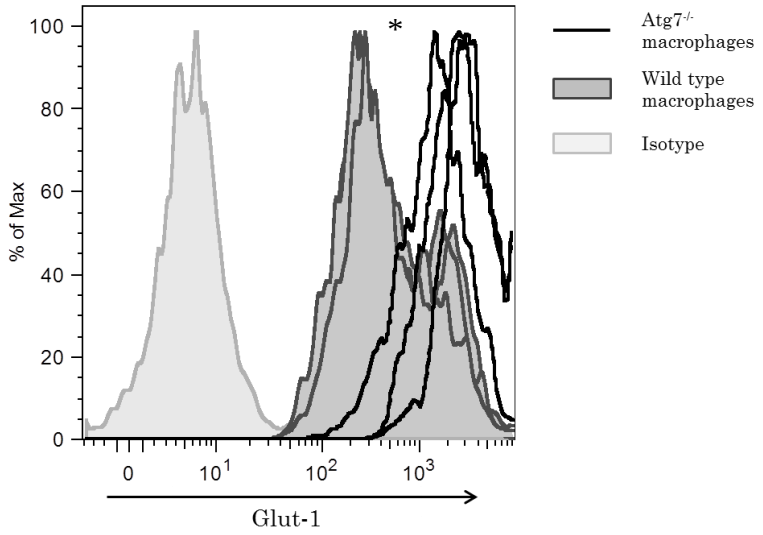

Figure 5.6: *Increased expression of the glucose transporter Glut-1 on Atg7$^{-/-}$ macrophages. Bone marrow macrophages were cultured for 7 days as described above and stained for the surface markers F4/80, CD11b and Glut-1. The histogram above shows overlaid histograms of Glut-1 expression on F4/80^{+} CD11b^{+} macrophages, n = 3. *p<0.05, un-paired t-test.*

5.7 Atg7$^{-/-}$ macrophages are more glycolytic than wildtype macrophages

The contribution of glycolysis to bioenergetic maintenance in macrophages was assessed using the Seahorse Bioscience XF24 analyser, which uses two sensors to simultaneously measure extracellular acidification rate (ECAR) and oxygen consumption rate (OCR), reporting on glycolytic and mitochondrial respiration respectively. Measurements of both parameters are taken at regular time intervals, during which it is possible to sequentially add drugs that enhance or inhibit specific points or targets in either pathway. Oligomycin is an ATP synthase inhibitor that blocks OxPhos, resulting in increased energy generation by glycolysis(267). Trifluorocarbonylcyanide Phenylhydrazone (FCCP) uncouples the electron transport chain from the OxPhos system, resulting in a large release of electrons as well as an increase in glycolytic rate. Finally, rotenone acts as a mitochondrial NADPH dehydrogenase/complex I inhibitor, specifically inhibiting mitochondrial respiration and forcing cells to increase glycolysis. Seahorse analysis showed that Atg7$^{-/-}$ peritoneal

macrophages have an average ECAR of 65 mpH/min, more than twice that of wildtype macrophages (figure 5.7). Furthermore, addition of oligomycin and FCCP resulted in a further increase of $Atg7^{-/-}$ macrophage ECAR, to 70 and 79 mpH/min respectively, compared to 30 and 35 mpH/min in wildtype macrophages. Rotenone resulted in no further increases in ECAR in either $Atg7^{-/-}$ or wildtype macrophages, possibly because they were already at their maximum rate.

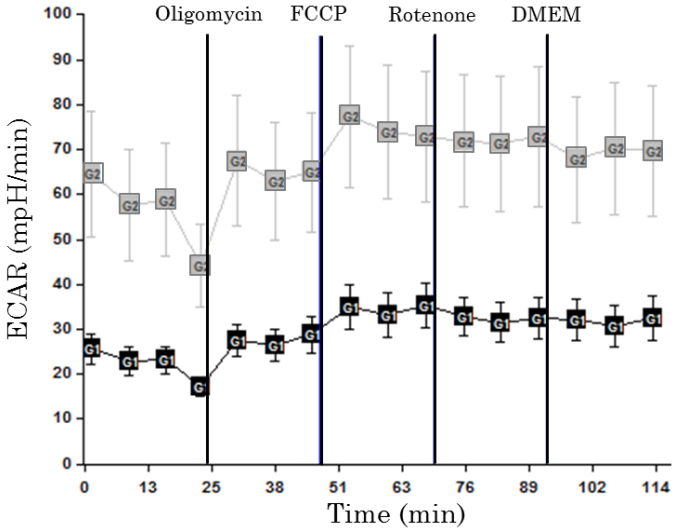

***Figure 5.7**: $Atg7^{-/-}$ macrophages have higher glycolytic flux as assessed by ECAR. Peritoneal macrophages were harvested from 4 wildtype and 4 Vav-Atg7 mice, seeded into a Seahorse 24 well plate at 2 × 10^5 cells per well and cultured overnight in R10 at 37° C, 5% CO_2. Prior to analysis, macrophages were washed in unbuffered DMEM and allowed to equilibrate at 37° C, no CO_2, prior to analysis. Oligomycin (400 nM), FCCP (400 nM) and rotenone (1 µM) were added at the indicated time points, DMEM was added at the fourth indicated time point. Each time point is calculated from 10 replicates of pooled wildtype or $Atg7^{-/-}$ macrophages, error bars represent standard deviation. With acknowledgements to Professors Marion McFarlane and Kelvin Cain for their help and expertise.*

5.8 $Atg7^{-/-}$ macrophages have increased respiratory reserves but no ATP-related oxygen consumption

Cells which predominantly produce their energy by glycolysis typically have reduced reliance on OxPhos and few mitochondria(253). Macrophages, however, are known for their plasticity and are able to switch between oxidative phosphorylation and glycolysis

depending on their activation state, with M1 macrophages favouring glycolysis, and M2 macrophages generating their energy predominantly by OxPhos(254). Oxygen consumption can be analysed using the Seahorse Bioscience XF24 analyser, simultaneous to measurements for ECAR. $Atg7^{-/-}$ macrophages were found to have a higher basal OCR than wildtype macrophages, of 180 pMoles/min compared to 110 pMoles/min by wildtype macrophages (figure 5.8). However, oxygen consumption by $Atg7^{-/-}$ macrophages appears to be independent of ATP generation, as treatment with oligomycin, had no influence on the OCR. In wildtype macrophages, however, oligomycin resulted in a drop in the OCR to 50 pMoles/min, suggesting that 50% of basal oxygen consumption in wildtype macrophages is related to ATP generation. Treatment with FCCP uncouples the proton transport chain from ATP synthesis, allowing assessment of maximal potential oxygen consumption in the absence of mitochondrial ATP generation and indicating the maximum respiratory capacity (MRC) of the cells(268). FCCP showed that $Atg7^{-/-}$ macrophages had a significantly higher MRC than wildtype macrophages, even considering that wildtype macrophages increased from a lower level following oligomycin treatment. Furthermore, $Atg7^{-/-}$ macrophages sustained their high consumption throughout the FCCP treatment period, whereas wildtype macrophages peaked quickly after treatment and then dropped over time. Spare respiratory capacity can be determined by subtracting the basal OCR from the FCCP induced OCR, giving a wildtype spare respiratory capacity on the order of 150 pMoles/min, half that of $Atg7^{-/-}$ macrophages, which have 300 pMoles/min spare respiratory capacity(269). Finally, rotenone, a mitochondrial NADPH dehydrogenase inhibitor, was added to assess non-mitochondrial respiration. Treatment of $Atg7^{-/-}$ macrophages with rotenone caused an OCR reduction to basal levels, implying that basal oxygen consumption in autophagy-deficient macrophages is ATP independent. In wildtype macrophages, OCR dropped down to the same level as following oligomycin

treatment, indicating that wildtype macrophages are utilising their mitochondria to make a proportion of their basal ATP and energy requirements.

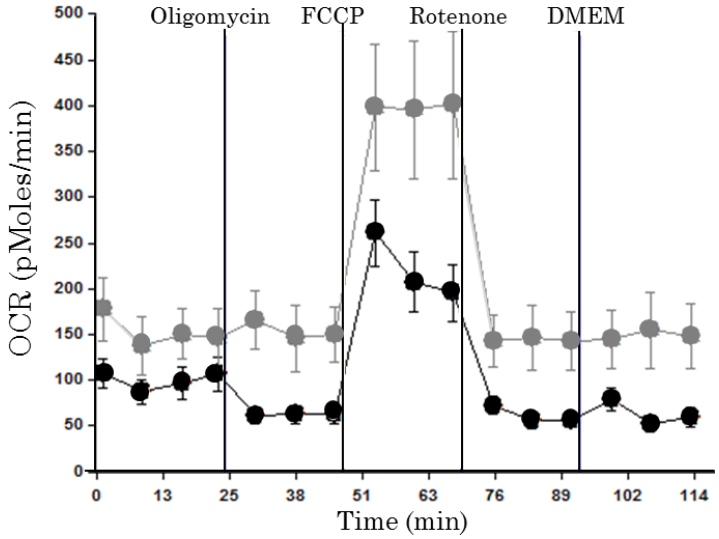

Figure 5.8: *Atg7$^{-/-}$ macrophages have an altered oxygen consumption profile. Peritoneal macrophages were harvested from 4 wildtype and 4 Vav-Atg7 mice, seeded into a Seahorse 24 well plate at 2 × 10^5 cells per well and cultured overnight in R10 at 37° C, 5% CO_2. Prior to analysis, macrophages were washed in unbuffered DMEM and allowed to equilibrate at 37° C, no CO_2, prior to analysis. Oligomycin (400 nM), FCCP (400 nM) and rotenone (1 µM) were added at the indicated time points, DMEM was added at the fourth indicated time point. Each time point is calculated from 10 replicates of pooled wildtype or Atg7$^{-/-}$ macrophages, error bars represent standard deviation. With acknowledgements to Professors Marion McFarlane and Kelvin Cain for their help and expertise.*

5.9 Atg7$^{-/-}$ macrophages have altered expression of many metabolic proteins

Bioenergetic analysis of Atg7$^{-/-}$ macrophages using Seahorse revealed significant differences in macrophage metabolism in the absence of autophagy. However, Seahorse only looks at the output of 2 metabolic pathways, not intermediates or other components such as lipid metabolism or the pentose phosphate pathway (PPP). Proteomic analysis provides a snapshot of protein expression within cells at the time of analysis, enabling a general overview of pathways and proteins up- or down-regulated following treatment or when comparing two cell phenotypes. Cell extracts from sorted Atg7$^{-/-}$ and wildtype bone

marrow derived macrophages were analysed by un-labelled tandem mass spectrometry. As expected, Atg7$^{-/-}$ macrophages showed increased levels of many proteins associated with glycolysis, including triosephosphate isomerase, transketolase and phosphoglycerate mutase (Figure 5.9). Furthermore, they showed decreased expression of lactate dehydrogenase, an enzyme that catalyses the conversion between pyruvate and lactate. Wildtype macrophages, on the other hand, showed increased expression of proteins involved with the PPP, including transaldolase and phosphoglucomutase that could only be detected in wildtype samples.

Protein ID	**Protein Name**	**Score**	**WT:KO ratio**	**p value**
Glycolysis Proteins				
P17751	Triosephosphate isomerase	971.09	0.8	0
Q3TRM8	Hexokinase-3	709.61	KO only	KO only
P40142	Transketolase	681.69	0.81	0.01
Q9DBJ1	Phosphoglycerate mutase 1	430.13	0.58	0
P06151	L-lactate dehydrogenase A chain	627.97	1.8	1
Pentose Phosphate Pathway				
Q93092	Transaldolase	218.96	WT only	WT only
Q00612	Glucose-6-phosphate 1-dehydrogenase X	435.05	1.9	1
Q9D0F9	Phosphoglucomutase-1	467.46	WT only	WT only
Q9DCD0	6-phosphogluconate dehydrogenase	499.22	1.8	1

Figure 5.9: *Atg7$^{-/-}$ macrophages show increased expression of glycolytic enzymes, but reduced expression of proteins associated with the pentose phosphate pathway. Bone marrow derived macrophages were cultured for 7 days and stimulated overnight with LPS (1 µg/ml). Protein extracts were produced from pooled wildtype and Atg7$^{-/-}$ macrophages, adjusted to the same protein concentration and analysed by tandem mass spectrometry. Protein score is a measure of protein abundance. Significance is denoted as $p<0.05$ for proteins with increased expression in Atg7$^{-/-}$ macrophages, and $p>0.95$ for proteins with increased expression in wildtype macrophages. Grateful acknowledgements to Dr Benedikt Kessler for performing the proteomic experiments and assisting with their analysis.*

5.10 Atg7$^{-/-}$ macrophages show upregulated expression of antioxidant pathways

In addition to changes in the glycolytic and pentose phosphate pathways, a number of proteins associated with the anti-oxidant response were increased in Atg7$^{-/-}$ macrophages (figure 5.10), including Peroxiredoxin 1, 2 and 5, thioredoxin and heme oxygenase 1. Peroxiredoxins help to protect cells against excessive levels of ROS, thereby protecting DNA integrity and preventing damage to organelles(270). Furthermore, wildtype macrophages showed expression of Obg-like ATPase 1, an inhibitor of the antioxidant response(271), which was not detectable in Atg7$^{-/-}$ macrophages.

Protein ID	Protein Name		Score	WT:KO ratio
Antioxidant Proteins				
P35700	Peroxiredoxin 1	865.1	0.9	0
Q61171	Peroxiredoxin 2	154.38	KO only	KO only
P99029	Peroxiredoxin 5	556.5	0.6	0
P14901	Heme Oxygenase 1	596.9	0.8	0.02
P10639	Thioredoxin	152.54	KO only	KO only
Q9CZ30	Obg-like ATPase 1	341.59	WT only	WT only

Figure 5.10: *Atg7$^{-/-}$ macrophages show increased expression of antioxidant enzymes. Protein extracts were produced from pooled wildtype and Atg7$^{-/-}$ macrophages, adjusted to the same protein concentration and analysed by tandem mass spectrometry. Protein score is a measure of protein abundance. Significance is denoted as $p<0.05$ for proteins with increased expression in Atg7$^{-/-}$ macrophages, and $p>0.95$ for proteins with increased expression in wildtype macrophages. Grateful acknowledgements to Dr Benedikt Kessler for performing the proteomic experiments and assisting with their analysis.*

Peroxiredoxins and many other cellular antioxidants are expressed under the control of nuclear factor erythroid 2-related factor 2 (Nrf2), which regulates cellular resistance to ROS and other oxidants(272, 273). As such, relative expression of Nrf2 regulated antioxidants peroxiredoxin 1 (Prxn1), peroxiredoxin 2 (Prxn2), Peroxiredoxin 5 (Prxn5)

and glutaredoxin (Glrx), and Nrf2 was assessed in BMMϕ by qPCR. Prxn1 and Glrx were significantly increased in LPS stimulated Atg7$^{-/-}$ macrophages, but not in unstimulated macrophages (figure 5.11), whereas Prxn5 was significantly increased in both unstimulated and LPS stimulated Atg7$^{-/-}$ macrophages, but showed no further increase following LPS stimulation. Prxn2 mRNA was expressed at similar levels in wildtype and Atg7$^{-/-}$ macrophages. Nrf2 mRNA expression was also significantly increased in Atg7$^{-/-}$ macrophages, in both LPS and unstimulated macrophages.

Hypoxia inducible factors (HIF) are transcription factors that respond to decreased oxygen and coordinate adaptive responses to hypoxic environments. HIF-1α suppresses mitochondrial respiration and enables a switch to glycolysis by transactivating pyruvate dehydrogenase kinase 1, which suppresses the citric acid cycle and promotes glycolytic production of ATP(258). Expression of HIF-1α mRNA expression in BMMϕ was also assessed by qPCR. HIF-1α mRNA was increased 1.7 fold in unstimulated macrophages, and by 2 fold following stimulation with LPS.

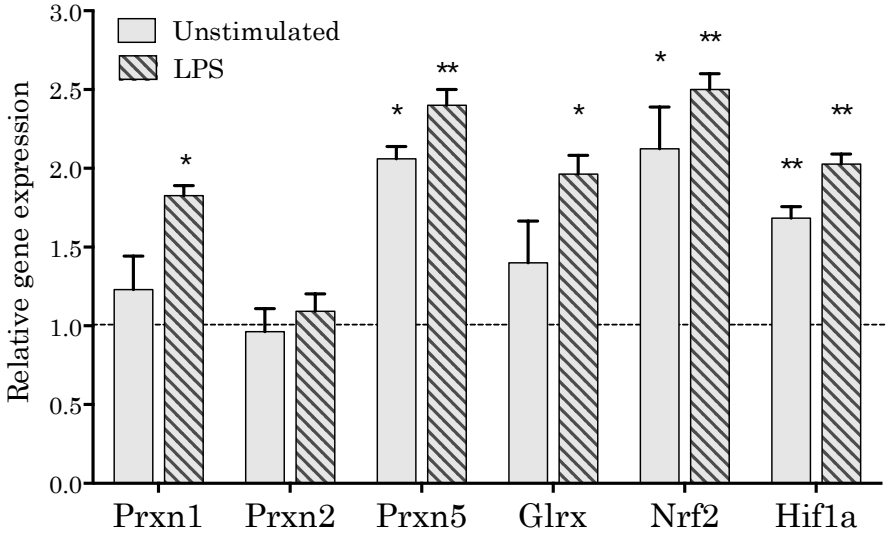

***Figure 5.11**: Increased expression of antioxidant and glycolytic genes in Atg7$^{-/-}$ macrophages. RNA was extracted from BMMϕ stimulated overnight with LPS (1 μg/ml). Values were determined using the ΔΔCT method, normalised to GAPDH and compared to wildtype macrophages cultured under the same conditions. Wildtype gene expression is represented by the dotted line on the graph at a relative expression of 1. Error bars represent standard deviation of 3 replicates, *p<0.05, **p<0.01, all other values ns.*

Increased expression of Prxn1in LPS stimulated Atg7$^{-/-}$ macrophages was also detectable by confocal microscopy (figure 5.12), and showed a different staining pattern to that of wildtype macrophages. Wildtype macrophage Prxn1 expression was limited to punctate cytoplasmic staining whereas staining in Atg7$^{-/-}$ macrophages was brighter, but more diffuse, possibly representing released Prxn1.

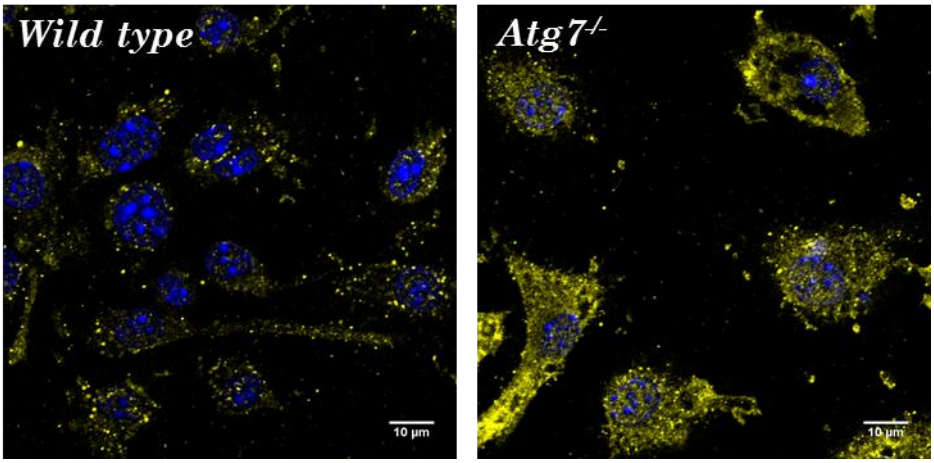

***Figure 5.12**: Increased Prxn1 expression in Atg7$^{-/-}$ macrophages. BMMϕ were cultured on glass coverslips for 7 days and stimulated overnight with LPS (1 µg/ml). Cells were fixed with 4% paraformaldehyde and permeabilised with 0.1% triton-X100 in PBS prior to staining with anti-mouse Prxn1. Nuclei were counterstained with DAPI. Slides were visualised by confocal microscopy, 60x lens. Representative images from 8 samples.*

5.11 Atg7$^{-/-}$ macrophages have a high mitochondrial burden and increased reactive oxygen species

Under normal conditions, macrophages have few mitochondria(149) compared with lymphocytes and other cells that rely on OxPhos for metabolism, although numbers of mitochondria increase upon M2 type stimulation(269). However, the unusual oxygen consumption profile of Atg7$^{-/-}$ macrophages suggests a role for increased mitochondria. Furthermore, autophagy is known to play a role in mitochondrial maintenance and removal in other immune cells(46, 54). Mitochondrial content was assessed using MitoTracker

Green, which localises to mitochondria regardless of their membrane potential. Atg7$^{-/-}$ macrophages had significantly higher levels of mitochondrial staining than wildtype macrophages (figure 5.13), with approximately 40% higher mitochondrial content. No changes in either wildtype or Atg7$^{-/-}$ mitochondrial content were observed following LPS or IFNγ stimulation. This suggests that increased mitochondrial content may contribute to the increased respiratory reserve available in Atg7$^{-/-}$ macrophages.

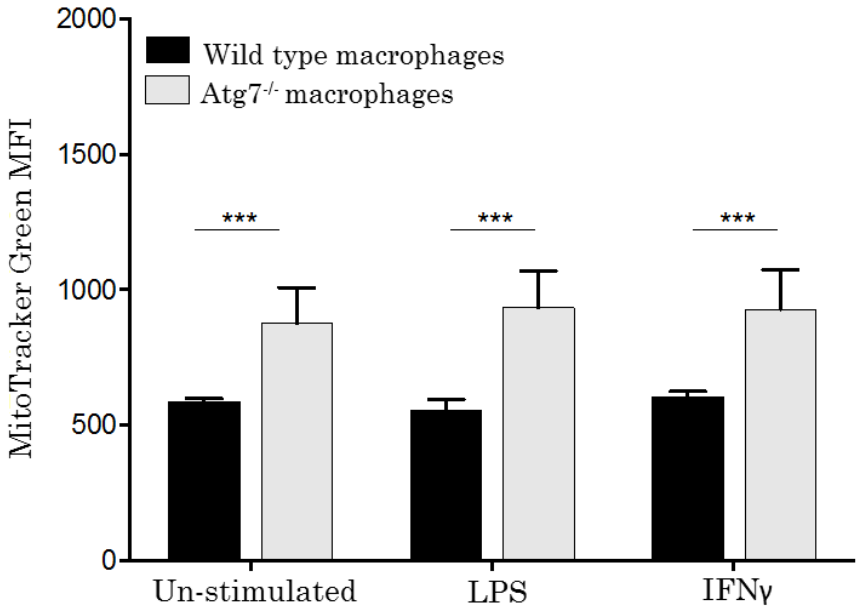

***Figure 5.13**: Mitochondrial Staining using MitoTracker Green staining in bone marrow derived macrophages. BMMϕ were cultured and stimulated overnight with LPS or IFNγ, followed by staining with MitoTracker Green (200 nM) for analysis by flow cytometry. Average MitoTracker green MFI for F4/80^{+} CD11b^{+} macrophages shown, error bars represent SEM. *p<0.05, un-paired t-test.*

Mitochondria are significant generators of mitochondrial ROS (mROS), produced as a by-product from OxPhos. Autophagy is known to play a role in limiting ROS accumulation within cells, thereby maintaining cellular integrity(274), and thus generation of mROS was assessed in Atg7$^{-/-}$ BMMϕ using MitoSOX, a fluorogenic dye that specifically targets mitochondria, where it is oxidised by mitochondrial superoxide producing fluorescence. Levels of mROS were significantly higher in Atg7$^{-/-}$ macrophages than in wildtype

macrophages (figure 5.14). No significant increase in mitochondrial ROS was observed following LPS stimulation in either wildtype or Atg7$^{-/-}$ macrophages.

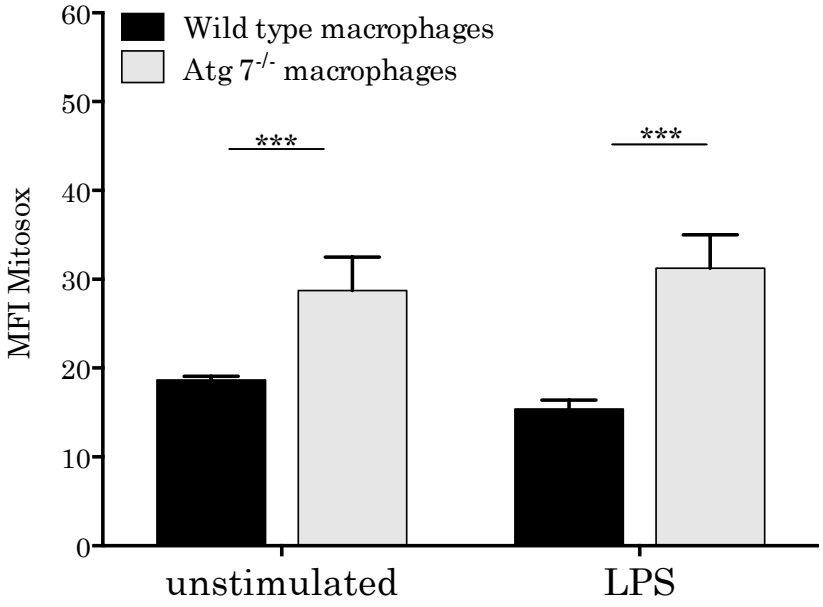

Figure 5.14: *Atg7$^{-/-}$ macrophages have increased levels of mitochondrial ROS. BMMϕ were stimulated overnight with LPS (1 µg/ml), washed, stained with surface markers as previously, followed by MitoSOX (5 µM) for 20 min at 37° C and analysed immediately by flow cytometry. Graph shows average MFI of MitoSOX staining, error bars represent SEM, n = 5. ***p<0.001, un-paired t-test.*

5.12 Perturbation of energy generation pathways influences the inflammatory response and cell death

Given the influence of metabolic pathways on inflammatory responses, cytokine production was assessed in BMMϕ that were stimulated with LPS in the presence of chemical metabolic inhibitors. Oxamate, an LDH inhibitor, was used to block the glycolytic pathway(275), and dehydroepiandrosterone (DHEA) treatment was used to block the PPP(276). Galactose was also used as a substitute for glucose, enabling the energy contribution of glycolysis to be assessed since breakdown of galactose yields no net production of ATP. As expected, LPS stimulation resulted in a significant up-regulation of IL-6, IL-10 and TNF-α (figures 5.15 – 5.17). Chemical modulation of metabolic

pathways resulted in visible decreases in cytokine production in both Atg7$^{-/-}$ and wildtype macrophages, though to different extents depending on the specific pathway inhibited. Galactose metabolism resulted in only a small decrease in IL-6 and IL-10 production, but had little or no effect on TNF-α secretion at all. Inhibition of glycolysis resulted in a reduction in IL-6, IL-10 and TNF-α in all macrophages, with a smaller reduction in secretion of IL-10 and TNF-α, but not IL-6, in Atg7$^{-/-}$ macrophages than wildtype macrophages. However, Atg7$^{-/-}$ macrophages appear more sensitive to PPP blockade by DHEA, with treatment almost abolishing LPS mediated IL-6 and IL-10 production, and significantly reducing TNF-α production. Decreased cytokine expression following PPP blockade was also present in wildtype macrophages, but not so much as Atg7$^{-/-}$ macrophages.

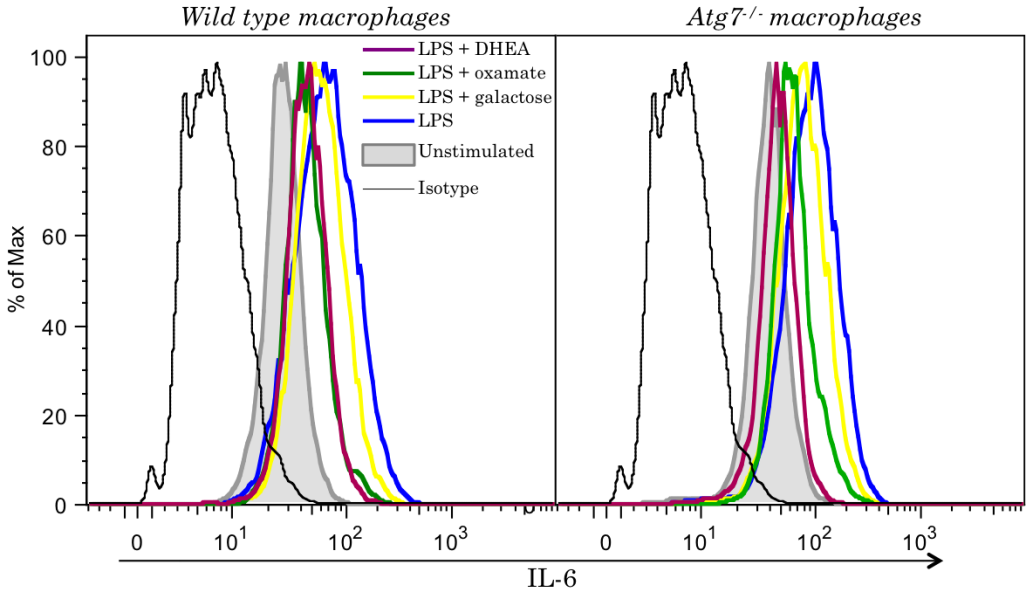

Figure 5.15: *Reduced IL-6 production by macrophages following chemical inhibition of metabolic pathways. BMMϕ were stimulated overnight with LPS in the presence of DHEA (200 μM), oxamate (40 mM) or galactose (2 mg/ml). Brefeldin A (1×) was added for 3 hr prior to staining to block protein secretion. Macrophages were stained for surface markers F4/80 and CD11b and then fixed and permeabilised for intracellular IL-6 staining. Representative histograms of wildtype (left) and Atg7$^{-/-}$ (right) macrophage IL-6 production following metabolic block.*

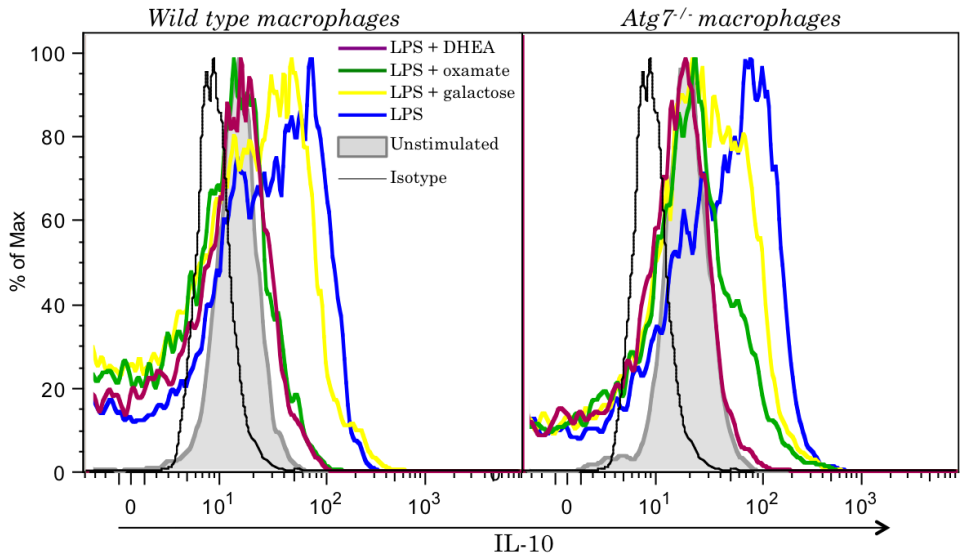

Figure 5.16: *Reduced IL-10 production by macrophages following chemical inhibition of metabolic pathways. BMMϕ were stimulated overnight with LPS in the presence of DHEA (200 µM), oxamate (40 mM) or galactose (2 mg/ml). Brefeldin A (1×) was added for 3 hr prior to staining to block protein secretion. Macrophages were stained for surface markers F4/80 and CD11b and then fixed and permeabilised for intracellular IL-10 staining. Representative histograms of wildtype (left) and Atg7$^{-/-}$ (right) macrophage IL-10 production following chemical metabolic block.*

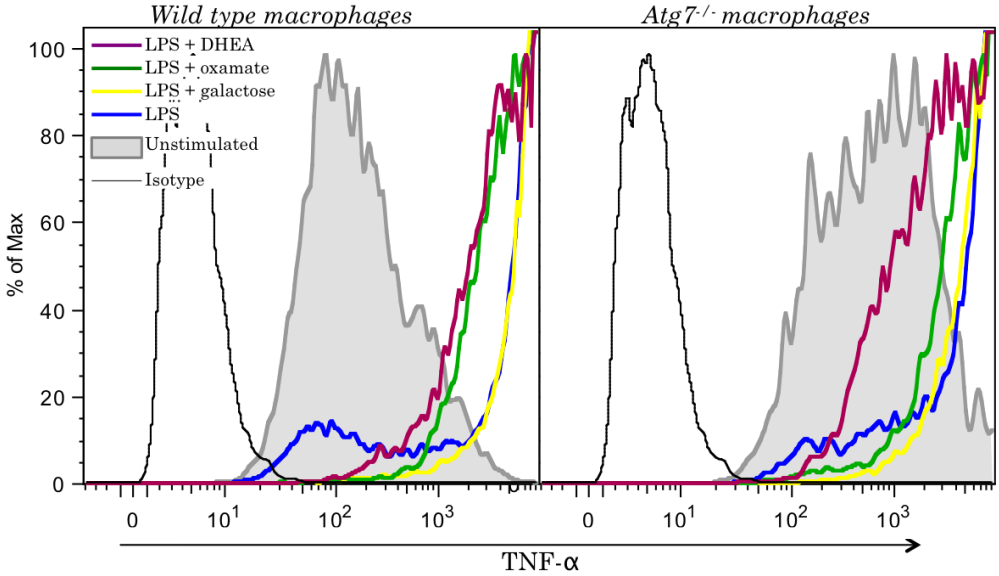

Figure 5.17*: Reduced TNF-α production by macrophages following chemical inhibition of metabolic pathways. BMMϕ were stimulated overnight with LPS in the presence of DHEA (200 µM), oxamate (40 mM) or galactose (2 mg/ml). Brefeldin A (1×) was added for 3 hr prior to staining to block protein secretion. Macrophages were stained for surface markers F4/80 and CD11b and then fixed and permeabilised for intracellular TNF-α staining. Representative histograms of wildtype (left) and Atg7$^{-/-}$ (right) macrophage TNF-α production following metabolic block.*

As discussed in chapter 3, Atg7$^{-/-}$ macrophages are more susceptible to cell death than wildtype macrophages, but not to the same extent as lymphocytes or RBCs. As such, the effect of inhibiting various metabolic pathways on cell death was investigated using the pathway inhibitors described above, in addition to media which contained no glutamine, another macrophage metabolic substrate(277). Cell death was variable in all cultures, resulting in no significant difference between average live cells in unstimulated Atg7$^{-/-}$ and wildtype cultures (figure 5.18). LPS stimulation and DHEA treatment resulted in a similar decrease in viability in both cultures, with significantly fewer viable cells in Atg7$^{-/-}$ macrophage cultures. Oxamate or glutamine treatment appeared to cause a slightly higher increase in cell death in Atg7$^{-/-}$ macrophages than in wildtype macrophages, though viability was variable in both cultures. Galactose substitution for glucose resulted in an equally large drop in viability in both cultures. However, this does not appear to be beyond the increased cell death visible in unstimulated cultures.

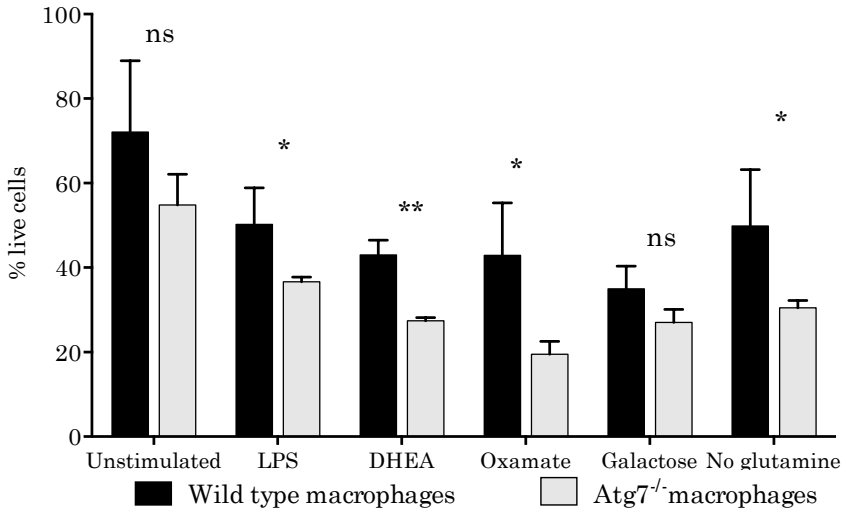

Figure 5.18: *Blockage of metabolic pathways increases cell death in Atg7$^{-/-}$ and wildtype macrophages. BMMϕ were cultured for 7 days and stimulated with LPS (1µg/ml) overnight in the presence of metabolic inhibitors, DHEA (200 µM), Oxamate (40 mM), Galactose (2 mg/ml) or in glutamine free R10. Cell death was assessed using a commercial fixable live dead stain. Graph shows percentages of live F4/80^{+} CD11b^{+} cells, error bars represent SEM, n = 4. *p<0.05, **p<0.01, ns is non-significant (un-paired t-test).*

Chapter 5: Discussion

Loss of autophagy skews macrophage metabolism to glycolysis

5.13 Atg7$^{-/-}$ macrophages are more glycolytic than wildtype macrophages

A number of experimental observations and bioenergenic profiling of Atg7$^{-/-}$ macrophages demonstrated that loss of autophagy in macrophages results in upregulation of glycolysis above wildtype levels. Glucose is the main metabolic substrate of macrophages, and uptake is increased following activation or stimulation with LPS, TNF-α and certain types of cellular injury(264). Activated M1 macrophages favour glycolysis as their primary mechanism for generating ATP(278), enabling them to adapt readily to hypoxic sites of inflammation(279), and as such generally high glycolysis is to be expected. However, the significantly increased levels of glycolysis in Atg7$^{-/-}$ macrophages suggest that, in the absence of autophagy, macrophages need increased levels of ATP or other glycolytic intermediates. Although glycolysis is less efficient per glucose molecule than OxPhos, glycolysis has other advantages for immune cells, being able to take place under oxygen-rich or hypoxic conditions, providing increased protein/nucleotide metabolism and a faster rate of ATP production(255, 280). Glycolysis guarantees that sufficient energy is produced in the required time frame to drive macromolecule synthesis (via anabolic metabolism), which is ultimately crucial for pathogen clearance and cell survival(281). Macrophages require increased ATP for functions such as phagocytosis, antigen presentation, migration and effector responses such as production of inflammatory cytokines. Inflammation and glycolysis are also intimately linked in macrophages, with M1 (inflammatory) macrophages upregulating glycolysis, whereas M2 (wound healing/anti-inflammatory) macrophages favour OxPhos(254). Furthermore, stimulation of OxPhos results in upregulation of macrophage anti-inflammatory responses(265), whereas overexpression of Glut-1 and upregulated glycolysis results in a hyper-inflammatory state(282). These data

suggest that there may be a link between the inflammatory phenotype of Atg7$^{-/-}$ macrophages and their increased rate of glycolysis.

Mitochondrial and glycolytic pathways are sensitive to changing conditions within the cell, enabling rapid shifts between forms of energy generation and allowing up- or downregulation of metabolic pathways to allow adaptation to changing ATP requirements. Glycolysis is frequently upregulated in tumours(283), providing similar advantages in terms of energy generation as it does in macrophages – increased rate of ATP production, oxygen independence and metabolic intermediates(255). Upregulation of autophagy in tumours is also common, with autophagy playing a pro-survival adaptive role, enabling tumours to survive in low oxygen, low nutrient environments and improving resistance against chemotherapeutic treatment(4, 284). One mechanism by which autophagy promotes tumour cell survival is in maintenance of tumour-associated glycolysis(285), with deletion of autophagy genes resulting in attenuated transformation, proliferation and reduced glycolytic capacity(286). Glycolysis also positively regulates autophagy by promotion of Atg12 transcription(115) and prevention of mTOR activation(287). Conversely, inhibition of glycolysis by TIGAR directs glycolytic intermediates toward the PPP, causing suppression of autophagy by glutathione-dependent reduction of ROS(288). Several questions then arise from our data: How does increased glycolysis benefit Atg7$^{-/-}$ macrophages, how does it affect the Atg7$^{-/-}$ inflammatory phenotype, and how does loss of autophagy contribute to the upregulation of glycolysis in macrophages, when in other systems loss of autophagy results in decreased glycolytic capacity? As discussed above, ATP generation by glycolysis has several advantages, particularly in terms of the rate of ATP production – ATP can be generated much faster by glycolysis than by OxPhos when glucose is not limiting. Loss of autophagy blocks several energy-generating sources, particularly energy released from degradation of amino acids, glycogen(289) and

lipids(290), which make a valuable energy source in autophagy-competent cells(291). In the absence of autophagy, glycolysis could potentially be upregulated to make up the energy shortfall.

Glycolysis has also been shown to be important for generating ATP to maintain mitochondrial membrane potential in macrophages following activation, thereby preventing apoptosis by the intrinsic pathway(292). Atg7$^{-/-}$ macrophages have a significantly higher mitochondrial burden and increased production of mROS. An increased burden of faulty mitochondria would require increased ATP generation to maintain mitochondrial potential and prevent apoptosis. This hypothesis could be assessed by incubation of Atg7$^{-/-}$ and wildtype macrophages in galactose, metabolism of which does not yield net ATP, and then following mitochondrial membrane potential with Tetramethylrhodamine (TMRM). This experiment would also indicate whether the glycolytic switch in Atg7$^{-/-}$ macrophages is permanent, or whether OxPhos could meet ATP demands when forced.

Recently, chaperone-mediated autophagy has been shown to be responsible for degrading the transcription factor HIF-1α(293). In addition to regulating inflammation(294, 295), HIF-1α facilitates glycolysis by transactivating pyruvate dehydrogenase kinase 1(258). Analysis of gene expression from Atg7$^{-/-}$ macrophages demonstrated increased HIF-1α expression, which would increase both inflammation and autophagy. HIF-1α as an autophagic substrate suggests that HIF-1α protein would accumulate in Atg7$^{-/-}$ macrophages, further enhancing glycolytic capacity and inflammatory cytokine production. Furthermore, ROS and inflammatory cytokines have also been shown to increase HIF-1α expression(296, 297), both of which are features of Atg7$^{-/-}$ macrophages, and could potentially drive increased glycolysis.

Inflammatory cytokine signalling has also been shown to increase glycolysis under other conditions. IL-6 enhanced glycolysis in mouse embryonic fibroblasts and human cell lines(298), and TNF-α and IFN-γ stimulation of human dermal fibroblasts has shown similar effects(299). As such, increased production of inflammatory cytokines by $Atg7^{-/-}$ macrophages could result in upregulation and maintenance of glycolysis, resulting in the phenotype observed. This effect may be bi-directional, as increased glycolysis results in production of increased mROS, which can then increase pro-inflammatory cytokine production(151).

Stimulation of TLR4 by LPS or other ligands results in glycolytic upregulation(266). As discussed in the previous chapter, increased secretion of inflammatory cytokines by 'unstimulated' $Atg7^{-/-}$ macrophages suggests that they are, in fact, likely pre-stimulated by an endogenous stimulus such as Prxn1 or other DAMPs. As such, it is difficult to rule out the possibility of the increased glycolysis observed in $Atg7^{-/-}$ peritoneal macrophages being due to pre-stimulation *in vivo* by cytokine signalling or DAMP-mediated TLR4 engagement from the present data. Nevertheless, unstimulated $Atg7^{-/-}$ BMMϕ had greater glucose uptake than wildtype BMMϕ, and an even greater increase following LPS stimulation. Although not conclusive, this does suggest that $Atg7^{-/-}$ macrophages have greater glycolytic capacity, even considering their potential pre-activated state, and it highlights a potential difficulty with comparing 'unstimulated' $Atg7^{-/-}$ macrophages with wildtype macrophages, since unstimulated macrophages may not truly exist in our model. As such, it may be instructive to use chemical or siRNA knockdown methods to inhibit autophagy in wildtype macrophages and observe changes in glycolytic capacity. This would also establish if increased glycolysis is specific to loss of Atg7 or autophagy in general.

As discussed above, increased glycolysis in tumour cells often requires autophagic support to prevent metabolic stress caused by the generation of increased ROS(300), which is vital in cells that are not adapted to a high level of glycolysis and ROS. However, macrophages are specially tailored to utilise glycolytic ATP and ROS for activation and cell killing, and therefore have adaptions that allow them to survive increased metabolic stress, such as upregulation of antioxidant genes(273). Furthermore, macrophage proliferation is inhibited following stimulation(301), whereas tumour cells are by their nature highly proliferative. This may explain why Atg7$^{-/-}$ macrophages are able to undergo such high levels of glycolysis in the absence of autophagy, whereas fast dividing tumour cells that do not normally utilise glycolysis or experience high levels of ROS, cannot.

5.14 Atg7$^{-/-}$ macrophages have increased respiratory reserves but no ATP-related oxygen consumption

Analysis of oxygen consumption in Atg7$^{-/-}$ and wildtype macrophages revealed a significantly higher basal OCR in the absence of autophagy, compared with wildtype macrophages. However, this basal oxygen consumption appears to be independent of ATP generation, as treatment with the stage 3 OxPhos inhibitor Oligomycin resulted in no change in OCR, whereas OCR in wildtype macrophages decreased to around half the basal levels. This suggests that wildtype macrophages are generating a proportion of their energy from OxPhos, whereas Atg7$^{-/-}$ macrophages are relying solely on glycolysis for their energy needs, with little residual OxPhos-related ATP production. As discussed previously, this may indicate that Atg7$^{-/-}$ macrophages are already partly activated *in vivo* and have thus downregulated OxPhos(292). However, while LPS stimulation of macrophages does normally lead to an increased ECAR, this usually occurs with a simultaneous drop in OCR(302). Furthermore, activation with LPS has previously been

shown to result in a lower basal OCR than unstimulated macrophages(269). Since increased, not decreased, oxygen consumption is a feature of Atg7$^{-/-}$ macrophages, their lack of ATP-related oxygen consumption may not indicate activation.

FCCP is used to assess maximal potential oxygen consumption, known as maximum respiratory capacity (MCR), by uncoupling the proton transport chain from ATP synthesis. Atg7$^{-/-}$ macrophages were shown to have a significantly increased MRC compared to wildtype macrophages, and also held their oxygen consumption steady during FCCP treatment, whereas wildtype macrophage OCR showed an initial peak that slowly dropped as time passed. Spare respiratory capacity (SRC) can then be calculated by the difference between the MRC and the basal OCR. The increased SRC in Atg7$^{-/-}$ macrophages may be due to the increased number of mitochondria present in their cytoplasm, and therefore higher consumption of oxygen upon FCCP treatment. Interestingly, a high SRC has previously been associated with M2 macrophages, due to increased mitochondrial biogenesis(269), whereas in the same experiments, LPS stimulated and M1 macrophages had a SRC comparable to their basal OCR. Although increased mitochondria in Atg7$^{-/-}$ macrophages are likely due to reduced clearance by autophagy, increased mitochondrial biogenesis cannot be ruled out. Biogenesis could be assessed by analysis of Tfam and Cox-1 expression, a major regulator of mitochondrial biogenesis and an essential component of the respiratory chain, respectively(303). It has been proposed that increased SRC under conditions of maximum physiological stress is a major factor determining the survival of cells(268), by reducing their reliance on glycolysis and increasing the variety of potential energetic substrates(304). This may provide a survival advantage for Atg7$^{-/-}$ macrophages, potentially allowing them to revert to OxPhos if required. It would be interesting to repeat the bioenergetic Seahorse experiment using glycolytic inhibitors, such as 2-Deoxyglucose or oxamate, and observe whether any of the SRC observed in Atg7$^{-/-}$ macrophages could

be utilised, or whether mitochondrial damage in the absence of autophagy renders this impossible, or severely reduced.

Treatment of macrophages with the mitochondrial NADPH dehydrogenase inhibitor, rotenone, allowed assessment of non-mitochondrial respiration. Rotenone treatment of $Atg7^{-/-}$ macrophages resulted in a decrease in OCR from the MRC back to basal levels, implying that basal oxygen consumption in $Atg7^{-/-}$ macrophages is independent of the mitochondrial route. In wildtype macrophages, however, OCR decreased to the oligomycin treated rate, suggesting that part of the basal rate in wildtype macrophages is ATP-related, with a smaller proportion of mitochondria exhibiting independent respiration. Non-mitochondrial respiration has been shown to include consumption of oxygen at the cell surface via trans-plasma membrane electron transport (tPMET)(305), which is particularly prevalent in cells undergoing high levels of proliferation or glycolysis. This form of non-mitochondrial respiration may assist glycolytic energy production by facilitating re-oxidation of cytosolic NADH, allowing continued glycolysis. tPMET helps alleviate the intracellular reductive stress caused by persistent glycolysis(306), and has been shown to take place in macrophages(307). Use of such a pathway in $Atg7^{-/-}$ macrophages would make sense to help maintain their high rate of glycolysis and explain their high ATP-independent oxygen consumption. The contribution of tPMET to oxygen consumption can be assessed using reduction of the water-soluble tetrazolium salt (WST-1) to the chromogenic formazan, which can then be assessed by spectrophotometry(308). In this experiment, OCR and ECAR were both investigated after treatment with compounds that directly influence various aspects of OxPhos. Given the high reliance of $Atg7^{-/-}$ macrophages on glycolysis and their apparently high SRC, it would be instructive to conduct a similar experiment using glycolytic inhibitors. An experimental setup could investigate changes in ECAR and OCR following macrophages incubated in galactose

initially, followed by injection of glucose to increase the glycolytic rate, oligomycin to show maximum glycolysis, and 2DG to completely inhibit glycolysis and give an indication of non-glycolytic acidification.

5.15 Altered metabolism in Atg7$^{-/-}$ macrophages may include changes in the Pentose Phosphate Pathway

In addition to altered expression of glycolytic proteins suggested by proteomic analysis, and verified experimentally, proteomics showed a decrease in expression of several proteins associated with the PPP in Atg7$^{-/-}$ macrophages. Although these alterations remain to be verified by western blot or other assays to demonstrate levels of the vital enzymes involved, it is interesting to consider the potential contribution of an altered PPP to the Atg7$^{-/-}$ phenotype. The PPP is an essential supplier of the reducing agent NADPH for glycolysis and a major source of other metabolic intermediates(309). Proteomic analysis suggests that Glucose-6-phosphate 1-dehydrogenase (G6PD) and 6-phosphogluconate dehydrogenase, two enzymes in the oxidative phase of the PPP, have reduced expression in Atg7$^{-/-}$ macrophages. NADPH is an important reductant, with key roles in many biological processes including maintenance of the antioxidant system(310). Research has shown that overexpression of macrophage G6PD and associated NADPH production, caused increased expression of pro-inflammatory and pro-oxidative genes(311). Thus, decreased production in Atg7$^{-/-}$ macrophages may play a protective role in limiting oxidative damage in the absence of autophagy. However, macrophage G6PD deficiency has also been shown to increase cytokine responses following LPS stimulation(312), paralleling the phenotype observed in our macrophages, suggesting that reduced G6PD expression may be contributing to the increased inflammatory cytokine production observed from our macrophages. The polarised responses to G6PD expression in various

cells and experimental conditions(311-314) suggest that the role of G6PD, and potentially the significance of the initial phase of the PPP, are influenced by cell type, redox signalling, activation state and other experimental conditions. Further investigation using PPP modulators and quantitative assessment of PPP enzyme levels would be required to determine its true role in autophagy-deficient macrophages.

5.16 Atg7$^{-/-}$ macrophages show upregulated expression of antioxidant pathways

As so many macrophage processes and effector functions rely on the production of ROS, macrophages have adapted comprehensive antioxidant defences to allow regulation of oxidant production at a safe level for homeostasis and signalling(152). A significant upregulation of antioxidant pathways in Atg7$^{-/-}$ macrophages was indicated in the proteomic analysis, and confirmed by qPCR analysis. Increased Prxn1 staining was also found in LPS-stimulated Atg7$^{-/-}$ macrophages by immunofluorescence staining. A major instrument in cellular defences against oxidative stress is the activation of the Nrf2-antioxidant response element signalling pathway, to which the Prxns, heme oxygenase and thioredoxin all belong(315). Nrf2 directs expression of genes involved in detoxification and removal of reactive oxidants via chemical reactions and enhancement of antioxidant capacity. Nrf2 is activated in macrophages during oxidative stress(316), with Nrf2$^{-/-}$ macrophages showing a marked increase in their susceptibility to oxidative cell death induced by l-chloro-2,4-dinitrobenzene(273). In unstressed cells, Nrf2 is maintained at low cytoplasmic levels by its inhibitor Keap1, which directs its degradation via the proteasome. During oxidative stress, Keap-mediated degradation is inhibited, and the stabilised protein is able to translocate to the nucleus(153), allowing expression of genes including antioxidants, DNA repair enzymes, and anti-inflammatory response proteins. Much like

the autophagy pathway, there is controversy over the exact role of Nrf2 in cancer, as it appears to play a dual role as both a tumour suppressor and an oncogenic factor – preventing tumorigenesis, but contributing to enhanced survival of tumour cells. Atg7$^{-/-}$ macrophages produce significantly higher levels of ROS than wildtype macrophages, due to increased levels of damaged mitochondria, and potentially also to their increased levels of glycolysis, which has been shown to increase oxidative stress(278). As such, increased expression of antioxidants such as Prxn1 is likely an adaptive response by Atg7$^{-/-}$ macrophages to enable survival in the presence of increased ROS. Furthermore, p62 accumulation in liver cells defective in autophagy has been shown to increase the action of Nrf2, by interacting with the Nrf2 binding site on Keap1 and allowing Nrf2 translocation to the nucleus(190). A similar build-up of p62 in Atg7$^{-/-}$ macrophages may also contribute to Nrf2 activation, further upregulating antioxidant activation. Interestingly, proteomic analysis also indicated reduced expression of Obg-like ATPase 1 (OLA1), a negative regulator of the antioxidant pathway(271). Activation of antioxidant enzymes and other defensive proteins leads to a reduction in cellular free radicals, many of which are vital for normal cell signalling. Furthermore, overexpression of extracellular Prxns, such as Prxn1, can have detrimental effects by acting as DAMPs, as discussed previously. Thus, cells may require regulatory factors such as OLA1 to prevent free radicals from falling below a critical threshold. This suggests that over-activation of the antioxidant response via persistent Nrf2 activation could have detrimental effects, which contribute to their inflammatory phenotype. This could be assessed using overexpression of OLA1 to selectively blunt the antioxidant response, and investigating increases in cell death, oxidative stress and inflammatory cytokine production.

5.17 Perturbation of energy generation pathways influences the inflammatory response and cell death

Loss of Atg7 in macrophages results in increased glycolysis and potential perturbation of the PPP. As both the PPP and glycolytic pathways have been linked to increased production of inflammatory cytokines(282, 317), cytokine expression in $Atg7^{-/-}$ macrophages was assessed following overnight incubation of macrophages with metabolism modulators. Oxamate, an LDH inhibitor, was used to inhibit glycolytic ATP production and the PPP was inhibited by DHEA, a G6PD inhibitor. Galactose was also substituted for glucose in some cultures, enabling an assessment of the energy contribution of glycolysis to cytokine production, since metabolism of galactose by glycolysis yields no net ATP.

Galactose metabolism resulted in only a very small reduction in cytokine expression, with no differences observed between wildtype and $Atg7^{-/-}$ macrophages, suggesting that cytokine production is not significantly influenced by reduction in glycolytic ATP production, and that the increased ATP production by $Atg7^{-/-}$ macrophages is likely not the cause of increased cytokine expression. Interestingly, galactose treatment resulted in a significant increase in cell death, in both wildtype and $Atg7^{-/-}$ macrophages, suggesting that activated macrophages do struggle to convert their energy production mechanism to OxPhos, at least for an overnight period. This experiment could be repeated using different durations of galactose replacement, to determine whether short term galactose treatment results in OxPhos upregulation and whether any macrophages managed to adapt over longer periods of galactose incubation. Glucose could also be replaced by pyruvate as an energy source, which would feed directly into the OxPhos pathway and possibly stimulate its energetic output.

Direct inhibition of glycolysis using oxamate resulted in decreased cytokine expression in both wildtype and Atg7$^{-/-}$ macrophages, confirming that glycolytic rate does impact cytokine secretion. As Atg7$^{-/-}$ macrophages have a higher glycolytic rate, it was expected that blockade of the glycolysis pathway would have a greater influence on cytokine secretion than in wildtype macrophages. However, this was not the case, with wildtype macrophages showing a greater decrease in expression of IL-10 and TNF-α than Atg7$^{-/-}$ macrophages, though the drop in IL-6 secretion was similar. This could be due to activation of respiratory reserves in Atg7$^{-/-}$ macrophages, to make up for the ATP shortfall, or it may be that the concentration of oxamate used was not sufficient to blockade the level of glycolysis occurring in Atg7$^{-/-}$ macrophages. Experiments with longer duration of oxamate treatment (in this experiment overnight treatment was used) or a higher concentration of oxamate may give a clearer indication of the role of increased glycolysis in excess cytokine production by Atg7$^{-/-}$ macrophages. Glycolytic blockade also increased cell death, as expected, due to macrophage reliance on glycolytically-derived ATP. Unlike galactose treatment, which resulted in similar levels of cell death in both cultures, oxamate treatment resulted in a significantly higher increase in cell death in Atg7$^{-/-}$ macrophages than wildtype macrophages, suggesting increased glycolysis is indeed a survival adaption to the loss of autophagy. However, cell death in all cultures was quite variable in this experiment, and further experiments, possibly experimenting with different oxamate concentrations or durations, would be useful to clarify the contribution of glycolytic blockage to increased macrophage cell death.

Interestingly, Atg7$^{-/-}$ macrophages did appear to be more sensitive to PPP blockade than wildtype macrophages. Following overnight treatment with DHEA, LPS-stimulated Atg7$^{-/-}$ macrophages showed no induction of IL-6 or IL-10 expression above unstimulated levels. TNF-α expression was also significantly reduced in Atg7$^{-/-}$ macrophages, though

there was still an induction of expression above unstimulated levels. Wildtype macrophage cytokine expression was also reduced in the presence of DHEA, but to similar levels as those observed following oxamate treatment. This strongly implicates the PPP in modulation of increased inflammatory cytokines in macrophages, since interruption of the pathway leads to reduced expression. Possibly Atg7$^{-/-}$ macrophages were more affected by PPP blockade due to reduced expression of G6DP, meaning the blockade was more effective. However, if this was the whole story, one would expect general cytokine secretion in untreated Atg7$^{-/-}$ macrophages to also be lower, again due to apparently decreased G6DP. Clarification of actual PPP metabolic rates in wildtype and Atg7$^{-/-}$ macrophages would assist in interpretation of these data.

5.18 Conclusions

Loss of Atg7 and autophagy in macrophages results in a dramatic skewing of metabolism toward glycolysis, while maintaining elevated rates of oxygen consumption and increased respiratory reserve. Upregulation of glycolysis may function as a survival mechanism, allowing generation of additional ATP to substitute for lost energy production in the absence of autophagic degradation of intracellular substrates. To our knowledge, this is the first report of increased glycolysis in the absence of autophagy, with previous reports showing a requirement for autophagy in glycolytic energy production. Altered glycolysis and oxygen consumption may also be accompanied by alterations in the PPP, which could further influence oxidative stress and cytokine production. Atg7$^{-/-}$ macrophages are able to adapt to the oxidative stress caused by increased mitochondrial load and production of mROS in the absence of autophagy through upregulation of antioxidant pathways, such as the Nrf2 family of antioxidants. The ability to upregulate glycolysis and antioxidant pathways, two pathways fundamental to normal macrophage function, may enable

macrophages to survive and adapt to loss of autophagy, whereas immune cells that are less adapted to oxidative stress, such as T-cells, or more reliant on OxPhos succumb more quickly when stressed.

Chapter 6: Introduction

Aged macrophages have a similar phenotype to Atg7$^{-/-}$ macrophages

6.1 Autophagy and aging

Aging is an inevitable physiological phenomenon characterised by accumulation of molecular damage within cells and tissues, resulting in functional changes and impairment caused by continuous decline in essential maintenance and repair pathways(318). Further contributions to the rate and extent of aging include predetermined genetic factors, environmental influences, and disease(5). Common changes associated with aging include changes in tissue composition, decreased physiological capacity (for example reduced cardiovascular function), diminished response to external stimuli and increased incidence of disease(319, 320). The link between autophagy and aging was first revealed by genetic studies of yeast, and later of *C. elegans*, where siRNA mediated knockdown of Beclin-1 resulted in a significant decrease in lifespan(46, 47, 321, 322). Complete or tissue specific ablation of autophagy genes in other models has shown a similar link between lack of autophagy and aging, whereas genetic overexpression of the autophagy gene Atg5 has been shown to increase lifespan(323).

Autophagy has also been linked to aging through studies investigating the benefits of caloric restriction on lifespan(324). Caloric restriction (CR) is achieved by reducing calorie consumption without causing malnutrition, and appears to be the crucial anti-aging intervention that extends life span in most animals, including rhesus monkeys, in which it reduces the incidence of cardiovascular, cancer, disease diabetes, and brain atrophy(325). Epidemiological studies suggest that CR is also beneficial to human health(326). CR is the most potent physiological inducer of autophagy, whereas inhibition of autophagy prevents the anti-aging benefits of CR in all species in which it has been investigated(327). Significant evidence has accumulated to suggest that maintenance of autophagy levels extends lifespan(328, 329). Furthermore, several studies have implicated autophagy in protection against a variety of age-related diseases, such as Alzheimer's disease,

Huntington's disease, Parkinson's disease and oculopharyngeal muscular dystrophy(12, 13, 48, 330). The mechanisms by which autophagy is thought to increase lifespan and reduce age-related decline include the removal of accumulated toxic protein aggregates, degradation of damaged mitochondria and improved mitochondrial function, and reduced cell death arising from enhanced homeostasis and hormesis(331). Furthermore, autophagy protects against stem cell loss and damage, as shown by our group(57, 332), and reduces oncogenic transformation(4, 333), thereby limiting the incidence of cancer.

Although the link between reduced autophagy and aging is now well established, little is known about why autophagy levels decline with age. Some studies have suggested that expression of autophagy genes declines with age(334), though the mechanism for reduced expression was not explored. Further research is required into the mechanism of age-related autophagy decline and into effective, accessible methods to maintain autophagy levels with age in addition to CR.

6.2 Aging of the immune system

In addition to the myriad of other systems whose function declines with age, aging is associated with a decline in effective immune function and a corresponding increase in susceptibility to infection and attendant mortality(335). Aging causes changes in both the innate and adaptive arms of the immune system, both in cell number and function.

Aging results in an overall decrease in HSC number and renewal capacity, resulting in reductions in total hematopoietic tissue volume in bone marrow(336-338), and changes in lineage commitment, with a skewing toward myeloid progenitors at the expense of lymphoid progenitors(339). Adaptive immunity is significantly impaired in the elderly, resulting in increased susceptibility to infection and reduced response to vaccinations. Numbers of T- and B-cells decline significantly with age(340, 341), and their function is

also affected. Antibodies produced by B-cells from elderly people exhibit decreased affinity for antigen and class-switching ability is impaired compared with B-cells from younger individuals(342). A simultaneous decline in the function of $CD4^+$ T-helper cells might also be a contributing factor to B-cell changes(343). There are several other changes in T-cell number and function with age, including reduced numbers of naive T-cells, diminished response to antigenic stimulation, decreased proliferation, and increased numbers of memory cells(344).

There are also a number of alterations in innate immunity that occur with aging. However, whereas the adaptive immune system shows almost universal decline with age, changes in the innate immune system are more enigmatic. Although functions of some immune cells do appear decreased, a chronic, low level of inflammation is frequently observed in the elderly due to increased inflammatory cytokine production from innate cells such as neutrophils and macrophages, a process known as 'inflammaging'(345). Numbers of NK cells have been shown to increase with age but their cytotoxicity is decreased and secretion of cytokines and chemokines such as RANTES, MIP1α, and IL-8 are also reduced(346). Neutrophil effector functions are decreased with age, including phagocytosis and superoxide generation(347, 348). DCs also show some alterations in function, though it appears that some aspects of the DC response are unchanged. Aged DCs retain their capacity for stimulation of a T-cell response(349), however expression of DC-SIGN is reduced and DC trafficking *in vivo* is significantly impaired(350). Decreased stimulated cytokine production has also been observed from aged DCs(351), though basal levels of production were found to be increased. Macrophages also exhibit a variety of age related changes. Increased numbers of monocytes and macrophages have been observed in the elderly(352, 353), though their functional capacity is reduced(354). Aged macrophages exhibit a decrease in oxidative and NO burst(355) and have reduced phagocytic

capacity(356). TLR expression on macrophages decreases during aging(236), which may be responsible for the decreased cytokine production observed by some researchers. However, several other studies have shown increased inflammatory cytokine production by aged macrophages(357, 358). Expression of important antigen presentation receptors such as MHC II and the co-receptor CD86 has also been shown to be decreased on aged macrophages(359, 360), potentially altering antigen presentation capacity.

There is considerable variation in the specific alterations recorded in studies of aged immune systems, partly as a result of different methods of analysis, background conditions and the difficulty in identifying 'healthy' aged participants with no other underlying conditions that could alter immune function(354).

6.3 Similarities between autophagy-deficient and aged macrophages

This chapter demonstrates decreased levels of autophagy in aged macrophages and draws parallels between the phenotypes of aged and Atg7$^{-/-}$ macrophages. We show that aged macrophages have several features in common with autophagy-deficient macrophages and link further functional changes in aged macrophages observed in the literature with the altered functions observed in Atg7$^{-/-}$ macrophages. Loss of autophagy in macrophages appears to dramatically accelerate the appearance of aged macrophage features, suggesting that the decreased autophagy observed in aged macrophages contributes to their functional decline and increased production of inflammatory cytokines, potentially implicating autophagy in the regulation of inflammaging.

Chapter 6: Results

Aged macrophages have a similar phenotype to Atg7$^{-/-}$ macrophages

6.4 Aged macrophages have reduced autophagy

The reduction in innate and adaptive immune responses and increased inflammatory status in Atg7$^{-/-}$ macrophages is caused by lack of autophagy directly interacting with vital cellular processes (e.g. reducing antigen processing or clearance of activated inflammasomes) or indirect effects such as increased reactive oxygen species. Reductions in the innate and adaptive immune responses produced by aged macrophages may also have a similar origin and be caused by reduced autophagy. Autophagy levels were assessed in BMMϕ from aged mice using a novel imaging flow cytometry assay developed by our lab(361). Autophagy was assessed by evaluating mean numbers of autophagic 'puncta' per cell, which are formed when lipidated LC3 is recruited into autophagosomes, and by assessing the colocalisation of autophagosomes and lysosomes as defined by Bright Detail Similarity (% BDS). BDS is a feature of the Image Stream that calculates the proportion of overlapping pixel intensities of different channels of fluorescence(362). BMMϕ from aged mice have significantly fewer mean LC3 puncta per cell, particularly following inhibition of autophagic flux using E64D and PepstatinA (figure 6.1). Autophagy was inducible with IFNγ and LPS in both macrophages from 7 week and 107 week mice, but remained significantly lower in aged macrophages than in young macrophages.

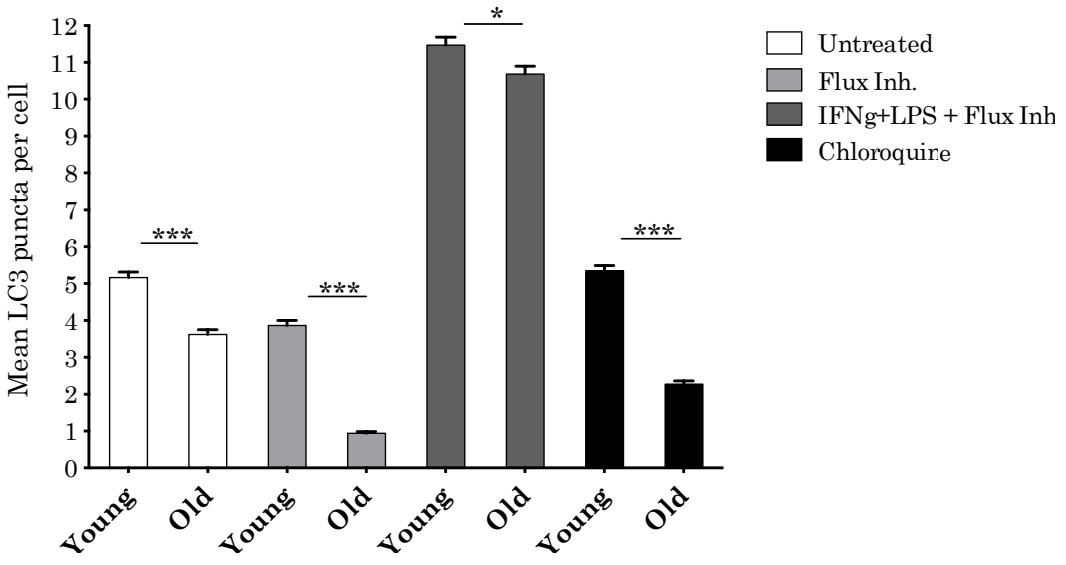

Figure 6.1*: Aged macrophages have reduced LC3 puncta even after autophagic induction. BMMϕ were cultured for 7 days and stimulated overnight with IFNγ (10 ng/ml) and LPS (1 µg/ml) to induce autophagy. Autophagic flux was inhibited for 2 hours with E64D (10 µg/ml) and Pepstatin A (2 µg/ml) or Chloroquine (20 µM). Samples were then stained for F4/80, followed by fixation and permeabilisation to allow LC3 and lysoID staining. Dead cells were excluded by live/dead staining. Mean LC3 puncta/cell was assessed using the ImageStream Spot Count wizard. Graph shows mean LC3 puncta/cell, error bars represent SD. *p<0.05, ***p<0.001, one-way ANOVA. Grateful acknowledgments to Anne Hansen for running and analysing the samples and for help and advice with autophagy assays.*

Autophagy starts with the formation of LC3^{+} autophagosomes around autophagic substrates. However, it is a highly dynamic process that is not considered complete until the fusion of autophagosomes with lysosomes to give the degradative autolysosomes capable of recycling components into the cytoplasm. As such, increased presence of autophagosomes alone is not ideal as a measure of autophagy. Measuring co-localisation of LC3^{+} autophagosomes with lysosomes gives a further measure of the level of autophagy flux in cells, by measuring the BDS between the two fluorescent markers as described above. BDS (and co-localisation of autophagosomes and lysosomes) was significantly reduced in macrophages derived from 107 week old mice, compared with macrophages from 7 week old mice (figure 6.2). Chloroquine treatment reduced BDS in young macrophages, but not in old macrophages, suggesting low levels of autophagy already

present in aged macrophages that cannot be further reduced. Flux inhibitors and autophagic stimuli (LPS and IFNγ) resulted in increased BDS in both young and old macrophages over untreated macrophages, though was still significantly lower in aged compared to young macrophages. Together, reduced numbers of LC3 puncta and reduced co-localisation between autophagosomes and lysosomes as indicated by BDS is indicative of lower autophagy in aged macrophages than in young macrophages.

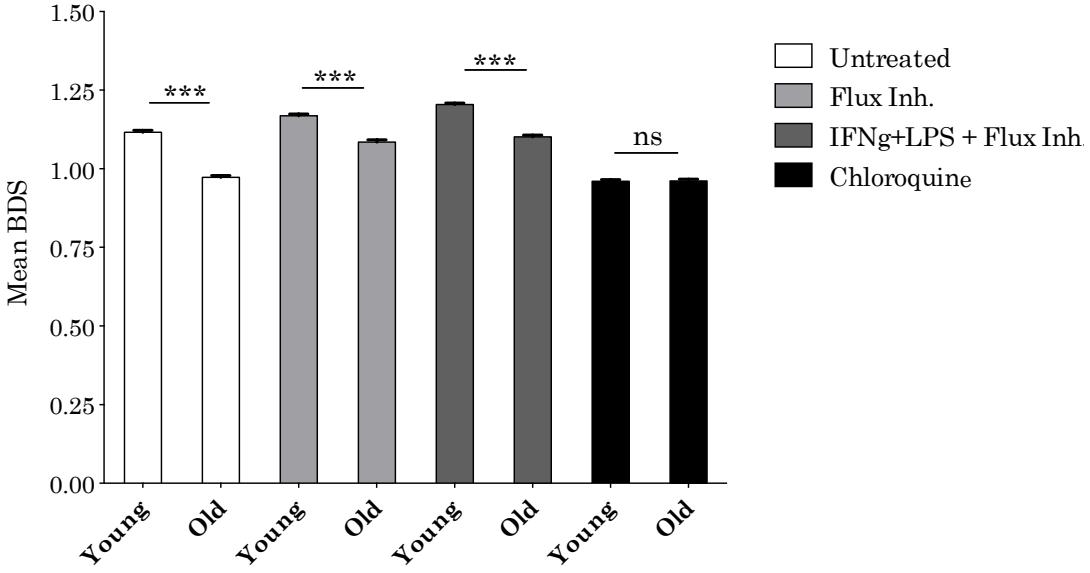

Figure 6.2: *Reduced colocalisation between LC3^{+} autophagosomes and lysosomes in aged mice. BMMϕ were cultured for 7 days and stimulated for 3hrs with IFNγ (10 ng/ml) and LPS (1 μg/ml) to induce autophagy. Autophagic flux was inhibited for 2 hours with E64D (10 μg/ml) and Pepstatin A (2 μg/ml) or Chloroquine (20 μM). Samples were then stained for F4/80, followed by fixation and permeabilisation to allow LC3 and lysoID staining. Dead cells were excluded by live/dead staining. Grateful acknowledgments to Anne Hansen for running and analysing the samples and for help and advice with autophagy assays. ***p<0.001, t-test.*

6.5 Aged mice have increased numbers of myeloid cells

Human and animal aging is accompanied by a decline in immune function, causing increased susceptibility to infection and reduced quality of life, as well as being a major cause of mortality. Immune aging is associated with a decline in numbers and function of the lymphoid cells of the adaptive immune system, with fewer immature T- and B-

cells(363) released from the bone marrow and a significant reduction in T-cell diversity(364). Aging of the innate immune system can also be accompanied by changes in cell numbers, with increases in circulating neutrophils(353) and macrophages(365) observed, and a general skewing of haematopoiesis toward the myeloid lineages(366, 367). Furthermore, the elderly are significantly more susceptible to myeloproliferative and myelodysplastic syndromes than young individuals.

This bias toward myeloid cell production is reminiscent of the Vav-Atg7$^{-/-}$ mouse model, which has significantly decreased T and B lymphocytes(147) and increased numbers of macrophages and neutrophils (Chapters 3 and 7). Macrophage numbers were assessed by flow cytometry from 107 week old C57BL/6 mice and compared to 7 week old wildtype mice, the same age at which Atg7$^{-/-}$ macrophage numbers were assessed at. Macrophage numbers were found to be significantly increased in the blood and spleen of aged mice, similar to Vav-Atg7 (figure 6.3).

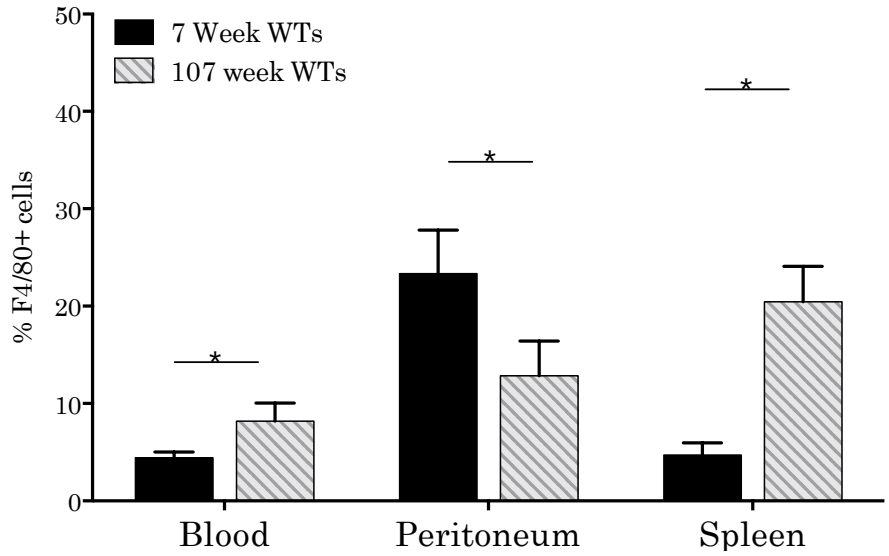

Figure 6.3: *Increased numbers of F4/80^{+} cells in the blood and spleen of 107 week old mice, but reduced numbers in the peritoneal cavity. Blood, peritoneal and splenic single cell suspensions from 7 and 107 week old C57BL/6 mice had RBC lysed prior to staining for analysis by flow cytometry. Graph shows average % of F4/80^{+} cells/sample, error bars represent SEM and n = 3. *p<0.05, un-paired t-test.*

However, significantly fewer macrophages were found in the peritoneal cavity of aged mice, relative to 7 week old mice, in contrast to Vav-Atg7 mice, which also had increased peritoneal macrophages.

6.6 Altered expression of surface marker and autophagy genes in aged macrophages

Reduced expression of genes encoding the surface marker receptors for MHC II and TLR4 was a feature of Atg7$^{-/-}$ macrophages (see results chapter 4), potentially contributing to reduced surface expression of these vital immune recognition and signalling molecules and thereby reducing the ability of the macrophages to mount an effective response to immune challenge. IFNγ stimulated MHC II mRNA expression has previously been found to be reduced in aged mice(360), as has reduced expression of TLRs on peritoneal and splenic macrophages from aged mice(236). BMMϕ were derived from 107 week old mice and RNA extracted for analysis by qPCR. Expression of MHC II and TLR4 mRNA was compared to that from BMMϕ derived from 7 week old mice, and found to be significantly reduced to 60% and 45% of young mice expression, respectively (figure 6.4). This is very similar to the reduced levels of MHC II and TLR4 mRNA expression seen in unstimulated Atg7$^{-/-}$ macrophages.

Levels of the transcription factors controlling antioxidant expression and adaptation to hypoxic conditions, Nrf2 and HIF-1α, were also assessed by qPCR, as these had been found to be increased in Atg7$^{-/-}$ macrophages (see results chapter 5). Neither Nrf2 nor HIF-1α expression was upregulated in BMMϕ derived from old mice compared with young mice. Finally, levels of autophagy gene expression were compared in macrophages derived from young and old mice, to determine whether low expression of autophagy genes contributes to the reduced autophagy observed in macrophages derived from aged mice. Levels of

Atg7 and Atg6 mRNA were both significantly reduced from aged macrophages, with Atg7 particularly reduced to less than 50% of that seen in young macrophages. The reduction in Atg6 mRNA was more modest, to 90% of young macrophage levels. Atg5 expression was particularly variable between replicates, but showed a trend of increased expression in aged macrophages. However, the increase was not significant. The reduction in expression of essential autophagy genes Atg6 and Atg7 may contribute to the reduced autophagy observed in macrophages derived from aged mice.

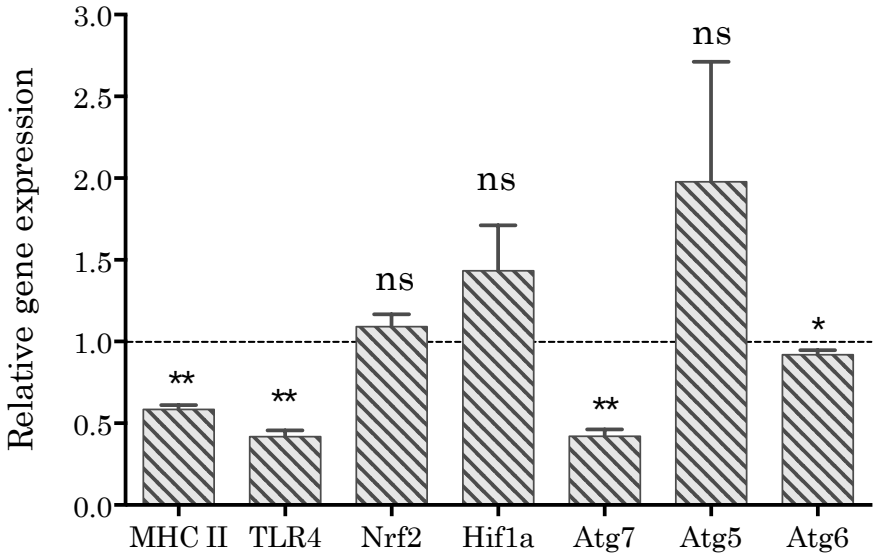

Figure 6.4: *Decreased relative surface marker and autophagy gene mRNA expression in aged macrophages. BMMϕ from 7 and 107 week old mice were cultured for 7 days as previously described. Macrophages from 3 aged or 3 young mice were pooled, total RNA was extracted using Trizol reagent and reverse transcribed to cDNA. Values determined using the ΔΔCT method, normalised to GAPDH and compared to 7 week old macrophages cultured under the same conditions. Dotted line represents young mouse expression levels. Error bars represent standard deviation of 3 replicates, *p<0.05, **p<0.01, un-paired t-test.*

6.7 Aged macrophages have increased lipid droplets

Atherosclerotic cardiovascular disease is a major, age related, cause of morbidity and mortality worldwide(368), with excessive lipid accumulation and release of inflammatory cytokines by macrophages within atherosclerotic plaques a major contributor to disease(369). We (chapter 3) and others(122) have shown higher lipid levels in autophagy-

deficient macrophages, as autophagosomes help breakdown and recycle droplets to prevent their build-up. Reductions in autophagy in aged macrophages may also contribute to increased lipid droplets, and hence lipid levels in aged macrophages were assessed using the lipid stain Nile Red. Like Atg7$^{-/-}$ macrophages, macrophages derived from 107 week old bone marrow were found to stain significantly higher for lipid than young mice (figure 6.5).

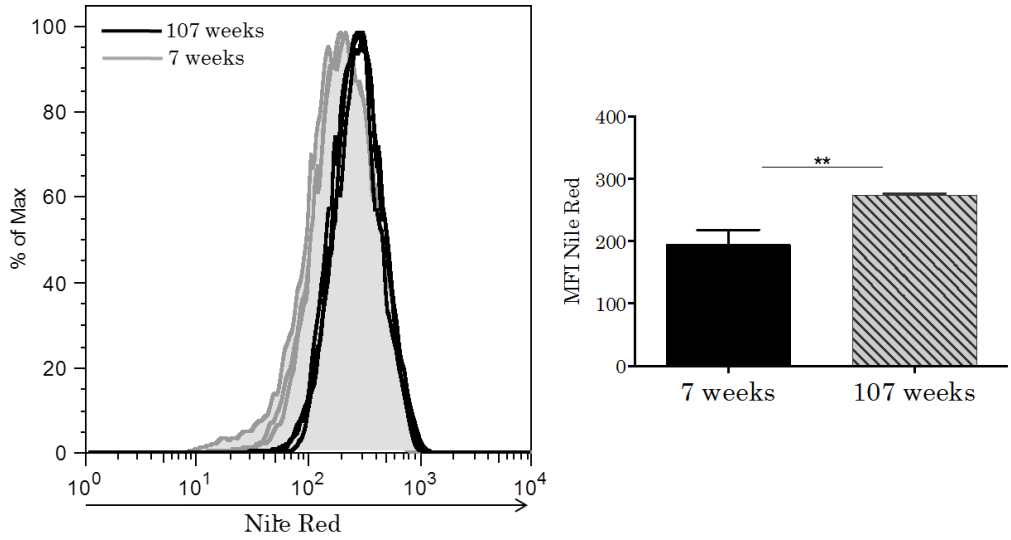

***Figure 6.5**: Increased Nile Red Lipid droplet staining in bone marrow derived macrophages from aged mice. BMMϕ were cultured from 7 and 107 week old mice for 7 days as previously described. Macrophages were stained for F4/80 and CD11b, followed by staining with Nile red (1 μM) for 20 min at 37° C. Left: overlaid histograms of Nile red staining in F4/80$^+$ CD11b$^+$ cells. Right: Graphical representation of average MFI of Nile red fluorescence for F4/80$^+$ CD11b$^+$ macrophages. Error bars represent SEM, n = 3. **p<0.01, un-paired t-test.*

6.8 Aged macrophages are more granular

Macrophages have a characteristic high light scatter profile when assessed by flow cytometry. As discussed in chapter 1, high SS results from increased cellular complexity and can be caused build-up of organelles or other components, such as lipid droplets, in the cytoplasm(370). As Atg7$^{-/-}$ macrophages exhibited significantly higher side scatter than wildtype macrophages, aged macrophages were assessed for the same characteristic. Side scatter in both young and old bone marrow derived macrophages was very high. Similarly

to Atg7$^{-/-}$ macrophages, however, aged macrophages had significantly higher side scatter and therefore granularity, than young macrophages (figure 6.6).

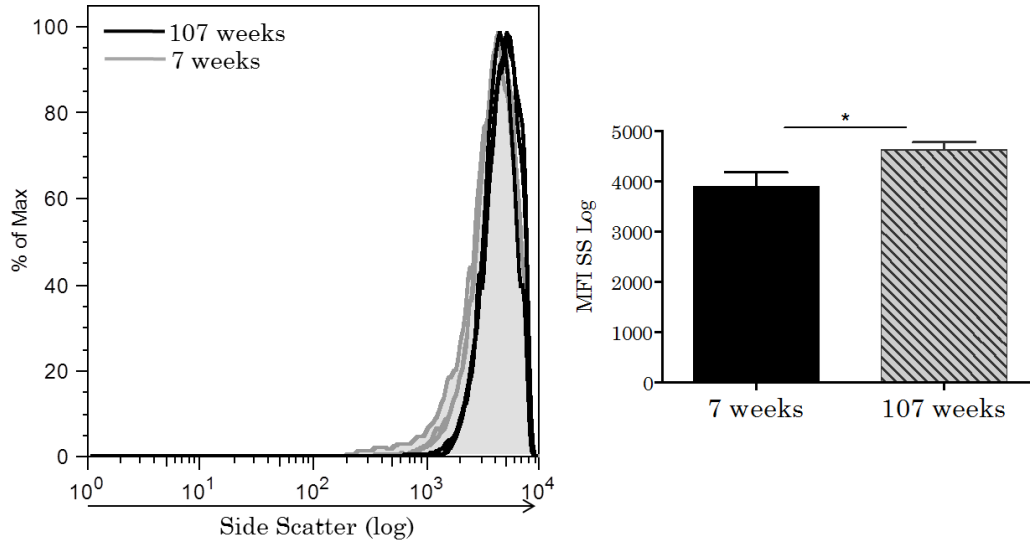

***Figure 6.6**: Flow cytometric analysis of BMMϕ cultures based on their FS vs. SS profile. BMMϕ were cultured for 7 days in the presence of M-CSF (20 ng/ml) and stained for flow cytometry. Left: Overlaid histograms of macrophages side scatter (log). Gated on F4/80$^+$ CD11b$^+$ cells. Right: Statistical comparison of SS MFI, error bars represent SEM, n = 3. *p<0.05.*

6.9 Aged macrophages show increased mitochondria and mROS after LPS activation

Several aging studies have uncovered a link between mitochondrial quality and longevity(371), with several showing that mitochondrial health can be improved by caloric restriction(325, 326). As caloric restriction results in upregulation of autophagy(324), this implicates autophagy in regulation of aging associated damage to mitochondria. Furthermore, we have shown that lack of autophagy in macrophages leads to an accumulation of mitochondria and increased mROS. Due to the connection between autophagy, aging and mitochondrial damage, we assessed mitochondrial content and mROS in macrophages derived from 7 week and 107 week old mice. No significant differences were observed between mitochondrial loads in unstimulated and IFNγ stimulated young

and aged macrophages (figure 6.7). However, following LPS stimulation, aged macrophages were found to contain significantly more mitochondria than wildtype macrophages.

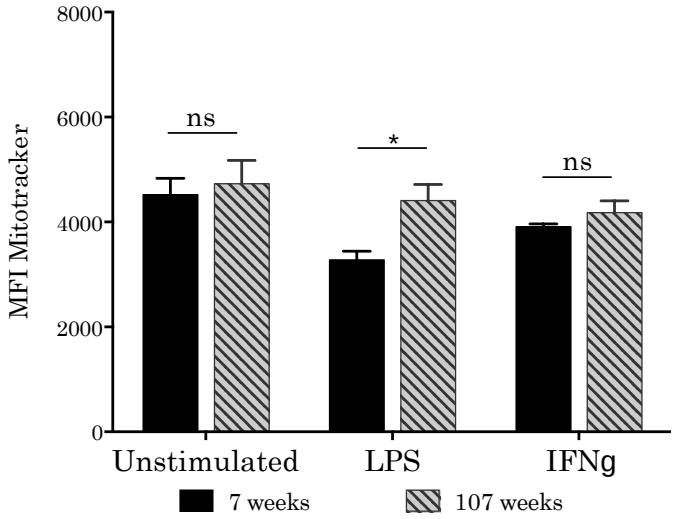

Figure 6.7: *Mitochondrial levels in bone marrow derived macrophages from 7 and 107 week old mice. BMMϕ were cultured and stimulated overnight with LPS or IFNγ, followed by staining with MitoTracker Green (200 nM). Macrophages were analysed on an LSRII flow cytometer (BD). Average MitoTracker green MFI for F4/80^{+} CD11b^{+} macrophages shown, error bars represent SEM. *p<0.05, un-paired t-test. Acknowledgments to Anne Hansen for running and analysing the samples.*

Aging is also associated with increased production of mROS due to accumulation of damaged mitochondria in major organs(372), and in macrophages(373). Similarly, we have shown that loss of autophagy causes an increase in mROS in macrophages. To confirm increased mROS production in aged macrophages, BMMϕ from 7 and 107 week old mice were stained with MitoSOX dye. Aged macrophages showed a trend of increased mROS across all stimuli; however this only reached significance following LPS stimulation due to staining variability between samples (figure 6.8).

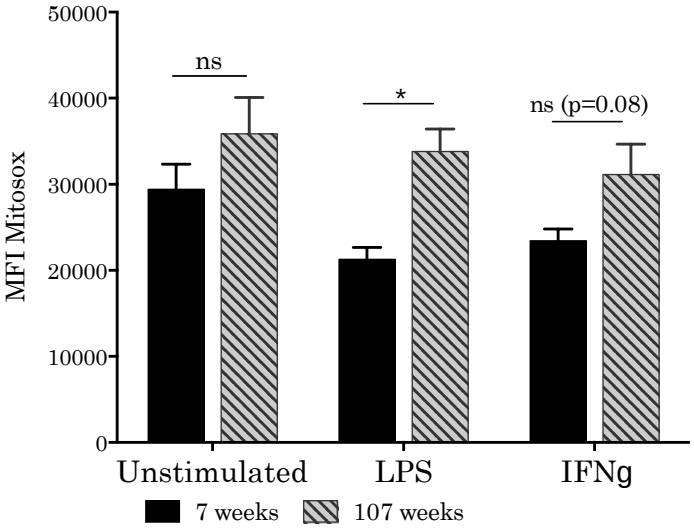

***Figure 6.8**: Atg7$^{-/-}$ macrophages have increased levels of mitochondrial ROS. BMMϕ from 7 week and 107 week old mice were cultured for 7 days and stimulated overnight with LPS (1 µg/ml) or IFNγ (10 ng/ml). Cells were washed and stained with MitoSOX (5 µM) for 20 min at 37° C. Macrophages were analysed on an LSRII flow cytometer (BD). Graph shows average MFI of MitoSOX staining, error bars represent SEM, n = 3. *p<0.05, un-paired t-test. Acknowledgments to Anne Hansen for running and analysing the samples.*

Chapter 6: Discussion

Aged macrophages have a similar phenotype to Atg7$^{-/-}$ macrophages

6.10 Aged macrophages have reduced autophagy

Age-related changes in the immune system contribute to the increased vulnerability of the elderly to infection, reduce the effectiveness of vaccination, and potentially increase autoimmunity and cancer(374). Immunosenescence affects multiple cell types in both the adaptive and the innate arms of the immune system, resulting in increased cell death, decreased function and a lower capacity to prevent and clear infections. Levels of autophagy also decline in many tissues with age, including the liver, heart and muscles, as well as in cells of the immune system(361), resulting in increased levels of oxidative stress, damaged mitochondria and ROS. However, increasing autophagy in aged cells and organisms, either by caloric restriction(375), chemical induction of autophagy(376) or genetic overexpression of autophagy genes(323), results in reduced aging-related damage and extension of lifespan. This suggests a strong link between reduced autophagy and cellular symptoms of aging. Investigation of BMMϕ from aged (107 weeks) mice shows that macrophages also undergo reduced autophagy with age, with fewer autophagosomes per cell and a reduction in autophagic flux, the fusion of autophagosomes with lysosomes. However, autophagic flux was not completely abolished and induction of autophagy using LPS and IFNγ was still possible, though not to the same extent as seen in young macrophages. Aged macrophages also showed a significant reduction in gene expression of the essential autophagy genes, Atg6 (Beclin-1) and Atg7, as has previously been seen in other aged tissues(377).

How aging results in reduced autophagy is the subject of much debate. It is thought that defective autophagy in aged cells arises partly from altered autophagic signaling and partly from poor clearance of autophagosomes by the lysosomal system(377). Experiments have suggested that reduced autophagosome formation results from alterations in the signaling cascades activating autophagy, rather than defects in components of the autophagy

pathway(377). Although many signaling pathways are likely influenced by aging, it is thought changes in Insulin Receptor (IR) signaling, caused by increased oxidative stress, may directly impact on autophagy levels in the elderly(378-380). Signaling via the IR inhibits autophagy, whereas signaling via glucagon, which occurs during periods of calorie restriction or starvation, initiates autophagy(381). However, aging results in impaired glucagon stimulation of autophagy while insulin signaling remains intact, causing an overall downregulation of autophagy(382). Furthermore, inactivating or deleting mutations in the IR results in increased autophagy levels and improved lifespan of model organisms(321). This indicates that insulin signaling negatively regulates the autophagy, aging and longevity interaction, and suggests manipulation of the IR as a possible mechanism for improving age-related decline in autophagy.

Recently, sirtuins have been implicated in the autophagy-aging axis(383). Sirtuins are NAD^+ dependent deacetylases and mono-ADP-ribosyl transferases, which regulate a variety of cellular processes such as metabolism, stress responses, cellular survival and senescence. SIRT1 plays a role in autophagosome formation and regulation of autophagy, deacetylating the essential autophagy genes Atg5, Atg7 and Atg8(384) and is involved in caloric restriction-mediated increases in lifespan(385), with downregulation of SIRT1 in mice resulting in an accelerated aging phenotype and dramatic decrease in lifespan to a median of 7 months (normal mouse lifespan is >24 months)(386). Thus, age-associated decreases in SIRT1 expression may result in decreased autophagy levels and a corresponding increase in age-related maladies. Research has also shown that SIRT1 exerts the greatest protective effect at 2.5 to 7.5-fold overexpression(387), and thus it may be that aging cells cannot efficiently upregulate SIRT1 in response to stress, and thus also not upregulate autophagy.

Aging also results in a general decline of ATP production within the cell, due to reductions in mitochondrial quality(388). Reduced ATP production may compromise the function of the ATP-dependent proton pumps that generate the acidic pH in lysosomes, allowing efficient degradation following lysosomal fusion with autophagosomes. This could contribute to accelerated buildup of lipofuscin, which in turn could cause impaired capacity to fuse and/or to degrade the autophagosomal contents(377). CMA has also been shown to decline with age, caused by a progressive decline in LAMP2a.

Age-related changes in oxidative stress, cell signalling and expression of important regulatory proteins all are likely to play a role in reduced autophagy in aging. As mentioned earlier, a decline in expression of essential autophagy genes, possibly caused by DNA mutations or other regulatory mechanisms, may also contribute to decreased autophagy in the elderly. Decreased autophagy, in turn, results in other deleterious cellular and organismal affects, such as impaired immune function.

6.11 Similarities between phenotypes of aged and Atg7$^{-/-}$ macrophages

Increasing age brings about alterations in function of cells from both the adaptive and innate immune systems. Interestingly, many of the age-related changes in macrophages are mirrored in autophagy-deficient macrophages, further underscoring the relationship between autophagy and aging and suggesting that loss of autophagy contributes to accelerated aging in macrophages. Furthermore, it suggests that many of the functional changes in aged macrophages can be related back to reduced levels of autophagy.

Increased numbers of macrophages is a common feature of aging in both mouse and human models(352, 353, 365, 389). Accordingly, macrophages from 107 week old mice were significantly increased in the blood and spleen, similar to Vav-Atg7 mice. However, unlike

Vav-Atg7 mice, a decrease in macrophages was observed in the peritoneal cavity. The reason for this reduction in the peritoneal cavity, but not in the bone marrow, is unclear. Some studies have shown variations in age-related changes in macrophages depending on the tissue the macrophages originated from(390), which could be due to the different environments present in each tissue. Potentially the peritoneal cavity represents a higher stress environment, relative to the blood and spleen, resulting in a higher level of apoptosis in macrophages in that area.

Both aged and autophagy-deficient macrophages have significantly increased numbers of lipid droplets present in the cytoplasm. In addition to degrading organelles and protein aggregates, autophagy has been shown to degrade lipid droplets, in a process called lipophagy(391). Lipophagy contributes to cellular energy production, and defects in lipophagy have been linked to age-related metabolic disorders such as atherosclerosis, fatty liver and obesity(392). It is hypothesised that reduced lipophagy with advanced age contributes to age-related metabolic syndrome(391).

Aged and autophagy-deficient macrophages also showed an increased granularity (SS) when analysed by flow cytometry. High SS is caused by complexity within the cell, which increases scattering of the light. Macrophages have a generally high side scatter (SS) due to their granule and organelle content, and are often identified in flow cytometry based on this feature(121). Increased protein content is a common feature of aged cells, due to decreased autophagy and proteosomal degradation(393). Thus, accumulation of undegraded proteins and organelles in aged and autophagy-deficient macrophages contributes to high SS. Increased lipid droplets and mitochondria can also contribute to increased side scatter(370, 394), which are also influenced by autophagy, further linking increased granularity in aged macrophages to reduced autophagy.

Aged macrophages also frequently have reduced expression of surface marker genes and receptors, including MHC II(360, 365) and TLR4(236), which was also seen in autophagy-deficient macrophages. We have shown that loss of autophagy results in a decrease in surface antigen presentation, possibly due to a requirement for autophagy or autophagic machinery in MVB or Rab-mediated surface marker expression. A decline in autophagy with age could result in a similar defect, particularly as endocytic transport in general is influenced by age(395). Furthermore, as discussed above, SIRT1 is implicated in regulation of both aging and autophagy, with decreased SIRT1 expression resulting in reduced autophagy. SIRT1 has also been implicated in regulation of MHC II expression by deacetylation of Class II transactivator (CIITA), drawing a further link between autophagy, aging and MHC II expression(396).

A significant increase in mitochondrial load and production of mROS was observed in autophagy-deficient macrophages, which was reflected in LPS-stimulated aged macrophages. Mitochondrial quality is known to decline with age(397), with an associated increase in ROS production, a trend which was reflected in macrophages from aged macrophages. Interestingly, LPS stimulation caused mitochondrial content to decrease in young mice in this experiment, possibly due to LPS-mediated induction of autophagy increasing mitochondrial degradation. No changes were observed in aged macrophages following stimulation, nor in young macrophages following IFNγ stimulus. In the samples that we analysed, we saw a large degree of variation between samples, in both young and aged mice, which prevented the trend in unstimulated and IFNγ stimulated macrophages from reaching statistical significance. This could be due to natural variations in autophagy levels between individuals, as has been seen previously(361), or individual differences in susceptibility to reactive oxygen damage and mitochondrial quality decline. Although autophagy levels show a strong trend of decreasing with age, there is nevertheless a degree

of individual variation, presumably resulting from genetic differences between individuals. Even in inbred Vav-Atg7 mice, we see a considerable variation between onset of symptoms and death of between 5 and 12 weeks, with a minority of Vav-Atg7$^{-/-}$ mice remaining almost symptom free until euthanasia at 9 -12 weeks. In order to confirm whether the trend was statistically significant, the experiment would need to be repeated on larger numbers. It would also be of interest to correlate levels of autophagy with ROS generation and mitochondrial load/quality from individual mice.

Similarly to autophagy-deficient macrophages, aged macrophages experience a decline in NO production following stimulation(355, 398), possibly due to impaired expression of iNOS mRNA or protein. Furthermore, phagocytosis has been shown to be impaired in aged macrophages in a variety of settings in aged mice and in elderly individuals(356, 399-401). The age-related impairment is hypothesised to be related to decreases in scavenger and adhesion receptor expression and to changes in membrane motility and fluidity, both of which are reflected in the reduced phagocytic capacity of autophagy-deficient macrophages. As autophagy is reduced, not abolished, in aged macrophages, treating aged macrophages with rapamycin or subjecting them to controlled starvation in order to induce autophagy, may result in improved phagocytic capacity and therefore a more efficient macrophage response to bacterial infections.

Increased expression of inflammatory cytokines, such as seen in autophagy-deficient macrophages, is also regularly associated with aging, with many age-associated diseases occurring with a significant, low-level inflammatory background, termed 'inflammaging'(402). Elevated levels of inflammatory cytokines such as IL-6, TNF-α and IL-1β are found in the serum and tissues of the elderly, produced by inflammatory macrophages(357, 358). Increased inflammation in aged macrophages is thought to be due to increased activation of the inflammasome(403), and increased signalling through TLRs

by ROS and DAMPs(404, 405). As discussed in chapter 4, loss or reduction in autophagy is also implicated in the activation of the inflammasome through several mechanisms(186, 187), though inflammasome-independent activation of inflammatory cytokine production has also been observed(188). Furthermore, the aging and autophagy-regulating protein SIRT1 has been implicated in controlling inflammatory cytokine production in macrophages(406). SIRT1 knockdown in peritoneal macrophages results in increased activation of the JNK and IKK inflammatory pathways and enhances LPS-stimulated TNF-α production. Furthermore, SIRT1 activators were able to reduce LPS-associated inflammation by macrophages and, in an animal model, reduce the inflammation associated with obesity(406), potentially explaining how SIRT1 overexpression is able to increase life- and healthspan in model organisms. Given the links between reduced autophagy and increased inflammatory cytokine production, it seems highly likely that increased inflammatory signalling and inflammasome activation associated with aging is also related, at least in part, to age-associated reductions in autophagy and corresponding increases in damaged mitochondria and ROS(403, 407).

As discussed in chapter 5, loss of autophagy in macrophages results in a significant upregulation of glycolytic ATP production, with a corresponding decrease in OxPhos. Chronic glycolysis has also been associated with aging-related damage, and it is hypothesised that one of the mechanisms behind the benefits of caloric restriction in increasing lifespan is reduced glycolysis(408). Some glycolytic intermediates can cause glycation of intracellular components, resulting in advanced glycosylation end-products (AGEs) that are implicated in age-related pathologies, such as diabetes and Alzheimer's disease(409-411). Thus, increased glycolysis, such as seen in autophagy-deficient cells, can contribute to age-associated damage by producing reactive intermediates, which normally induce autophagy. Potentially, stimulation of autophagy in aged macrophages may be able

to reduce chronic glycolysis, thereby preventing build-up of deleterious glycolytic intermediates and reducing age-related damage.

Loss of autophagy in macrophages mimics many of the age-related changes in macrophage function, as summarised in the table below, which strongly suggests that reduced autophagy levels with aging contribute to such functional changes and the development of inflammaging. However, autophagy in aged macrophages is reduced, not abolished, and autophagy levels and aging symptoms vary greatly between individuals. It is difficult to determine what, if any, 'level' of autophagy is required to be protective, and whether it is basal or inducible autophagy that is most important. Some studies have shown that initiation of caloric restriction during late middle age has a beneficial outcome on lifespan(412, 413), and reduced caloric intake even among the elderly improves memory function(414). This suggests that increased autophagy at any time can improve aging outcomes, though there is little research on whether benefits continue after cessation of a calorie restricted diet. Although there are many reports of declining immune function and increased inflammatory cytokine production with aging, some of which were discussed above, there is much variation in the literature regarding immune responses in the elderly. In some studies no changes in cell number or function are found with aging(415, 416), and there are several studies that show a decrease in macrophage secretion of inflammatory cytokines with aging(236, 359, 417). Although there are multiple possibilities for such differences in outcomes, from different types of macrophages, different experimental setups, antibody markers and the problems selecting 'healthy' aged people, it is possible that individual autophagy levels also influence immune response preservation in the elderly. As mentioned previously, autophagy levels vary dramatically in both aged and young mice and humans(361). It would be very interesting to investigate whether elderly people with (relatively) high functioning immune systems and low inflammation correlate

with high levels of autophagy, and conversely whether increased inflammatory background and circulating inflammatory cells is related to lower than average levels of autophagy. Investigating genetic links to high basal autophagy levels and healthy immune aging could also provide information on a potential link. This would provide further clarification of the role of autophagy in immunosenescence and inflammaging, and possibly shed light on why there are such great differences in immune parameters amongst the elderly.

Aged macrophages	**Macrophage Function**	**Atg7$^{-/-}$ macrophages**
✓ **(decreased in peritoneum)**	Increased numbers of macrophages	✓
✓ **(after LPS stimulation)**	Increased mitochondria and mROS	✓
✓	Decreased phagocytosis	✓
✓	Decreased NO	✓
✓	Reduced surface marker expression	✓
✓	Reduced antigen presentation	✓
✓	Increased inflammatory cytokine production	✓
✓	Metabolism alterations	✓

Table: 6.2*: Similarities between aged and autophagy-deficient macrophages. Loss of autophagy in macrophages results in a similar range of phenotypic changes, as are commonly seen in aged macrophages. As aged macrophages also show significant decreases in autophagy, this suggests that loss of autophagy may accelerate aging in macrophages and cause or contribute to many of the phenotypic changes associated with aged macrophages.*

6.12 Conclusions

Aging results in a decline in function of both the adaptive and innate immune systems, often accompanied by chronic low-level inflammation. Autophagy levels also decline with age, and loss of autophagy in macrophages results in a similar phenotype of increased inflammation, altered metabolism and decreased innate functions, to that of aged macrophages. Together, these data suggest a link between autophagy and aging of the immune system and immune cells, whereby declining autophagy rates cause increased oxidative stress and accumulation of damaged organelles and proteins, which together alter function and promote inflammation. Caloric restriction may therefore improve lifespan, partly due to its autophagy-enhancing effects reducing inflammation and improving immune function, thereby providing better protection from infection and other age-related conditions.

Chapter 7: Introduction

Atg7 has a role in neutrophil maturation

7.1 Normal Neutrophil Development

Neutrophil differentiation is orchestrated by the sequential activation of specific gene expression patterns and regulatory factors, which together induce transcription of characteristic lineage markers. The interaction between the key neutrophil transcription factors and their relative expression levels during crucial developmental stages are key parameters in the establishment of cellular fate(418). Maturation of haematopoietic precursors into neutrophils requires two essential processes: reduction in self-renewal potential, and acquisition of a specific lineage identity. During granulopoiesis, HSCs give rise to common myeloid progenitors (CMP) and then to granulocyte/macrophage progenitors (GMPs), characterised by expression of CD34 and Fc Receptor II/III(419). GMPs then give rise to granulocyte-, monocyte-, and granulocyte/monocyte-forming units (CFU-G, CFU-M and CFU-GM), of which CFU-Gs can give rise to mature neutrophils in response to signalling via G-CSF and other factors. Neutrophil maturation then proceeds through six stages: myeloblasts to promyelocytes to myelocytes to metamyelocytes, band cells and, finally, to mature neutrophils, characterised by their three-lobed nuclei and the presence of tertiary granules(420).

Myeloid differentiation is orchestrated by relatively few transcription factors, including PU.1, CCAAT/enhancer binding proteins (C/EBPα, C/EBPβ and C/EBPε), and growth-factor independent 1 (GFI-1)(421-425). Many myeloid genes are regulated by these transcriptions, such as those that encode G-CSF and GM-CSF, as well as granule components such as lactoferrin and neutrophil gelatinase (NGAL)(426). Additionally, transcription of genes normally expressed in other lineages is frequently actively suppressed. This balance of activation of neutrophil-specific genes and repression of other lineage genes orchestrates overall neutrophil maturation. C/EBPα activation is required for GMP production from CMPs, with GMPs and all subsequent lineages absent from C/EBPα-

deficient mice(422). C/EBPα also regulates exit from the cell cycle(427), resulting in the inhibition of further proliferation from the myelocyte stage onward(420). Following the GMP stage, two further transcription factors orchestrate final neutrophil differentiation, GFI-1 and C/EBPε. GFI-1 is a transcriptional repressor that regulates repression of macrophage lineage gene expression, thereby promoting terminal neutrophilic differentiation. In mice lacking expression of GFI-1, neutrophilic differentiation is blocked beyond the promyelocyte stage(425). C/EBPε is required for transcription of granule proteins at the myelocyte stage and beyond, with C/EBPε deficient mice developing myelodysplasia, characterized by proliferation of atypical granulocytes that lack secondary and subsequent granules(424).

Granules begin to appear from the promyelocyte stage and production continues until the segmented stage of maturation is reached. Neutrophil granules are classified into three subsets based on characteristic granule proteins: primary granules (myeloperoxidase [MPO]), secondary/specific granules (lactoferrin), and tertiary granules (gelatinase). Each subset is formed sequentially during differentiation, at the promyelocyte stage (primary), the myelocyte-metamyelocyte stage (secondary), and the band cell stage (tertiary)(428). The different subsets not only reflect the differences in granule content, but also in their mobilization, with the granules formed last the first ones to be released(428). A fourth type of granule, termed the secretory vesicles, contains membrane proteins wrapped around a matrix of plasma proteins(429) and is formed by endocytosis during late maturation(430). Stages of neutrophil development with associated transcriptional changes and granule formation are summarised in figure 7.1 below.

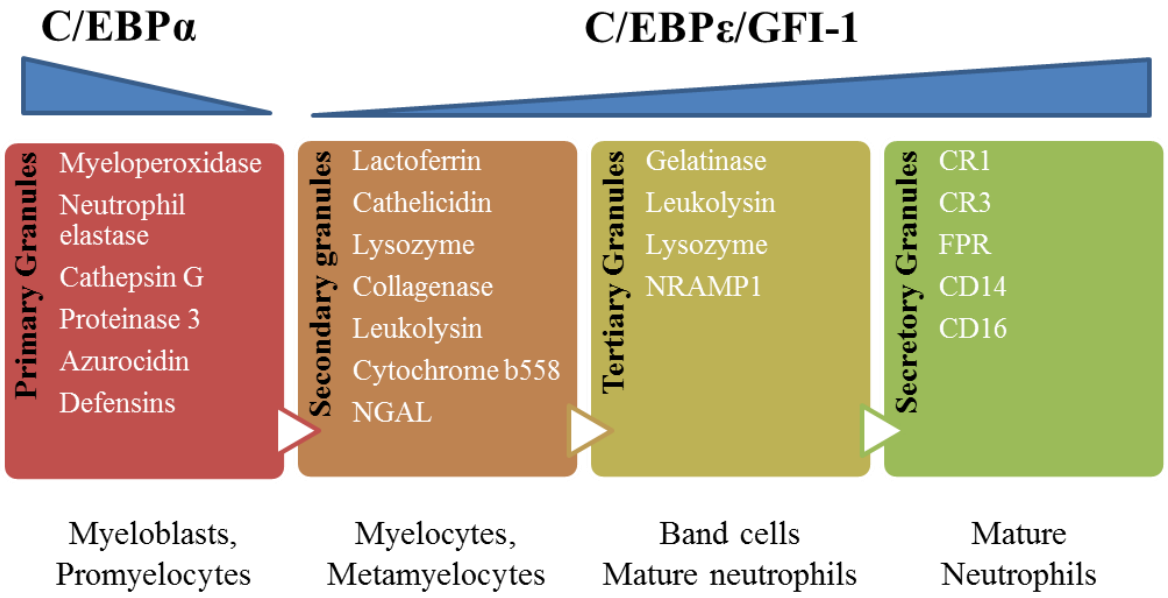

***Figure 7.1**: Features of neutrophil development. Neutrophil development is regulated by sequential expression of transcription factors C/EBPα, C/EBPε and GFI-1. Granules become visible in the cytoplasm from the myeloblast stage, and granule formation continues until the mature, segmented neutrophil stage. NRAMP1 is natural resistance-associated macrophage protein 1. FPR is formyl peptide receptor. Adapted from Refs (431) and (432).*

7.2 Autophagy in non-transformed neutrophil development

This chapter explores a novel role for autophagy in the development of normal, non-transformed neutrophils from bone marrow. Bone marrow neutrophils from $Atg7^{-/-}$ mice have features consistent with immaturity, including reduced nuclear lobularity and changes in granule expression. Furthermore, treatment with stimuli that normally induce maturation cannot overcome the maturational block and restore mature neutrophil morphology. This suggests a vital role for autophagy in the acquisition of normal neutrophil nuclear morphology and granule formation.

Chapter 7: Results

Atg7 has a role in neutrophil maturation

7.3 Increased neutrophils in Vav-Atg7 mice

Neutrophils are short lived cells, with estimated half-lives of between 1.5 and 12.5 hours(433) under basal conditions and increasing several-fold during inflammatory responses(434). The number of neutrophils present in blood and tissue varies according to immune activation state, age(435, 436), sex(437), mouse strain(438, 439), and sampling method and location(440). As such, quantitative reporting of 'normal' numbers of neutrophils in blood or other tissues is difficult. Several conditions result in a relative or absolute increase in neutrophil counts, including myeloid leukaemia(441), MDS(442) and acute or chronic inflammation or infection. Loss of Atg7 in the hematopoietic system results in severe anaemia and lymphopenia, with significant myeloid infiltration into many organs, including the lungs, liver, stomach and spleen(57). To assess neutrophil numbers from Vav-Atg7 mice, blood, spleen, bone marrow and peritoneal wash samples were collected and analysed by flow cytometry. Neutrophils were identified using the neutrophil specific markers Ly6g or Gr1(443) and the pan-myeloid marker CD11b. Significantly increased numbers of neutrophils were found in each analysed tissue of Vav-Atg7 mice (figure 7.2), particularly in the bone marrow, in which close to 80% of cells were $Ly6g^{+}$ $CD11b^{+}$.

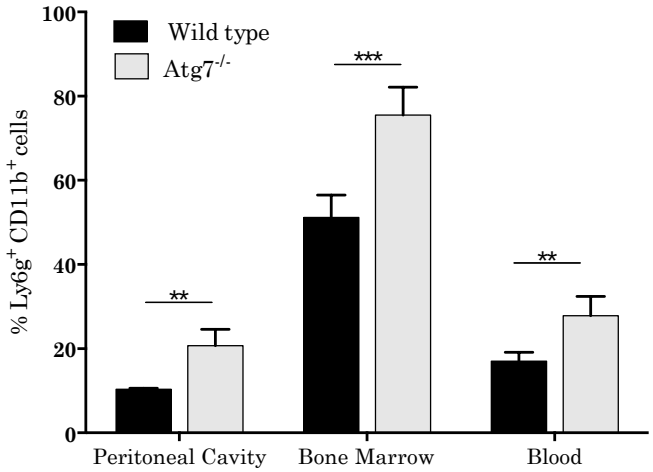

Figure 7.2*: Increased proportions of Ly6g$^+$ CD11b$^+$ neutrophils in the peritoneal cavity, bone marrow and blood of 8 week old mice. Data shows mean percentages of Ly6g$^+$ CD11b$^+$ cells of a single cell suspension following red blood cell lysis. Error bars represent SEM, n = 4. **p<0.01, ***p<0.001.*

Atg7 excision was confirmed in sorted Ly6g$^+$ CD11b$^+$ neutrophils using qPCR analysis of Atg7 gene expression, and found to be decreased by over 80% in neutrophils from Vav-Atg7 bone marrow, indicating that Atg7 is efficiently excised (figure 7.3).

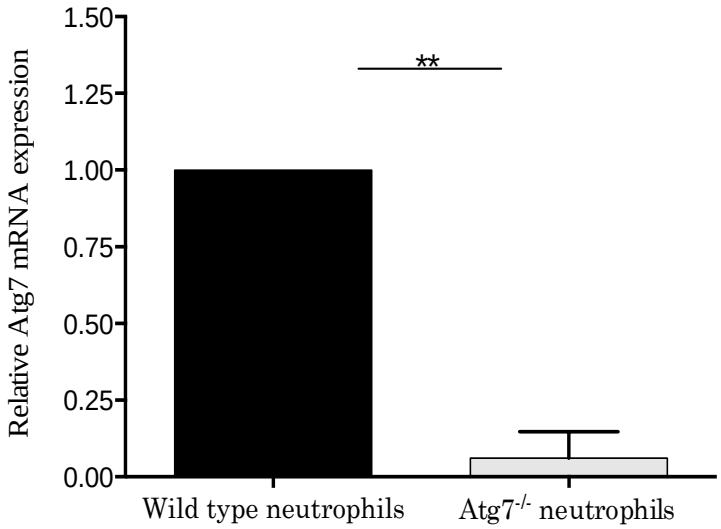

Figure 7.3: *Significantly decreased Atg7 mRNA expression in Ly6g+ CD11b+ neutrophils sorted from bone marrow. Values determined using the ΔΔCT method, normalised to GAPDH and compared to wild Ly6g+ CD11b+ neutrophils. Error bars represent standard deviation of 3 experiments, **p<0.01.*

7.4 Atg7$^{-/-}$ neutrophils show altered expression of common surface markers

Ly6g is expressed exclusively on neutrophils(443), and is thought to play a role in neutrophil recruitment to sites of inflammation(444). Expression increases with neutrophil maturation, with highest levels found on end stage neutrophils, whereas Ly6g^{low} cells are generally immature myeloid cells or myelocytes(445). CD11b (also known as Macrophage-1 antigen) functions as both an integrin(446), and a membrane receptor capable of recognising various ligands, such as the cleaved complement fragment iC3b(447). CD11b is surface expressed, with cytoplasmic granule stores for rapid mobilisation following stimulation. Hence, up-regulation of CD11b expression is an indicator of neutrophil activation. Bone marrow neutrophils were stained with both Ly6g and CD11b in order to assess their development and activation state and to determine whether loss of Atg7$^{-/-}$ altered neutrophil development. Wildtype neutrophils appeared as a distinct CD11b^{+} Gr1^{+} population that was clearly separate from the Ly6g$^{low/negative}$ population (figure 7.4). Many Atg7$^{-/-}$ neutrophils also expressed high levels of both Ly6g and CD11b, however there existed a spectrum of Ly6g expression that was difficult to gate from the Ly6g$^{low/negative}$ cells. CD11b expression was similarly distinct in both populations, with a clear CD11b^{+} and CD11b^{neg} population in wildtype and Atg7$^{-/-}$ cells (figure 7.4, bottom left panel). Histograms of Ly6g expression show the distinct neutrophil population visible in wildtype bone marrow (figure 7.4, bottom right panel), whereas Atg7$^{-/-}$ bone marrow gives rise to a much broader Ly6g peak, with no clear positive population.

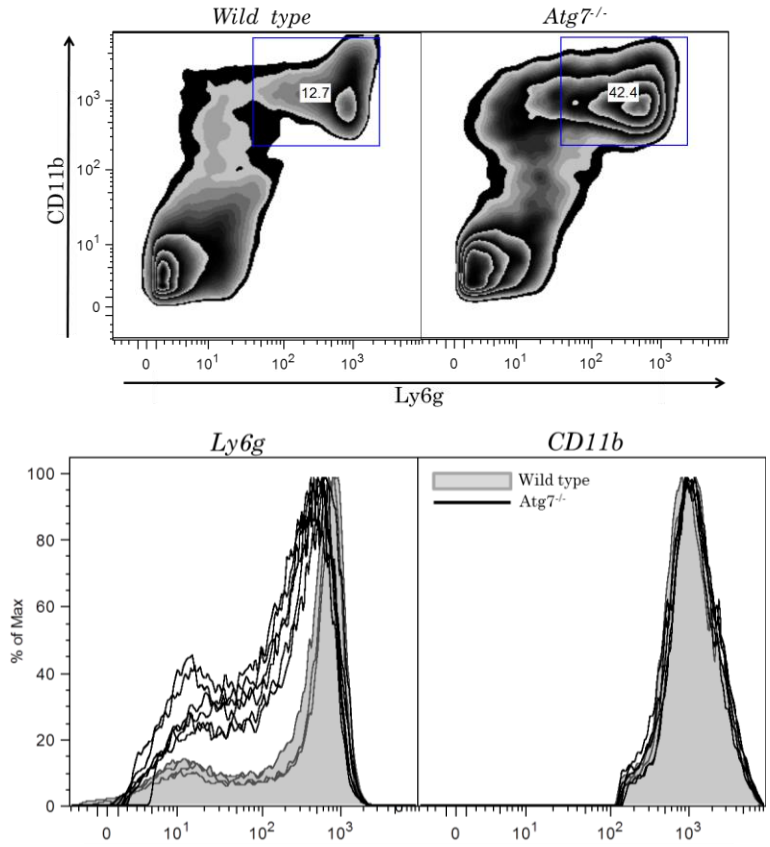

***Figure 7.4**: Ly6g^{+} CD11b^{+} neutrophil populations from bone marrow. Bone marrow neutrophils were harvested and stained for flow cytometry analysis using the neutrophil surface marker Ly6g and the pan-myeloid marker CD11b. Representative histograms of wildtype (left) and Atg7$^{-/-}$ (right) neutrophils extracted ex vivo from bone marrow. Histograms representative of >20 experiments.*

Neutrophils also express other surface receptors, vital for pathogen recognition and response to inflammatory environments. The neutrophil Fcγ (II/III) receptor (CD16/CD32) plays several roles in neutrophil function, including phagocytosis, degranulation, and triggering of transcriptional activation of inflammatory cytokine genes(448). CD16 typically appears late in neutrophil development(449), reaching maximum expression at the segmented nucleus stage. CD32 appears early in development, but expression peaks at maturity. Fc receptor expression was investigated on neutrophils using flow cytometry. Unexpectedly, given the lower levels of Ly6g expression, Fc receptor expression using an antibody that recognises CD16 and CD32 was found to be significantly higher, in neutrophils from the bone marrow, blood and spleen (figure 7.5).

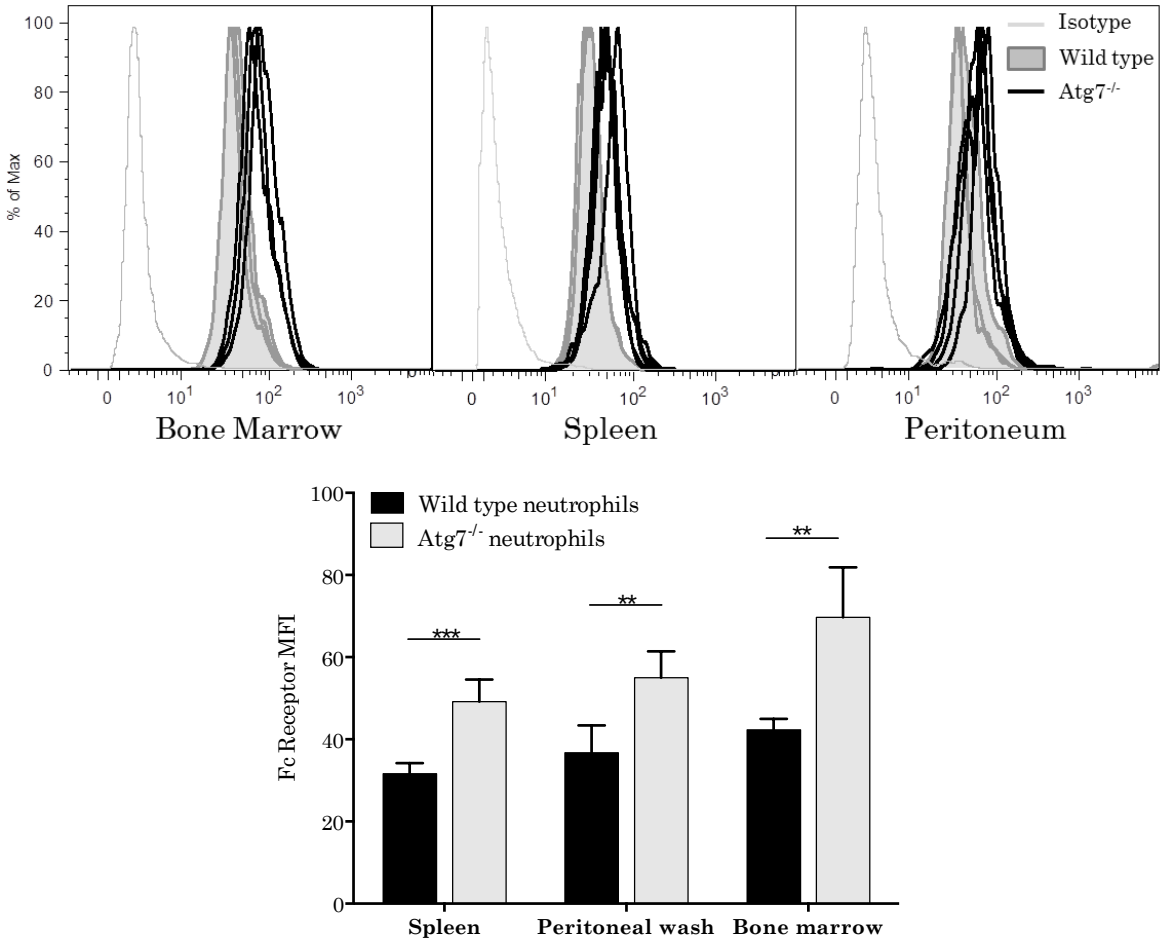

Figure 7.5: *Increased expression of Fcγ Receptor on Atg7$^{-/-}$ neutrophils. Top panels: Overlaid histograms of Fc Receptor expression on Ly6g^{+} CD11b^{+} neutrophils. Lightest grey line shows isotype control staining. Bottom graph: Statistical analysis of expression based on mean MFI, error bars represent SEM, n = 4. **p<0.01, ***p<0.001, un-paired t-test.*

CXCR4 regulates neutrophil trafficking from the bone marrow into the periphery through its interaction with the chemokine CXCL12(450). Dysregulated signalling through CXCR4, is associated with metastasis in several cancers(451, 452) and with neutrophilia in the periphery(453). Furthermore, increased expression is an adverse prognostic factor in myeloid dysplastic syndrome(454) and acute myeloid leukaemia(455). As neutrophil numbers are increased in this mouse model, expression of CXCR4 on neutrophils was assessed. Atg7$^{-/-}$ bone marrow neutrophils were found to express significantly higher levels of CXCR4 than wildtype neutrophils, expressing close to 50% more as assessed by relative mean fluorescence intervals of staining (figure 7.6).

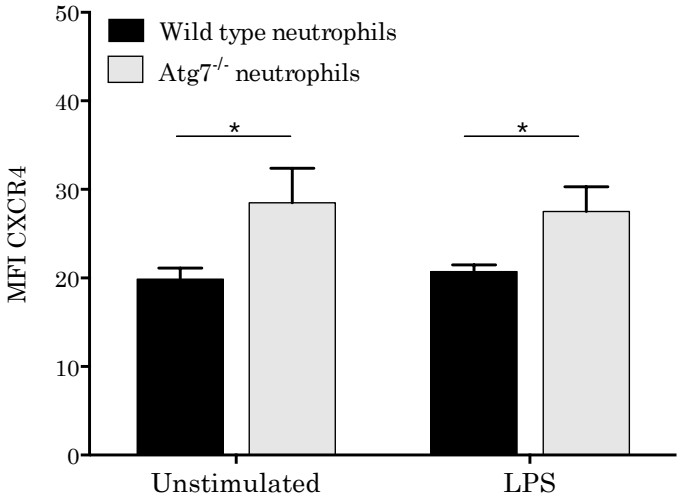

Figure 7.6: *Increased expression of the chemokine receptor CXCR4 on Atg7$^{-/-}$ neutrophils. Bone marrow neutrophils were isolated from the bone marrow and cultured overnight in the presence of LPS (1 µg/ml). Statistical analysis of expression based on mean MFI, error bars represent SEM, n = 4. *p<0.05, un-paired t-test.*

Neutrophil activation results in up-regulation of adhesion molecules required for adhesion to the vascular wall and extravasation into tissues at the site of infection or inflammation. L-selectin (CD62L) is one such adhesion molecule, which plays a role in 'tethering' of neutrophils as they roll along the vascular surface and in the subsequent arrest of movement following activation. Stimulation results in receptor 'shedding'(456), indicating neutrophil activation. CD62L expression was significantly higher on Atg7$^{-/-}$ neutrophils, though expression was low overall (figure 7.7). Overnight stimulation in LPS resulted in a small, but insignificant decrease in L-selectin expression on both wildtype and Atg7$^{-/-}$ neutrophils. Higher L-selectin expression in Atg7$^{-/-}$ neutrophils may be an indication of reduced activation/maturation or problems with receptor shedding.

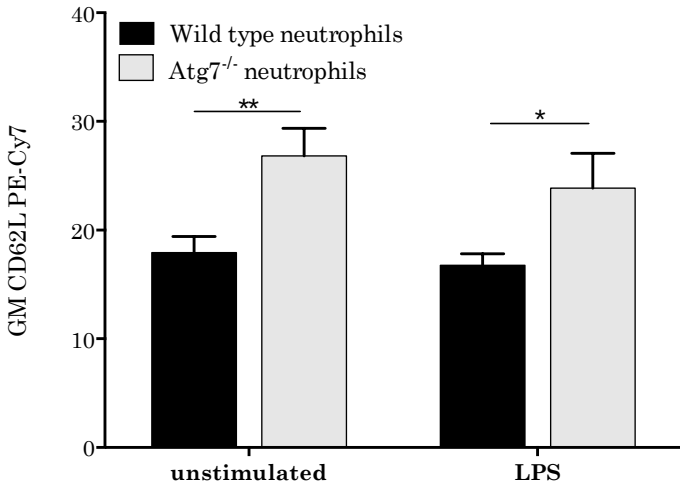

Figure 7.7: *Higher L-selectin (CD62L) expression on Atg7$^{-/-}$ neutrophils. Bone marrow neutrophils were isolated from the bone marrow and cultured overnight in the presence of LPS (1 µg/ml). Statistical analysis of expression based on mean MFI, error bars represent SEM, n = 4. *p<0.05,**p<0.01, un-paired t-test.*

7.5 Atg7$^{-/-}$ neutrophils have features consistent with immaturity

Mature neutrophils can be identified by their morphological features, particularly their characteristic multi-lobed (usually ≥ 3) nuclei and the presence of cytoplasmic granules. These features can be viewed by light microscopy, but electron microscopy provides greater detail. Cells expressing the mature neutrophil markers Gr1 and CD11b were sorted by flow cytometry and the resultant population analysed by transmission electron microscopy. Despite expression of mature surface markers, Atg7$^{-/-}$ neutrophils showed a number of features consistent with immaturity. The micrographs showed differences in nuclear characteristics, with many Atg7$^{-/-}$ neutrophils exhibiting non-lobed or bi-lobed nuclei, rather than the multi-lobed nuclei present in the majority of wildtype neutrophils (figure 7.8, top panel). 57% of Atg7$^{-/-}$ neutrophils showed no visible nuclear segmentation, compared with 8% of wildtype neutrophils (figure 7.8, bottom panel). The majority of Atg7$^{-/-}$ neutrophils had morphological appearance closer to that of neutrophil bands, precursors to mature neutrophils. Furthermore, less than 5% of Atg7 deficient neutrophils

had nuclei with mature morphology, whereas > 60% of wildtype neutrophils had mature morphology.

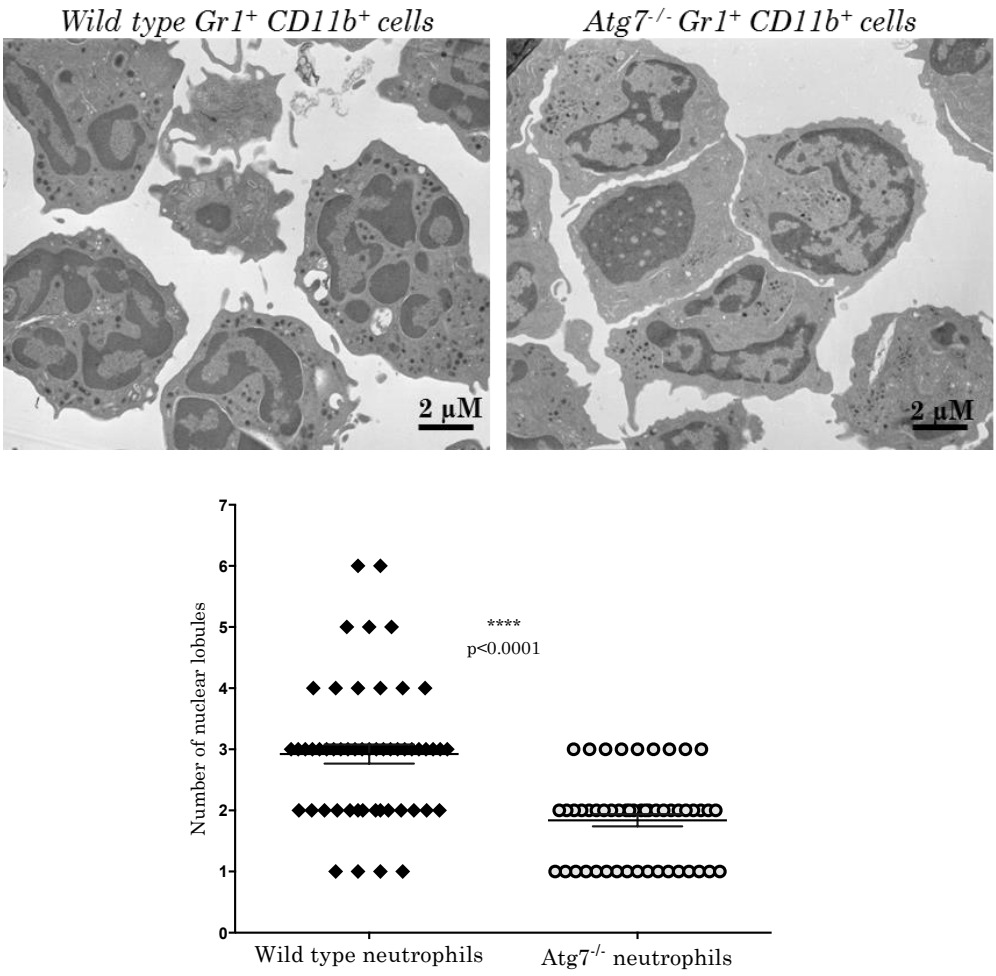

Figure 7.8: *Atg7$^{-/-}$ neutrophils show reduced nuclear lobularity compared with wildtype neutrophils. CD11b^{+} Gr1^{+} cells were sorted from bone marrow pooled from 4 mice by flow cytometry and fixed for analysis by electron microscopy. Top: Representative micrographs from wildtype (left) and Atg7$^{-/-}$ (right) neutrophils, showing reduced segmentation in Atg7$^{-/-}$ neutrophils. Bottom: Comparison of visible nuclear segments from 50 neutrophils from each sample. Un-paired t-test. Grateful acknowledgments to Professor David Fergusson for acquiring the TEM images.*

In addition to altered neutrophil morphology, the electron micrographs revealed alterations in the number, size and nature of the granules present in the cytoplasm (figure 7.9, top panel). Atg7$^{-/-}$ neutrophils (right) contained half the granules of wildtype neutrophils (figure 7.9, bottom graph), and their granules were smaller and less electron dense.

Furthermore, Atg7$^{-/-}$ neutrophil granules were unevenly distributed, often clustered together in one part of the cell, whereas wildtype granules were more evenly distributed.

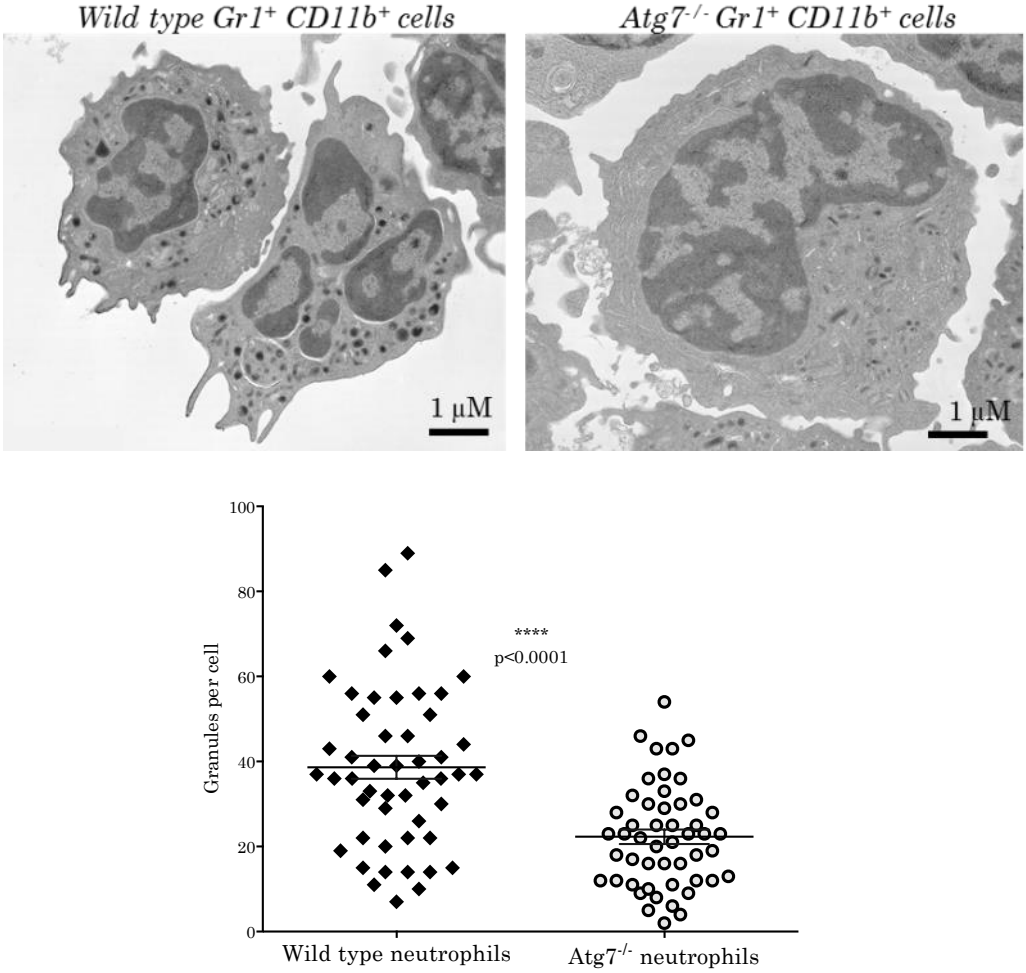

Figure 7.9: *Atg7$^{-/-}$ neutrophils have fewer cytoplasmic granules compared with wildtype neutrophils. CD11b^{+} Gr1^{+} cells were sorted from bone marrow pooled from 4 mice by flow cytometry and fixed for analysis by electron microscopy. Top: Representative micrographs from wildtype (left) and Atg7$^{-/-}$ (right) neutrophils, showing reduced granule number in Atg7$^{-/-}$ neutrophils. Bottom: Comparison of enumerated granules from 50 neutrophils from each sample. Un-paired t-test. Grateful acknowledgments to Professor David Fergusson for acquiring the TEM images.*

In order to more quantitatively assess the distribution of immature subsets according to nuclear morphology, bone marrow neutrophils were analysed using an imaging flow cytometer to categorise them based on number of nuclear lobules. Neutrophils were divided into 5 categories: bands (bean-shaped nuclei, no lobules), doughnuts (circular nuclei with a central hole, little lobulation), 2 lobes, 3 lobes and 4 or more lobes, using a

specially designed wizard. The results showed a significant skewing toward immature cells in Atg7$^{-/-}$ samples (figure 7.10), with higher numbers of doughnut and 2 lobed nuclei, and a slightly higher (though insignificant) increase in band-shaped nuclei. Wildtype neutrophils, on the other hand, were skewed toward 3 and 4 lobed nuclei, with fewer immature neutrophils present.

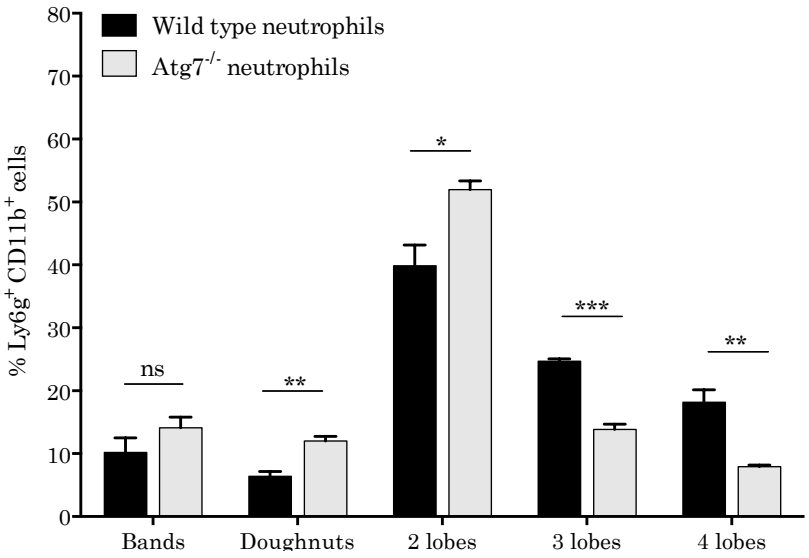

Figure 7.10: *Increased numbers of immature neutrophils in Atg7$^{-/-}$ bone marrow samples. Bone marrow was stained with the neutrophil specific marker Ly6g and the pan-myeloid marker CD11b and categorised according to nuclear segmentation based on Draq5 staining. Dead cells were excluded from analysis using a live/dead stain. Data shows % of total cells in each category, error bars represent SEM, n = 4. *p<0.05, **p<0.01, ***p<0.001, ns = not significant, un-paired t-test. Grateful acknowledgments to Dr Sharon Sanderson for helping to run the samples and designing and analysing the assay.*

Neutrophil differentiation and proliferation are controlled by the growth factors G-CSF and GM-CSF, secreted by stromal and other cells within the bone marrow and hematopoietic tissues(457), though knockout studies have demonstrated that other factors are also involved(458). Nevertheless, alterations in expression of these cytokine receptors may contribute to maturational changes. However, when levels of GM-CSFR and G-CSFR were assessed on neutrophils from the bone marrow or spleen, similar expression was observed to wildtype neutrophils (figure 7.11), suggests that alternations in neutrophil numbers and maturational status are not due to changes in cytokine receptor levels.

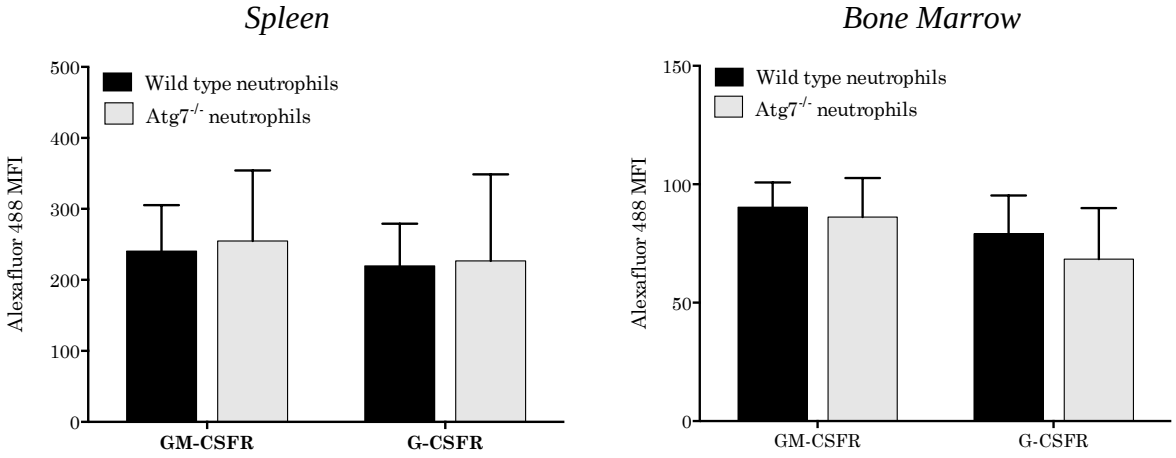

Figure 7.11: *Levels of growth factor receptors GM-CSFR and G-CSFR are unaltered on Atg7$^{-/-}$ neutrophils. Spleen (left) and bone marrow (right) neutrophils were stained with the neutrophil markers Ly6g and CD11b and antibodies against the receptors for GM-CSF and G-CSF. Data shown is average MFI, error bars represent SEM, n = 5. No significant differences were detected using the un-paired t-test.*

Neutrophil granules can be grouped into primary, secondary and tertiary granules, each with different components and appearing at different stages of neutrophil development. Due to the differences in granules observed in Atg7$^{-/-}$ neutrophils, granule contents were investigated using several different assays. Degranulation of primary granules was assessed using a colorimetric assay in which total and exocytosed MPO is determined using 3,3',5,5'-tetramethlybenzidine (TMB) as a substrate(459). Released MPO was assessed by TMB reaction with the supernatant of unstimulated or LPS stimulated bone marrow neutrophils, and total cellular MPO content was assessed using cell lysates. As no samples of known MPO concentration were available, MPO release was determined in Atg7$^{-/-}$ neutrophils relative to wildtype by comparing absorbance at 405 nm. Surprisingly, Atg7$^{-/-}$ neutrophils extracted from bone marrow released significantly higher amounts of MPO than wildtype neutrophils (figure 7.12), though LPS stimulation had no apparent effect on neutrophil degranulation. However, total MPO content in Atg7$^{-/-}$ neutrophils was similar to released MPO, suggesting that upon degranulation Atg7$^{-/-}$ neutrophils released their entire internal stores of MPO. Total MPO content in wildtype neutrophils, on the other hand, was

significantly higher than degranulated MPO, suggesting that they retain intracellular MPO stores following degranulation, or that fewer wildtype neutrophils had degranulated at the time of the assay. Total cellular MPO content was comparable between wildtype and Atg7$^{-/-}$ bone marrow neutrophils.

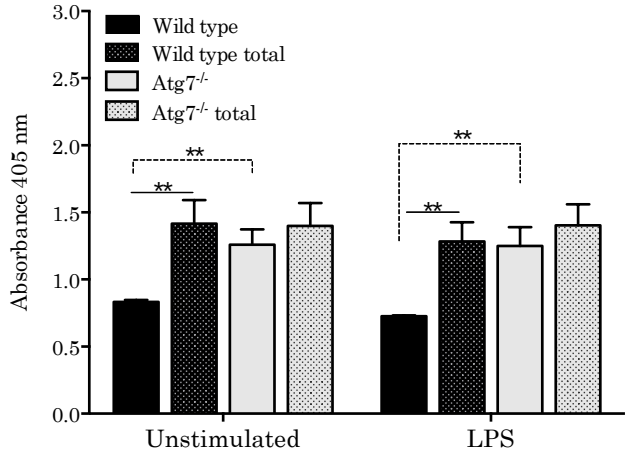

***Figure 7.12**: Increased MPO release in Atg7$^{-/-}$ neutrophils from bone marrow neutrophils. Degranulated and total MPO was assessed by reaction with the substrate TMB. MPO content and release was assessed from unstimulated neutrophils and neutrophils stimulated overnight with LPS (1µg/ml). Relative MPO levels were determined by comparison of absorbance 405 nm in triplicate. Error bars represent SEM, n = 3. **p<0.01, un-paired t-test.*

Intracellular flow cytometry was used to assess the content of secondary granules, by staining for lactoferrin and NGAL. Intriguingly, higher levels of staining were observed for both lactoferrin and NGAL in Atg7$^{-/-}$ neutrophils (figure 7.13), which could suggest increased intracellular stores of these secondary granule proteins.

As neutrophils differentiate, they express a series of genes that regulate development, and activate proteins required for granule development and maturation. For example, suppressor of cytokine signaling-3 (SOCS3) is a negative regulator of granulopoiesis and G-CSF signalling in neutrophils, and may contribute to changes in neutrophil numbers(460).

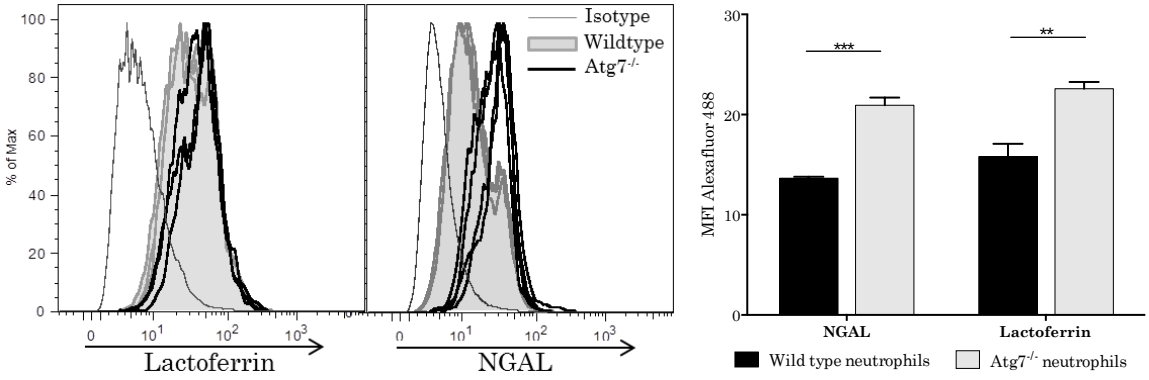

Figure 7.13: *Higher expression of secondary granule proteins neutrophil gelatinase (NGAL) and Lactoferrin. Bone marrow was stained for neutrophil surface markers Ly6g and CD11b, and then fixed and permeabilised to allow staining of NGAL and lactoferrin. Overlaid histograms of Lactoferrin and NGAL staining, leftmost open histogram is isotype control. Graph shows mean MFI of granule staining, error bars represent SEM, n = 5. **p<0.01, ***p<0.001, un-paired t-test.*

C/EBPε is a transcription factor involved in myeloid differentiation and granule maturation(461). MPO, lactoferrin (Ltf) and Matrix metalloproteinase-9 (MMP-9) are proteins found in primary, secondary and tertiary granules, respectively. Expression of these developmental genes was assessed by qPCR analysis of $Ly6g^{+}$ MACS sorted neutrophils from bone marrow (figure 7.14). Levels of SOCS3, C/EBPε and MMP9 were all significantly decreased in $Atg7^{-/-}$ neutrophils, whereas the primary and secondary granule protein genes MPO and Ltf were significantly upregulated, suggesting that proliferation and granule maturation may be altered in $Atg7^{-/-}$ neutrophils. Levels of Nrf2, the antioxidant pathway regulator, and HIF-1α, which regulated the hypoxia adaptation response, were also assessed and found to be significantly increased in $Atg7^{-/-}$ neutrophils.

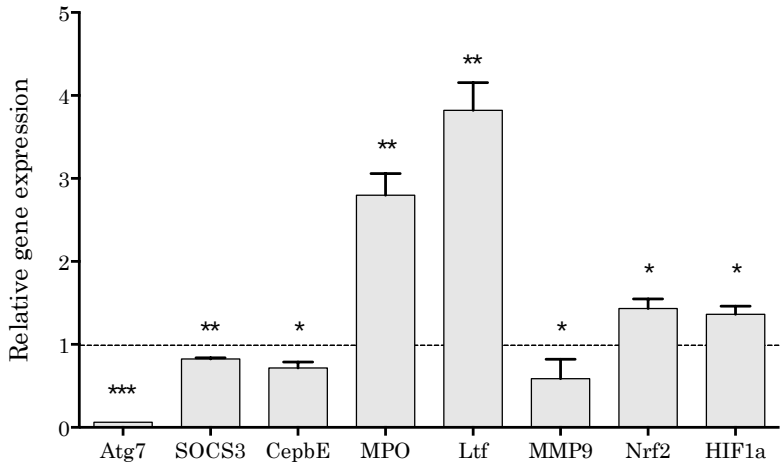

Figure 7.14: *Atg7$^{-/-}$ neutrophils show altered expression of developmental and inflammation genes. RNA was extracted from Ly6g+ BM using Trizol reagent. Values were determined using the ΔΔCT method, normalised to GAPDH and compared to wildtype macrophages cultured under the same conditions. Wildtype gene expression is represented by the dotted line on the graph at a relative expression of 1. Error bars represent standard deviation of 3 replicates, *p<0.05, **p<0.01, un-paired t-test.*

7.6 Stimulation cannot overcome the maturation defect

Neutrophil maturation is modulated by growth factors such as G-CSF and GM-CSF, and immune stimuli such as bacterial products or cytokines, all of which activate transcription pathways and signalling leading to maturation(457). All-trans retinoic acid (ATRA) is a form of vitamin A used to force neutrophil maturation in the treatment of acute promyelocytic leukaemia (APL)(462), a process modulated by autophagy(463). Wildtype and Atg7$^{-/-}$ bone marrow samples were treated overnight with maturational stimuli and then analysed by flow cytometry and light microscopy. Treatment with LPS, TNF-α, G-CSF, GM-CSF and ATRA resulted in up-regulation of Ly6g and CD11b expression in wildtype cells, producing a distinct Ly6g^{+} CD11b^{+} population that was clearly distinguishable from Ly6g^{neg} cells (figure 7.15). However, no stimulant was able to produce a distinct population of mature Ly6g^{+} neutrophils that was clearly distinguishable from negative cells, suggesting that many Atg7$^{-/-}$ neutrophils could not mature further in response to maturational stimuli.

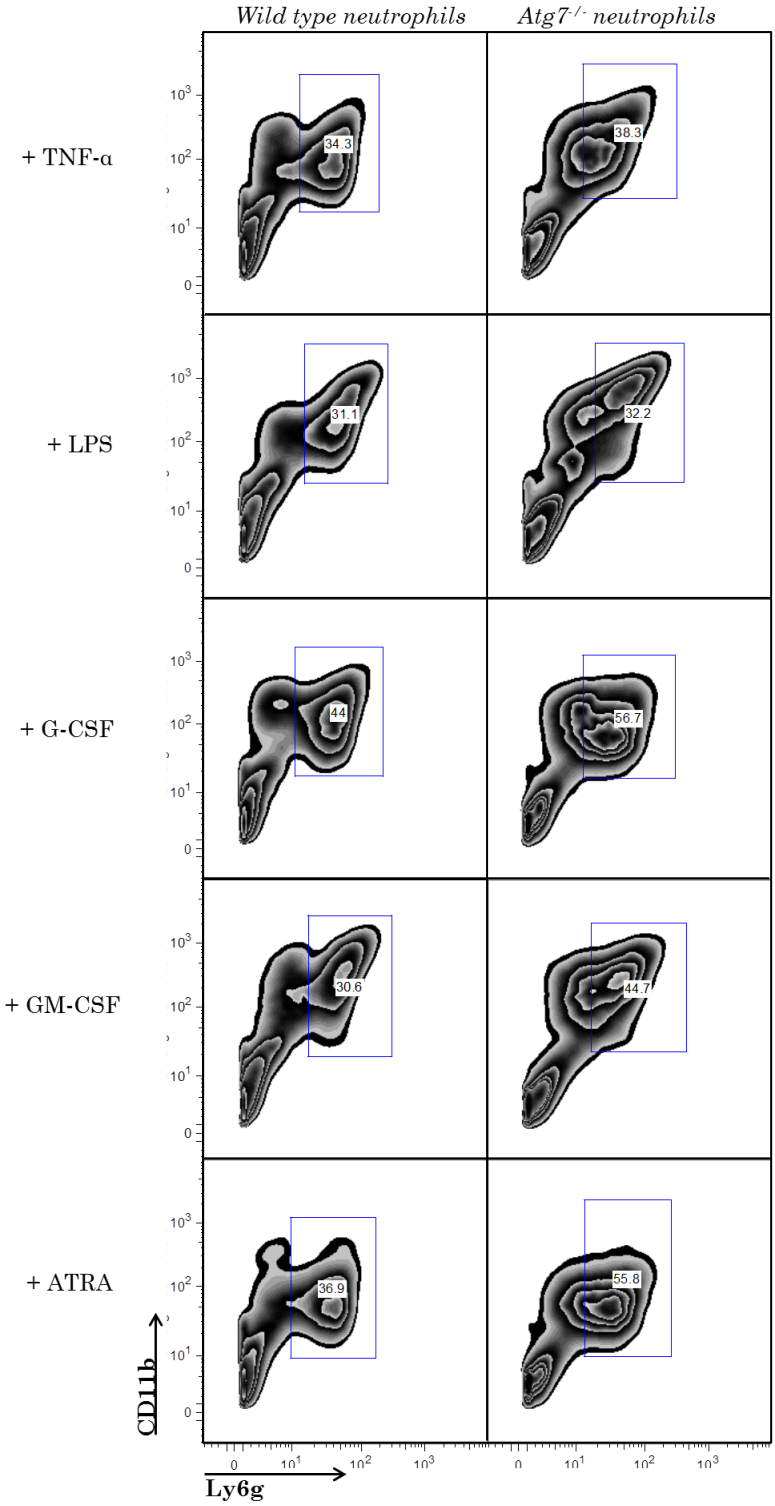

***Figure 7.15**: Addition of exogenous growth factors, cytokines or maturational drugs does not give rise to a distinct population of Ly6g$^+$ CD11b$^+$ neutrophils. Bone marrow neutrophils were cultured overnight in R10 supplemented with TNF-α (1 µg/ml), LPS (1 µg/ml), G-CSF (40 ng/ml), GM-CSF (40 ng/ml) or ATRA (1µM). Cells were harvested and stained for the neutrophil surface markers Ly6g and CD11b and analysed by flow cytometry. Representative plots of wildtype and Atg7$^{-/-}$ neutrophils treated with the stimuli shown.*

Neutrophils treated overnight with G-CSF or GM-CSF were also analysed by light microscopy to determine whether treatment induced mature nuclear morphology in $Atg7^{-/-}$ neutrophils. Samples from treated samples were cytospun onto glass slides and stained to highlight their morphological features and enable easy identification of neutrophils. With the staining kit used (QuickDiff), neutrophil nuclei stain dark blue and the cytoplasm stains a very light pink-purple. Neutrophils were present in high numbers in both wildtype and $Atg7^{-/-}$ bone marrow samples, with $Atg7^{-/-}$ neutrophils showing some nuclear abnormalities. Wildtype nuclei stained dark blue and showed clear evidence of complex, lobular nuclei, whereas $Atg7^{-/-}$ nuclei stained a lighter blue-purple colour, and had little evidence of lobularity; rather the nuclei were rounded and doughnut shaped (figure 7.16). Furthermore, $Atg7^{-/-}$ neutrophils had a lower nuclei:cytoplasmic ratio, and the cytoplasm stained a light purple colour, rather than the very light pink seen in the wildtype cultures.

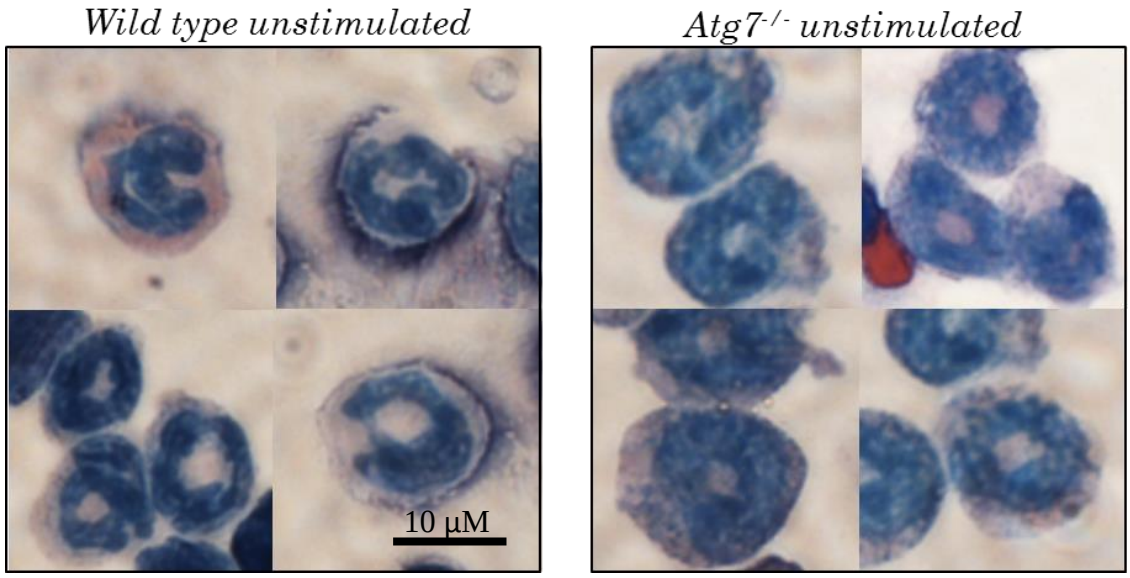

Figure 7.16: *Light microscopy reveals changes in nuclei and cytoplasm of $Atg7^{-/-}$ neutrophils. Bone marrow samples were cultured in R10 overnight, spun onto slides and stained with QuikDiff differential stain. Slides were visualised using a 100x oil inversion lens, with images taken of >20 neutrophils from each culture. Representative images from 4 samples shown.*

Overnight stimulation with G-CSF, the growth factor primarily involved in neutrophil differentiation and proliferation(464), resulted in a significant increase in the numbers of neutrophils in wildtype bone marrow cultures, but very little morphological change in wildtype neutrophils (figure 7.17). G-CSF treatment did not appear to greatly increase neutrophil numbers in $Atg7^{-/-}$ bone marrow, though this was difficult to distinguish due to significant changes in the staining and morphology of $Atg7^{-/-}$ neutrophils. Following overnight incubation with G-CSF, $Atg7^{-/-}$ neutrophils increased in size, with a concomitant increase in nuclear volume, though not lobularity. Furthermore, there was a reversal in staining pattern, with the cytoplasm staining darker than the nucleus, which stained a light purple. Vacuoles also appeared in the cytoplasm of many $Atg7^{-/-}$, but not wildtype, neutrophils following G-CSF treatment.

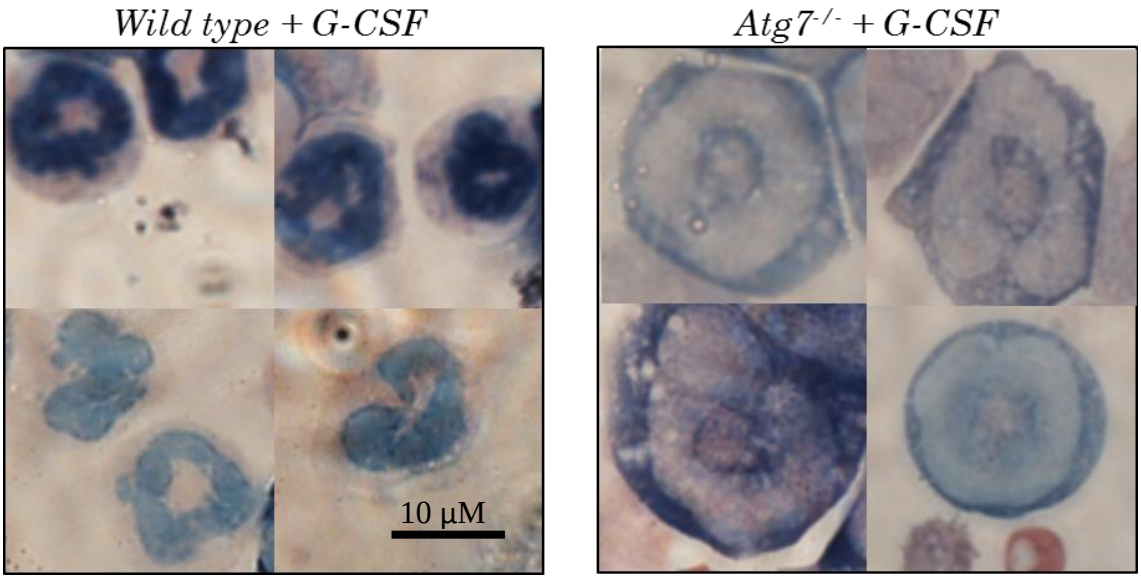

Figure 7.17: *Overnight treatment with G-CSF results in morphological changes in $Atg7^{-/-}$ neutrophils, but does not increase maturity. Bone marrow samples were cultured in R10 + G-CSF (40 ng/ml) overnight, spun onto slides and stained with QuikDiff differential stain. Slides were visualised using a 100x oil inversion lens, with images taken of >20 neutrophils from each culture. Representative images from 4 samples shown.*

Overnight treatment with GM-CSF also resulted in increased numbers of mature neutrophils in wildtype cultures, and appeared to cause an overall increase in cell size and cytoplasmic volume, as well as producing further nuclear complexity (figure 7.18).

Following treatment with GM-CSF, the cytoplasm in wildtype nuclei also stained lighter, such that it could hardly be seen following staining. GM-CSF treatment did not result in the production of mature neutrophils in $Atg7^{-/-}$ cultures, nor was there an apparent increase in neutrophil numbers. As with G-CSF stimulation, neutrophils were harder to identify than in unstimulated cultures due to morphological and staining changes. Neutrophil-like cells increased in size, and there was nuclear swelling, as in G-CSF stimulation. Large and numerous vacuoles were present in many bone marrow cells from $Atg7^{-/-}$ GM-CSF treated cultures, particularly in neutrophils and macrophage like cells, and the cytoplasm stained much darker than in wildtype cells. There were also many cells that appeared to have intermediate morphology between neutrophils and macrophages, which were not clearly identifiable as either cell type. There were, however, a small number (less than 10 counted) of more normal (though immature) staining neutrophils in $Atg7^{-/-}$ cultures, as shown in the top left image of the $Atg7^{-/-}$ panel below.

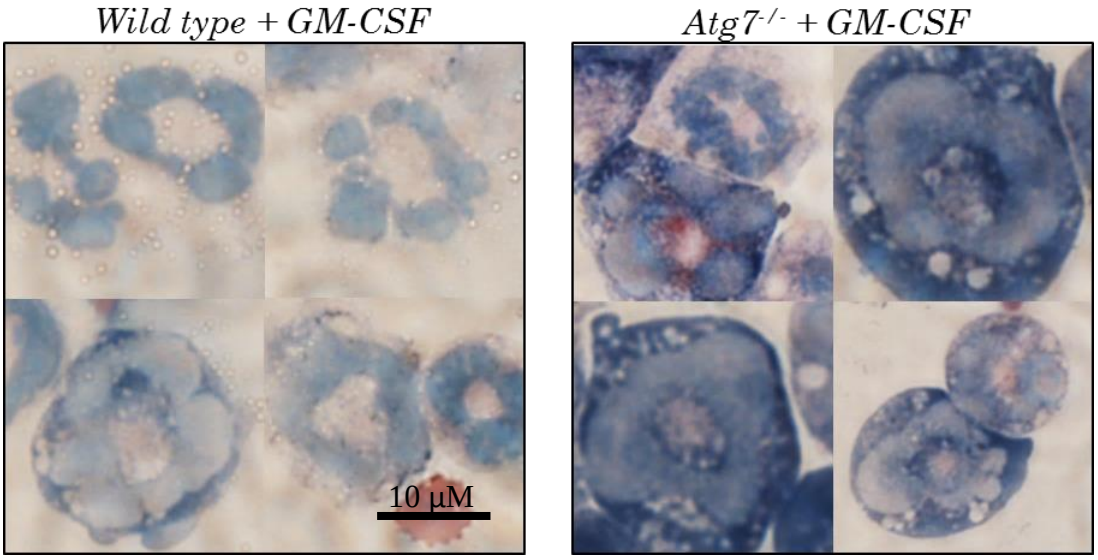

Figure 7.18: *Overnight treatment with GM-CSF results in morphological changes in nuclei and cytoplasm of $Atg7^{-/-}$ neutrophils, but does not increase maturity. Bone marrow samples were cultured in R10 + GM-CSF (40 ng/ml) overnight, spun onto slides and stained with QuikDiff differential stain. Slides were visualised using a 100x oil inversion lens, with images taken of >20 neutrophils from each culture. Representative images from 4 samples shown.*

7.7 Loss of Atg7 results in reduced innate functions of neutrophils

Neutrophils play a vital role in the innate host defence by direct phagocytosis of pathogens, release of inflammatory and cytotoxic mediators such as reactive oxygen and nitrogen species and production of neutrophil extracellular traps (NETs). Phagocytosis is one of the most fundamental neutrophil processes, defects of which can lead to serious immunodeficiency, typically due to increased dissemination of infection(465, 466). Phagocytic capacity was assessed in neutrophils by observing the ability to take up fluorescent latex beads in the presence or absence of LPS. No difference in phagocytic capacity was observed in unstimulated bone marrow neutrophils (figure 7.19), and addition of LPS concurrently with the beads increased the percentage of bead positive neutrophils in both cultures. However, the number of bead positive neutrophils following LPS stimulation was significantly lower in Atg7$^{-/-}$ neutrophils than in wildtype neutrophils,

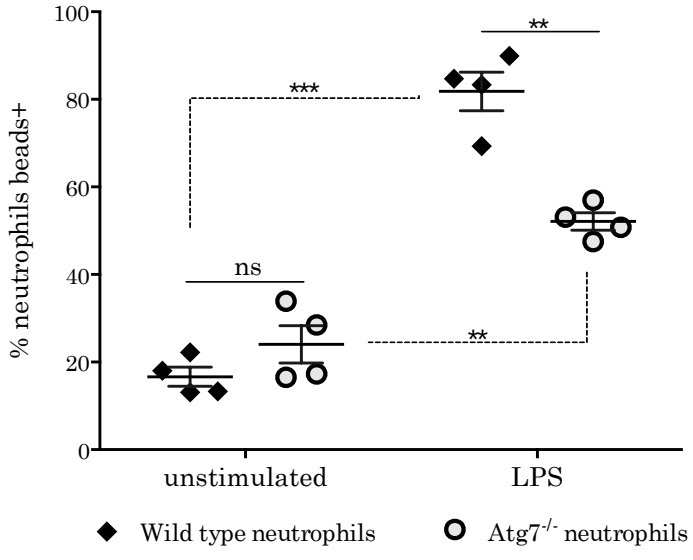

Figure 7.19: *Decreased phagocytic capacity of Atg7$^{-/-}$ bone marrow neutrophils in the presence or absence of LPS. FITC labelled latex beads were cultured for 3 hours with neutrophils with or without LPS (1 µg/ml), and analysed by flow cytometry. Surface associated bead fluorescence was quenched with trypan blue. Error bars represent SEM (n = 4), **p<0.01, ***p<0.001, unpaired t-test.*

where almost 80% of neutrophils contained fluorescent beads compared with 50% of autophagy-deficient neutrophils, indicating significantly reduced phagocytic capacity, and potentially reduced ability to respond to pathogens.

Immature neutrophil-like cells expressing Ly6g and CD11b could also indicate the presence of myeloid derived suppressor cells (MDSCs), which are characterised by inducible nitric oxide synthase (iNOS) and high arginase expression(467). They are frequently found in cancers(468), autoimmune conditions(469), and chronic infections(470), where their main characteristic is a potent ability to suppress T-cell responses(471). As MDSCs express similar surface markers to mature neutrophils, their identification can be challenging, and they are usually classified according to their suppressive capacity or production of suppressive mediators such as iNOS or arginase. To determine whether the immature neutrophil-like cells found in $Atg7^{-/-}$ mice were MDSCs, intracellular expression of iNOS in $Ly6g^{+}$ $CD11b^{+}$ cells was determined by flow cytometry. Although a subset of $Atg7^{-/-}$ neutrophils were indeed positive for iNOS expression (figure 7.20), it was a much smaller percentage than that present in wildtype bone marrow, with less than 2% of $Atg7^{-/-}$ neutrophils staining positive for iNOS, compared with just over 5% of wildtype neutrophils. This suggests that the $Ly6g^{+}$ $CD11b^{+}$ population investigated is unlikely to have suppressive activity in either wildtype or vav-$Atg7^{-/-}$ mice under the conditions tested.

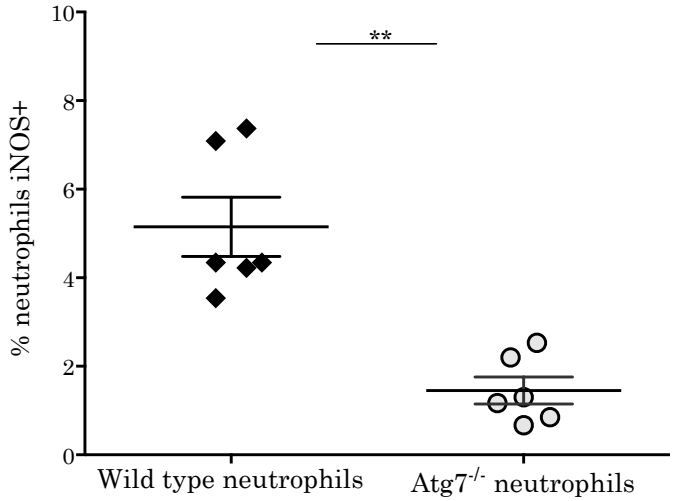

Figure 7.20: *Fewer iNOS$^+$ Ly6g$^+$ CD11b$^+$ cells in Atg7$^{-/-}$ bone marrow. Bone marrow was harvested and stained for neutrophil/MDSC surface markers CD11b and Ly6g prior to fixation and permeabilisation to allow intracellular iNOS staining. Graph shows mean percentage of cells iNOS+, error bars represent SEM and n = 6. **p<0.01, un-paired t-test.*

NO compounds represent one of the main weapons in neutrophil defence, possessing cytotoxic and bactericidal activity, and are particularly effective against intracellular bacteria(472). NO released by neutrophils rapidly reacts with reactive oxygen (O_2^-) to form peroxynitrite, with even more effective killing capacity(473). Given the vital role of NO in neutrophil function, supernatant levels were assessed for nitrite concentration using the Griess reaction. Nitrite concentration in unstimulated neutrophil supernatants was comparable between wildtype Atg7$^{-/-}$ samples, at around 2 µM. However, LPS stimulated Atg7$^{-/-}$ neutrophils produced only half the amount of nitrite compared to wildtype neutrophils, with average supernatant nitrite concentrations of 6 µM, compared with 12 µM in wildtype supernatants (figure 7.21).

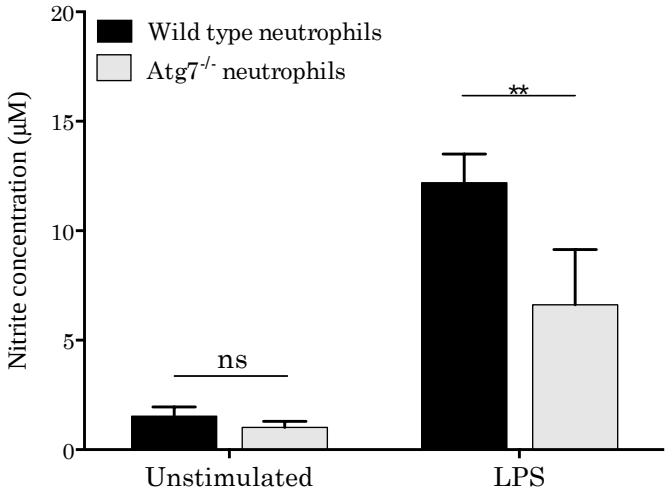

Figure 7.21: *Reduced nitrite burst from Atg7$^{-/-}$ bone marrow neutrophils. Bone marrow neutrophils were stimulated overnight with LPS (1µg/ml) or IFNγ (10 ng/ml) and supernatant samples taken the following day for nitrite analysis using the Griess reagent. Error bars represent SD, n = 4. **p<0.01, un-paired t-test.*

7.8 Autophagy-deficient neutrophils are highly inflammatory

In addition to phagocytosis and degranulation, neutrophils are also significant producers of inflammatory cytokines that initiate and shape the immune response to invading pathogens(474). Although not as significant producers as macrophages and T-cells on a per cell basis, their large numbers mean they make an important contribution to the inflammatory cytokine milieu during many immune responses(475). Autophagy-deficient macrophages produce significantly higher levels of inflammatory cytokines than wildtype macrophages, as discussed in chapter 2. As such, cytokine expression from *ex vivo* neutrophils was assessed to determine whether their apparent inability to mature alters their inflammatory cytokine responses. As seen in autophagy-deficient macrophages, Atg7$^{-/-}$ neutrophils isolated from the peritoneal cavity or spleen express significantly higher levels of the inflammatory cytokines TNF-α and IL-12 than their wildtype counterparts (figure 7.22, top and bottom). Furthermore, increased cytokine expression was observed without

externally applied immune stimulation. In addition to the inflammatory cytokines, the anti-inflammatory cytokine IL-10 was also found to be significantly increased in splenic and peritoneal neutrophils from vav-Atg7 mice.

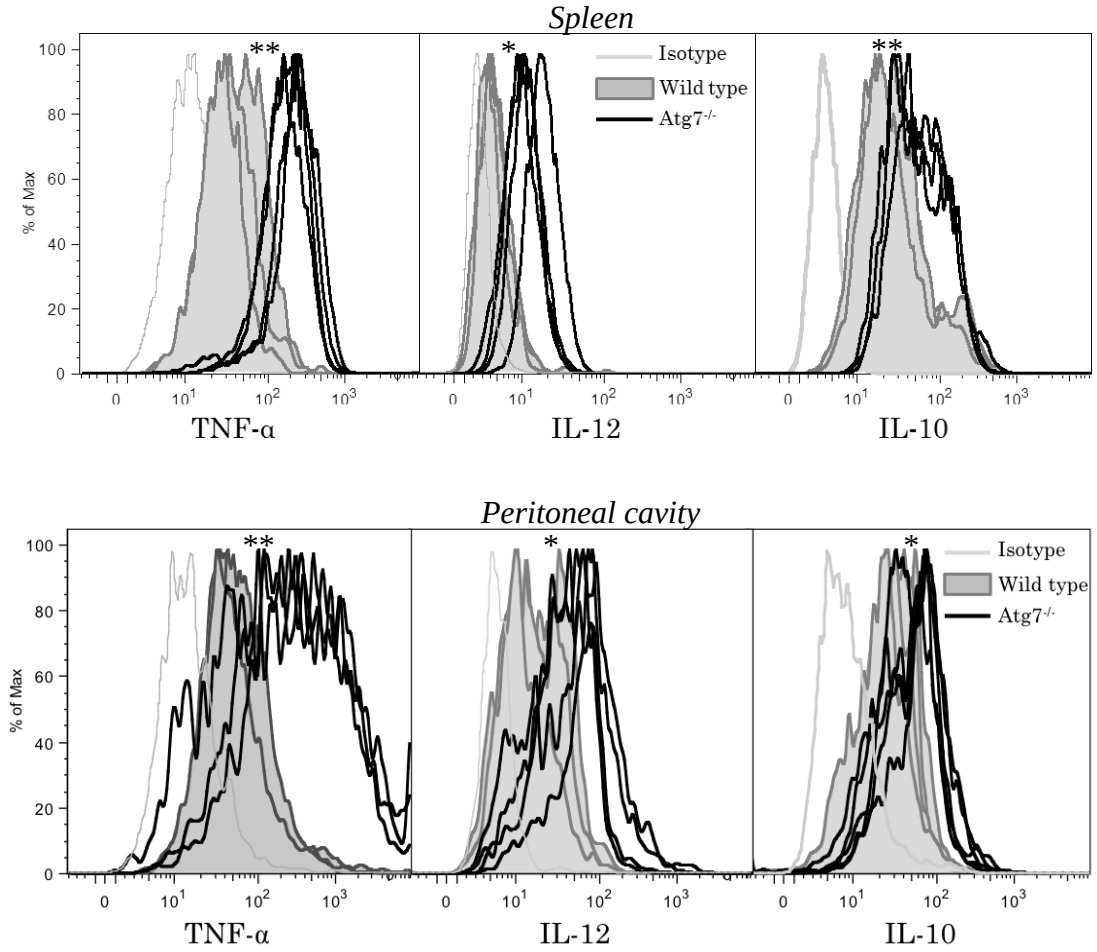

Figure 7.22: Ex vivo *Atg7$^{-/-}$ neutrophils express significantly more cytokines than wildtype neutrophils. Neutrophils were harvested from the spleen (top panels) and the peritoneal cavity (bottom panels) and RBC lysed prior to overnight culture in R10 in the presence of 1x Brefeldin A to block protein secretion. Neutrophils were surface stained for Ly6g and CD11b, followed by fixation and permeabilisation for intracellular cytokine staining. Left-most lightest grey histograms are isotype control peaks. *p<0.05, **p<0.01, statistics generated by un-paired t-test on MFI of each peak.*

Neutrophils extracted from bone marrow were also analysed for cytokine secretion following overnight stimulation with LPS. As found in the splenic and peritoneal neutrophils, unstimulated bone marrow neutrophils expressed significantly higher levels of TNF-α and IL-10 than wildtype neutrophils, despite their apparently immature state (figure

7.23, left and right). Furthermore, stimulation with LPS led to a small, but significant, increase in cytokine expression in Atg7$^{-/-}$ neutrophils, but not wildtype neutrophils.

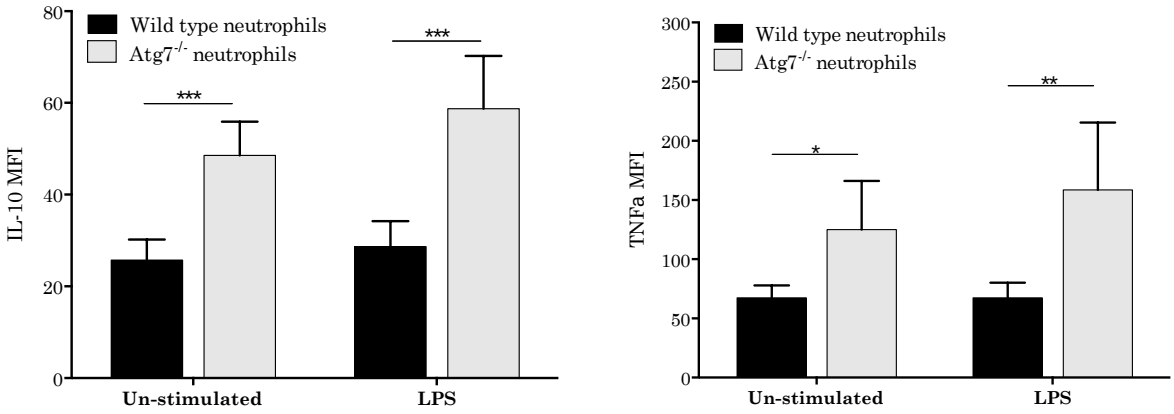

Figure 7.23: Ex vivo *Atg7$^{-/-}$ bone marrow neutrophils express significantly more cytokines than wildtype neutrophils following stimulation with LPS. Neutrophils were harvested from the bone marrow and cultured overnight in R10, supplemented in some cases with LPS (1µg/ml). The following day, 1x Brefeldin A was added for 3hr to block protein secretion. Neutrophils were surface stained for Ly6g and CD11b, followed by fixation and permeabilisation for intracellular cytokine staining. Graphs show mean MFI, error bars represent SEM, n = 4. *p<0.05, **p<0.01, un-paired t-test.*

Chapter 7: Discussion

Atg7 has a role in neutrophil maturation

7.9 Increased neutrophils in Vav-Atg7 mice

As with the macrophages, numbers of neutrophils in the blood, bone marrow and tissues were significantly increased in Vav-Atg7 mice. Although small numbers of neutrophils can commonly be found in many tissues, such large numbers are unusual. The myeloid infiltrate stained positive for CD68, CD11b and myeloperoxidase, and included a high number of immature neutrophils, described as reminiscent of MDS or AML. The cause of the neutrophilia is likely in response to a similar trigger as resulted in increased numbers of macrophages, namely increased proliferation of progenitors, reduced cell death, response to infection, aseptic inflammation or as a result of a proliferative, dysplastic or malignant syndrome. Increased proliferation appears unlikely, as overnight stimulation of bone marrow with G-CSF gave rise to far fewer neutrophil-like cells in $Atg7^{-/-}$ bone marrow cultures than in wildtype cultures, and levels of cell death were increased in $Atg7^{-/-}$ neutrophils, just as in the macrophages, suggesting that decreased cell death was not the cause. No signs of infection were present in any of the mice at dissection or autopsy, nor in any of the tissue samples or cell cultures established from the mice, suggesting that infection as a cause for neutrophilia is unlikely in this instance.

Severe myeloid infiltration is also associated with MDS, myeloproliferative disorders and myeloid leukaemias. Transplanted bone marrow and bone marrow progenitors from Vav-$Atg7^{-/-}$ mice could not successfully transfer the infiltration to other mice(57) and *ex vivo* proliferative capacity of myeloid precursors from Vav-Atg7 bone marrow is severely diminished (*Alec Watson, unpublished data*). As no evidence of translocations or major deletions was found in either bone marrow, myeloid precursors or neutrophil-like cells, it appears unlikely that the myeloid infiltrates present in the tissue of Vav-Atg7 mice are leukemic in origin. Nevertheless, there is evidence that decreased (as opposed to absent) autophagy is involved in the development and pathogenesis of MDS and AML, with

autophagy genes found within the commonly deleted regions (CDRs) of chromosomes associated with leukaemia(476). Immature cells did make up a large proportion of the tissue infiltrates, reminiscent of a myeloproliferative condition, which suggests that autophagy has a role in normal neutrophil maturation or in preventing conditions that result in the artificially increased production of neutrophils.

The severely inflammatory phenotype of $Atg7^{-/-}$ macrophages could result in increased numbers of neutrophils and infiltration into tissues. Increased GM-CSF and G-CSF production by $Atg7^{-/-}$ macrophages could result in egress of neutrophils and precursors from the bone marrow(477). Furthermore, excessive G-CSF signalling can cause neutrophil ROS-mediated apoptosis of mesenchymal progenitor cells in the bone marrow that produce cytokines and adhesion molecules important for maintenance of remaining hematopoietic stem cell populations(478). In otherwise healthy individuals, this effect is transient, however, due to defective stem cell production in Vav-Atg7 mice; this could speed stem cell exhaustion and contribute to increased numbers of neutrophils and neutrophil precursors in the periphery. Furthermore, macrophage recruitment of neutrophils through MIP-1α and TNF-α expression(479) could cause migration into tissues to sites of macrophage-driven inflammation. $Atg7^{-/-}$ neutrophils produce significantly higher levels of inflammatory cytokines themselves, further increasing the inflammatory signalling and potentially driving further production of neutrophils. This has been shown in a model of heart failure, where lack of autophagy-mediated clearance of mitochondrial DNA led to cell autonomous activation of TLR9 and inflammation and infiltration of $CD68^{+}$ macrophages and $Ly6g^{+}$ neutrophils in the heart(480). Thus, loss of autophagy in macrophages and neutrophils could cause a chronically inflammatory environment that fuels production of increased numbers of myeloid cells from the bone marrow, recruiting them into tissues and contributing to increased rapidity of bone marrow failure in Vav-$Atg7^{-/-}$ mice. This

hypothesis could be explored by attempting to reduce levels of inflammatory cytokines or chemokines in the blood of young Vav-Atg7 mice. Anti-GM-CSF (mAb 22E9) has been used successfully to treat inflammatory conditions such as arthritis(481, 482), and anti-G-CSF antibodies have been used to prevent G-CSF-mediated infiltration of $Ly6g^{+}$ cells into organs(483), suggesting administration of either could be used in Vav-Atg7 mice. Injections could be administered weekly or in a single, large dose and levels of inflammatory cells and cytokine production assessed from blood and tissue sections by flow cytometry. Enumeration of HSCs and progenitors from the blood and bone marrow of treated mice would also give an indication of whether α-G-CSF or α-GM-CSF treatment reduced the severity of the decline in progenitor numbers as Vav-Atg7 mice age.

7.10 $Atg7^{-/-}$ neutrophils show altered expression of common neutrophil surface markers

Neutrophils express a range of surface markers throughout development, and on maturity are considered to express high levels of the surface marker Ly6g(443, 445) and the adhesion molecule CD11b. Flow cytometric analysis of neutrophils from Vav-Atg mice revealed differences in Ly6g expression between the neutrophil populations, whereas expression of CD11b was comparable between groups. This suggests that some $Atg7^{-/-}$ neutrophils express 'mature' levels of Ly6g, but a large proportion of them express reduced levels, possibly due to reduced maturation. CD11b is expressed at fairly consistent levels throughout the later stages of maturation (from myelocyte to segmented nuclei)(449), suggesting that the population in $Atg7^{-/-}$ mice may contain an even spread of these maturation states, whereas the wildtype population contains predominately band and segmented neutrophils expressing high Ly6g. Levels of Fc receptor (CD16/32), CXCR4 and CD62L were all found to be elevated on $Atg7^{-/-}$ neutrophils relative to wildtype. This is

unexpected both due to their potential immaturity, based on Ly6g expression and morphology, but also because Atg7$^{-/-}$ macrophages had reduced expression of many surface markers. However, CD11b expression was found to be similar on macrophages, and the expression of F4/80 was found to be variable. As previously discussed, it is possible that not all surface antigens utilise autophagy as a mechanism for surface presentation. Furthermore, macrophage alterations in morphology and neutrophil and macrophage deficiencies in phagocytosis suggest a wider role for autophagy in regulation of membrane motility. Higher L-selectin expression in Atg7$^{-/-}$ neutrophils could be an indication of reduced activation/maturation or problems with receptor shedding. It may be that CD62L, shedding of which is a marker of activation(484), is shed normally in wildtype neutrophils, but is fixed in the membrane following loss of autophagy, thus causing them to appear to have higher expression.

Similarly, FcγRIII (CD16) is constantly shed by activated neutrophils, suggesting it is lack of shedding rather than increased expression responsible for higher cell surface levels on Atg7$^{-/-}$ neutrophils(485). This could be assessed by quantification of shed CD62L and CD16 in the supernatants of neutrophil cultures via western blot or ELISA. GM-CSF has been shown to increase expression of Fc Receptor(486), though this would normally also result in upregulation of Ly6g.

CXCR4 negatively regulates neutrophil trafficking from the bone marrow(450), with increased expression usually related to increased retention of neutrophils in the bone marrow. As neutrophils are increased in both the bone marrow and the tissues of Vav-Atg7 mice, it is difficult to assess whether CXCR4 signalling on Atg7$^{-/-}$ neutrophils is successful. However, it may be upregulated as a responsive mechanism in Atg7$^{-/-}$ mice to prevent the egress of such large numbers of neutrophils from the bone marrow.

Loss of autophagy in neutrophils results in a disruption of normal surface marker expression, which is in some ways similar to that observed in $Atg7^{-/-}$ macrophages. However, changes in some of the surface markers (decreased Ly6g expression and increased CD62L expression) are indicative of reduced maturation, whereas others may be adaptive responses to attempt to regulate neutrophil trafficking out of the bone marrow.

7.11 $Atg7^{-/-}$ neutrophils have features consistent with immaturity

In addition to decreased expression of Ly6g, morphologic analysis of $Atg7^{-/-}$ neutrophils showed significant immaturity among $Gr1^{high}CD11b^{high}$ cells. High expression of these markers is usually accepted to represent mature neutrophils, although no studies in mice have assigned surface markers to particular stages of neutrophil development. Despite cells being sorted from the same 'maturity' gate by flow cytometry, there was a significant majority of immature neutrophils in $Atg7^{-/-}$ cultures, most of which exhibited round or bean-shaped nuclei consistent with metamyelocyte and band stages of development(432). More than 60% of wildtype $Gr1^{high}CD11b^{high}$ neutrophils had the characteristic ≥3 lobed appearance, whereas less than 5% of $Atg7^{-/-}$ $Gr1^{high}CD11b^{high}$ cells from the same gate had 3 or more visible nuclear lobules. Furthermore, 57% of $Atg7^{-/-}$ $Gr1^{high}CD11b^{high}$ neutrophils showed no evidence of nuclear lobulation at all, compared with 8% of wildtype cells. Neutrophils were also assessed by image stream analysis, based on $Ly6g^{high}CD11b^{high}$ staining and nuclear staining with Draq5, and assigned to different maturation characteristics based on their nuclear lobularity. This also revealed a significant shift toward less mature forms of neutrophil, confirming that $Atg7^{-/-}$ $Ly6g^{high}$ $CD11b^{high}$ cells are less mature. This is in spite of using the same Gr1 and Ly6g gating and gating out the clearly less mature $Ly6g^{mid\text{-}low}$ population visible on flow cytometry. This suggests that

even those Atg7$^{-/-}$ neutrophils expressing comparable levels of Ly6g surface antigen are less morphologically mature, based on nuclear shape, than their wildtype counterparts.

In addition to immature nuclear morphology, there were significant differences in the number, appearance and location of neutrophil granules. Atg7$^{-/-}$ neutrophils contained, on average, half the granules of wildtype neutrophils and their granules were smaller in size and less electron dense with an uneven distribution in the cytoplasm when assessed by EM. Both primary (very dark round granules) and secondary (dark grey, slightly smaller granules)(487) appear reduced in the electron micrographs, though it is difficult to distinguish tertiary granules in either micrograph. However, a primary granule release assay showed similar levels of total MPO in Atg7$^{-/-}$ macrophages, albeit with a different release pattern. Higher levels of MPO were found in the supernatant of Atg7$^{-/-}$ bone marrow neutrophils, whereas total levels from lysed neutrophils were the same. This suggests that Atg7$^{-/-}$ macrophages released their granules un-primed (LPS had little effect on MPO in either samples), whereas wildtype macrophages retained their MPO granules. This makes some sense, as primary granules usually only undergo limited exocytosis and are generally thought to contribute mainly to the intracellular degradation of microorganisms in the phagolysosome(431). The bone marrow neutrophils in this assay underwent a similar staining regime prior to MACS sorting as the EM neutrophils underwent for staining by flow sorting. This raises the possibility that the lack of primary granules present in the EM images is due to prior release of MPO granules from Atg7$^{-/-}$ macrophages. Ideally, primary granule number would be clarified by more specific microscopic staining, in order to better compare relative expression, though if unstimulated MPO release from Atg7$^{-/-}$ neutrophils does occur, it may be difficult to stain them without causing them to lose their MPO. Secondary granule content was assessed by intracellular flow cytometry, and found to be unexpectedly higher in Atg7$^{-/-}$ neutrophils. This could arise from a number of factors, and

further investigations will be necessary to clarify the true extent of NGAL and lactoferrin content of secondary granules in Atg7$^{-/-}$ neutrophils. Lactoferrin ceases to be produced in mature granules, whereas it is continually being produced in immature granule forms(488), which could result in a build-up in immature Atg7$^{-/-}$ neutrophils over time. It is also possible that secondary (or any other) granules are autophagic substrates, either during general cytoplasmic turnover, or secretory granule autophagy, termed Zymophagy. Zymophagy was first described in the pancreas, as a mechanism that specifically detects and degrades secretory granules to prevent inflammation(489). Autophagic uptake of members of the lipocalin family, to which NGAL belongs, has also been observed in kidney cells(490, 491), suggesting such a mechanism may occur in neutrophils as an adaptation to prevent excess inflammation. Only total intracellular lactoferrin and NGAL were assessed in neutrophils, with no assessment of protein localisation, and therefore no confirmation that the increased protein production was located in granules. Further clarification could be achieved by fluorescence microscopy with labelled granules. Autophagy has previously been implicated in the degranulation of mast cells(98) and Paneth cell lysozyme mobilisation(492), suggesting that increased internal granule contents could also be due to a secretion defect in Atg7$^{-/-}$ neutrophils, though this was apparently not an issue for MPO.

Granule expression was also assessed at the mRNA level using qPCR. Gene expression of MPO and lactoferrin were significantly upregulated in Atg7$^{-/-}$ bone marrow neutrophils, which correlates with the MPO assay and Lactoferrin FACS staining. Expression of the tertiary granule protein MMP9 was found to be significantly reduced in Atg7$^{-/-}$ macrophages to around 60% of wildtype expression. Tertiary granule production is initiated at the band stage of neutrophil development(428), and thus this may reflect the reduced numbers of Atg7$^{-/-}$ neutrophils at this stage of development among the

$Ly6g^{+}CD11b^{+}$ population. Tertiary granule components, such as MMP9, could be assessed by fluorescence microscopy, western blot or ELISA. As primary and secondary granule components seem to be detectable, if not visible by EM, in $Atg7^{-/-}$ neutrophils, it would be of interest to determine whether similar levels of MMP9 protein were produced and secreted, to clarify whether the immaturity is limited to nuclear morphology, or overall reduced maturation (morphology and granule status).

It was also observed that $Atg7^{-/-}$ neutrophils express significantly decreased levels of SOCS3 mRNA, a negative regulator of neutrophil production. Mice in which SOCS3 has been specifically deleted in the granulocyte macrophage lineage had significantly more neutrophils than wildtype mice(460), suggesting that a decrease in SOCS3 signalling in $Atg7^{-/-}$ neutrophils and precursors could be responsible for their increased numbers. Autophagy is not known to directly regulate SOCS3 expression, but it is possible that reduced expression is a feedback mechanism to attempt to increase the numbers of mature neutrophils formed.

Granulopoiesis from HSC to mature, segmented neutrophil is presided over by 2 key regulators, C/EBPα and C/EBPε(493). C/EBPα is expressed in myeloid progenitors from the common myeloid progenitor (CMP) and is maintained during granulocytic differentiation(494). C/EBPα activates several granulocyte-specific genes, including the primary granule protein, MPO, and the G-CSFR(495), and also results in the activation of C/EBPε, a late neutrophil differentiation transcription factor. C/EBPε is upregulated by C/EBPα in concert with G-CSF signalling through the G-CSFR(496), and is responsible for induction of secondary/tertiary granule proteins such as lactoferrin and gelatinase(424). Analysis of C/EBPε gene expression indicated significantly reduced expression in $Atg7^{-/-}$ neutrophils, to around 70% of wildtype expression. However, from this information it is difficult to determine whether reduced C/EBPε expression is causing the reduced

differentiation, or whether merely having more immature cells in the $Ly6g^{+}CD11b^{+}$ population that was analysed means there are fewer C/EBPε-expressing cells present. Analysis of C/EBPε protein expression and transcription factor binding/transactivation may give a better indication of whether it is a cause or merely a symptom of reduced maturation. $Atg7^{-/-}$ neutrophils show a spectrum of characteristics suggestive of reduced maturational state, including reduced Ly6g expression, reduced nuclear lobularity and alterations in granule protein expression and/or localisation. Even $Atg7^{-/-}$ neutrophils expressing similar levels of Gr1 to wildtype neutrophils still appear morphologically immature despite their expression of 'maturity' markers. This conflicting combination of maturity and immaturity signs suggests a role for autophagy in specific aspects of neutrophil differentiation.

7.12 Maturational stimuli cannot overcome the maturation defect

Autophagy has previously been shown to be important for treatment-induced maturation of APL cells, by autophagic degradation of the fusion protein PML-RARα(463) in response to ATRA therapy(463). Furthermore, autophagy is required for the terminal differentiation of several neutrophilic cells lines, including HL-60 cells(497), and facilitates degradation of the oncoprotein BCR-ABL in chronic myeloid leukaemia (CML)(498). However, there is no research covering the role of autophagy in non-transformed neutrophils or how autophagy contributes to normal granulopoiesis.

In order to determine whether immature autophagy-deficient neutrophils could be induced to mature in response to maturational stimuli, bone marrow neutrophils were treated overnight with TNF-α, LPS, G-CSF, GM-CSF and ATRA, which has previously been shown to induce maturation in myeloid leukemic cell lines(499). None of the treatments applied were sufficient to induce a population of $Ly6g^{+}$ $CD11b^{+}$ cells that was clearly

distinct from $Ly6g^{neg}$ cells. Although several treatments resulted in a change in CD11b expression, none was able to make $Atg7^{-/-}$ neutrophils replicate the distinct neutrophil population of wildtype neutrophils. Furthermore, light microscopic analysis following treatment with G-CSF and GM-CSF showed changes in nuclear size, shape and staining characteristics. GM-CSF treatment also resulted in the appearance of large vacuoles, reminiscent of those seen in $Atg7^{-/-}$ macrophage micrographs. Some of the cells in $Atg7^{-/-}$ cultures were reminiscent of macrophages, potentially suggesting the presence of hybrid macrophage-neutrophil cells, which would be further evidence of altered maturity. Induction of autophagy facilitates differentiation of APL cells via degradation of the PML-RAR fusion protein(463). As autophagy is primarily a degradation mechanism, this suggests that non-transformed neutrophils cannot differentiate in the absence of autophagy due to accumulation or overexpression of a negative regulator or competitor of differentiation, analogous to the PML-RAR protein. Overexpression of a dominant negative retinoic acid receptor (RAR) in bone marrow neutrophils inhibited their differentiation(500), suggesting RAR or similar proteins could be autophagic targets under normal conditions. Overexpression or accumulation of repressors of C/EBPα/ε may also result in decreased differentiation potential of wildtype neutrophils. In support of this hypothesis, C/EBPε is rapidly induced in ATRA treated NB4 cells during granulocytic differentiation, suggesting a link between autophagy induction and C/EBPε activation. In ATRA resistant APL cell lines, C/EBPε was not induced, or only at very high ATRA concentrations(501). $C/EBP\varepsilon^{-/-}$ mice have similarities to the phenotype of $Atg7^{-/-}$ mice as well, with myelodysplasia characterized by proliferation of atypical granulocytes that infiltrate tissues, and similar morphological changes in neutrophils(424). Levels of neutrophil-development repressors, such as RAR and C/EBP repressors, could be assessed in $Atg7^{-/-}$ neutrophils by western blot, or intracellular staining. Additionally, dual staining

of known repressors and LC3 could be attempted in order to determine whether such repressors could be found in autophagosomes. Ectopic overexpression of pro-development transcription factors, such as C/EBPε and C/EBPα, could also be attempted to force neutrophil maturation.

Although granule expression was enigmatic in $Atg7^{-/-}$ neutrophils, and requires further investigation, nuclear morphology was unmistakably altered, with a significant lack of the lobularity that characterises a mature neutrophil. Although the exact purpose of neutrophil nuclear shape is not known, it is thought that the lobular shape allows flexibility for movement through tight spaces during extravasation and trafficking to sites of infection(502). Nuclear differentiation requires adequate expression of a protein called Lamin B Receptor (LBR), with expression increasing following ATRA treatment of HL-60 cells(503). Relative to ATRA differentiated HL-60 cells, normal neutrophil nuclei exhibit little LBR(504). The relative absence of LBR on normal mature nuclei, suggests that its downregulation or physical removal plays a role in nuclei development. Nuclear-specific autophagy, or nucleophagy, has been described in some cell types, allowing nuclear maintenance by removal of damaged, non-functional components(505). LBR or other nuclear proteins could potentially act as autophagy receptors, targeting portions of the nucleus for autophagic degradation during nuclear maturation. Senescent cells have also been shown to process chromatin via an autophagy/lysosomal pathway, in which portions of the nucleus bud off and are degraded by autophagy(506), suggesting an alternate mechanism by which autophagy could shape the neutrophil nucleus. The removal of nuclear envelope proteins upon maturation is also thought to stabilise the lobulated nucleus, while at the same time allowing the formation of post-mortem NETs(502), which is also thought to contribute to the characteristic dense chromatin pattern of mature neutrophils. If these proteins are not able to be removed by nucleophagy, this may also explain the

reduced chromatin density and light staining observed in Atg7$^{-/-}$ neutrophil electron micrographs and light microscope images, respectively.

Neutrophil morphology was only assessed in neutrophils extracted from the bone marrow of Vav-Atg7 mice. Although tissue sections and staining of surface markers indicated increased numbers of immature cells, which suggests the immature phenotype extends beyond the bone marrow, only detailed morphologic analysis of tissue and blood would be able to confirm this. Blood neutrophils are usually more mature than bone marrow neutrophils, and thus continued immaturity in the blood would further confirm the differentiation block in Atg7$^{-/-}$ neutrophils. Furthermore, adoptive transfer of Atg7$^{-/-}$ neutrophils into wildtype mice could be attempted to determine whether a normal, non-inflammatory environment could rectify their maturational defect. Although the autophagy defect is likely cell autonomous, the Vav-Atg7 model does have a significantly altered immune background, due to the anaemia, lymphopenia, stem cell defect and increased inflammatory signalling, which could contribute confounding effects on neutrophil differentiation and mask the physiological role of autophagy in differentiation.

7.13 Loss of Atg7 results in reduced innate functions of neutrophils and increased inflammation

Both phagocytosis and nitrite burst were reduced in neutrophils in the absence of autophagy, very similarly to Atg7$^{-/-}$ macrophages, and most likely with a similar mechanism of action. As with macrophages, neither function was completely abolished in Atg7$^{-/-}$ neutrophils, again suggesting that autophagy plays an indirect, rather than a direct, role in either.

Ly6g, Gr1 and CD11b are frequently used to identify MDSCs, in addition to mature neutrophils(467), and iNOS production is a known mechanism of suppressive action. The

immature Ly6g^{+} CD11b^{+} population in Vav-Atg7 mice have some similar features to MDSCs, but expression of iNOS was significantly lower in Atg7$^{-/-}$ neutrophils than in wildtype neutrophils, making it unlikely they have suppressive action. However, this would need to be confirmed by a suppressive assay to conclusively show that they have no suppressive activity. However, Atg7$^{-/-}$ neutrophils were also found to have significantly increased expression of inflammatory cytokines, despite their immature phenotype, which provides further evidence that they have no immune-suppressive capability. Similarly to Atg7$^{-/-}$ macrophages, unstimulated (or, at least, not exogenously stimulated) *ex vivo* neutrophils from the spleen, peritoneal cavity and direct from the bone marrow produced significantly higher levels of inflammatory cytokines than wildtype neutrophils. Interestingly, their immature phenotype does not appear to impair their capacity for cytokine production, suggesting that all cytokine activating genes are active in Atg7$^{-/-}$ neutrophils. Although neutrophils do not secrete cytokines to the same level as macrophages, their sheer numbers make them a formidable contributor to the overall cytokine milieu. Like macrophages, neutrophils can also be activated by DAMPs and recruited to sites of cellular damage and inflammation by DAMP production(507). The NLRP3 inflammasome also directs IL-1β secretion in neutrophils(508), suggesting a similar mechanism for autophagy-mediated cytokine control in neutrophils as in macrophages, namely increased expression of mROS(237), mitochondrial DNA(7) and increased inflammasome activation(186). Furthermore, qPCR analysis indicated increased expression of the antioxidant regulator Nrf2, and HIF-1α, suggesting that the neutrophils are attempting to adapt to and survive their inflammatory and oxidative environment by the production of antioxidants and other survival genes and potentially by altering their metabolism.

7.14 Conclusions

Loss of autophagy in neutrophils results in a significant increase in immature neutrophils in the blood and tissues of vav-Atg7 mice, characterised by reduced expression of Ly6g, altered expression of other neutrophil surface markers, enigmatic granule production and significant changes in nuclear morphology. Addition of exogenous stimuli is insufficient to bring about morphological maturity, outlining a role for autophagy in non-transformed neutrophil maturation. Although the mechanism for autophagic control of neutrophil differentiation is unclear from the present data, it could involve degradation of inhibitors of differentiation, analogous to fusion protein degradation in APL, or potentially through specific autophagic reshaping of the nuclei via nucleophagy. Reduced innate functions and increased inflammatory cytokine production are mirrored between the two major myeloid cell types, neutrophils and macrophages, in the absence of autophagy. This confirms a general, rather than cell-specific, role for autophagy in maintenance of optimal cell function and appropriate immune responses and further reiterates the master control of homeostasis and cell function that autophagy exerts within cells.

Chapter 8: Discussion & Conclusions

8.1 Myeloproliferation in Vav-Atg7 mice

Vav-Atg7 mice showed significantly increased numbers of macrophages and neutrophils, both in normal hematopoietic tissues and infiltrated into other, non-hematopoietic organs. The origin of the increased myeloid burden could be attributed to:

a. Chronic inflammation
b. MDS/myeloproliferative disease
c. AML
d. Combination of inflammation and MDS

The myeloid cells produced by Vav-Atg7 mice and derived from $Atg7^{-/-}$ bone marrow are highly inflammatory, even in the absence of exogenous stimuli and exhibit increased production of myeloid-supporting growth factors, chemokines, cytokines and ROS, any and all of which could certainly contribute to increased myelopoiesis. However, the initiating trigger for the inflammation is uncertain – did the presence of large numbers of myeloid cells (i.e. due to MDS or AML) occur first, thereby resulting in increased inflammation, or was there an initial or low level gradually increasing inflammatory signals? The potential sources of such inflammatory signals in this model are many; there are large numbers of dying RBCs and lymphocytes potentially releasing DAMPs, such as mitochondrial and genomic DNA, histones and other cellular constituents. Furthermore, both the macrophages and neutrophils appear to upregulate antioxidant pathways as an adaptation to increasing oxidative stress and, as previously discussed, Prxn1, a major antioxidant, may act as a DAMP signalling through TLR4(238). Overall this gradual buildup of inflammatory triggers could plausibly result in increasing production and infiltration of myeloid cells into the tissues. However, the inability of neutrophils to mature in the absence of autophagy is also highly reminiscent of AML cell lines such as NB4(499) and HL-60(463). Further genetic analysis of infiltrates may yet reveal mutations or translocations indicating that stable transformation in the complete absence of autophagy is

possible, although the stem cell defect present in $Atg7^{-/-}$ bone marrow could make them so highly fragile and susceptible to death as to be unable to support continued proliferation or immortality. Another confounding factor is the relative contribution or, in this model, the lack of contribution, of lymphocytes. Any tumours that did arise in this model, hematopoietic or otherwise, would not have experienced immunological selective pressure, potentially weakening their tumorigenic ability. Immuno-regulatory signalling, for example through T_H2 cells, may also prevent or partially ameliorate the excessive inflammation present in this model. Other models of Atg7 deletion may help clarify the myelospecific consequences of loss of autophagy in the absence of the confounding influence of fragile stem cells. For example, Atg7 deletion using the Cebpa-cre(509) would give rise to Atg7 deletion from very early myelopoiesis without influencing stem cell production. Later contributions to development could be assessed using LysM-Cre(169)-driven deletion of Atg7. There have been multiple studies using LysM mediated deletion of Atg7(92, 510) and, although none have shown as extreme a phenotype as the Vav-Atg7 model, some have reported reduced differentiation(511), spontaneous inflammation and infiltration of the lung(512) and activation of the inflammasome(513), suggesting HSC-independent roles for autophagy in myeloproliferation and inflammation. Use of such models may help to clarify the origin of increased myeloid cell numbers in Vav-Atg7 mice.

8.2 Autophagy and metabolism

Loss of autophagy in macrophages resulted in a significant upregulation of glycolysis, possibly as a substitute for lost autophagic energy production or to produce sufficient ATP to maintain mitochondrial potential and prevent cell death via the intrinsic apoptotic pathway. This is the first time that loss of autophagy has been shown to increase glycolysis, rather than decrease glycolysis, as has been shown in several cell line and cancer subtypes.

Macrophages, being naturally glycolytic cells, have a range of adaptions that allow for glycolytic energy production in the absence of autophagy without being overwhelmed by oxidative stress or overcome by build-up of toxic glycolytic intermediates. Neutrophils also preferentially produce energy via glycolysis(514), also maintaining their mitochondrial membrane potential in this manner. It appears likely that neutrophils also further increase their glycolytic output in the absence of autophagy, and it would be interesting to see how this varies between tissue locations, i.e. blood neutrophils versus bone marrow or peritoneal neutrophils (and macrophages), to determine whether their energy needs are dictated by their environment. It would be interesting to investigate metabolic pathways in autophagy-deficient lymphocytes to determine whether they are able to utilise this pathway as a survival mechanism in the same manner. Both B- and T-cells normally upregulate glycolysis following ligation of the BCR or TCR(515, 516), suggesting that it may also make a viable survival pathway in the absence of autophagy or aberrant OxPhos due to damaged mitochondria. Similarly, HSCs rely on glycolytic energy production due to the hypoxic nature of the stem cell niche(517), suggesting they may also potentially upregulate glycolysis in the absence of autophagy, particularly since mitochondrial instability is implicated in HSC failure in Vav-Atg7 mice(57). Although several lines of research have shown a requirement for autophagy in supporting tumorigenic glycolysis, in some instances autophagy appears to play a protective role in preventing glycolytic upregulation. For example, loss of PTEN, a positive regulator of autophagy(518), in leukaemia cells results in upregulation of autophagy(519), whereas inhibition of mTOR suppresses autophagy and sensitises AML cells to chemotherapy(520). Together, these data suggest a further contribution to autophagy's 'double-edged sword' role in cancer prevention and progression.

8.3 Autophagy and the aging innate immune system

The similarities between aged and autophagy-deficient macrophages suggest both that loss of autophagy accelerates aging of the immune system, and that many of the changes seen in the aged immune system may be due, at least in part, to reduced autophagy levels. Increased myeloid cell production in the elderly may also have an origin in decreased autophagy levels. Furthermore, the increased glycolysis that occurs with advancing age(408, 521) draws a further link to autophagy, and thereby potentially also to cancer progression. Our experiments in macrophages demonstrated significantly decreased autophagy in macrophages, but also that autophagy could still be increased using autophagic stimuli such as LPS and IFNγ. This suggests that positive modulation of autophagy in the elderly, either by caloric restriction or autophagy-inducing agents such as rapamycin or spermidine, has the potential to improve immune function in a variety of ways, supress excess inflammation and prevent induction of excessive glycolysis.

8.4 Conclusions

Analysis of the role of autophagy in the myeloid cells of the immune system has uncovered and clarified multiple roles in maturation, function, control of inflammation and metabolism, and, in the case of neutrophils, differentiation.

Loss of autophagy in Vav-Atg7 mice contributes to a significant increase of macrophages and neutrophils in the bone marrow, blood and tissues, potentially due to chronic inflammatory signalling by both the macrophages and neutrophils. In macrophages, loss of autophagy caused alterations in morphology and membrane shape, potentially influencing functions which rely on membrane motility, such as phagocytosis, migration and surface marker expression. In addition to increased levels of cell death, phagocytosis and NO burst were significantly reduced, but not abolished, in both macrophages and neutrophils.

Furthermore, antigen presentation by macrophages was significantly blunted, either due to reduced intracellular processing of antigens in the absence of autophagy, or due to reduced expression and upregulation of important antigen presentation markers, such as MHC II. The mechanism for autophagy's role in surface marker expression may be mediated through interaction of autophagosomes or autophagy machinery with MVBs or due to reduced expression and action of vital Rab proteins. Despite their inability to upregulate many surface antigens in response to stimulation, autophagy-deficient macrophages were found to be highly inflammatory, producing increased levels of inflammatory cytokines, chemokines and growth factors that mediate proliferation and differentiation of other myeloid cells, thereby potentially contributing to the increased numbers of myeloid cells present in Vav-Atg7 mice. Increased inflammatory mediator production by both macrophages and neutrophils was observed in the absence of exogenously applied stimuli, suggesting endogenous stimulation by DAMPs or mROS is further contributing to the inflammation observed *in vivo*.

In addition to altered macrophage function, a significant change in metabolism was observed in the absence of autophagy. Autophagy-deficient macrophages showed significantly increased glucose uptake and levels of glycolysis, as well as increased expression of HIF-1α. Furthermore, despite their increased levels of glycolysis, the macrophages had a higher basal OCR than wildtype macrophages and a significantly higher SRC, likely attributable to increased mitochondrial load.

Many of the changes observed in autophagy-deficient macrophages are mirrored in aged macrophages, drawing the connection between reduced autophagy and accelerated aging, and implying a role for autophagy in preventing the age-related decline in macrophage function and dysregulated inflammatory signalling.

Finally, a novel role for autophagy in normal neutrophil differentiation was also uncovered. Autophagy-deficient neutrophils showed signs of immaturity, particularly in altered granule expression and lack of lobulated nuclei. The mechanism by which autophagy facilitates neutrophil maturation could be through degradation of negative regulators of differentiation, analogous to degradation of leukemic fusion proteins in treatment of leukaemia, or via a new role for nucleophagy in remodelling of the neutrophil nucleus. These data further underscore the importance of autophagy in myeloid cell function and regulation, and opens up further avenues of exploration in the links between autophagy, inflammation, metabolism and aging. That autophagy can influence events as diverse as infection control, development and differentiation, metabolism and energy generation, and homeostasis, underscores its vital importance to cellular, and therefore organismal, well-being. Without the 'housekeeping' capacity of autophagy, cellular function declines over time, oxidative stress increases, and, in a subset of cells, inflammatory signalling becomes dysregulated – all features of cellular senescence(408), and so called 'inflamm-aging'(522). Furthermore, changes in metabolism, low level inflammation and DNA damage caused by high oxidative stress can contribute to the increased cancer susceptibility in the elderly. The challenge in future is to determine what genetic factors control basal autophagy levels in humans, and how autophagy can best be exploited to maintain optimal cellular quality.

Bibliography

1. Reggiori, F., and D. J. Klionsky. 2002. Autophagy in the eukaryotic cell. *Eukaryot Cell* 1: 11-21.
2. Mortensen, M., and A. K. Simon. 2010. Nonredundant role of Atg7 in mitochondrial clearance during erythroid development. *Autophagy* 6: 423-425.
3. Boya, P., R. A. Gonzalez-Polo, N. Casares, J. L. Perfettini, P. Dessen, N. Larochette, D. Metivier, D. Meley, S. Souquere, T. Yoshimori, G. Pierron, P. Codogno, and G. Kroemer. 2005. Inhibition of macroautophagy triggers apoptosis. *Mol Cell Biol* 25: 1025-1040.
4. Degenhardt, K., R. Mathew, B. Beaudoin, K. Bray, D. Anderson, G. Chen, C. Mukherjee, Y. Shi, C. Gelinas, Y. Fan, D. A. Nelson, S. Jin, and E. White. 2006. Autophagy promotes tumor cell survival and restricts necrosis, inflammation, and tumorigenesis. *Cancer Cell* 10: 51 - 64.
5. Rajawat, Y. S., Z. Hilioti, and I. Bossis. 2009. Aging: central role for autophagy and the lysosomal degradative system. *Ageing Res Rev* 8: 199-213.
6. Deretic, V., M. Delgado, I. Vergne, S. Master, S. De Haro, M. Ponpuak, and S. Singh. 2009. Autophagy in immunity against mycobacterium tuberculosis: a model system to dissect immunological roles of autophagy. *Curr Top Microbiol Immunol* 335: 169-188.
7. Nakahira, K., J. A. Haspel, V. A. Rathinam, S. J. Lee, T. Dolinay, H. C. Lam, J. A. Englert, M. Rabinovitch, M. Cernadas, H. P. Kim, K. A. Fitzgerald, S. W. Ryter, and A. M. Choi. 2010. Autophagy proteins regulate innate immune responses by inhibiting the release of mitochondrial DNA mediated by the NALP3 inflammasome. *Nat Immunol*.
8. Dengjel, J., O. Schoor, R. Fischer, M. Reich, M. Kraus, M. Muller, K. Kreymborg, F. Altenberend, J. Brandenburg, H. Kalbacher, R. Brock, C. Driessen, H. G. Rammensee, and S. Stevanovic. 2005. Autophagy promotes MHC class II presentation of peptides from intracellular source proteins. *Proc Natl Acad Sci U S A* 102: 7922-7927.
9. Lee, H. K., L. M. Mattei, B. E. Steinberg, P. Alberts, Y. H. Lee, A. Chervonsky, N. Mizushima, S. Grinstein, and A. Iwasaki. 2010. In vivo requirement for Atg5 in antigen presentation by dendritic cells. *Immunity* 32: 227-239.
10. Hruz, P., and L. Eckmann. 2011. Innate immune defence: NOD2 and autophagy in the pathogenesis of Crohn's disease. *Swiss Med Wkly* 140: w13135.
11. Gonzalez, C. D., M. S. Lee, P. Marchetti, M. Pietropaolo, R. Towns, M. I. Vaccaro, H. Watada, and J. W. Wiley. 2011. The emerging role of autophagy in the pathophysiology of diabetes mellitus. *Autophagy* 7: 2-11.
12. Li, L., X. Zhang, and W. Le. 2010. Autophagy dysfunction in Alzheimer's disease. *Neurodegener Dis* 7: 265-271.
13. Sarkar, S., and D. C. Rubinsztein. 2008. Huntington's disease: degradation of mutant huntingtin by autophagy. *FEBS J* 275: 4263-4270.
14. Dengjel, J., A. R. Kristensen, and J. S. Andersen. 2008. Ordered bulk degradation via autophagy. *Autophagy* 4: 1057-1059.

15. Bejarano, E., and A. M. Cuervo. 2010. Chaperone-mediated autophagy. *Proc Am Thorac Soc* 7: 29-39.

16. Kaushik, S., U. Bandyopadhyay, S. Sridhar, R. Kiffin, M. Martinez-Vicente, M. Kon, S. J. Orenstein, E. Wong, and A. M. Cuervo. 2011. Chaperone-mediated autophagy at a glance. *J Cell Sci* 124: 495-499.

17. Dice, J. F. 1990. Peptide sequences that target cytosolic proteins for lysosomal proteolysis. *Trends Biochem Sci* 15: 305-309.

18. Mizushima, N., and B. Levine. 2010. Autophagy in mammalian development and differentiation. *Nat Cell Biol* 12: 823-830.

19. Bains, M., M. L. Florez-McClure, and K. A. Heidenreich. 2009. Insulin-like growth factor-I prevents the accumulation of autophagic vesicles and cell death in Purkinje neurons by increasing the rate of autophagosome-to-lysosome fusion and degradation. *J Biol Chem* 284: 20398-20407.

20. Jia, G., G. Cheng, D. M. Gangahar, and D. K. Agrawal. 2006. Insulin-like growth factor-1 and TNF-alpha regulate autophagy through c-jun N-terminal kinase and Akt pathways in human atherosclerotic vascular smooth cells. *Immunol Cell Biol* 84: 448-454.

21. Waltz, P., E. H. Carchman, A. C. Young, J. Rao, M. R. Rosengart, D. Kaczorowski, and B. S. Zuckerbraun. 2011. Lipopolysaccaride induces autophagic signaling in macrophages via a TLR4, heme oxygenase-1 dependent pathway. *Autophagy* 7: 315-320.

22. Tsukada, M., and Y. Ohsumi. 1993. Isolation and characterization of autophagy-defective mutants of Saccharomyces cerevisiae. *FEBS Lett* 333: 169-174.

23. Tooze, S. A. 2013. Current views on the source of the autophagosome membrane. *Essays Biochem* 55: 29-38.

24. Arico, S., A. Petiot, C. Bauvy, P. F. Dubbelhuis, A. J. Meijer, P. Codogno, and E. Ogier-Denis. 2001. The tumor suppressor PTEN positively regulates macroautophagy by inhibiting the phosphatidylinositol 3-kinase/protein kinase B pathway. *J Biol Chem* 276: 35243-35246.

25. Tassa, A., M. P. Roux, D. Attaix, and D. M. Bechet. 2003. Class III phosphoinositide 3-kinase--Beclin1 complex mediates the amino acid-dependent regulation of autophagy in C2C12 myotubes. *Biochem J* 376: 577-586.

26. Blommaart, E. F., U. Krause, J. P. Schellens, H. Vreeling-Sindelarova, and A. J. Meijer. 1997. The phosphatidylinositol 3-kinase inhibitors wortmannin and LY294002 inhibit autophagy in isolated rat hepatocytes. *Eur J Biochem* 243: 240-246.

27. Meijer, A. J., and P. Codogno. 2007. AMP-activated protein kinase and autophagy. *Autophagy* 3: 238-240.

28. Noda, T., and Y. Ohsumi. 1998. Tor, a phosphatidylinositol kinase homologue, controls autophagy in yeast. *J Biol Chem* 273: 3963-3966.

29. Yan, J., H. Kuroyanagi, A. Kuroiwa, Y. Matsuda, H. Tokumitsu, T. Tomoda, T. Shirasawa, and M. Muramatsu. 1998. Identification of mouse ULK1, a novel protein kinase structurally related to C. elegans UNC-51. *Biochem Biophys Res Commun* 246: 222-227.

30. Hara, T., and N. Mizushima. 2009. Role of ULK-FIP200 complex in mammalian autophagy: FIP200, a counterpart of yeast Atg17? *Autophagy* 5: 85-87.

31. Hosokawa, N., T. Hara, T. Kaizuka, C. Kishi, A. Takamura, Y. Miura, S. Iemura, T. Natsume, K. Takehana, N. Yamada, J. L. Guan, N. Oshiro, and N. Mizushima. 2009. Nutrient-dependent mTORC1 association with the ULK1-Atg13-FIP200 complex required for autophagy. *Mol Biol Cell* 20: 1981-1991.

32. Itakura, E., and N. Mizushima. 2009. Atg14 and UVRAG: mutually exclusive subunits of mammalian Beclin 1-PI3K complexes. *Autophagy* 5: 534-536.

33. Itakura, E., C. Kishi, K. Inoue, and N. Mizushima. 2008. Beclin 1 forms two distinct phosphatidylinositol 3-kinase complexes with mammalian Atg14 and UVRAG. *Mol Biol Cell* 19: 5360-5372.

34. He, C., M. Baba, Y. Cao, and D. J. Klionsky. 2008. Self-interaction is critical for Atg9 transport and function at the phagophore assembly site during autophagy. *Mol Biol Cell* 19: 5506-5516.

35. Juhasz, G., and T. P. Neufeld. 2006. Autophagy: a forty-year search for a missing membrane source. *PLoS Biol* 4: e36.

36. Reggiori, F., T. Shintani, U. Nair, and D. J. Klionsky. 2005. Atg9 cycles between mitochondria and the pre-autophagosomal structure in yeasts. *Autophagy* 1: 101-109.

37. Mizushima, N., T. Noda, T. Yoshimori, Y. Tanaka, T. Ishii, M. D. George, D. J. Klionsky, M. Ohsumi, and Y. Ohsumi. 1998. A protein conjugation system essential for autophagy. *Nature* 395: 395 - 398.

38. Ichimura, Y., T. Kirisako, T. Takao, Y. Satomi, Y. Shimonishi, N. Ishihara, N. Mizushima, I. Tanida, E. Kominami, M. Ohsumi, T. Noda, and Y. Ohsumi. 2000. A ubiquitin-like system mediates protein lipidation. *Nature* 408: 488-492.

39. Ichimura, Y., Y. Imamura, K. Emoto, M. Umeda, T. Noda, and Y. Ohsumi. 2004. In vivo and in vitro reconstitution of Atg8 conjugation essential for autophagy. *J Biol Chem* 279: 40584-40592.

40. Yang, Z., and D. J. Klionsky. 2009. An overview of the molecular mechanism of autophagy. *Curr Top Microbiol Immunol* 335: 1-32.

41. Schmid, D., and C. Munz. 2007. Innate and adaptive immunity through autophagy. *Immunity* 27: 11-21.

42. Bjorkoy, G., T. Lamark, A. Brech, H. Outzen, M. Perander, A. Overvatn, H. Stenmark, and T. Johansen. 2005. p62/SQSTM1 forms protein aggregates degraded by autophagy and has a protective effect on huntingtin-induced cell death. *J Cell Biol* 171: 603-614.

43. Metcalf, D., and A. M. Isaacs. 2010. The role of ESCRT proteins in fusion events involving lysosomes, endosomes and autophagosomes. *Biochem Soc Trans* 38: 1469-1473.

44. Chua, C. E., B. Q. Gan, and B. L. Tang. 2011. Involvement of members of the Rab family and related small GTPases in autophagosome formation and maturation. *Cell Mol Life Sci* 68: 3349-3358.

45. Jager, S., C. Bucci, I. Tanida, T. Ueno, E. Kominami, P. Saftig, and E. L. Eskelinen. 2004. Role for Rab7 in maturation of late autophagic vacuoles. *J Cell Sci* 117: 4837-4848.

46. Komatsu, M., S. Waguri, T. Ueno, J. Iwata, S. Murata, I. Tanida, J. Ezaki, N. Mizushima, Y. Ohsumi, Y. Uchiyama, E. Kominami, K. Tanaka, and T. Chiba.

2005. Impairment of starvation-induced and constitutive autophagy in Atg7-deficient mice. *J Cell Biol* 169: 425-434.

47. Hara, T., K. Nakamura, M. Matsui, A. Yamamoto, Y. Nakahara, R. Suzuki-Migishima, M. Yokoyama, K. Mishima, I. Saito, H. Okano, and N. Mizushima. 2006. Suppression of basal autophagy in neural cells causes neurodegenerative disease in mice. *Nature* 441: 885-889.
48. Youle, R. J., and D. P. Narendra. 2011. Mechanisms of mitophagy. *Nat Rev Mol Cell Biol* 12: 9-14.
49. Manjithaya, R., T. Y. Nazarko, J. C. Farre, and S. Subramani. 2010. Molecular mechanism and physiological role of pexophagy. *FEBS Lett* 584: 1367-1373.
50. Krick, R., Y. Muehe, T. Prick, S. Bremer, P. Schlotterhose, E. L. Eskelinen, J. Millen, D. S. Goldfarb, and M. Thumm. 2008. Piecemeal microautophagy of the nucleus requires the core macroautophagy genes. *Mol Biol Cell* 19: 4492-4505.
51. Cebollero, E., F. Reggiori, and C. Kraft. 2012. Reticulophagy and ribophagy: regulated degradation of protein production factories. *International journal of cell biology* 2012: 182834.
52. Bernales, S., S. Schuck, and P. Walter. 2007. ER-phagy: selective autophagy of the endoplasmic reticulum. *Autophagy* 3: 285-287.
53. Levine, B. 2007. Cell biology: autophagy and cancer. *Nature* 446: 745-747.
54. Mortensen, M., D. J. Ferguson, M. Edelmann, B. Kessler, K. J. Morten, M. Komatsu, and A. K. Simon. 2010. Loss of autophagy in erythroid cells leads to defective removal of mitochondria and severe anemia in vivo. *Proc Natl Acad Sci U S A* 107: 832-837.
55. Pua, H. H., J. Guo, M. Komatsu, and Y. W. He. 2009. Autophagy is essential for mitochondrial clearance in mature T lymphocytes. *J Immunol* 182: 4046-4055.
56. Mizushima, N. 2007. Autophagy: process and function. *Genes Dev* 21: 2861-2873.
57. Mortensen, M., E. J. Soilleux, G. Djordjevic, R. Tripp, M. Lutteropp, E. Sadighi-Akha, A. J. Stranks, J. Glanville, S. Knight, W. J. SE, K. R. Kranc, and A. K. Simon. 2011. The autophagy protein Atg7 is essential for hematopoietic stem cell maintenance. *J Exp Med* 208: 455 - 467.
58. Xu, D., N. Suenaga, M. J. Edelmann, R. Fridman, R. J. Muschel, and B. M. Kessler. 2008. Novel MMP-9 substrates in cancer cells revealed by a label-free quantitative proteomics approach. *Mol Cell Proteomics* 7: 2215-2228.
59. Classen, A., J. Lloberas, and A. Celada. 2009. Macrophage activation: classical versus alternative. *Methods Mol Biol* 531: 29-43.
60. Shi, C. S., and J. H. Kehrl. 2010. TRAF6 and A20 regulate lysine 63-linked ubiquitination of Beclin-1 to control TLR4-induced autophagy. *Sci Signal* 3: ra42.
61. Delgado, M. A., and V. Deretic. 2009. Toll-like receptors in control of immunological autophagy. *Cell Death Differ* 16: 976-983.
62. Travassos, L. H., L. A. Carneiro, M. Ramjeet, S. Hussey, Y. G. Kim, J. G. Magalhaes, L. Yuan, F. Soares, E. Chea, L. Le Bourhis, I. G. Boneca, A. Allaoui, N. L. Jones, G. Nunez, S. E. Girardin, and D. J. Philpott. 2010. Nod1 and Nod2 direct autophagy by recruiting ATG16L1 to the plasma membrane at the site of bacterial entry. *Nat Immunol* 11: 55-62.

63. Lei, Y., H. Wen, Y. Yu, D. J. Taxman, L. Zhang, D. G. Widman, K. V. Swanson, K. W. Wen, B. Damania, C. B. Moore, P. M. Giguere, D. P. Siderovski, J. Hiscott, B. Razani, C. F. Semenkovich, X. Chen, and J. P. Ting. 2012. The mitochondrial proteins NLRX1 and TUFM form a complex that regulates type I interferon and autophagy. *Immunity* 36: 933-946.

64. McFarlane, S., J. Aitken, J. S. Sutherland, M. J. Nicholl, V. G. Preston, and C. M. Preston. 2011. Early induction of autophagy in human fibroblasts after infection with human cytomegalovirus or herpes simplex virus 1. *J Virol* 85: 4212-4221.

65. Scherz-Shouval, R., E. Shvets, E. Fass, H. Shorer, L. Gil, and Z. Elazar. 2007. Reactive oxygen species are essential for autophagy and specifically regulate the activity of Atg4. *Embo J* 26: 1749-1760.

66. Yang, C. S., J. S. Lee, M. Rodgers, C. K. Min, J. Y. Lee, H. J. Kim, K. H. Lee, C. J. Kim, B. Oh, E. Zandi, Z. Yue, I. Kramnik, C. Liang, and J. U. Jung. 2012. Autophagy protein Rubicon mediates phagocytic NADPH oxidase activation in response to microbial infection or TLR stimulation. *Cell Host Microbe* 11: 264-276.

67. Sarkar, S., V. I. Korolchuk, M. Renna, S. Imarisio, A. Fleming, A. Williams, M. Garcia-Arencibia, C. Rose, S. Luo, B. R. Underwood, G. Kroemer, C. J. O'Kane, and D. C. Rubinsztein. 2011. Complex inhibitory effects of nitric oxide on autophagy. *Mol Cell* 43: 19-32.

68. Zalckvar, E., H. Berissi, L. Mizrachy, Y. Idelchuk, I. Koren, M. Eisenstein, H. Sabanay, R. Pinkas-Kramarski, and A. Kimchi. 2009. DAP-kinase-mediated phosphorylation on the BH3 domain of beclin 1 promotes dissociation of beclin 1 from Bcl-XL and induction of autophagy. *EMBO Rep* 10: 285-292.

69. Mostowy, S., V. Sancho-Shimizu, M. A. Hamon, R. Simeone, R. Brosch, T. Johansen, and P. Cossart. 2011. p62 and NDP52 proteins target intracytosolic Shigella and Listeria to different autophagy pathways. *J Biol Chem* 286: 26987-26995.

70. Harris, J., S. A. De Haro, S. S. Master, J. Keane, E. A. Roberts, M. Delgado, and V. Deretic. 2007. T helper 2 cytokines inhibit autophagic control of intracellular Mycobacterium tuberculosis. *Immunity* 27: 505-517.

71. Van Grol, J., C. Subauste, R. M. Andrade, K. Fujinaga, J. Nelson, and C. S. Subauste. 2010. HIV-1 inhibits autophagy in bystander macrophage/monocytic cells through Src-Akt and STAT3. *PLoS ONE* 5: e11733.

72. Pua, H. H., I. Dzhagalov, M. Chuck, N. Mizushima, and Y. W. He. 2007. A critical role for the autophagy gene Atg5 in T cell survival and proliferation. *J Exp Med* 204: 25-31.

73. Wang, X., Y. Gao, J. Tan, K. Devadas, V. Ragupathy, K. Takeda, J. Zhao, and I. Hewlett. 2012. HIV-1 and HIV-2 infections induce autophagy in Jurkat and CD4+ T cells. *Cell Signal* 24: 1414-1419.

74. Hubbard, V. M., R. Valdor, B. Patel, R. Singh, A. M. Cuervo, and F. Macian. 2010. Macroautophagy regulates energy metabolism during effector T cell activation. *J Immunol* 185: 7349-7357.

75. Nedjic, J., M. Aichinger, J. Emmerich, N. Mizushima, and L. Klein. 2008. Autophagy in thymic epithelium shapes the T-cell repertoire and is essential for tolerance. *Nature* 455: 396-400.

76. Kasai, M., I. Tanida, T. Ueno, E. Kominami, S. Seki, T. Ikeda, and T. Mizuochi. 2009. Autophagic Compartments Gain Access to the MHC Class II Compartments in Thymic Epithelium. *The Journal of Immunology* 183: 7278-7285.

77. Miller, B. C., Z. Zhao, L. M. Stephenson, K. Cadwell, H. H. Pua, H. K. Lee, N. N. Mizushima, A. Iwasaki, Y. W. He, W. Swat, and H. W. t. Virgin. 2008. The autophagy gene ATG5 plays an essential role in B lymphocyte development. *Autophagy* 4: 309-314.

78. Pengo, N., M. Scolari, L. Oliva, E. Milan, F. Mainoldi, A. Raimondi, C. Fagioli, A. Merlini, E. Mariani, E. Pasqualetto, U. Orfanelli, M. Ponzoni, R. Sitia, S. Casola, and S. Cenci. 2013. Plasma cells require autophagy for sustainable immunoglobulin production. *Nat Immunol* 14: 298-305.

79. Lu, B., E. Capan, and C. Li. 2007. Autophagy induction and autophagic cell death in effector T cells. *Autophagy* 3: 158-159.

80. Watanabe, K., S. Ichinose, K. Hayashizaki, and T. Tsubata. 2008. Induction of autophagy by B cell antigen receptor stimulation and its inhibition by costimulation. *Biochemical and Biophysical Research Communications* 374: 274 - 281.

81. Xu, Y., C. Jagannath, X. D. Liu, A. Sharafkhaneh, K. E. Kolodziejska, and N. T. Eissa. 2007. Toll-like receptor 4 is a sensor for autophagy associated with innate immunity. *Immunity* 27: 135-144.

82. Shi, C. S., and J. H. Kehrl. 2008. MyD88 and Trif target Beclin 1 to trigger autophagy in macrophages. *J Biol Chem* 283: 33175-33182.

83. Lee, H. K., J. M. Lund, B. Ramanathan, N. Mizushima, and A. Iwasaki. 2007. Autophagy-dependent viral recognition by plasmacytoid dendritic cells. *Science* 315: 1398-1401.

84. Yoshikawa, Y., M. Ogawa, T. Hain, M. Yoshida, M. Fukumatsu, M. Kim, H. Mimuro, I. Nakagawa, T. Yanagawa, T. Ishii, A. Kakizuka, E. Sztul, T. Chakraborty, and C. Sasakawa. 2009. Listeria monocytogenes ActA-mediated escape from autophagic recognition. *Nat Cell Biol* 11: 1233-1240.

85. Rich, K. A., C. Burkett, and P. Webster. 2003. Cytoplasmic bacteria can be targets for autophagy. *Cell Microbiol* 5: 455-468.

86. Nakagawa, I., A. Amano, N. Mizushima, A. Yamamoto, H. Yamaguchi, T. Kamimoto, A. Nara, J. Funao, M. Nakata, K. Tsuda, S. Hamada, and T. Yoshimori. 2004. Autophagy defends cells against invading group A Streptococcus. *Science* 306: 1037-1040.

87. Gutierrez, M. G., S. S. Master, S. B. Singh, G. A. Taylor, M. I. Colombo, and V. Deretic. 2004. Autophagy is a defense mechanism inhibiting BCG and Mycobacterium tuberculosis survival in infected macrophages. *Cell* 119: 753-766.

88. Dorn, B. R., W. A. Dunn, Jr., and A. Progulske-Fox. 2002. Bacterial interactions with the autophagic pathway. *Cell Microbiol* 4: 1-10.

89. Al-Younes, H. M., V. Brinkmann, and T. F. Meyer. 2004. Interaction of Chlamydia trachomatis serovar L2 with the host autophagic pathway. *Infect Immun* 72: 4751-4762.

90. Amer, A. O., and M. S. Swanson. 2005. Autophagy is an immediate macrophage response to Legionella pneumophila. *Cell Microbiol* 7: 765-778.

91. Jacquel, A., S. Obba, L. Boyer, M. Dufies, G. Robert, P. Gounon, E. Lemichez, F. Luciano, E. Solary, and P. Auberger. 2012. Autophagy is required for CSF-1-

induced macrophagic differentiation and acquisition of phagocytic functions. *Blood* 119: 4527-4531.

92. Sanjuan, M. A., C. P. Dillon, S. W. G. Tait, S. Moshiach, F. Dorsey, S. Connell, M. Komatsu, K. Tanaka, J. L. Cleveland, S. Withoff, and D. R. Green. 2007. Toll-like receptor signalling in macrophages links the autophagy pathway to phagocytosis. *Nature* 450: 1253 - 1257.
93. Lima, J. G., C. de Freitas Vinhas, I. N. Gomes, C. M. Azevedo, R. R. Dos Santos, M. A. Vannier-Santos, and P. S. Veras. 2011. Phagocytosis is inhibited by autophagic induction in murine macrophages. *Biochem Biophys Res Commun* 405: 604-609.
94. Bonilla, D. L., A. Bhattacharya, Y. Sha, Y. Xu, Q. Xiang, A. Kan, C. Jagannath, M. Komatsu, and N. T. Eissa. 2013. Autophagy Regulates Phagocytosis by Modulating the Expression of Scavenger Receptors. *Immunity*.
95. Cadwell, K., and J. A. Philips. 2013. Autophagy meets phagocytosis. *Immunity* 39: 425-427.
96. Remijsen, Q., T. W. Kuijpers, E. Wirawan, S. Lippens, P. Vandenabeele, and T. Vanden Berghe. 2011. Dying for a cause: NETosis, mechanisms behind an antimicrobial cell death modality. *Cell Death Differ* 18: 581-588.
97. Remijsen, Q., T. Vanden Berghe, E. Wirawan, B. Asselbergh, E. Parthoens, R. De Rycke, S. Noppen, M. Delforge, J. Willems, and P. Vandenabeele. 2011. Neutrophil extracellular trap cell death requires both autophagy and superoxide generation. *Cell Res* 21: 290-304.
98. Ushio, H., T. Ueno, Y. Kojima, M. Komatsu, S. Tanaka, A. Yamamoto, Y. Ichimura, J. Ezaki, K. Nishida, S. Komazawa-Sakon, F. Niyonsaba, T. Ishii, T. Yanagawa, E. Kominami, H. Ogawa, K. Okumura, and H. Nakano. 2011. Crucial role for autophagy in degranulation of mast cells. *J Allergy Clin Immunol*.
99. Nakano, H., and H. Ushio. 2011. An unexpected role for autophagy in degranulation of mast cells. *Autophagy* 7: 657-659.
100. Schmid, D., M. Pypaert, and C. Munz. 2007. Antigen-loading compartments for major histocompatibility complex class II molecules continuously receive input from autophagosomes. *Immunity* 26: 79-92.
101. Nimmerjahn, F., S. Milosevic, U. Behrends, E. M. Jaffee, D. M. Pardoll, G. W. Bornkamm, and J. Mautner. 2003. Major histocompatibility complex class II-restricted presentation of a cytosolic antigen by autophagy. *Eur J Immunol* 33: 1250-1259.
102. Li, B., Z. Lei, B. D. Lichty, D. Li, G. M. Zhang, Z. H. Feng, Y. Wan, and B. Huang. 2010. Autophagy facilitates major histocompatibility complex class I expression induced by IFN-gamma in B16 melanoma cells. *Cancer Immunol Immunother* 59: 313-321.
103. English, L., M. Chemali, J. Duron, C. Rondeau, A. Laplante, D. Gingras, D. Alexander, D. Leib, C. Norbury, R. Lippe, and M. Desjardins. 2009. Autophagy enhances the presentation of endogenous viral antigens on MHC class I molecules during HSV-1 infection. *Nat Immunol* 10: 480-487.
104. Jagannath, C., D. R. Lindsey, S. Dhandayuthapani, Y. Xu, R. L. Hunter, Jr., and N. T. Eissa. 2009. Autophagy enhances the efficacy of BCG vaccine by increasing peptide presentation in mouse dendritic cells. *Nat Med* 15: 267-276.

105. Culshaw, S., O. R. Millington, J. M. Brewer, and I. B. McInnes. 2008. Murine neutrophils present Class II restricted antigen. *Immunol Lett* 118: 49-54.

106. Cooney, R., J. Baker, O. Brain, B. Danis, T. Pichulik, P. Allan, D. J. Ferguson, B. J. Campbell, D. Jewell, and A. Simmons. 2010. NOD2 stimulation induces autophagy in dendritic cells influencing bacterial handling and antigen presentation. *Nat Med* 16: 90-97.

107. Deretic, V., T. Saitoh, and S. Akira. 2013. Autophagy in infection, inflammation and immunity. *Nat Rev Immunol* 13: 722-737.

108. Elmore, S. 2007. Apoptosis: a review of programmed cell death. *Toxicol Pathol* 35: 495-516.

109. McQuade, T., Y. Cho, and F. K. Chan. 2013. Positive and Negative Phosphorylation Regulates RIP1 and RIP3-Induced Programmed Necrosis. *Biochem J*.

110. Galluzzi, L., T. Vanden Berghe, N. Vanlangenakker, S. Buettner, T. Eisenberg, P. Vandenabeele, F. Madeo, and G. Kroemer. 2011. Programmed necrosis from molecules to health and disease. *Int Rev Cell Mol Biol* 289: 1-35.

111. Kroemer, G., and B. Levine. 2008. Autophagic cell death: the story of a misnomer. *Nat Rev Mol Cell Biol* 9: 1004-1010.

112. Luo, S., and D. C. Rubinsztein. 2007. Atg5 and Bcl-2 provide novel insights into the interplay between apoptosis and autophagy. *Cell Death Differ* 14: 1247-1250.

113. Abedin, M. J., D. Wang, M. A. McDonnell, U. Lehmann, and A. Kelekar. 2007. Autophagy delays apoptotic death in breast cancer cells following DNA damage. *Cell Death and Differentiation* 14: 500 -510.

114. Kuma, A., M. Hatano, M. Matsui, A. Yamamoto, H. Nakaya, T. Yoshimori, Y. Ohsumi, T. Tokuhisa, and N. Mizushima. 2004. The role of autophagy during the early neonatal starvation period. *Nature* 432: 1032-1036.

115. Colell, A., J. E. Ricci, S. Tait, S. Milasta, U. Maurer, L. Bouchier-Hayes, P. Fitzgerald, A. Guio-Carrion, N. J. Waterhouse, C. W. Li, B. Mari, P. Barbry, D. D. Newmeyer, H. M. Beere, and D. R. Green. 2007. GAPDH and autophagy preserve survival after apoptotic cytochrome c release in the absence of caspase activation. *Cell* 129: 983-997.

116. Kang, C., and L. Avery. 2008. To be or not to be, the level of autophagy is the question: dual roles of autophagy in the survival response to starvation. *Autophagy* 4: 82-84.

117. Verderame, M., D. Alcorta, M. Egnor, K. Smith, and R. Pollack. 1980. Cytoskeletal F-actin patterns quantitated with fluorescein isothiocyanate-phalloidin in normal and transformed cells. *Proc Natl Acad Sci U S A* 77: 6624-6628.

118. Manzanero, S. 2012. Generation of mouse bone marrow-derived macrophages. *Methods Mol Biol* 844: 177-181.

119. Austyn, J. M., and S. Gordon. 1981. F4/80, a monoclonal antibody directed specifically against the mouse macrophage. *Eur J Immunol* 11: 805-815.

120. Zeger, D. L., N. Osman, M. Hennings, I. F. McKenzie, D. W. Sears, and P. M. Hogarth. 1990. Mouse macrophage beta subunit (CD11b) cDNA for the CR3 complement receptor/Mac-1 antigen. *Immunogenetics* 31: 191-197.

121. Daigneault, M., J. A. Preston, H. M. Marriott, M. K. Whyte, and D. H. Dockrell. 2010. The identification of markers of macrophage differentiation in PMA-stimulated THP-1 cells and monocyte-derived macrophages. *PLoS ONE* 5: e8668.

122. Ouimet, M., V. Franklin, E. Mak, X. Liao, I. Tabas, and Y. L. Marcel. 2011. Autophagy regulates cholesterol efflux from macrophage foam cells via lysosomal acid lipase. *Cell Metab* 13: 655-667.

123. Ahn, C. H., E. G. Jeong, J. W. Lee, M. S. Kim, S. H. Kim, S. S. Kim, N. J. Yoo, and S. H. Lee. 2007. Expression of beclin-1, an autophagy-related protein, in gastric and colorectal cancers. *Apmis* 115: 1344-1349.

124. Komatsu, M., S. Waguri, T. Chiba, S. Murata, J. Iwata, I. Tanida, T. Ueno, M. Koike, Y. Uchiyama, E. Kominami, and K. Tanaka. 2006. Loss of autophagy in the central nervous system causes neurodegeneration in mice. *Nature* 441: 880-884.

125. Ziegler, H. K. 1984. The processing and presentation of Listeria monocytogenes antigens by macrophages. *Clin Invest Med* 7: 269-272.

126. Palmowski, M. J., U. Gileadi, M. Salio, A. Gallimore, M. Millrain, E. James, C. Addey, D. Scott, J. Dyson, E. Simpson, and V. Cerundolo. 2006. Role of immunoproteasomes in cross-presentation. *J Immunol* 177: 983-990.

127. Luheshi, N. M., J. A. Giles, G. Lopez-Castejon, and D. Brough. 2012. Sphingosine regulates the NLRP3-inflammasome and IL-1beta release from macrophages. *Eur J Immunol* 42: 716-725.

128. Park, Y. M., J. A. Drazba, A. Vasanji, T. Egelhoff, M. Febbraio, and R. L. Silverstein. 2012. Oxidized LDL/CD36 interaction induces loss of cell polarity and inhibits macrophage locomotion. *Mol Biol Cell* 23: 3057-3068.

129. Ishihara, D., A. Dovas, H. Park, B. M. Isaac, and D. Cox. 2012. The chemotactic defect in wiskott-Aldrich syndrome macrophages is due to the reduced persistence of directional protrusions. *PLoS ONE* 7: e30033.

130. Patel, P. C., and R. E. Harrison. 2008. Membrane ruffles capture C3bi-opsonized particles in activated macrophages. *Mol Biol Cell* 19: 4628-4639.

131. DeMali, K. A., and K. Burridge. 2003. Coupling membrane protrusion and cell adhesion. *J Cell Sci* 116: 2389-2397.

132. Maloyan, A., and J. Robbins. 2010. Autophagy in desmin-related cardiomyopathy: Thoughts at the halfway point. *Autophagy* 6.

133. Benes, P., V. Maceckova, Z. Zdrahal, H. Konecna, E. Zahradnickova, J. Muzik, and J. Smarda. 2006. Role of vimentin in regulation of monocyte/macrophage differentiation. *Differentiation* 74: 265-276.

134. Kidd, M. E., D. K. Shumaker, and K. M. Ridge. 2013. The Role of Vimentin Intermediate Filaments in the Progression of Lung Cancer. *Am J Respir Cell Mol Biol*.

135. Nomura, H., K. Uzawa, T. Ishigami, Y. Kouzu, H. Koike, K. Ogawara, M. Siiba, H. Bukawa, H. Yokoe, H. Kubosawa, and H. Tanzawa. 2008. Clinical significance of gelsolin-like actin-capping protein expression in oral carcinogenesis: an immunohistochemical study of premalignant and malignant lesions of the oral cavity. *BMC Cancer* 8: 39.

136. Zadeh, A. D., and H. Keller. 2003. Chemotactically directed redistribution of alpha-actinin precedes morphological polarization and reversal of polarity in human polymorphonuclear leucocytes (PMNs). *Eur J Cell Biol* 82: 93-96.

137. Suraneni, P., B. Rubinstein, J. R. Unruh, M. Durnin, D. Hanein, and R. Li. 2012. The Arp2/3 complex is required for lamellipodia extension and directional fibroblast cell migration. *J Cell Biol* 197: 239-251.

138. Wu, C., S. B. Asokan, M. E. Berginski, E. M. Haynes, N. E. Sharpless, J. D. Griffith, S. M. Gomez, and J. E. Bear. 2012. Arp2/3 is critical for lamellipodia and response to extracellular matrix cues but is dispensable for chemotaxis. *Cell* 148: 973-987.

139. Monastyrska, I., C. He, J. Geng, A. D. Hoppe, Z. Li, and D. J. Klionsky. 2008. Arp2 links autophagic machinery with the actin cytoskeleton. *Mol Biol Cell* 19: 1962-1975.

140. Xia, P., S. Wang, Y. Du, Z. Zhao, L. Shi, L. Sun, G. Huang, B. Ye, C. Li, Z. Dai, N. Hou, X. Cheng, Q. Sun, L. Li, X. Yang, and Z. Fan. 2013. WASH inhibits autophagy through suppression of Beclin 1 ubiquitination. *Embo J*.

141. Kadandale, P., J. D. Stender, C. K. Glass, and A. A. Kiger. 2010. Conserved role for autophagy in Rho1-mediated cortical remodeling and blood cell recruitment. *Proc Natl Acad Sci U S A* 107: 10502-10507.

142. Razani, B., C. Feng, T. Coleman, R. Emanuel, H. Wen, S. Hwang, J. P. Ting, H. W. Virgin, M. B. Kastan, and C. F. Semenkovich. 2012. Autophagy links inflammasomes to atherosclerotic progression. *Cell Metab* 15: 534-544.

143. Kobayashi, S., T. Kojidani, H. Osakada, A. Yamamoto, T. Yoshimori, Y. Hiraoka, and T. Haraguchi. 2010. Artificial induction of autophagy around polystyrene beads in nonphagocytic cells. *Autophagy* 6: 36-45.

144. Dutta, D., and J. G. Donaldson. 2012. Search for inhibitors of endocytosis: Intended specificity and unintended consequences. *Cell Logist* 2: 203-208.

145. Lagana, A., J. Vadnais, P. U. Le, T. N. Nguyen, R. Laprade, I. R. Nabi, and J. Noel. 2000. Regulation of the formation of tumor cell pseudopodia by the Na(+)/H(+) exchanger NHE1. *J Cell Sci* 113 (Pt 20): 3649-3662.

146. Nishida, Y., S. Arakawa, K. Fujitani, H. Yamaguchi, T. Mizuta, T. Kanaseki, M. Komatsu, K. Otsu, Y. Tsujimoto, and S. Shimizu. 2009. Discovery of Atg5/Atg7-independent alternative macroautophagy. *Nature* 461: 654 - 655.

147. Mortensen, M. 2009. The Role of Autophagy in the Haematopoietic System *in vivo*. In *MRC Human Immunology Unit, Nuffield Department of Clinical Medicine*. University of Oxford, Oxford. 225.

148. Willinger, T., and R. A. Flavell. 2012. Canonical autophagy dependent on the class III phosphoinositide-3 kinase Vps34 is required for naive T-cell homeostasis. *Proc Natl Acad Sci U S A* 109: 8670-8675.

149. Sutton, J. S., and L. Weiss. 1966. Transformation of monocytes in tissue culture into macrophages, epithelioid cells, and multinucleated giant cells. An electron microscope study. *J Cell Biol* 28: 303-332.

150. Forman, H. J., and M. Torres. 2001. Redox signaling in macrophages. *Mol Aspects Med* 22: 189-216.

151. West, A. P., I. E. Brodsky, C. Rahner, D. K. Woo, H. Erdjument-Bromage, P. Tempst, M. C. Walsh, Y. Choi, G. S. Shadel, and S. Ghosh. 2011. TLR signalling augments macrophage bactericidal activity through mitochondrial ROS. *Nature* 472: 476-480.

152. Brune, B., N. Dehne, N. Grossmann, M. Jung, D. Namgaladze, T. Schmid, A. von Knethen, and A. Weigert. 2013. Redox control of inflammation in macrophages. *Antioxid Redox Signal* 19: 595-637.

153. Bryan, H. K., A. Olayanju, C. E. Goldring, and B. K. Park. 2013. The Nrf2 cell defence pathway: Keap1-dependent and -independent mechanisms of regulation. *Biochem Pharmacol* 85: 705-717.

154. Karna, P., S. Zughaier, V. Pannu, R. Simmons, S. Narayan, and R. Aneja. 2010. Induction of reactive oxygen species-mediated autophagy by a novel microtubule-modulating agent. *J Biol Chem* 285: 18737-18748.

155. Moore, M. N. 2008. Autophagy as a second level protective process in conferring resistance to environmentally-induced oxidative stress. *Autophagy* 4: 254-256.

156. Bulua, A. C., A. Simon, R. Maddipati, M. Pelletier, H. Park, K. Y. Kim, M. N. Sack, D. L. Kastner, and R. M. Siegel. 2011. Mitochondrial reactive oxygen species promote production of proinflammatory cytokines and are elevated in TNFR1-associated periodic syndrome (TRAPS). *J Exp Med* 208: 519-533.

157. Oczypok, E. A., T. D. Oury, and C. T. Chu. 2013. It's a cell-eat-cell world: autophagy and phagocytosis. *Am J Pathol* 182: 612-622.

158. Miyahara, K., H. Murayama, H. Wakabayashi, T. Kurihara, K. Hashimoto, K. Satoh, N. Motohashi, and H. Sakagami. 2008. Inhibition of LPS-stimulated NO production in mouse macrophage-like cells by benzocycloheptoxazines. *Anticancer Res* 28: 2657-2662.

159. Xie, Q. W., H. J. Cho, J. Calaycay, R. A. Mumford, K. M. Swiderek, T. D. Lee, A. Ding, T. Troso, and C. Nathan. 1992. Cloning and characterization of inducible nitric oxide synthase from mouse macrophages. *Science* 256: 225-228.

160. Grisham, M. B., D. Jourd'Heuil, and D. A. Wink. 1999. Nitric oxide. I. Physiological chemistry of nitric oxide and its metabolites:implications in inflammation. *Am J Physiol* 276: G315-321.

161. Domitrovic, R., O. Cvijanovic, E. Pernjak-Pugel, M. Skoda, L. Mikelic, and Z. Crncevic-Orlic. 2013. Berberine exerts nephroprotective effect against cisplatin-induced kidney damage through inhibition of oxidative/nitrosative stress, inflammation, autophagy and apoptosis. *Food Chem Toxicol*.

162. Chen, Y., M. B. Azad, and S. B. Gibson. 2009. Superoxide is the major reactive oxygen species regulating autophagy. *Cell Death Differ* 16: 1040-1052.

163. Zhang, L., J. S. Cardinal, R. Bahar, J. Evankovich, H. Huang, G. Nace, T. R. Billiar, M. R. Rosengart, P. Pan, and A. Tsung. 2012. Interferon regulatory factor-1 regulates the autophagic response in LPS-stimulated macrophages through nitric oxide. *Mol Med* 18: 201-208.

164. Millrain, M., D. Scott, C. Addey, H. Dewchand, P. Ellis, I. Ehrmann, M. Mitchell, P. Burgoyne, E. Simpson, and J. Dyson. 2005. Identification of the Immunodominant HY H2-D k Epitope and Evaluation of the Role of Direct and Indirect Antigen Presentation in HY Responses. *The Journal of Immunology* 175: 7209-7217.

165. Chemali, M., K. Radtke, M. Desjardins, and L. English. 2011. Alternative pathways for MHC class I presentation: a new function for autophagy. *Cell Mol Life Sci*.

166. Li, Y., L.-X. Wang, G. Yang, F. Hao, W. J. Urba, and H.-M. Hu. 2008. Efficient cross-presentation depends on autophagy in tumor cells. *Cancer Research* 68: 6889-6895.

167. Strawbridge, A. B., and J. S. Blum. 2007. Autophagy in MHC class II antigen processing. *Curr Opin Immunol* 19: 87-92.

168. Sakai, T., E. Shuto, T. Taki, H. Imamura, M. Kioka, A. Nakamoto, S. Mizoguchi, S. Amano, Y. Kawano, M. Nakamoto, R. Tsutumi, and T. Hosaka. 2012. Decreased expression of MHC class II and cathepsin E in dendritic cells might contribute to impaired induction of antigen-specific T cell response in NC/Nga mice. *J Med Invest* 59: 95-101.

169. Clausen, B. E., C. Burkhardt, W. Reith, R. Renkawitz, and I. Förster. 1999. Conditional Gene Targeting in Macrophages and Granulocytes Using LysMcre mice. *Transgenic Research* 8: 265 - 277.

170. De Matteis, M. A., and J. S. Morrow. 2000. Spectrin tethers and mesh in the biosynthetic pathway. *J Cell Sci* 113 (Pt 13): 2331-2343.

171. Ang, S. F., and H. Folsch. 2012. The role of secretory and endocytic pathways in the maintenance of cell polarity. *Essays Biochem* 53: 29-39.

172. Yewdell, J. W., E. Reits, and J. Neefjes. 2003. Making sense of mass destruction: quantitating MHC class I antigen presentation. *Nat Rev Immunol* 3: 952-961.

173. Berger, A. C., and P. A. Roche. 2009. MHC class II transport at a glance. *J Cell Sci* 122: 1-4.

174. Rothman, J. E. 1994. Mechanisms of intracellular protein transport. *Nature* 372: 55-63.

175. Hiltbold, E. M., and P. A. Roche. 2002. Trafficking of MHC class II molecules in the late secretory pathway. *Curr Opin Immunol* 14: 30-35.

176. Murk, J. L., W. Stoorvogel, M. J. Kleijmeer, and H. J. Geuze. 2002. The plasticity of multivesicular bodies and the regulation of antigen presentation. *Semin Cell Dev Biol* 13: 303-311.

177. Wubbolts, R., M. Fernandez-Borja, L. Oomen, D. Verwoerd, H. Janssen, J. Calafat, A. Tulp, S. Dusseljee, and J. Neefjes. 1996. Direct vesicular transport of MHC class II molecules from lysosomal structures to the cell surface. *J Cell Biol* 135: 611-622.

178. Kleijmeer, M., G. Ramm, D. Schuurhuis, J. Griffith, M. Rescigno, P. Ricciardi-Castagnoli, A. Y. Rudensky, F. Ossendorp, C. J. Melief, W. Stoorvogel, and H. J. Geuze. 2001. Reorganization of multivesicular bodies regulates MHC class II antigen presentation by dendritic cells. *J Cell Biol* 155: 53-63.

179. 2007. Genome-wide association study of 14,000 cases of seven common diseases and 3,000 shared controls. *Nature* 447: 661-678.

180. Jostins, L., S. Ripke, R. K. Weersma, R. H. Duerr, D. P. McGovern, K. Y. Hui, J. C. Lee, L. P. Schumm, Y. Sharma, C. A. Anderson, J. Essers, M. Mitrovic, K. Ning, I. Cleynen, E. Theatre, S. L. Spain, S. Raychaudhuri, P. Goyette, Z. Wei, C. Abraham, J. P. Achkar, T. Ahmad, L. Amininejad, A. N. Ananthakrishnan, V. Andersen, J. M. Andrews, L. Baidoo, T. Balschun, P. A. Bampton, A. Bitton, G. Boucher, S. Brand, C. Buning, A. Cohain, S. Cichon, M. D'Amato, D. De Jong, K. L. Devaney, M. Dubinsky, C. Edwards, D. Ellinghaus, L. R. Ferguson, D. Franchimont, K. Fransen, R. Gearry, M. Georges, C. Gieger, J. Glas, T. Haritunians, A. Hart, C. Hawkey, M. Hedl, X. Hu, T. H. Karlsen, L. Kupcinskas, S. Kugathasan, A. Latiano, D. Laukens,

I. C. Lawrance, C. W. Lees, E. Louis, G. Mahy, J. Mansfield, A. R. Morgan, C. Mowat, W. Newman, O. Palmieri, C. Y. Ponsioen, U. Potocnik, N. J. Prescott, M. Regueiro, J. I. Rotter, R. K. Russell, J. D. Sanderson, M. Sans, J. Satsangi, S. Schreiber, L. A. Simms, J. Sventoraityte, S. R. Targan, K. D. Taylor, M. Tremelling, H. W. Verspaget, M. De Vos, C. Wijmenga, D. C. Wilson, J. Winkelmann, R. J. Xavier, S. Zeissig, B. Zhang, C. K. Zhang, H. Zhao, M. S. Silverberg, V. Annese, H. Hakonarson, S. R. Brant, G. Radford-Smith, C. G. Mathew, J. D. Rioux, E. E. Schadt, M. J. Daly, A. Franke, M. Parkes, S. Vermeire, J. C. Barrett, and J. H. Cho. 2012. Host-microbe interactions have shaped the genetic architecture of inflammatory bowel disease. *Nature* 491: 119-124.

181. Henckaerts, L., I. Cleynen, M. Brinar, J. M. John, K. Van Steen, P. Rutgeerts, and S. Vermeire. 2011. Genetic variation in the autophagy gene ULK1 and risk of Crohn's disease. *Inflamm Bowel Dis* 17: 1392-1397.

182. Ramos, P. S., L. A. Criswell, K. L. Moser, M. E. Comeau, A. H. Williams, N. M. Pajewski, S. A. Chung, R. R. Graham, R. Zidovetzki, J. A. Kelly, K. M. Kaufman, C. O. Jacob, T. J. Vyse, B. P. Tsao, R. P. Kimberly, P. M. Gaffney, M. E. Alarcon-Riquelme, J. B. Harley, and C. D. Langefeld. 2011. A comprehensive analysis of shared loci between systemic lupus erythematosus (SLE) and sixteen autoimmune diseases reveals limited genetic overlap. *PLoS Genet* 7: e1002406.

183. Martin, L. J., J. Gupta, S. S. Jyothula, M. Butsch Kovacic, J. M. Biagini Myers, T. L. Patterson, M. B. Ericksen, H. He, A. M. Gibson, T. M. Baye, S. Amirisetty, A. M. Tsoras, Y. Sha, N. T. Eissa, and G. K. Hershey. 2012. Functional variant in the autophagy-related 5 gene promotor is associated with childhood asthma. *PLoS ONE* 7: e33454.

184. Raychaudhuri, S., B. P. Thomson, E. F. Remmers, S. Eyre, A. Hinks, C. Guiducci, J. J. Catanese, G. Xie, E. A. Stahl, R. Chen, L. Alfredsson, C. I. Amos, K. G. Ardlie, A. Barton, J. Bowes, N. P. Burtt, M. Chang, J. Coblyn, K. H. Costenbader, L. A. Criswell, J. B. Crusius, J. Cui, P. L. De Jager, B. Ding, P. Emery, E. Flynn, P. Harrison, L. J. Hocking, T. W. Huizinga, D. L. Kastner, X. Ke, F. A. Kurreeman, A. T. Lee, X. Liu, Y. Li, P. Martin, A. W. Morgan, L. Padyukov, D. M. Reid, M. Seielstad, M. F. Seldin, N. A. Shadick, S. Steer, P. P. Tak, W. Thomson, A. H. van der Helm-van Mil, I. E. van der Horst-Bruinsma, M. E. Weinblatt, A. G. Wilson, G. J. Wolbink, P. Wordsworth, D. Altshuler, E. W. Karlson, R. E. Toes, N. de Vries, A. B. Begovich, K. A. Siminovitch, J. Worthington, L. Klareskog, P. K. Gregersen, M. J. Daly, and R. M. Plenge. 2009. Genetic variants at CD28, PRDM1 and CD2/CD58 are associated with rheumatoid arthritis risk. *Nat Genet* 41: 1313-1318.

185. Schroder, K., and J. Tschopp. 2010. The inflammasomes. *Cell* 140: 821-832.

186. Saitoh, T., N. Fujita, M. H. Jang, S. Uematsu, B. G. Yang, T. Satoh, H. Omori, T. Noda, N. Yamamoto, M. Komatsu, K. Tanaka, T. Kawai, T. Tsujimura, O. Takeuchi, T. Yoshimori, and S. Akira. 2008. Loss of the autophagy protein Atg16L1 enhances endotoxin-induced IL-1beta production. *Nature* 456: 264-268.

187. Shi, C. S., K. Shenderov, N. N. Huang, J. Kabat, M. Abu-Asab, K. A. Fitzgerald, A. Sher, and J. H. Kehrl. 2012. Activation of autophagy by inflammatory signals limits IL-1beta production by targeting ubiquitinated inflammasomes for destruction. *Nat Immunol* 13: 255-263.

188. Crisan, T. O., T. S. Plantinga, F. L. van de Veerdonk, M. F. Farcas, M. Stoffels, B. J. Kullberg, J. W. van der Meer, L. A. Joosten, and M. G. Netea. 2011.

Inflammasome-independent modulation of cytokine response by autophagy in human cells. *PLoS ONE* 6: e18666.

189. Duran, A., J. F. Linares, A. S. Galvez, K. Wikenheiser, J. M. Flores, M. T. Diaz-Meco, and J. Moscat. 2008. The signaling adaptor p62 is an important NF-kappaB mediator in tumorigenesis. *Cancer Cell* 13: 343-354.

190. Komatsu, M., H. Kurokawa, S. Waguri, K. Taguchi, A. Kobayashi, Y. Ichimura, Y. S. Sou, I. Ueno, A. Sakamoto, K. I. Tong, M. Kim, Y. Nishito, S. Iemura, T. Natsume, T. Ueno, E. Kominami, H. Motohashi, K. Tanaka, and M. Yamamoto. 2010. The selective autophagy substrate p62 activates the stress responsive transcription factor Nrf2 through inactivation of Keap1. *Nat Cell Biol* 12: 213-223.

191. Chow, J. C., D. W. Young, D. T. Golenbock, W. J. Christ, and F. Gusovsky. 1999. Toll-like receptor-4 mediates lipopolysaccharide-induced signal transduction. *J Biol Chem* 274: 10689-10692.

192. Aladzsity, I., M. L. Toth, T. Sigmond, E. Szabo, B. Bicsak, J. Barna, A. Regos, L. Orosz, A. L. Kovacs, and T. Vellai. 2007. Autophagy genes unc-51 and bec-1 are required for normal cell size in Caenorhabditis elegans. *Genetics* 177: 655-660.

193. Jones, B. W., K. A. Heldwein, T. K. Means, J. J. Saukkonen, and M. J. Fenton. 2001. Differential roles of Toll-like receptors in the elicitation of proinflammatory responses by macrophages. *Ann Rheum Dis* 60 Suppl 3: iii6-12.

194. Stein, M., S. Keshav, N. Harris, and S. Gordon. 1992. Interleukin 4 potently enhances murine macrophage mannose receptor activity: a marker of alternative immunologic macrophage activation. *J Exp Med* 176: 287-292.

195. Ivaska, J., K. Vuoriluoto, T. Huovinen, I. Izawa, M. Inagaki, and P. J. Parker. 2005. PKCepsilon-mediated phosphorylation of vimentin controls integrin recycling and motility. *Embo J* 24: 3834-3845.

196. Stanasila, L., L. Abuin, D. Diviani, and S. Cotecchia. 2006. Ezrin directly interacts with the alpha1b-adrenergic receptor and plays a role in receptor recycling. *J Biol Chem* 281: 4354-4363.

197. MacNeil, A. J., and B. Pohajdak. 2009. Getting a GRASP on CASP: properties and role of the cytohesin-associated scaffolding protein in immunity. *Immunol Cell Biol* 87: 72-80.

198. Stenmark, H., and V. M. Olkkonen. 2001. The Rab GTPase family. *Genome Biol* 2: REVIEWS3007.

199. Zhuang, X., K. A. Adipietro, S. Datta, J. K. Northup, and K. Ray. 2010. Rab1 small GTP-binding protein regulates cell surface trafficking of the human calcium-sensing receptor. *Endocrinology* 151: 5114-5123.

200. BasuRay, S., S. Mukherjee, E. G. Romero, M. N. Seaman, and A. Wandinger-Ness. 2013. Rab7 mutants associated with Charcot-Marie-Tooth disease cause delayed growth factor receptor transport and altered endosomal and nuclear signaling. *J Biol Chem* 288: 1135-1149.

201. Reed, S. E., L. R. Hodgson, S. Song, M. T. May, E. E. Kelly, M. W. McCaffrey, C. C. Mastick, P. Verkade, and J. M. Tavare. 2013. A role for Rab14 in the endocytic trafficking of GLUT4 in 3T3-L1 adipocytes. *J Cell Sci* 126: 1931-1941.

202. Strisciuglio, C., M. Duijvestein, A. P. Verhaar, A. C. Vos, G. R. van den Brink, D. W. Hommes, and M. E. Wildenberg. 2013. Impaired autophagy leads to abnormal dendritic cell-epithelial cell interactions. *J Crohns Colitis* 7: 534-541.

203. Maurer, M., and E. von Stebut. 2004. Macrophage inflammatory protein-1. *Int J Biochem Cell Biol* 36: 1882-1886.

204. Baravalle, G., H. Park, M. McSweeney, M. Ohmura-Hoshino, Y. Matsuki, S. Ishido, and J. S. Shin. 2011. Ubiquitination of CD86 is a key mechanism in regulating antigen presentation by dendritic cells. *J Immunol* 187: 2966-2973.

205. Dahlen, E., G. Hedlund, and K. Dawe. 2000. Low CD86 expression in the nonobese diabetic mouse results in the impairment of both T cell activation and CTLA-4 up-regulation. *J Immunol* 164: 2444-2456.

206. Paludan, C., D. Schmid, M. Landhalter, M. Vockerodt, D. Kube, T. Tuschl, and C. Munz. 2005. Endogenous MHC Class II Processing of a Viral Nuclear Antigen After Autophagy. *Science* 307: 593 - 596.

207. Tsukamoto, H., K. Fukudome, S. Takao, N. Tsuneyoshi, S. Ohta, Y. Nagai, H. Ihara, K. Miyake, Y. Ikeda, and M. Kimoto. 2013. Reduced surface expression of TLR4 by a V254I point mutation accounts for the low lipopolysaccharide responder phenotype of BALB/c B cells. *J Immunol* 190: 195-204.

208. Hoshino, K., O. Takeuchi, T. Kawai, H. Sanjo, T. Ogawa, Y. Takeda, K. Takeda, and S. Akira. 1999. Cutting edge: Toll-like receptor 4 (TLR4)-deficient mice are hyporesponsive to lipopolysaccharide: evidence for TLR4 as the Lps gene product. *J Immunol* 162: 3749-3752.

209. Song, W., N. M. Wagle, T. Banh, C. C. Whiteford, E. Ulug, and S. K. Pierce. 1997. Wortmannin, a phosphatidylinositol 3-kinase inhibitor, blocks the assembly of peptide-MHC class II complexes. *Int Immunol* 9: 1709-1722.

210. Weichhart, T., G. Costantino, M. Poglitsch, M. Rosner, M. Zeyda, K. M. Stuhlmeier, T. Kolbe, T. M. Stulnig, W. H. Horl, M. Hengstschlager, M. Muller, and M. D. Saemann. 2008. The TSC-mTOR signaling pathway regulates the innate inflammatory response. *Immunity* 29: 565-577.

211. Romieu-Mourez, R., M. Francois, M. N. Boivin, J. Stagg, and J. Galipeau. 2007. Regulation of MHC class II expression and antigen processing in murine and human mesenchymal stromal cells by IFN-gamma, TGF-beta, and cell density. *J Immunol* 179: 1549-1558.

212. Monti, P., A. Mercalli, B. E. Leone, D. C. Valerio, P. Allavena, and L. Piemonti. 2003. Rapamycin impairs antigen uptake of human dendritic cells. *Transplantation* 75: 137-145.

213. Mosser, D. M., and J. P. Edwards. 2008. Exploring the full spectrum of macrophage activation. *Nat Rev Immunol* 8: 958-969.

214. Juhasz, G., J. H. Hill, Y. Yan, M. Sass, E. H. Baehrecke, J. M. Backer, and T. P. Neufeld. 2008. The class III PI(3)K Vps34 promotes autophagy and endocytosis but not TOR signaling in Drosophila. *J Cell Biol* 181: 655-666.

215. Shravage, B. V., J. H. Hill, C. M. Powers, L. Wu, and E. H. Baehrecke. 2013. Atg6 is required for multiple vesicle trafficking pathways and hematopoiesis in Drosophila. *Development*.

216. Rocha, N., and J. Neefjes. 2008. MHC class II molecules on the move for successful antigen presentation. *Embo J* 27: 1-5.

217. Fernandez-Borja, M., R. Wubbolts, J. Calafat, H. Janssen, N. Divecha, S. Dusseljee, and J. Neefjes. 1999. Multivesicular body morphogenesis requires phosphatidyl-inositol 3-kinase activity. *Curr Biol* 9: 55-58.

218. Brown, W. J., D. B. DeWald, S. D. Emr, H. Plutner, and W. E. Balch. 1995. Role for phosphatidylinositol 3-kinase in the sorting and transport of newly synthesized lysosomal enzymes in mammalian cells. *J Cell Biol* 130: 781-796.

219. Fader, C. M., D. Sanchez, M. Furlan, and M. I. Colombo. 2008. Induction of autophagy promotes fusion of multivesicular bodies with autophagic vacuoles in k562 cells. *Traffic* 9: 230-250.

220. Fader, C. M., and M. I. Colombo. 2009. Autophagy and multivesicular bodies: two closely related partners. *Cell Death Differ* 16: 70-78.

221. Kondylis, V., H. E. van Nispen Tot Pannerden, S. van Dijk, T. Ten Broeke, R. Wubbolts, W. J. Geerts, C. Seinen, T. Mutis, and H. F. Heijnen. 2013. Endosome-mediated autophagy: an unconventional MIIC-driven autophagic pathway operational in dendritic cells. *Autophagy* 9: 861-880.

222. Bento, C. F., C. Puri, K. Moreau, and D. C. Rubinsztein. 2013. The role of membrane-trafficking small GTPases in the regulation of autophagy. *J Cell Sci* 126: 1059-1069.

223. Popovic, D., M. Akutsu, I. Novak, J. W. Harper, C. Behrends, and I. Dikic. 2012. Rab GTPase-activating proteins in autophagy: regulation of endocytic and autophagy pathways by direct binding to human ATG8 modifiers. *Mol Cell Biol* 32: 1733-1744.

224. Ng, E. L., B. Q. Gan, F. Ng, and B. L. Tang. 2012. Rab GTPases regulating receptor trafficking at the late endosome-lysosome membranes. *Cell Biochem Funct* 30: 515-523.

225. Longatti, A., C. A. Lamb, M. Razi, S. Yoshimura, F. A. Barr, and S. A. Tooze. 2012. TBC1D14 regulates autophagosome formation via Rab11- and ULK1-positive recycling endosomes. *J Cell Biol* 197: 659-675.

226. Dupont, N., S. Jiang, M. Pilli, W. Ornatowski, D. Bhattacharya, and V. Deretic. 2011. Autophagy-based unconventional secretory pathway for extracellular delivery of IL-1beta. *Embo J* 30: 4701-4711.

227. Duran, J. M., C. Anjard, C. Stefan, W. F. Loomis, and V. Malhotra. 2010. Unconventional secretion of Acb1 is mediated by autophagosomes. *J Cell Biol* 188: 527-536.

228. Manjithaya, R., and S. Subramani. 2010. Autophagy: a broad role in unconventional protein secretion? *Cell*.

229. Gutierrez, M. G., D. B. Munafo, W. Beron, and M. I. Colombo. 2004. Rab7 is required for the normal progression of the autophagic pathway in mammalian cells. *J Cell Sci* 117: 2687-2697.

230. Eskelinen, E. L. 2005. Maturation of autophagic vacuoles in Mammalian cells. *Autophagy* 1: 1-10.

231. Lazzarino, D. A., P. Blier, and I. Mellman. 1998. The monomeric guanosine triphosphatase rab4 controls an essential step on the pathway of receptor-mediated antigen processing in B cells. *J Exp Med* 188: 1769-1774.

232. Vieira, O. V., C. Bucci, R. E. Harrison, W. S. Trimble, L. Lanzetti, J. Gruenberg, A. D. Schreiber, P. D. Stahl, and S. Grinstein. 2003. Modulation of Rab5 and Rab7 recruitment to phagosomes by phosphatidylinositol 3-kinase. *Mol Cell Biol* 23: 2501-2514.

233. Bertram, E. M., R. G. Hawley, and T. H. Watts. 2002. Overexpression of rab7 enhances the kinetics of antigen processing and presentation with MHC class II molecules in B cells. *Int Immunol* 14: 309-318.

234. Chaudhry, A., S. R. Das, S. Jameel, A. George, V. Bal, S. Mayor, and S. Rath. 2008. HIV-1 Nef induces a Rab11-dependent routing of endocytosed immune costimulatory proteins CD80 and CD86 to the Golgi. *Traffic* 9: 1925-1935.

235. Berg-Larsen, A., O. J. Landsverk, C. Progida, T. F. Gregers, and O. Bakke. 2013. Differential Regulation of Rab GTPase Expression in Monocyte-Derived Dendritic Cells upon Lipopolysaccharide Activation: A Correlation to Maturation-Dependent Functional Properties. *PLoS ONE* 8: e73538.

236. Renshaw, M., J. Rockwell, C. Engleman, A. Gewirtz, J. Katz, and S. Sambhara. 2002. Cutting edge: impaired Toll-like receptor expression and function in aging. *J Immunol* 169: 4697-4701.

237. Naik, E., and V. M. Dixit. 2011. Mitochondrial reactive oxygen species drive proinflammatory cytokine production. *J Exp Med* 208: 417-420.

238. Riddell, J. R., X. Y. Wang, H. Minderman, and S. O. Gollnick. 2010. Peroxiredoxin 1 stimulates secretion of proinflammatory cytokines by binding to TLR4. *J Immunol* 184: 1022-1030.

239. Robinson, M. W., A. T. Hutchinson, J. P. Dalton, and S. Donnelly. 2010. Peroxiredoxin: a central player in immune modulation. *Parasite Immunol* 32: 305-313.

240. Ren, P., H. Ye, L. Dai, M. Liu, X. Liu, Y. Chai, Q. Shao, Y. Li, N. Lei, B. Peng, W. Yao, and J. Zhang. 2013. Peroxiredoxin 1 is a tumor-associated antigen in esophageal squamous cell carcinoma. *Oncol Rep* 30: 2297-2303.

241. Poynton, R. A., and M. B. Hampton. 2013. Peroxiredoxins as biomarkers of oxidative stress. *Biochim Biophys Acta*.

242. Ishii, T., E. Warabi, and T. Yanagawa. 2012. Novel roles of peroxiredoxins in inflammation, cancer and innate immunity. *J Clin Biochem Nutr* 50: 91-105.

243. Bianchi, M. E. 2007. DAMPs, PAMPs and alarmins: all we need to know about danger. *J Leukoc Biol* 81: 1-5.

244. Zhang, X., and D. M. Mosser. 2008. Macrophage activation by endogenous danger signals. *J Pathol* 214: 161-178.

245. Bosmann, M., N. F. Russkamp, and P. A. Ward. 2012. Fingerprinting of the TLR4-induced acute inflammatory response. *Exp Mol Pathol* 93: 319-323.

246. Chong, I. W., S. R. Lin, J. J. Hwang, M. S. Huang, T. H. Wang, J. Y. Hung, and J. D. Paulauskis. 2002. Expression and regulation of the macrophage inflammatory protein-1 alpha gene by nicotine in rat alveolar macrophages. *Eur Cytokine Netw* 13: 242-249.

247. Lee, M. T., K. Kaushansky, P. Ralph, and M. B. Ladner. 1990. Differential expression of M-CSF, G-CSF, and GM-CSF by human monocytes. *J Leukoc Biol* 47: 275-282.

248. He, R. L., J. Zhou, C. Z. Hanson, J. Chen, N. Cheng, and R. D. Ye. 2009. Serum amyloid A induces G-CSF expression and neutrophilia via Toll-like receptor 2. *Blood* 113: 429-437.

249. Xiang, M., Y. Yuan, L. Fan, Y. Li, A. Li, L. Yin, M. J. Scott, G. Xiao, T. R. Billiar, M. A. Wilson, and J. Fan. 2012. Role of macrophages in mobilization of hematopoietic progenitor cells from bone marrow after hemorrhagic shock. *Shock* 37: 518-523.

250. Pelicano, H., D. S. Martin, R. H. Xu, and P. Huang. 2006. Glycolysis inhibition for anticancer treatment. *Oncogene* 25: 4633-4646.

251. Shapiro, H., A. Lutaty, and A. Ariel. 2011. Macrophages, meta-inflammation, and immuno-metabolism. *ScientificWorldJournal* 11: 2509-2529.

252. Biswas, S. K., and A. Mantovani. 2012. Orchestration of metabolism by macrophages. *Cell Metab* 15: 432-437.

253. Borregaard, N., and T. Herlin. 1982. Energy metabolism of human neutrophils during phagocytosis. *J Clin Invest* 70: 550-557.

254. Odegaard, J. I., and A. Chawla. 2011. Alternative macrophage activation and metabolism. *Annu Rev Pathol* 6: 275-297.

255. Lunt, S. Y., and M. G. Vander Heiden. 2011. Aerobic glycolysis: meeting the metabolic requirements of cell proliferation. *Annu Rev Cell Dev Biol* 27: 441-464.

256. Zu, X. L., and M. Guppy. 2004. Cancer metabolism: facts, fantasy, and fiction. *Biochem Biophys Res Commun* 313: 459-465.

257. Vander Heiden, M. G., L. C. Cantley, and C. B. Thompson. 2009. Understanding the Warburg effect: the metabolic requirements of cell proliferation. *Science* 324: 1029-1033.

258. Kim, J. W., I. Tchernyshyov, G. L. Semenza, and C. V. Dang. 2006. HIF-1-mediated expression of pyruvate dehydrogenase kinase: a metabolic switch required for cellular adaptation to hypoxia. *Cell Metab* 3: 177-185.

259. Nizet, V., and R. S. Johnson. 2009. Interdependence of hypoxic and innate immune responses. *Nat Rev Immunol* 9: 609-617.

260. Sakamoto, T., and M. Seiki. 2010. A membrane protease regulates energy production in macrophages by activating hypoxia-inducible factor-1 via a non-proteolytic mechanism. *J Biol Chem* 285: 29951-29964.

261. Sakamoto, T., D. Niiya, and M. Seiki. 2011. Targeting the Warburg effect that arises in tumor cells expressing membrane type-1 matrix metalloproteinase. *J Biol Chem* 286: 14691-14704.

262. Osellame, L. D., T. S. Blacker, and M. R. Duchen. 2012. Cellular and molecular mechanisms of mitochondrial function. *Best Pract Res Clin Endocrinol Metab* 26: 711-723.

263. Huttemann, M., I. Lee, L. Samavati, H. Yu, and J. W. Doan. 2007. Regulation of mitochondrial oxidative phosphorylation through cell signaling. *Biochim Biophys Acta* 1773: 1701-1720.

264. Gamelli, R. L., H. Liu, L. K. He, and C. A. Hofmann. 1996. Augmentations of glucose uptake and glucose transporter-1 in macrophages following thermal injury and sepsis in mice. *J Leukoc Biol* 59: 639-647.

265. Vats, D., L. Mukundan, J. I. Odegaard, L. Zhang, K. L. Smith, C. R. Morel, R. A. Wagner, D. R. Greaves, P. J. Murray, and A. Chawla. 2006. Oxidative metabolism and PGC-1beta attenuate macrophage-mediated inflammation. *Cell Metab* 4: 13-24.

266. O'Neill, L. A., and D. G. Hardie. 2013. Metabolism of inflammation limited by AMPK and pseudo-starvation. *Nature* 493: 346-355.

267. Shchepina, L. A., O. Y. Pletjushkina, A. V. Avetisyan, L. E. Bakeeva, E. K. Fetisova, D. S. Izyumov, V. B. Saprunova, M. Y. Vyssokikh, B. V. Chernyak, and V. P. Skulachev. 2002. Oligomycin, inhibitor of the F0 part of H+-ATP-synthase, suppresses the TNF-induced apoptosis. *Oncogene* 21: 8149-8157.

268. Nicholls, D. G., V. M. Darley-Usmar, M. Wu, P. B. Jensen, G. W. Rogers, and D. A. Ferrick. 2010. Bioenergetic profile experiment using C2C12 myoblast cells. *J Vis Exp*.

269. Tavakoli, S., D. Zamora, S. Ullevig, and R. Asmis. 2013. Bioenergetic Profiles Diverge During Macrophage Polarization: Implications for the Interpretation of 18F-FDG PET Imaging of Atherosclerosis. *J Nucl Med* 54: 1661-1667.

270. Liu, C. X., H. C. Zhou, Q. Q. Yin, Y. L. Wu, and G. Q. Chen. 2013. Targeting peroxiredoxins against leukemia. *Exp Cell Res* 319: 170-176.

271. Zhang, J., V. Rubio, M. W. Lieberman, and Z. Z. Shi. 2009. OLA1, an Obg-like ATPase, suppresses antioxidant response via nontranscriptional mechanisms. *Proc Natl Acad Sci U S A* 106: 15356-15361.

272. Ma, Q. 2013. Role of nrf2 in oxidative stress and toxicity. *Annu Rev Pharmacol Toxicol* 53: 401-426.

273. Ishii, T., K. Itoh, S. Takahashi, H. Sato, T. Yanagawa, Y. Katoh, S. Bannai, and M. Yamamoto. 2000. Transcription factor Nrf2 coordinately regulates a group of oxidative stress-inducible genes in macrophages. *J Biol Chem* 275: 16023-16029.

274. Chen, Y., and S. B. Gibson. 2008. Is mitochondrial generation of reactive oxygen species a trigger for autophagy? *Autophagy* 4: 246 - 248.

275. Li, X., W. Lu, Y. Hu, S. Wen, C. Qian, W. Wu, and P. Huang. 2013. Effective inhibition of nasopharyngeal carcinoma in vitro and in vivo by targeting glycolysis with oxamate. *Int J Oncol*.

276. Butler, R. N., W. J. Butler, D. Antoniou, and V. Pascoe. 1993. Effect of dehydroepiandrosterone on pentose phosphate pathway activity in the rat colon. *Int J Biochem* 25: 1601-1607.

277. Murphy, C., and P. Newsholme. 1998. Importance of glutamine metabolism in murine macrophages and human monocytes to L-arginine biosynthesis and rates of nitrite or urea production. *Clin Sci (Lond)* 95: 397-407.

278. Pearce, E. L., and E. J. Pearce. 2013. Metabolic pathways in immune cell activation and quiescence. *Immunity* 38: 633-643.

279. Roiniotis, J., H. Dinh, P. Masendycz, A. Turner, C. L. Elsegood, G. M. Scholz, and J. A. Hamilton. 2009. Hypoxia prolongs monocyte/macrophage survival and enhanced glycolysis is associated with their maturation under aerobic conditions. *J Immunol* 182: 7974-7981.

280. Pfeiffer, T., S. Schuster, and S. Bonhoeffer. 2001. Cooperation and competition in the evolution of ATP-producing pathways. *Science* 292: 504-507.

281. Lu, H., R. A. Forbes, and A. Verma. 2002. Hypoxia-inducible factor 1 activation by aerobic glycolysis implicates the Warburg effect in carcinogenesis. *J Biol Chem* 277: 23111-23115.

282. Johnson, A. R., A. J. Freemerman, E. D. Abel, J. Rathmell, and L. Makowski. 2012. Glucose metabolism is linked to the inflammatory status of macrophages. *BMC Proceedings* 6: 62.

283. Fajas, L. 2013. Metabolic control in cancer cells. *Ann Endocrinol (Paris)* 74: 71-73.

284. Ma, X. H., S. Piao, D. Wang, Q. W. McAfee, K. L. Nathanson, J. J. Lum, L. Z. Li, and R. K. Amaravadi. 2011. Measurements of tumor cell autophagy predict invasiveness, resistance to chemotherapy, and survival in melanoma. *Clin Cancer Res* 17: 3478-3489.

285. Ferraro, E., A. Pulicati, M. T. Cencioni, M. Cozzolino, F. Navoni, S. di Martino, R. Nardacci, M. T. Carri, and F. Cecconi. 2008. Apoptosome-deficient cells lose cytochrome c through proteasomal degradation but survive by autophagy-dependent glycolysis. *Mol Biol Cell* 19: 3576-3588.

286. Lock, R., S. Roy, C. M. Kenific, J. S. Su, E. Salas, S. M. Ronen, and J. Debnath. 2011. Autophagy facilitates glycolysis during Ras-mediated oncogenic transformation. *Mol Biol Cell* 22: 165-178.

287. Lee, M. N., S. H. Ha, J. Kim, A. Koh, C. S. Lee, J. H. Kim, H. Jeon, D. H. Kim, P. G. Suh, and S. H. Ryu. 2009. Glycolytic flux signals to mTOR through glyceraldehyde-3-phosphate dehydrogenase-mediated regulation of Rheb. *Mol Cell Biol* 29: 3991-4001.

288. Bensaad, K., E. C. Cheung, and K. H. Vousden. 2009. Modulation of intracellular ROS levels by TIGAR controls autophagy. *Embo J* 28: 3015-3026.

289. Kotoulas, O. B., S. A. Kalamidas, and D. J. Kondomerkos. 2006. Glycogen autophagy in glucose homeostasis. *Pathol Res Pract* 202: 631-638.

290. Singh, R., S. Kaushik, Y. Wang, Y. Xiang, I. Novak, M. Komatsu, K. Tanaka, A. M. Cuervo, and M. J. Czaja. 2009. Autophagy regulates lipid metabolism. *Nature* 458: 1131-1135.

291. Rabinowitz, J. D., and E. White. 2010. Autophagy and metabolism. *Science* 330: 1344-1348.

292. Garedew, A., S. O. Henderson, and S. Moncada. 2010. Activated macrophages utilize glycolytic ATP to maintain mitochondrial membrane potential and prevent apoptotic cell death. *Cell Death Differ* 17: 1540-1550.

293. Hubbi, M. E., H. Hu, Kshitiz, I. Ahmed, A. Levchenko, and G. L. Semenza. 2013. Chaperone-mediated autophagy targets hypoxia-inducible factor-1alpha (HIF-1alpha) for lysosomal degradation. *J Biol Chem* 288: 10703-10714.

294. Cramer, T., Y. Yamanishi, B. E. Clausen, I. Forster, R. Pawlinski, N. Mackman, V. H. Haase, R. Jaenisch, M. Corr, V. Nizet, G. S. Firestein, H. P. Gerber, N. Ferrara, and R. S. Johnson. 2003. HIF-1alpha is essential for myeloid cell-mediated inflammation. *Cell* 112: 645-657.

295. Imtiyaz, H. Z., and M. C. Simon. 2010. Hypoxia-inducible factors as essential regulators of inflammation. *Curr Top Microbiol Immunol* 345: 105-120.

296. Gerald, D., E. Berra, Y. M. Frapart, D. A. Chan, A. J. Giaccia, D. Mansuy, J. Pouyssegur, M. Yaniv, and F. Mechta-Grigoriou. 2004. JunD reduces tumor angiogenesis by protecting cells from oxidative stress. *Cell* 118: 781-794.

297. Hellwig-Burgel, T., K. Rutkowski, E. Metzen, J. Fandrey, and W. Jelkmann. 1999. Interleukin-1beta and tumor necrosis factor-alpha stimulate DNA binding of hypoxia-inducible factor-1. *Blood* 94: 1561-1567.

298. Ando, M., I. Uehara, K. Kogure, Y. Asano, W. Nakajima, Y. Abe, K. Kawauchi, and N. Tanaka. 2010. Interleukin 6 enhances glycolysis through expression of the glycolytic enzymes hexokinase 2 and 6-phosphofructo-2-kinase/fructose-2,6-bisphosphatase-3. *J Nippon Med Sch* 77: 97-105.

299. Taylor, D. J., E. B. Faragher, and J. M. Evanson. 1992. Inflammatory cytokines stimulate glucose uptake and glycolysis but reduce glucose oxidation in human dermal fibroblasts in vitro. *Circ Shock* 37: 105-110.

300. Pavlides, S., I. Vera, R. Gandara, S. Sneddon, R. G. Pestell, I. Mercier, U. E. Martinez-Outschoorn, D. Whitaker-Menezes, A. Howell, F. Sotgia, and M. P. Lisanti. 2012. Warburg meets autophagy: cancer-associated fibroblasts accelerate tumor growth and metastasis via oxidative stress, mitophagy, and aerobic glycolysis. *Antioxid Redox Signal* 16: 1264-1284.

301. Xaus, J., M. Comalada, A. F. Valledor, M. Cardo, C. Herrero, C. Soler, J. Lloberas, and A. Celada. 2001. Molecular mechanisms involved in macrophage survival, proliferation, activation or apoptosis. *Immunobiology* 204: 543-550.

302. Haschemi, A., P. Kosma, L. Gille, C. R. Evans, C. F. Burant, P. Starkl, B. Knapp, R. Haas, J. A. Schmid, C. Jandl, S. Amir, G. Lubec, J. Park, H. Esterbauer, M. Bilban, L. Brizuela, J. A. Pospisilik, L. E. Otterbein, and O. Wagner. 2012. The sedoheptulose kinase CARKL directs macrophage polarization through control of glucose metabolism. *Cell Metab* 15: 813-826.

303. Kelly, D. P., and R. C. Scarpulla. 2004. Transcriptional regulatory circuits controlling mitochondrial biogenesis and function. *Genes Dev* 18: 357-368.

304. van der Windt, G. J., B. Everts, C. H. Chang, J. D. Curtis, T. C. Freitas, E. Amiel, E. J. Pearce, and E. L. Pearce. 2012. Mitochondrial respiratory capacity is a critical regulator of CD8+ T cell memory development. *Immunity* 36: 68-78.

305. Herst, P. M., and M. V. Berridge. 2007. Cell surface oxygen consumption: a major contributor to cellular oxygen consumption in glycolytic cancer cell lines. *Biochim Biophys Acta* 1767: 170-177.

306. Berridge, M. V., and A. S. Tan. 2000. High-capacity redox control at the plasma membrane of mammalian cells: trans-membrane, cell surface, and serum NADH-oxidases. *Antioxid Redox Signal* 2: 231-242.

307. Wood, J. L., and A. Graham. 1999. Reduction of transition metals by human (THP-1) monocytes is enhanced by activators of protein kinase C. *Free Radic Res* 31: 367-379.

308. Weir, L., D. Robertson, I. M. Leigh, and A. A. Panteleyev. 2011. The reduction of water-soluble tetrazolium salt reagent on the plasma membrane of epidermal keratinocytes is oxygen dependent. *Anal Biochem* 414: 31-37.

309. Kruger, N. J., and A. von Schaewen. 2003. The oxidative pentose phosphate pathway: structure and organisation. *Curr Opin Plant Biol* 6: 236-246.

310. Heiss, E. H., D. Schachner, K. Zimmermann, and V. M. Dirsch. 2013. Glucose availability is a decisive factor for Nrf2-mediated gene expression. *Redox Biol* 1: 359-365.

311. Ham, M., J. W. Lee, A. H. Choi, H. Jang, G. Choi, J. Park, C. Kozuka, D. D. Sears, H. Masuzaki, and J. B. Kim. 2013. Macrophage glucose-6-phosphate dehydrogenase stimulates proinflammatory responses with oxidative stress. *Mol Cell Biol* 33: 2425-2435.

312. Wilmanski, J., E. Villanueva, E. A. Deitch, and Z. Spolarics. 2007. Glucose-6-phosphate dehydrogenase deficiency and the inflammatory response to endotoxin and polymicrobial sepsis. *Crit Care Med* 35: 510-518.

313. Xu, Y., Z. Zhang, J. Hu, I. E. Stillman, J. A. Leopold, D. E. Handy, J. Loscalzo, and R. C. Stanton. 2010. Glucose-6-phosphate dehydrogenase-deficient mice have increased renal oxidative stress and increased albuminuria. *FASEB J* 24: 609-616.

314. Wilmanski, J., M. Siddiqi, E. A. Deitch, and Z. Spolarics. 2005. Augmented IL-10 production and redox-dependent signaling pathways in glucose-6-phosphate dehydrogenase-deficient mouse peritoneal macrophages. *J Leukoc Biol* 78: 85-94.

315. Nguyen, T., P. Nioi, and C. B. Pickett. 2009. The Nrf2-antioxidant response element signaling pathway and its activation by oxidative stress. *J Biol Chem* 284: 13291-13295.

316. Abbas, K., J. Breton, A. G. Planson, C. Bouton, J. Bignon, C. Seguin, S. Riquier, M. B. Toledano, and J. C. Drapier. 2011. Nitric oxide activates an Nrf2/sulfiredoxin antioxidant pathway in macrophages. *Free Radic Biol Med* 51: 107-114.

317. Perl, A., R. Hanczko, T. Telarico, Z. Oaks, and S. Landas. 2011. Oxidative stress, inflammation and carcinogenesis are controlled through the pentose phosphate pathway by transaldolase. *Trends Mol Med* 17: 395-403.

318. Rattan, S. I. 2006. Theories of biological aging: genes, proteins, and free radicals. *Free Radic Res* 40: 1230-1238.

319. Fleg, J. L. 1996. Normative Aging Changes in Cardiovascular Structure and Function. *Am J Geriatr Cardiol* 5: 7-15.

320. Hitt, R., Y. Young-Xu, M. Silver, and T. Perls. 1999. Centenarians: the older you get, the healthier you have been. *Lancet* 354: 652.

321. Melendez, A., Z. Talloczy, M. Seaman, E. L. Eskelinen, D. H. Hall, and B. Levine. 2003. Autophagy genes are essential for dauer development and life-span extension in C. elegans. *Science* 301: 1387-1391.

322. Simonsen, A., R. C. Cumming, A. Brech, P. Isakson, D. R. Schubert, and K. D. Finley. 2008. Promoting basal levels of autophagy in the nervous system enhances longevity and oxidant resistance in adult Drosophila. *Autophagy* 4: 176-184.

323. Pyo, J. O., S. M. Yoo, H. H. Ahn, J. Nah, S. H. Hong, T. I. Kam, S. Jung, and Y. K. Jung. 2013. Overexpression of Atg5 in mice activates autophagy and extends lifespan. *Nat Commun* 4: 2300.

324. Bergamini, E., G. Cavallini, A. Donati, and Z. Gori. 2007. The role of autophagy in aging: its essential part in the anti-aging mechanism of caloric restriction. *Ann N Y Acad Sci* 1114: 69-78.

325. Colman, R. J., R. M. Anderson, S. C. Johnson, E. K. Kastman, K. J. Kosmatka, T. M. Beasley, D. B. Allison, C. Cruzen, H. A. Simmons, J. W. Kemnitz, and R. Weindruch. 2009. Caloric restriction delays disease onset and mortality in rhesus monkeys. *Science* 325: 201-204.

326. Park, S. K., and T. A. Prolla. 2005. Lessons learned from gene expression profile studies of aging and caloric restriction. *Ageing Res Rev* 4: 55-65.

327. Levine, B., and G. Kroemer. 2008. Autophagy in the Pathogenesis of Disease. *Cell* 132: 27 - 42.

328. Hansen, M., A. Chandra, L. L. Mitic, B. Onken, M. Driscoll, and C. Kenyon. 2008. A role for autophagy in the extension of lifespan by dietary restriction in C. elegans. *PLoS Genet* 4: e24.

329. Salminen, A., and K. Kaarniranta. 2009. SIRT1: regulation of longevity via autophagy. *Cell Signal* 21: 1356-1360.

330. Ravikumar, B., R. Duden, and D. C. Rubinsztein. 2002. Aggregate-prone proteins with polyglutamine and polyalanine expansions are degraded by autophagy. *Hum Mol Genet* 11: 1107-1117.

331. Rubinsztein, D. C., G. Marino, and G. Kroemer. 2011. Autophagy and aging. *Cell* 146: 682-695.

332. Chen, C., Y. Liu, and P. Zheng. 2009. mTOR regulation and therapeutic rejuvenation of aging hematopoietic stem cells. *Sci Signal* 2: ra75.

333. Maiuri, M. C., E. Tasdemir, A. Criollo, E. Morselli, J. M. Vicencio, R. Carnuccio, and G. Kroemer. 2009. Control of autophagy by oncogenes and tumor suppressor genes. *Cell Death Differ* 16: 87-93.

334. Shibata, M., T. Lu, T. Furuya, A. Degterev, N. Mizushima, T. Yoshimori, M. MacDonald, B. Yankner, and J. Yuan. 2006. Regulation of intracellular accumulation of mutant Huntingtin by Beclin 1. *J Biol Chem* 281: 14474-14485.

335. Pawelec, G., J. E. McElhaney, A. E. Aiello, and E. Derhovanessian. 2012. The impact of CMV infection on survival in older humans. *Curr Opin Immunol* 24: 507-511.

336. Lansdorp, P. M., W. Dragowska, T. E. Thomas, M. T. Little, and H. Mayani. 1994. Age-related decline in proliferative potential of purified stem cell candidates. *Blood Cells* 20: 376-380; discussion 380-371.

337. Hartsock, R. J., E. B. Smith, and C. S. Petty. 1965. Normal variations with aging of the amount of hematopoietic tissue in bone marrow from the anterior iliac crest. A study made from 177 cases of sudden death examined by necropsy. *Am J Clin Pathol* 43: 326-331.

338. Dykstra, B., and G. de Haan. 2008. Hematopoietic stem cell aging and self-renewal. *Cell Tissue Res* 331: 91-101.

339. Beerman, I., D. Bhattacharya, S. Zandi, M. Sigvardsson, I. L. Weissman, D. Bryder, and D. J. Rossi. 2010. Functionally distinct hematopoietic stem cells modulate hematopoietic lineage potential during aging by a mechanism of clonal expansion. *Proc Natl Acad Sci U S A* 107: 5465-5470.

340. Jamieson, B. D., D. C. Douek, S. Killian, L. E. Hultin, D. D. Scripture-Adams, J. V. Giorgi, D. Marelli, R. A. Koup, and J. A. Zack. 1999. Generation of functional thymocytes in the human adult. *Immunity* 10: 569-575.

341. Rossi, M. I., T. Yokota, K. L. Medina, K. P. Garrett, P. C. Comp, A. H. Schipul, Jr., and P. W. Kincade. 2003. B lymphopoiesis is active throughout human life, but there are developmental age-related changes. *Blood* 101: 576-584.

342. Frasca, D., A. M. Landin, S. C. Lechner, J. G. Ryan, R. Schwartz, R. L. Riley, and B. B. Blomberg. 2008. Aging down-regulates the transcription factor E2A, activation-induced cytidine deaminase, and Ig class switch in human B cells. *J Immunol* 180: 5283-5290.

343. Haynes, L., and S. L. Swain. 2006. Why aging T cells fail: implications for vaccination. *Immunity* 24: 663-666.

344. Agarwal, S., and P. J. Busse. 2010. Innate and adaptive immunosenescence. *Ann Allergy Asthma Immunol* 104: 183-190; quiz 190-182, 210.

345. Giunta, S. 2006. Is inflammaging an auto[innate]immunity subclinical syndrome? *Immun Ageing* 3: 12.

346. Mocchegiani, E., R. Giacconi, C. Cipriano, and M. Malavolta. 2009. NK and NKT cells in aging and longevity: role of zinc and metallothioneins. *J Clin Immunol* 29: 416-425.

347. Shaw, A. C., S. Joshi, H. Greenwood, A. Panda, and J. M. Lord. 2010. Aging of the innate immune system. *Curr Opin Immunol* 22: 507-513.

348. Lord, J. M., S. Butcher, V. Killampali, D. Lascelles, and M. Salmon. 2001. Neutrophil ageing and immunesenescence. *Mech Ageing Dev* 122: 1521-1535.

349. Tesar, B. M., W. E. Walker, J. Unternaehrer, N. S. Joshi, A. Chandele, L. Haynes, S. Kaech, and D. R. Goldstein. 2006. Murine [corrected] myeloid dendritic cell-dependent toll-like receptor immunity is preserved with aging. *Aging Cell* 5: 473-486.

350. Grolleau-Julius, A., E. K. Harning, L. M. Abernathy, and R. L. Yung. 2008. Impaired dendritic cell function in aging leads to defective antitumor immunity. *Cancer Res* 68: 6341-6349.

351. Panda, A., F. Qian, S. Mohanty, D. van Duin, F. K. Newman, L. Zhang, S. Chen, V. Towle, R. B. Belshe, E. Fikrig, H. G. Allore, R. R. Montgomery, and A. C. Shaw. 2010. Age-associated decrease in TLR function in primary human dendritic cells predicts influenza vaccine response. *J Immunol* 184: 2518-2527.

352. Della Bella, S., L. Bierti, P. Presicce, R. Arienti, M. Valenti, M. Saresella, C. Vergani, and M. L. Villa. 2007. Peripheral blood dendritic cells and monocytes are differently regulated in the elderly. *Clin Immunol* 122: 220-228.

353. Boggs, D., K. Patrene, and H. Steinberg. 1986. Aging and hematopoiesis. VI. Neutrophilia and other leukocyte changes in aged mice. *Exp Hematol* 14: 372-379.

354. Sebastian, C., M. Espia, M. Serra, A. Celada, and J. Lloberas. 2005. MacrophAging: a cellular and molecular review. *Immunobiology* 210: 121-126.

355. Koike, E., T. Kobayashi, K. Mochitate, and M. Murakami. 1999. Effect of aging on nitric oxide production by rat alveolar macrophages. *Exp Gerontol* 34: 889-894.

356. Cannizzo, E. S., C. C. Clement, R. Sahu, C. Follo, and L. Santambrogio. 2011. Oxidative stress, inflamm-aging and immunosenescence. *J Proteomics* 74: 2313-2323.

357. Bruunsgaard, H., M. Pedersen, and B. K. Pedersen. 2001. Aging and proinflammatory cytokines. *Curr Opin Hematol* 8: 131-136.

358. Henry, C. J., Y. Huang, A. M. Wynne, and J. P. Godbout. 2009. Peripheral lipopolysaccharide (LPS) challenge promotes microglial hyperactivity in aged mice that is associated with exaggerated induction of both pro-inflammatory IL-1beta and anti-inflammatory IL-10 cytokines. *Brain Behav Immun* 23: 309-317.

359. van Duin, D., S. Mohanty, V. Thomas, S. Ginter, R. R. Montgomery, E. Fikrig, H. G. Allore, R. Medzhitov, and A. C. Shaw. 2007. Age-associated defect in human TLR-1/2 function. *J Immunol* 178: 970-975.

360. Herrero, C., L. Marques, J. Lloberas, and A. Celada. 2001. IFN-gamma-dependent transcription of MHC class II IA is impaired in macrophages from aged mice. *J Clin Invest* 107: 485-493.

361. Phadwal, K., J. Alegre-Abarrategui, A. S. Watson, L. Pike, S. Anbalagan, E. M. Hammond, R. Wade-Martins, A. McMichael, P. Klenerman, and A. K. Simon. 2012. A novel method for autophagy detection in primary cells: impaired levels of macroautophagy in immunosenescent T cells. *Autophagy* 8: 677-689.

362. Beum, P. V., M. A. Lindorfer, B. E. Hall, T. C. George, K. Frost, P. J. Morrissey, and R. P. Taylor. 2006. Quantitative analysis of protein co-localization on B cells opsonized with rituximab and complement using the ImageStream multispectral imaging flow cytometer. *J Immunol Methods* 317: 90-99.

363. Cancro, M. P. 2005. B cells and aging: gauging the interplay of generative, selective, and homeostatic events. *Immunol Rev* 205: 48-59.

364. Goronzy, J. J., and C. M. Weyand. 2005. T cell development and receptor diversity during aging. *Curr Opin Immunol* 17: 468-475.

365. Strohacker, K., W. L. Breslin, K. C. Carpenter, and B. K. McFarlin. 2012. Aged mice have increased inflammatory monocyte concentration and altered expression of cell-surface functional receptors. *J Biosci* 37: 55-62.

366. Tang, Q., L. K. Koh, D. Jiang, and H. Schwarz. 2013. CD137 ligand reverse signaling skews hematopoiesis towards myelopoiesis during aging. *Aging (Albany NY)* 5.

367. Wang, J., H. Geiger, and K. L. Rudolph. 2011. Immunoaging induced by hematopoietic stem cell aging. *Curr Opin Immunol* 23: 532-536.

368. Hennekens, C. H. 1998. Increasing burden of cardiovascular disease: current knowledge and future directions for research on risk factors. *Circulation* 97: 1095-1102.

369. Libby, P., A. H. Lichtman, and G. K. Hansson. 2013. Immune effector mechanisms implicated in atherosclerosis: from mice to humans. *Immunity* 38: 1092-1104.

370. Wojcik, A. J., M. D. Skaflen, S. Srinivasan, and C. C. Hedrick. 2008. A critical role for ABCG1 in macrophage inflammation and lung homeostasis. *J Immunol* 180: 4273-4282.

371. Lee, H. C., and Y. H. Wei. 2012. Mitochondria and aging. *Adv Exp Med Biol* 942: 311-327.

372. Sohal, R. S., H. H. Ku, S. Agarwal, M. J. Forster, and H. Lal. 1994. Oxidative damage, mitochondrial oxidant generation and antioxidant defenses during aging and in response to food restriction in the mouse. *Mech Ageing Dev* 74: 121-133.

373. Smallwood, H. S., D. Lopez-Ferrer, and T. C. Squier. 2011. Aging enhances the production of reactive oxygen species and bactericidal activity in peritoneal macrophages by upregulating classical activation pathways. *Biochemistry* 50: 9911-9922.

374. Dorshkind, K., E. Montecino-Rodriguez, and R. A. Signer. 2009. The ageing immune system: is it ever too old to become young again? *Nat Rev Immunol* 9: 57-62.

375. Trepanowski, J. F., R. E. Canale, K. E. Marshall, M. M. Kabir, and R. J. Bloomer. 2011. Impact of caloric and dietary restriction regimens on markers of health and longevity in humans and animals: a summary of available findings. *Nutr J* 10: 107.

376. Chen, T., L. Shen, J. Yu, H. Wan, A. Guo, J. Chen, Y. Long, J. Zhao, and G. Pei. 2011. Rapamycin and other longevity-promoting compounds enhance the generation of mouse induced pluripotent stem cells. *Aging Cell* 10: 908-911.

377. Cuervo, A. M., E. Bergamini, U. T. Brunk, W. Droge, M. Ffrench, and A. Terman. 2005. Autophagy and aging: the importance of maintaining "clean" cells. *Autophagy* 1: 131-140.

378. Greer El Fau - Brunet, A., and A. Brunet. 2008. Signaling networks in aging. *Journal of Cell Science* 121: 407 - 412.

379. Holzenberger M Fau - Dupont, J., B. Dupont J Fau - Ducos, P. Ducos B Fau - Leneuve, A. Leneuve P Fau - Geloen, P. C. Geloen A Fau - Even, P. Even Pc Fau - Cervera, Y. Cervera P Fau - Le Bouc, and Y. Le Bouc. 2003. IGF-1 receptor regulates lifespan and resistance to oxidative stress in mice. *Nature* 421: 182 - 187.

380. Kasapoglu, M., and T. Ozben. 2001. Alterations of antioxidant enzymes and oxidative stress markers in aging. *Exp Gerontol* 36: 209-220.

381. Schworer, C. M., and G. E. Mortimore. 1979. Glucagon-induced autophagy and proteolysis in rat liver: mediation by selective deprivation of intracellular amino acids. *Proc Natl Acad Sci U S A* 76: 3169-3173.

382. Bergamini, E., A. Del Roso, V. Fierabracci, Z. Gori, P. Masiello, M. Masini, and M. Pollera. 1993. A new method for the investigation of endocrine-regulated autophagy and protein degradation in rat liver. *Exp Mol Pathol* 59: 13-26.

383. Michan, S., and D. Sinclair. 2007. Sirtuins in mammals: insights into their biological function. *Biochem J* 404: 1-13.

384. Lee, I. H., L. Cao, R. Mostoslavsky, D. B. Lombard, J. Liu, N. E. Bruns, M. Tsokos, F. W. Alt, and T. Finkel. 2008. A role for the NAD-dependent deacetylase Sirt1 in the regulation of autophagy. *Proc Natl Acad Sci U S A* 105: 3374-3379.

385. Longo, V. D., and B. K. Kennedy. 2006. Sirtuins in aging and age-related disease. *Cell* 126: 257-268.

386. Sommer, M., N. Poliak, S. Upadhyay, E. Ratovitski, B. D. Nelkin, L. A. Donehower, and D. Sidransky. 2006. DeltaNp63alpha overexpression induces downregulation of Sirt1 and an accelerated aging phenotype in the mouse. *Cell Cycle* 5: 2005-2011.

387. Sedding, D., and J. Haendeler. 2007. Do we age on Sirt1 expression? *Circ Res* 100: 1396-1398.

388. Miyoshi, N., H. Oubrahim, P. B. Chock, and E. R. Stadtman. 2006. Age-dependent cell death and the role of ATP in hydrogen peroxide-induced apoptosis and necrosis. *Proc Natl Acad Sci U S A* 103: 1727-1731.

389. Wang, C. Q., K. B. Udupa, H. Xiao, and D. A. Lipschitz. 1995. Effect of age on marrow macrophage number and function. *Aging (Milano)* 7: 379-384.

390. Kohut, M. L., D. S. Senchina, K. S. Madden, A. E. Martin, D. L. Felten, and J. A. Moynihan. 2004. Age effects on macrophage function vary by tissue site, nature of stimulant, and exercise behavior. *Exp Gerontol* 39: 1347-1360.

391. Singh, R., and A. M. Cuervo. 2012. Lipophagy: connecting autophagy and lipid metabolism. *International journal of cell biology* 2012: 282041.

392. Liu, K., and M. J. Czaja. 2013. Regulation of lipid stores and metabolism by lipophagy. *Cell Death Differ* 20: 3-11.

393. Martinez-Vicente, M., G. Sovak, and A. M. Cuervo. 2005. Protein degradation and aging. *Exp Gerontol* 40: 622-633.

394. Marina, O. C., C. K. Sanders, and J. R. Mourant. 2012. Correlating light scattering with internal cellular structures. *Biomedical optics express* 3: 296-312.

395. Blanpied, T. A., D. B. Scott, and M. D. Ehlers. 2003. Age-related regulation of dendritic endocytosis associated with altered clathrin dynamics. *Neurobiology of aging* 24: 1095-1104.

396. Wu, X., X. Kong, D. Chen, H. Li, Y. Zhao, M. Xia, M. Fang, P. Li, F. Fang, L. Sun, W. Tian, H. Xu, Y. Yang, X. Qi, Y. Gao, J. Sha, Q. Chen, and Y. Xu. 2011. SIRT1 links CIITA deacetylation to MHC II activation. *Nucleic acids research* 39: 9549-9558.

397. Conley, K. E., D. J. Marcinek, and J. Villarin. 2007. Mitochondrial dysfunction and age. *Current opinion in clinical nutrition and metabolic care* 10: 688-692.

398. Kissin, E., M. Tomasi, N. McCartney-Francis, C. L. Gibbs, and P. D. Smith. 1997. Age-related decline in murine macrophage production of nitric oxide. *The Journal of infectious diseases* 175: 1004-1007.

399. Khare, V., A. Sodhi, and S. M. Singh. 1996. Effect of aging on the tumoricidal functions of murine peritoneal macrophages. *Nat Immun* 15: 285-294.

400. Hazlett, L. D., F. B. Kreindler, R. S. Berk, and R. Barrett. 1990. Aging alters the phagocytic capability of inflammatory cells induced into cornea. *Curr Eye Res* 9: 129-138.

401. Fietta, A., C. Merlini, P. M. De Bernardi, L. Gandola, P. D. Piccioni, and C. Grassi. 1993. Non specific immunity in aged healthy subjects and in patients with chronic bronchitis. *Aging (Milano)* 5: 357-361.

402. De la Fuente, M., and J. Miquel. 2009. An update of the oxidation-inflammation theory of aging: the involvement of the immune system in oxi-inflamm-aging. *Curr Pharm Des* 15: 3003-3026.

403. Salminen, A., J. Ojala, K. Kaarniranta, and A. Kauppinen. 2012. Mitochondrial dysfunction and oxidative stress activate inflammasomes: impact on the aging process and age-related diseases. *Cell Mol Life Sci* 69: 2999-3013.

404. Chen, G. Y., and G. Nunez. 2010. Sterile inflammation: sensing and reacting to damage. *Nat Rev Immunol* 10: 826-837.

405. Gill, R., A. Tsung, and T. Billiar. 2010. Linking oxidative stress to inflammation: Toll-like receptors. *Free Radic Biol Med* 48: 1121-1132.

406. Yoshizaki, T., S. Schenk, T. Imamura, J. L. Babendure, N. Sonoda, E. J. Bae, D. Y. Oh, M. Lu, J. C. Milne, C. Westphal, G. Bandyopadhyay, and J. M. Olefsky. 2010. SIRT1 inhibits inflammatory pathways in macrophages and modulates insulin sensitivity. *Am J Physiol Endocrinol Metab* 298: E419-428.

407. Salminen, A., K. Kaarniranta, and A. Kauppinen. 2012. Inflammaging: disturbed interplay between autophagy and inflammasomes. *Aging (Albany NY)* 4: 166-175.

408. Hipkiss, A. R. 2006. Does chronic glycolysis accelerate aging? Could this explain how dietary restriction works? *Ann N Y Acad Sci* 1067: 361-368.

409. Brownlee, M. 2001. Biochemistry and molecular cell biology of diabetic complications. *Nature* 414: 813-820.

410. Dukic-Stefanovic, S., R. Schinzel, P. Riederer, and G. Munch. 2001. AGES in brain ageing: AGE-inhibitors as neuroprotective and anti-dementia drugs? *Biogerontology* 2: 19-34.

411. Reddy, V. P., M. E. Obrenovich, C. S. Atwood, G. Perry, and M. A. Smith. 2002. Involvement of Maillard reactions in Alzheimer disease. *Neurotox Res* 4: 191-209.

412. Lee, C. K., D. B. Allison, J. Brand, R. Weindruch, and T. A. Prolla. 2002. Transcriptional profiles associated with aging and middle age-onset caloric restriction in mouse hearts. *Proc Natl Acad Sci U S A* 99: 14988-14993.

413. Pugh, T. D., T. D. Oberley, and R. Weindruch. 1999. Dietary intervention at middle age: caloric restriction but not dehydroepiandrosterone sulfate increases lifespan and lifetime cancer incidence in mice. *Cancer Res* 59: 1642-1648.

414. Witte, A. V., M. Fobker, R. Gellner, S. Knecht, and A. Floel. 2009. Caloric restriction improves memory in elderly humans. *Proc Natl Acad Sci U S A* 106: 1255-1260.

415. Butcher, S., H. Chahel, and J. M. Lord. 2000. Review article: ageing and the neutrophil: no appetite for killing? *Immunology* 100: 411-416.

416. Plowden, J., M. Renshaw-Hoelscher, C. Engleman, J. Katz, and S. Sambhara. 2004. Innate immunity in aging: impact on macrophage function. *Aging Cell* 3: 161-167.

417. Boehmer, E. D., J. Goral, D. E. Faunce, and E. J. Kovacs. 2004. Age-dependent decrease in Toll-like receptor 4-mediated proinflammatory cytokine production and mitogen-activated protein kinase expression. *J Leukoc Biol* 75: 342-349.

418. Orkin, S. H. 2000. Diversification of haematopoietic stem cells to specific lineages. *Nat Rev Genet* 1: 57-64.

419. Traver, D., T. Miyamoto, J. Christensen, J. Iwasaki-Arai, K. Akashi, and I. L. Weissman. 2001. Fetal liver myelopoiesis occurs through distinct, prospectively isolatable progenitor subsets. *Blood* 98: 627-635.

420. Friedman, A. D. 2002. Transcriptional regulation of granulocyte and monocyte development. *Oncogene* 21: 3377-3390.

421. Singh, H. 2008. PU.1, a shared transcriptional regulator of innate and adaptive immune cell fates. *J Immunol* 181: 1595-1596.

422. Zhang, D. E., P. Zhang, N. D. Wang, C. J. Hetherington, G. J. Darlington, and D. G. Tenen. 1997. Absence of granulocyte colony-stimulating factor signaling and neutrophil development in CCAAT enhancer binding protein alpha-deficient mice. *Proc Natl Acad Sci U S A* 94: 569-574.

423. Tanaka, T., S. Akira, K. Yoshida, M. Umemoto, Y. Yoneda, N. Shirafuji, H. Fujiwara, S. Suematsu, N. Yoshida, and T. Kishimoto. 1995. Targeted disruption of the NF-IL6 gene discloses its essential role in bacteria killing and tumor cytotoxicity by macrophages. *Cell* 80: 353-361.

424. Yamanaka, R., C. Barlow, J. Lekstrom-Himes, L. H. Castilla, P. P. Liu, M. Eckhaus, T. Decker, A. Wynshaw-Boris, and K. G. Xanthopoulos. 1997. Impaired granulopoiesis, myelodysplasia, and early lethality in CCAAT/enhancer binding protein epsilon-deficient mice. *Proc Natl Acad Sci U S A* 94: 13187-13192.

425. Hock, H., M. J. Hamblen, H. M. Rooke, D. Traver, R. T. Bronson, S. Cameron, and S. H. Orkin. 2003. Intrinsic requirement for zinc finger transcription factor Gfi-1 in neutrophil differentiation. *Immunity* 18: 109-120.

426. Laiosa, C. V., M. Stadtfeld, and T. Graf. 2006. Determinants of lymphoid-myeloid lineage diversification. *Annu Rev Immunol* 24: 705-738.

427. Johnson, P. F. 2005. Molecular stop signs: regulation of cell-cycle arrest by C/EBP transcription factors. *J Cell Sci* 118: 2545-2555.

428. Borregaard, N., and J. B. Cowland. 1997. Granules of the human neutrophilic polymorphonuclear leukocyte. *Blood* 89: 3503-3521.

429. Borregaard, N., L. Kjeldsen, K. Rygaard, L. Bastholm, M. H. Nielsen, H. Sengelov, O. W. Bjerrum, and A. H. Johnsen. 1992. Stimulus-dependent secretion of plasma proteins from human neutrophils. *J Clin Invest* 90: 86-96.

430. Sengelov, H., L. Kjeldsen, W. Kroeze, M. Berger, and N. Borregaard. 1994. Secretory vesicles are the intracellular reservoir of complement receptor 1 in human neutrophils. *J Immunol* 153: 804-810.

431. Pham, C. T. 2006. Neutrophil serine proteases: specific regulators of inflammation. *Nat Rev Immunol* 6: 541-550.

432. Borregaard, N. 2010. Neutrophils, from marrow to microbes. *Immunity* 33: 657-670.

433. Pillay, J., I. den Braber, N. Vrisekoop, L. M. Kwast, R. J. de Boer, J. A. Borghans, K. Tesselaar, and L. Koenderman. 2010. In vivo labeling with 2H2O reveals a human neutrophil lifespan of 5.4 days. *Blood* 116: 625-627.

434. Colotta, F., F. Re, N. Polentarutti, S. Sozzani, and A. Mantovani. 1992. Modulation of granulocyte survival and programmed cell death by cytokines and bacterial products. *Blood* 80: 2012-2020.

435. Wong, C. P., K. R. Magnusson, and E. Ho. 2013. Increased inflammatory response in aged mice is associated with age-related zinc deficiency and zinc transporter dysregulation. *J Nutr Biochem* 24: 353-359.

436. Leuenberger, H. G., and I. Kunstyr. 1976. Gerontological data of C57BL/6J mice. II. Changes in blood cell counts in the course of natural aging. *J Gerontol* 31: 648-653.

437. Kile, B. T., C. L. Mason-Garrison, and M. J. Justice. 2003. Sex and strain-related differences in the peripheral blood cell values of inbred mouse strains. *Mamm Genome* 14: 81-85.

438. Laboratory, T. S. o. T. J. 1966. *Biology of the Laboratory Mouse*. Dover Publications, New York.

439. Wirth-Dzięciołowska, E., J. Karaszewska, K. Pyśniak, M. Smolińska, and M. Gajewska. 2009. Selected peripheral blood cell parameters in twelve inbred strains of laboratory mice. *Animal Science Papers and Reports* 27: 69 - 77.

440. Nemzek, J. A., G. L. Bolgos, B. A. Williams, and D. G. Remick. 2001. Differences in normal values for murine white blood cell counts and other hematological parameters based on sampling site. *Inflamm Res* 50: 523-527.

441. Stone, R. M., M. R. O'Donnell, and M. A. Sekeres. 2004. Acute myeloid leukemia. *Hematology Am Soc Hematol Educ Program*: 98-117.

442. Mano, H. 2006. DNA micro-array analysis of myelodysplastic syndrome. *Leuk Lymphoma* 47: 9-14.

443. Fleming, T. J., M. L. Fleming, and T. R. Malek. 1993. Selective expression of Ly-6G on myeloid lineage cells in mouse bone marrow. RB6-8C5 mAb to granulocyte-

differentiation antigen (Gr-1) detects members of the Ly-6 family. *J Immunol* 151: 2399-2408.

444. Hickey, M. J. 2012. Has Ly6G finally found a job? *Blood* 120: 1352-1353.

445. Hestdal, K., F. W. Ruscetti, J. N. Ihle, S. E. Jacobsen, C. M. Dubois, W. C. Kopp, D. L. Longo, and J. R. Keller. 1991. Characterization and regulation of RB6-8C5 antigen expression on murine bone marrow cells. *J Immunol* 147: 22-28.

446. Anderson, S. I., N. A. Hotchin, and G. B. Nash. 2000. Role of the cytoskeleton in rapid activation of CD11b/CD18 function and its subsequent downregulation in neutrophils. *J Cell Sci* 113 (Pt 15): 2737-2745.

447. Ross, G. D., and V. Vetvicka. 1993. CR3 (CD11b, CD18): a phagocyte and NK cell membrane receptor with multiple ligand specificities and functions. *Clin Exp Immunol* 92: 181-184.

448. Takai, T. 2002. Roles of Fc receptors in autoimmunity. *Nat Rev Immunol* 2: 580-592.

449. Elghetany, M. T. 2002. Surface antigen changes during normal neutrophilic development: a critical review. *Blood Cells Mol Dis* 28: 260-274.

450. Eash, K. J., J. M. Means, D. W. White, and D. C. Link. 2009. CXCR4 is a key regulator of neutrophil release from the bone marrow under basal and stress granulopoiesis conditions. *Blood* 113: 4711-4719.

451. Park, B. H., S. Kook, S. Lee, J. H. Jeong, A. Brufsky, and B. C. Lee. 2013. An isoform of C/EBP beta, LIP, regulates expression of the chemokine receptor CXCR4 and modulates breast cancer cell migration. *J Biol Chem*.

452. He, H., C. Wang, Z. Shen, Y. Fang, X. Wang, W. Chen, F. Liu, X. Qin, and Y. Sun. 2013. Upregulated expression of C-x-C chemokine receptor 4 is an independent prognostic predictor for patients with gastric cancer. *PLoS ONE* 8: e71864.

453. Kim, H. K., J. E. Kim, J. Chung, K. H. Park, K. S. Han, and H. I. Cho. 2007. Lithium down-regulates the expression of CXCR4 in human neutrophils. *J Trace Elem Med Biol* 21: 204-209.

454. Zhang, Y., Q. Guo, H. Zhao, D. Zhao, X. Wu, W. Zhao, Y. Wang, B. Xia, and W. Da. 2013. Expression of CXCR4 is an independent prognostic factor for overall survival and progression-free survival in patients with myelodysplastic syndrome. *Med Oncol* 30: 341.

455. Ahn, J. Y., K. Seo, O. K. Weinberg, and D. A. Arber. 2013. The prognostic value of CXCR4 in acute myeloid leukemia. *Appl Immunohistochem Mol Morphol* 21: 79-84.

456. Ivetic, A. 2013. Signals regulating L-selectin-dependent leucocyte adhesion and transmigration. *Int J Biochem Cell Biol* 45: 550-555.

457. Barreda, D. R., P. C. Hanington, and M. Belosevic. 2004. Regulation of myeloid development and function by colony stimulating factors. *Dev Comp Immunol* 28: 509-554.

458. Liu, F., J. Poursine-Laurent, H. Y. Wu, and D. C. Link. 1997. Interleukin-6 and the granulocyte colony-stimulating factor receptor are major independent regulators of granulopoiesis in vivo but are not required for lineage commitment or terminal differentiation. *Blood* 90: 2583-2590.

459. Palic, D., C. B. Andreasen, B. W. Menzel, and J. A. Roth. 2005. A rapid, direct assay to measure degranulation of primary granules in neutrophils from kidney of fathead minnow (Pimephales promelas Rafinesque, 1820). *Fish Shellfish Immunol* 19: 217-227.

460. Kimura, A., I. Kinjyo, Y. Matsumura, H. Mori, R. Mashima, M. Harada, K. R. Chien, H. Yasukawa, and A. Yoshimura. 2004. SOCS3 is a physiological negative regulator for granulopoiesis and granulocyte colony-stimulating factor receptor signaling. *J Biol Chem* 279: 6905-6910.

461. Khanna-Gupta, A., T. Zibello, H. Sun, J. Lekstrom-Himes, and N. Berliner. 2001. C/EBP epsilon mediates myeloid differentiation and is regulated by the CCAAT displacement protein (CDP/cut). *Proc Natl Acad Sci U S A* 98: 8000-8005.

462. White, K. L., J. S. Wiley, T. Frost, J. J. McKendrick, R. P. Hermann, M. Seldon, A. Enno, R. Bell, I. Bunce, K. Taylor, and et al. 1992. All-trans retinoic acid in the treatment of acute promyelocytic leukaemia. *Aust N Z J Med* 22: 449-454.

463. Wang, Z., L. Cao, R. Kang, M. Yang, L. Liu, Y. Zhao, Y. Yu, M. Xie, X. Yin, K. M. Livesey, and D. Tang. 2011. Autophagy regulates myeloid cell differentiation by p62/SQSTM1-mediated degradation of PML-RARalpha oncoprotein. *Autophagy* 7: 401-411.

464. Panopoulos, A. D., and S. S. Watowich. 2008. Granulocyte colony-stimulating factor: molecular mechanisms of action during steady state and 'emergency' hematopoiesis. *Cytokine* 42: 277-288.

465. Lekstrom-Himes, J. A., and J. I. Gallin. 2000. Immunodeficiency diseases caused by defects in phagocytes. *N Engl J Med* 343: 1703-1714.

466. Andrews, T., and K. E. Sullivan. 2003. Infections in patients with inherited defects in phagocytic function. *Clin Microbiol Rev* 16: 597-621.

467. Condamine, T., and D. I. Gabrilovich. 2011. Molecular mechanisms regulating myeloid-derived suppressor cell differentiation and function. *Trends Immunol* 32: 19-25.

468. Almand, B., J. I. Clark, E. Nikitina, J. van Beynen, N. R. English, S. C. Knight, D. P. Carbone, and D. I. Gabrilovich. 2001. Increased production of immature myeloid cells in cancer patients: a mechanism of immunosuppression in cancer. *J Immunol* 166: 678-689.

469. Ioannou, M., T. Alissafi, I. Lazaridis, G. Deraos, J. Matsoukas, A. Gravanis, V. Mastorodemos, A. Plaitakis, A. Sharpe, D. Boumpas, and P. Verginis. 2012. Crucial role of granulocytic myeloid-derived suppressor cells in the regulation of central nervous system autoimmune disease. *J Immunol* 188: 1136-1146.

470. Norris, B. A., L. S. Uebelhoer, H. I. Nakaya, A. A. Price, A. Grakoui, and B. Pulendran. 2013. Chronic but not acute virus infection induces sustained expansion of myeloid suppressor cell numbers that inhibit viral-specific T cell immunity. *Immunity* 38: 309-321.

471. Srivastava, M. K., P. Sinha, V. K. Clements, P. Rodriguez, and S. Ostrand-Rosenberg. 2010. Myeloid-derived suppressor cells inhibit T-cell activation by depleting cystine and cysteine. *Cancer Res* 70: 68-77.

472. Ahlin, A., G. Larfars, G. Elinder, J. Palmblad, and H. Gyllenhammar. 1999. Gamma interferon treatment of patients with chronic granulomatous disease is associated

with augmented production of nitric oxide by polymorphonuclear neutrophils. *Clin Diagn Lab Immunol* 6: 420-424.

473. Beckman, J. S., T. W. Beckman, J. Chen, P. A. Marshall, and B. A. Freeman. 1990. Apparent hydroxyl radical production by peroxynitrite: implications for endothelial injury from nitric oxide and superoxide. *Proc Natl Acad Sci U S A* 87: 1620-1624.
474. Cassatella, M. A. 1995. The production of cytokines by polymorphonuclear neutrophils. *Immunol Today* 16: 21-26.
475. Wright, H. L., R. J. Moots, R. C. Bucknall, and S. W. Edwards. 2010. Neutrophil function in inflammation and inflammatory diseases. *Rheumatology (Oxford)* 49: 1618-1631.
476. Watson, A. S., M. Mortensen, and A. K. Simon. 2011. Autophagy in the pathogenesis of myelodysplastic syndrome and acute myeloid leukemia. *Cell Cycle* 10: 1719-1725.
477. Cairo, M. S. 1989. Review of G-CSF and GM-CSF. Effects on neonatal neutrophil kinetics. *Am J Pediatr Hematol Oncol* 11: 238-244.
478. Singh, P., P. Hu, J. Hoggatt, A. Moh, and L. M. Pelus. 2012. Expansion of bone marrow neutrophils following G-CSF administration in mice results in osteolineage cell apoptosis and mobilization of hematopoietic stem and progenitor cells. *Leukemia* 26: 2375-2383.
479. Ramos, C. D., C. Canetti, J. T. Souto, J. S. Silva, C. M. Hogaboam, S. H. Ferreira, and F. Q. Cunha. 2005. MIP-1alpha[CCL3] acting on the CCR1 receptor mediates neutrophil migration in immune inflammation via sequential release of TNF-alpha and LTB4. *J Leukoc Biol* 78: 167-177.
480. Oka, T., S. Hikoso, O. Yamaguchi, M. Taneike, T. Takeda, T. Tamai, J. Oyabu, T. Murakawa, H. Nakayama, K. Nishida, S. Akira, A. Yamamoto, I. Komuro, and K. Otsu. 2012. Mitochondrial DNA that escapes from autophagy causes inflammation and heart failure. *Nature* 485: 251-255.
481. Plater-Zyberk, C., L. A. Joosten, M. M. Helsen, J. Hepp, P. A. Baeuerle, and W. B. van den Berg. 2007. GM-CSF neutralisation suppresses inflammation and protects cartilage in acute streptococcal cell wall arthritis of mice. *Ann Rheum Dis* 66: 452-457.
482. Krinner, E. M., T. Raum, S. Petsch, S. Bruckmaier, I. Schuster, L. Petersen, R. Cierpka, D. Abebe, M. Molhoj, A. Wolf, P. Sorensen, M. Locher, P. A. Baeuerle, and J. Hepp. 2007. A human monoclonal IgG1 potently neutralizing the pro-inflammatory cytokine GM-CSF. *Mol Immunol* 44: 916-925.
483. Kowanetz, M., X. Wu, J. Lee, M. Tan, T. Hagenbeek, X. Qu, L. Yu, J. Ross, N. Korsisaari, T. Cao, H. Bou-Reslan, D. Kallop, R. Weimer, M. J. Ludlam, J. S. Kaminker, Z. Modrusan, N. van Bruggen, F. V. Peale, R. Carano, Y. G. Meng, and N. Ferrara. 2010. Granulocyte-colony stimulating factor promotes lung metastasis through mobilization of Ly6G+Ly6C+ granulocytes. *Proc Natl Acad Sci U S A* 107: 21248-21255.
484. Sengstake, S., E. M. Boneberg, and H. Illges. 2006. CD21 and CD62L shedding are both inducible via P2X7Rs. *Int Immunol* 18: 1171-1178.
485. Fossati, G., R. C. Bucknall, and S. W. Edwards. 2002. Insoluble and soluble immune complexes activate neutrophils by distinct activation mechanisms: changes

in functional responses induced by priming with cytokines. *Ann Rheum Dis* 61: 13-19.

486. Scott, C. S. 1979. Maturation-linked expression of the Fc (IgG) receptor on developing human bone marrow and peripheral blood granulocytes. *Clin Exp Immunol* 38: 300-305.

487. Witko-Sarsat, V., P. Rieu, B. Descamps-Latscha, P. Lesavre, and L. Halbwachs-Mecarelli. 2000. Neutrophils: molecules, functions and pathophysiological aspects. *Lab Invest* 80: 617-653.

488. Masson, P. L., J. F. Heremans, and E. Schonne. 1969. Lactoferrin, an iron-binding protein in neutrophilic leukocytes. *J Exp Med* 130: 643-658.

489. Vaccaro, M. I. 2012. Zymophagy: selective autophagy of secretory granules. *International journal of cell biology* 2012: 396705.

490. Cuervo, A. M., H. Hildebrand, E. M. Bomhard, and J. F. Dice. 1999. Direct lysosomal uptake of alpha 2-microglobulin contributes to chemically induced nephropathy. *Kidney Int* 55: 529-545.

491. Heymann, D. 2006. Autophagy: A protective mechanism in response to stress and inflammation. *Curr Opin Investig Drugs* 7: 443-450.

492. Cadwell, K., J. Y. Liu, S. L. Brown, H. Miyoshi, J. Loh, J. K. Lennerz, C. Kishi, W. Kc, J. A. Carrero, S. Hunt, C. D. Stone, E. M. Brunt, R. J. Xavier, B. P. Sleckman, E. Li, N. Mizushima, T. S. Stappenbeck, and H. W. t. Virgin. 2008. A key role for autophagy and the autophagy gene Atg16l1 in mouse and human intestinal Paneth cells. *Nature* 456: 259-263.

493. Borregaard, N., K. Theilgaard-Monch, O. E. Sorensen, and J. B. Cowland. 2001. Regulation of human neutrophil granule protein expression. *Curr Opin Hematol* 8: 23-27.

494. Theilgaard-Monch, K., L. C. Jacobsen, R. Borup, T. Rasmussen, M. D. Bjerregaard, F. C. Nielsen, J. B. Cowland, and N. Borregaard. 2005. The transcriptional program of terminal granulocytic differentiation. *Blood* 105: 1785-1796.

495. Radomska, H. S., C. S. Huettner, P. Zhang, T. Cheng, D. T. Scadden, and D. G. Tenen. 1998. CCAAT/enhancer binding protein alpha is a regulatory switch sufficient for induction of granulocytic development from bipotential myeloid progenitors. *Mol Cell Biol* 18: 4301-4314.

496. Nakajima, H., and J. N. Ihle. 2001. Granulocyte colony-stimulating factor regulates myeloid differentiation through CCAAT/enhancer-binding protein epsilon. *Blood* 98: 897-905.

497. Wang, J., H. Lian, Y. Zhao, M. A. Kauss, and S. Spindel. 2008. Vitamin D3 induces autophagy of human myeloid leukemia cells. *J Biol Chem* 283: 25596-25605.

498. Goussetis, D. J., E. Gounaris, E. J. Wu, E. Vakana, B. Sharma, M. Bogyo, J. K. Altman, and L. C. Platanias. 2012. Autophagic degradation of the BCR-ABL oncoprotein and generation of antileukemic responses by arsenic trioxide. *Blood* 120: 3555-3562.

499. Humbert, M., C. Mueller, M. F. Fey, and M. P. Tschan. 2012. Inhibition of damage-regulated autophagy modulator-1 (DRAM-1) impairs neutrophil differentiation of NB4 APL cells. *Leuk Res* 36: 1552-1556.

500. Tsai, S., and S. J. Collins. 1993. A dominant negative retinoic acid receptor blocks neutrophil differentiation at the promyelocyte stage. *Proc Natl Acad Sci U S A* 90: 7153-7157.

501. Park, D. J., A. M. Chumakov, P. T. Vuong, D. Y. Chih, A. F. Gombart, W. H. Miller, Jr., and H. P. Koeffler. 1999. CCAAT/enhancer binding protein epsilon is a potential retinoid target gene in acute promyelocytic leukemia treatment. *J Clin Invest* 103: 1399-1408.

502. Olins, A. L., M. Zwerger, H. Herrmann, H. Zentgraf, A. J. Simon, M. Monestier, and D. E. Olins. 2008. The human granulocyte nucleus: Unusual nuclear envelope and heterochromatin composition. *Eur J Cell Biol* 87: 279-290.

503. Olins, A. L., H. Herrmann, P. Lichter, M. Kratzmeier, D. Doenecke, and D. E. Olins. 2001. Nuclear envelope and chromatin compositional differences comparing undifferentiated and retinoic acid- and phorbol ester-treated HL-60 cells. *Exp Cell Res* 268: 115-127.

504. Somech, R., E. N. Gal-Yam, S. Shaklai, O. Geller, N. Amariglio, G. Rechavi, and A. J. Simon. 2007. Enhanced expression of the nuclear envelope LAP2 transcriptional repressors in normal and malignant activated lymphocytes. *Ann Hematol* 86: 393-401.

505. Mijaljica, D., M. Prescott, and R. J. Devenish. 2010. The intricacy of nuclear membrane dynamics during nucleophagy. *Nucleus* 1: 213-223.

506. Ivanov, A., J. Pawlikowski, I. Manoharan, J. van Tuyn, D. M. Nelson, T. S. Rai, P. P. Shah, G. Hewitt, V. I. Korolchuk, J. F. Passos, H. Wu, S. L. Berger, and P. D. Adams. 2013. Lysosome-mediated processing of chromatin in senescence. *J Cell Biol* 202: 129-143.

507. Pittman, K., and P. Kubes. 2013. Damage-associated molecular patterns control neutrophil recruitment. *J Innate Immun* 5: 315-323.

508. Tamassia, N., M. Zimmermann, and M. A. Cassatella. 2012. An additional piece in the puzzle of neutrophil-derived IL-1beta: the NLRP3 inflammasome. *Eur J Immunol* 42: 565-568.

509. Alemdehy, M. F., N. G. van Boxtel, H. W. de Looper, I. J. van den Berge, M. A. Sanders, T. Cupedo, I. P. Touw, and S. J. Erkeland. 2012. Dicer1 deletion in myeloid-committed progenitors causes neutrophil dysplasia and blocks macrophage/dendritic cell development in mice. *Blood* 119: 4723-4730.

510. Martinet, W., S. Verheye, I. De Meyer, J. P. Timmermans, D. M. Schrijvers, I. Van Brussel, H. Bult, and G. R. De Meyer. 2012. Everolimus triggers cytokine release by macrophages: rationale for stents eluting everolimus and a glucocorticoid. *Arterioscler Thromb Vasc Biol* 32: 1228-1235.

511. Lin, N. Y., C. Beyer, A. Giessl, T. Kireva, C. Scholtysek, S. Uderhardt, L. E. Munoz, C. Dees, A. Distler, S. Wirtz, G. Kronke, B. Spencer, O. Distler, G. Schett, and J. H. Distler. 2013. Autophagy regulates TNFalpha-mediated joint destruction in experimental arthritis. *Ann Rheum Dis* 72: 761-768.

512. Abdel Fattah, E. A. H., A. Bhattacharya, D. LiuX, J. Shin, Q. Wei, Y. Xu, A. Herron, and N. T. Eissa. 2012. Autophagy Deficiency In Myeloid Cells Results In Spontaneous Lung Inflammation. In *American Thoracic Society 2013 International Conference*. American Thoracic Society, Philadelphia Pennsylvania.

513. Lupfer, C., P. G. Thomas, P. K. Anand, P. Vogel, S. Milasta, J. Martinez, G. Huang, M. Green, M. Kundu, H. Chi, R. J. Xavier, D. R. Green, M. Lamkanfi, C. A. Dinarello, P. C. Doherty, and T. D. Kanneganti. 2013. Receptor interacting protein kinase 2-mediated mitophagy regulates inflammasome activation during virus infection. *Nat Immunol* 14: 480-488.

514. van Raam, B. J., W. Sluiter, E. de Wit, D. Roos, A. J. Verhoeven, and T. W. Kuijpers. 2008. Mitochondrial membrane potential in human neutrophils is maintained by complex III activity in the absence of supercomplex organisation. *PLoS ONE* 3: e2013.

515. Blair, D., F. J. Dufort, and T. C. Chiles. 2012. Protein kinase Cbeta is critical for the metabolic switch to glycolysis following B-cell antigen receptor engagement. *Biochem J* 448: 165-169.

516. Chang, C. H., J. D. Curtis, L. B. Maggi, Jr., B. Faubert, A. V. Villarino, D. O'Sullivan, S. C. Huang, G. J. van der Windt, J. Blagih, J. Qiu, J. D. Weber, E. J. Pearce, R. G. Jones, and E. L. Pearce. 2013. Posttranscriptional control of T cell effector function by aerobic glycolysis. *Cell* 153: 1239-1251.

517. Simsek, T., F. Kocabas, J. Zheng, R. J. Deberardinis, A. I. Mahmoud, E. N. Olson, J. W. Schneider, C. C. Zhang, and H. A. Sadek. 2010. The distinct metabolic profile of hematopoietic stem cells reflects their location in a hypoxic niche. *Cell Stem Cell* 7: 380-390.

518. Ueno, T., W. Sato, Y. Horie, M. Komatsu, I. Tanida, M. Yoshida, S. Ohshima, T. W. Mak, S. Watanabe, and E. Kominami. 2008. Loss of Pten, a tumor suppressor, causes the strong inhibition of autophagy without affecting LC3 lipidation. *Autophagy* 4: 692-700.

519. Tandon, P., C. A. Gallo, S. Khatri, J. F. Barger, H. Yepiskoposyan, and D. R. Plas. 2011. Requirement for ribosomal protein S6 kinase 1 to mediate glycolysis and apoptosis resistance induced by Pten deficiency. *Proc Natl Acad Sci U S A* 108: 2361-2365.

520. Liu, L. L., Z. J. Long, L. X. Wang, F. M. Zheng, Z. G. Fang, M. Yan, D. F. Xu, J. J. Chen, S. W. Wang, D. J. Lin, and Q. Liu. 2013. Inhibition of mTOR pathway sensitizes acute myeloid leukemia cells to Aurora inhibitors by suppression of glycolytic metabolism. *Mol Cancer Res*.

521. Salminen, A., and K. Kaarniranta. 2010. Glycolysis links p53 function with NF-kappaB signaling: impact on cancer and aging process. *J Cell Physiol* 224: 1-6.

522. Franceschi, C., M. Capri, D. Monti, S. Giunta, F. Olivieri, F. Sevini, M. P. Panourgia, L. Invidia, L. Celani, M. Scurti, E. Cevenini, G. C. Castellani, and S. Salvioli. 2007. Inflammaging and anti-inflammaging: a systemic perspective on aging and longevity emerged from studies in humans. *Mech Ageing Dev* 128: 92-105.

Authors Publications

A J Stranks, M Mortensen, D Ferguson, D Puleston, K Shenderov, A Watson, K Phadwal, V Cerundolo, and A K Simon. *"Reduced maturation and antigen presentation in autophagy-deficient macrophages is consistent with inflamm-aging".* Manuscript in preparation for submission to Aging Cell

A S Watson, **A J Stranks**, O Williams, K Cain, M McFarlane, J McGouran, B Kessler, S Khandwala, M Lutterop, P Woll, K Phadwal, M Mortensen, D Puleston, G Djordjevic, D Ferguson, E Soilleux, S E Jacobsen, and A K Simon. *Deficient autophagy drives hematopoietic stem cell dysfunction, myeloid dysplasia and leukemic proliferation and metabolism*. Resubmitted to Nature Cell Biology, September 2013

A Clarke, U Ellinghaus, A Cortini, **A J Stranks**, A K Simon, M Botto and Timothy Vyse, *Autophagy is activated in SLE and required for plasmablast development*. Submitted to Science Translational Medicine, July 2013

S B Rasmussen, K A Horan, C K Holm, **A J Stranks**, T C Mettenleiter, K A Simon, S B Jensen, F J Rixon, R E Vance, B He, S R Paludan, *Activation of autophagy by alpha-herpesviruses in myeloid cells is mediated by cytoplasmic viral DNA though a mechanism dependent on STING*. Journal of Immunology, 2011. **187**(10): p. 5268 - 5276

M Mortensen, E. J Soilleux, G. Djordjevic, R. Tripp, M. Lutteropp, E. Sadighi-Akha, **A. J. Stranks,** J. Glanville, S. Knight, S. E. Jacobsen, K. R. Kranc and A. K. Simon, *The autophagy protein Atg7 is essential for hematopoietic stem cell maintenance.* Journal of Experimental Medicine, 2011. **208**(3): p. 455 – 467